



**GUIDELINES FOR ATMOSPHERIC MEASUREMENTS IN SUPPORT OF
ELECTRO-OPTICAL SYSTEMS TESTING**

**ABERDEEN TEST CENTER
DUGWAY PROVING GROUND
ELECTRONIC PROVING GROUND
REAGAN TEST SITE
REDSTONE TEST CENTER
WHITE SANDS TEST CENTER
YUMA PROVING GROUND**

**NAVAL AIR WARFARE CENTER AIRCRAFT DIVISION PATUXENT RIVER
NAVAL AIR WARFARE CENTER WEAPONS DIVISION CHINA LAKE
NAVAL AIR WARFARE CENTER WEAPONS DIVISION POINT MUGU
NAVAL SURFACE WARFARE CENTER DAHLGREN DIVISION
NAVAL UNDERSEA WARFARE CENTER DIVISION KEYPORT
NAVAL UNDERSEA WARFARE CENTER DIVISION NEWPORT
PACIFIC MISSILE RANGE FACILITY**

**96TH TEST WING
412TH TEST WING
ARNOLD ENGINEERING DEVELOPMENT CENTER**

**SPACE LAUNCH DELTA 30
SPACE LAUNCH DELTA 45**

NATIONAL AERONAUTICS AND SPACE ADMINISTRATION

**DISTRIBUTION A: APPROVED FOR PUBLIC RELEASE;
DISTRIBUTION IS UNLIMITED**

This page intentionally left blank.

DOCUMENT 356-22

**GUIDELINES FOR ATMOSPHERIC MEASUREMENTS IN SUPPORT OF
ELECTRO-OPTICAL SYSTEMS TESTING**

August 2022

Prepared by

**Electro-Optics Committee
Meteorology Group**

Published by

**Secretariat
Range Commanders Council
U.S. Army White Sands Missile Range
New Mexico 88002-5110**

This page intentionally left blank.

Table of Contents

Preface	vii
Summary of Change	ix
Acronyms	xi
Chapter 1. Introduction	1-1
Chapter 2. Measurement Guidelines	2-1
2.1 Total Quality Data Management.....	2-1
2.1.1 TQDM Methods for Identifying and Quantifying Qualified Data.....	2-6
2.1.2 Development of Information Bases	2-8
2.2 Test Data Requirements	2-12
2.2.1 Visual Sensor Tests.....	2-16
2.2.2 Infrared Sensor Tests	2-17
2.2.3 Laser Range Finder Tests.....	2-18
2.2.4 Millimeter Wave Sensor Tests.....	2-20
2.2.5 Test Programs	2-21
2.3 Recommended Measurement Methods.....	2-23
2.3.1 Visual Range (Visibility)	2-23
2.3.2 Wind.....	2-28
2.3.3 Absorbing Gases	2-33
2.3.4 Aerosols	2-34
2.3.5 Aerosol Speciation	2-36
2.3.6 Precipitation	2-36
2.3.7 Terrain Signatures	2-38
2.3.8 Humidity and Temperature Structure Constants.....	2-40
2.3.9 Sea State.....	2-42
2.3.10 Background Radiation	2-43
2.3.11 Spectral Transmittance.....	2-45
2.3.12 Index of Refraction Structure Constant	2-49
2.3.13 Surface and Aloft Meteorological Situation	2-50
2.3.14 Air Temperature, Humidity, and Pressure	2-54
2.4 Test Data Evaluation.....	2-55
2.4.1 RMS Errors	2-55
2.4.2 Impact of Measurement Error on Sensor Evaluation.....	2-57
2.4.3 Temporal and Spatial Averaging Intervals	2-58
2.5 Data and Information Bases.....	2-59
2.5.1 Data Archival Formats and Storage	2-60
2.5.2 Information Base Generation and Storage	2-61
2.5.3 Identifying and Reporting Data Gaps	2-61

2.5.4	Identifying and Tracking Future Test Requirements	2-61
Appendix A. Summary of Atmospheric Environmental Parameter Requirements in Support of Electro-Optical Systems Testing		
A.1	Purpose.....	A-1
A.2	Scope.....	A-1
Appendix B. Relative Uncertainty in Visual 50 Percent Probability of Detection		
B.1	Purpose.....	B-1
B.2	Scope.....	B-1
Appendix C. Relative Uncertainty in Infrared (Thermal Bands) 50 Percent Probability of Detection		
C.1	Purpose.....	C-1
C.2	Scope.....	C-1
Appendix D. Relative Uncertainty in 1.06 and 10.6 μm Laser Wavelength Probability of Successful Ranging.....		
D.1	Purpose.....	D-1
D.2	Scope.....	D-1
Appendix E. Relative Uncertainty in 1.06 and 10.6 μm Laser Wavelength Laser Power, on Target		
E.1	Purpose.....	E-1
E.2	Scope.....	E-1
Appendix F. Relative Uncertainty in 8-12 μm Transmittance because of Air Temperature, Relative Humidity, and Visual Range.....		
F.1	Purpose.....	F-1
F.2	Scope.....	F-1
Appendix G. Relative Uncertainty in Millimeter Wave Extinction and Transmittance Parameters as a Function of Ice and Liquid Water Precipitation Temperatures		
G.1	Purpose.....	G-1
G.2	Scope.....	G-1
Appendix H. Citations		
H-1		
Table of Figures		
Figure 1-1.	Targets-Atmospheres-Sensors Sequential Influence Synopsis	1-4
Figure 2-1.	Data Management Approach Now Used for Acquiring Data in an Electro-Optical Sensor Atmospheric Test	2-1

Figure 2-2.	The Data Cycle with No Total Quality Data Management Operations	2-2
Figure 2-3.	TQDM-required Measurement Standards.....	2-3
Figure 2-4.	TQDM Experimental Design.....	2-3
Figure 2-5.	TQDM Data Acquisition.....	2-4
Figure 2-6.	TQDM Data Evaluation.....	2-4
Figure 2-7.	The Information Base Concept	2-5
Figure 2-8.	A Visual Impression of Measurement Uncertainty for Well-Maintained Instruments of Different 2018 Pyranometer Classes	2-12
Figure 2-9.	Typical Probability of Detection Curves for Visual/Near-Infrared Band Imaging Systems.....	2-17
Figure 2-10.	Example of 8-4 μm Band FLIR Probability of Detection of a Tank on a Grass Background as a Function of Time of Day	2-18
Figure 2-11.	Example Probability of Successful Ranging.....	2-19
Figure 2-12.	Illustration of the Dependence of the Sky (S)-to-Ground (G) Illuminance Ratio on Viewing Direction	2-25
Figure 2-13.	The Effect of Sky-to-Ground Ratio on Visual Range.....	2-26
Figure 2-14.	Ratio of Seeing ϵ_0 to Full Width Half Maximum (ϵvK) as a Function of the Wavelength for Several Values of L_0	2-31
Figure 2-15.	Sea-Level Transmittance over a 1820 m Horizontal Path	2-33
Figure 2-16.	Bulk Log Estimates for Different Values of Relative Humidity (RH) and Temperature-specific Humidity Correlation Coefficient (rTq) as Indicated, vs. Air-Sea Temperature Difference	2-42
Figure 2-17.	3-5 μm Band Spectral Irradiance Distributions for a 27 °C (300 K) Blackbody Target and 1500 °C (1773 K) Blackbody Radiometric Source	2-47
Figure 2-18.	3-5 μm Transmittance to ah 27 °C (300 K) Blackbody Target or a 1500 °C (1773 K) Radiometric Source	2-48
Figure 2-19.	MZA DELTA Concept of Operations	2-50

Table of Tables

Table 2-1.	Summary Atmospheric Environmental Parameters in Support of Electro- Optical Systems Testing	2-13
Table A-1.	Summary Atmospheric Environmental Parameters in Support of Electro- Optical Visual Image Detection Testing.....	A-2
Table A-2.	Summary Atmospheric Environmental Parameters in Support of Electro- Optical Infrared Image Detection Testing	A-4
Table A-3.	Summary Atmospheric Environmental Parameters in Support of Electro- Optical Rangefinder/Designator Testing	A-6

This page intentionally left blank.

Preface

The original release of this document provided guidance to test ranges and programs for acquiring adequate data to specify electro-optical sensor performance under a range of atmospheric conditions. The purpose of this report is to update RCC document 356-95 in view of modern test and evaluation requirements and technological advances in recent years, and to provide guidelines for atmospheric and oceanographic measurements used to support test and evaluation of electro-optical sensor system performance. The guidelines approach is employed to illustrate the context in which the measurements will be used, to show the impact of measurement error on measurement applications, and to emphasize that atmospheric measurements are an interactive, complex set of variables that must be viewed as a whole.

Demands for high-quality atmospheric measurements to support electro-optical performance evaluation have increased during the past 10 years for at least three reasons.

- a. It is impractical to test electro-optical sensor performance under all operational atmospheric conditions. Thus, electro-optical sensor atmospheric field tests produce “calibration points” that are used to ensure models predicting system performance under all conditions are accurate and that the sensor functions as expected.
- b. Field test data now serve as the basis for the development of simulations used to develop high-energy laser (HEL) weapons, and to train sensor users.
- c. The number of test ranges supporting electro-optical testing in the atmosphere and the budgets for testing have dramatically increased in recent years, and technology as well as understanding of the atmosphere has been transforming electro-optic measurement techniques.

Determination of data accuracy by the method of root-mean-square (RMS) error analysis is reviewed and recommended as a means of qualifying data. Application to sensors employed for target detection and ranging and multispectral transmissometry are discussed as examples. The impact of spatial and temporal sampling intervals on data interpretation is shown to play a fundamental role in test design considerations.

Test data that support the understanding of electro-optical sensor or HEL operation in atmospheric conditions worldwide are required. As the popularity of electro-optical sensor-based weapons spreads, the United States’ forces must increasingly be able to anticipate threat force capability as a function of atmospheric conditions. The recommended methods of data measurement and analysis in these guidelines are basic tools for ensuring the production of reliable data for predicting and interpreting worldwide electro-optical sensor performance.

For questions about this document, contact the Range Commanders Council Secretariat.

Secretariat, Range Commanders Council
ATTN: TEWS-TDR
1510 Headquarters Avenue
White Sands Missile Range, New Mexico 88002-5110
Telephone: (575) 678-1107, DSN 258-1107
E-mail: rcc-feedback@trmc.osd.mil

This page intentionally left blank.

Summary of Change

The primary changes to this document are the following.

- Material moved from the Preface to Chapter 1.
- New section describing maritime laser test environments.
- Review of all formulas to integrate some updates and resolve small translation errors from the previous version.
- Descriptions of new sensors and systems applicable to the atmospheric characterization techniques for laser test and evaluation.
- Removal of section on classifying laser testing.

This page intentionally left blank.

Acronyms

ACU	acquisition control unit
AOD	aerosol optical depth
BRDF	bidirectional reflectance distribution function
DELTA	Delayed Tilt Anisoplanatism
DIMM	Differential Image Motion Monitor
DoD	Department of Defense
E-O	electro-optical
FLIR	forward-looking infrared
FTS	Fourier-transform spectrometer
GPS	Global Positioning System
HEL	high-energy laser
LDV	laser Doppler velocimeter
LRF	laser range finder
MMW	millimeter wave
MRTD	minimum resolvable temperature difference
NIST	National Institute of Standards and Technology
PROPS	Path-Resolved Optical Profiler System
RASS	Radio Acoustic Sounding System
RMS	root mean square
SWOE	Smart Weapons Operability Enhancement
T&E	test and evaluation
TASS	Targets-Atmospheres-Sensors Synopsis
TQDM	Total Quality Data Management
UHF	ultra-high frequency

This page intentionally left blank.

CHAPTER 1

Introduction

Recent armed conflicts have demonstrated the superiority of weapons systems using electro-optical (E-O) sensors that operate in spectral bands throughout the ultraviolet through millimeter wave (MMW) spectrum. In addition, some DoD components are exploiting the value of an almost unlimited magazine available to solid-state lasers, along with other battlefield advantages. The performance of these sensors and weapon systems, including kinetic weapons using E-O targeting, depends on countermeasures effectiveness, atmospheric conditions, background and target signatures, and the sensor response envelope. Without careful specification of all these parameters and variables, the probability of operational success for systems using these sensors is unknown.

In 1983, the Meteorology Group of the Range Commanders Council (RCC) recognized the need to provide guidelines for E-O sensor and weapon testing in the atmosphere. A workshop attended by experts in atmospheric transmission, meteorology, particulate characterization, and gaseous constituents was convened. The experts were asked to define state-of-the-art measurement methods and capabilities in atmospheric measurements relevant to E-O sensor testing. The resulting *Proceedings of Workshop to Standardize Atmospheric Measurements in Support of Electro-Optical Systems*, compiled and edited by the University of Dayton staff, formed the basis for the initial publication of this document, in 1984. In deciding what atmospheric measurements should be made in support of electro-optical systems testing, these three questions should be addressed.

- a. What information will be required to determine the reasons for variations in observed system performance?
- b. What information will be required to determine how the system or similar systems would perform under environmental conditions other than those during which the tests were conducted?
- c. What information is needed to predict the performance of the system after deployment?

These requirements have not changed; although, modern E-O sensor and weapon applications require expanded and more comprehensive measurement approaches to answer these questions.

During the 38 years since the publication of document 356-84, E-O system development and testing have become increasingly complex and demanding. Weapons and surveillance systems increasingly rely on multiple spectral bands (so called “sensor fusion”). The MMW sensors are playing an increasingly important role in multisensor packages. Effective multispectral remote sensing information interpretation from satellites requires accurate ground truth and reliable surface and aloft atmospheric measurements. Aided target recognition technology development and evaluation require detailed and sophisticated atmospheric measurements and specifications. Recently all Services have started to develop laser weapons for fielding in the near future. The value of E-O weapons and surveillance systems and atmospheric

effects on performance were clearly demonstrated in the 1991 Persian Gulf War with Iraq. As a result of this and other successes worldwide, the demand and development activity for these systems has increased. The worldwide distribution of these weapons has increased demand for knowledge of effective countermeasures and methods for effective operations in a measure-countermeasure environment. Available sensor development and testing budgets are increasing, so pressure is increasing on test ranges to acquire atmospheric data not normally acquired and with accuracies not required when E-O systems were in their infancy. All these factors have led to the blurring of the borders of responsibility for particular kinds of measurements to support E-O sensor test and evaluation (T&E).

A focused effort encompassing comprehensive management in all phases of the data cycle is required to achieve the data quality and quantity demanded by current sensor T&E, simulation developments, and future applications. Total Quality Data Management (TQDM) is the approach taken by these guidelines to attain a high standard of data quality. The objectives of TQDM are:

- comprehensive management of all phases of the data cycle;
- continuous measurable improvement in all aspects of the data cycle;
- quantifiable data standards, in particular National Institute for Standards and Technology (NIST) – traceable parameters; and
- accessible and distributable data and information.

These guidelines describe how TQDM accomplishes these objectives by planning:

- all test phases in accordance with instrumentation accuracy capability and required final product accuracy;
- measurement cross-checks and verifications, in particular the use of intercomparison techniques;
- data accuracy determination;
- data evaluation and archival; and
- standardized data available to current and future users in information base formats.

Every test program is unique; however, experience shows that all test programs share many common measurements. To illustrate, these guidelines discuss measurements required by two major Army E-O test programs: Smart Weapons Operability Enhancement (SWOE) tests, and Smoke Week. In addition, experiences from a Navy E-O atmospheric measurement campaign for laser performance assessment called CABLE/TRAX-West will be cited.

Additionally, this standard reviews measurements for specific E-O sensors (multispectral imaging systems and laser range finders [LRFs]/designators) used by all military Services. Typical required sampling rates, data averaging times, and a suggested level of measurement accuracy are given. Note that the specification of single values of instrument measurement accuracy is inappropriate for many test data applications.

This standard provides general information guidelines for desirable measurement methods. Please note that, in many cases, measurements at a specific range must be made with existing hardware; however, as the guidelines show, many previous measurements have not acquired the necessary supporting data, calibration records were not maintained, and measurement errors were not determined. Such fundamental requirements are the focus of these measurement method guidelines.

This standard also provides data evaluation guidelines. Those who test systems understand best the limitations of test support data. Examination of existing atmospheric databases shows that measurement errors are rarely recorded with the data. Data accuracy and methods of qualifying data must be acquired and specified as a normal part of test procedures if data now acquired are to be used effectively in future E-O system evaluations and simulations.

Section [2.4](#) reviews and recommends determination of data accuracy by the method of root-mean-square (RMS) error analysis as a means of qualifying data. The section discusses as examples application to sensors employed for target detection and ranging and multispectral transmissometry. The impact of spatial and temporal sampling intervals on data interpretation is shown to play a fundamental role in test design considerations.

This document draws a distinction between databases (archived data) and information bases (summaries of results from data applications). It also provides guidelines for developing and making data and information accessible. In many cases, users do not require or want archived data. Their interest is in the information the data yields. Making data accessible and meaningful through information bases developed to reside with the archived database ensures that data is accessible in an immediately useful form. This document recommends two new types of information base for test range operational planning and use. These information bases are identification of data gaps and tracking of anticipated test requirements. With this information, test designers can often structure tests to acquire missing data, and range operators can anticipate new instrumentation requirements.

Developmental and acquisition programs require test data that support the understanding of E-O sensor or high-energy laser (HEL) operation in atmospheric conditions worldwide. As the popularity of E-O sensor-based weapons spreads, the United States' forces must increasingly be able to anticipate threat force capability as a function of atmospheric conditions. The recommended methods of data measurement and analysis in these guidelines are basic tools for ensuring the production of reliable data for predicting and interpreting worldwide E-O sensor performance.

The difficulty in supporting E-O sensor T&E with reliable atmospheric measurements is illustrated in [Figure 1-1](#).

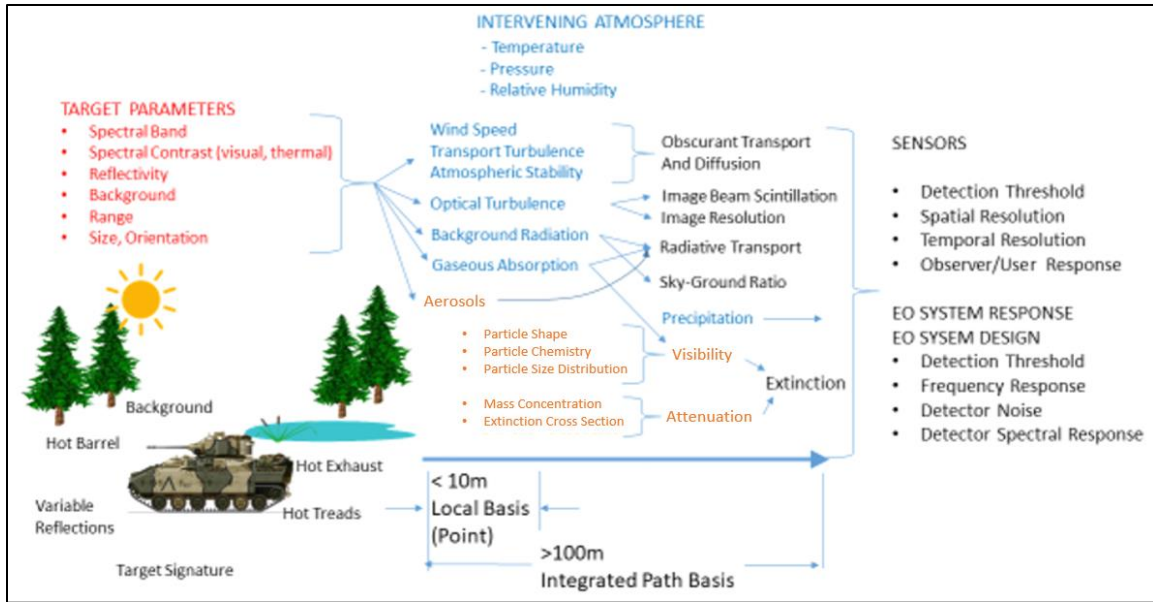


Figure 1-1. Targets-Atmospheres-Sensors Synopsis

[Figure 1-1](#) shows the Targets-Atmospheres-Sensors Synopsis (TASS) that must be recognized to effectively evaluate E-O sensor performance in the atmosphere. The propagation effects of the atmosphere on the shorter wavelengths of the electromagnetic spectrum act as a filter that modifies background and target signature information reaching the E-O sensor system. The target signature depends on background spectral band and texture (defined by the sensor under test), spectral contrast, reflectivity, range, size, and orientation. The atmosphere filters the target spectral image through a dynamic lens that fluctuates in time and transmittance. The refractivity dynamics and attenuation of the atmosphere will impact the performance envelope of the sensor or weapon design and response. Modeling, interpreting, and, in some cases, measuring atmospheric characteristics begin on a localized basis involving distances typically less than 10 meters and extends to the integrated path basis (distances involving hundreds to thousands of meters between the sensor system and the target) by operationally simulating localized basis results. For example, integrated path attenuation results from the summation of highly variable (in space, time, and magnitude) localized aerosol and gas concentrations along the transmission path, which may be horizontal or a slant path. Proper characterization of the atmosphere for sensor evaluation requires effective spatial representation of the localized basis with sampling rates that satisfy the Nyquist criteria that requires data be sampled at a rate at least twice as high as the highest frequency of the measured variable. In numerous cases, the Nyquist sampling rate is too slow because the mean of the measurement is not constant during the sample averaging duration. Therefore, atmospheric testing and characterization in both a localized and an integrated path basis are key elements in specifying sensor performance. Furthermore, the data acquired in either basis must be accurate to a tolerance that depends on the sensor and its applications.

The need to accurately measure the atmosphere on the first attempt in which a sensor is tested calls for focused and intensive data management, from identifying the need to test through to making the data accessible to the sensor development and T&E community. The TQDM is a method and philosophy for achieving intensive data management, and it forms the guiding principle for the recommended guidelines.

The TQDM method provides the opportunity for ensuring significant improvements in cost-effective E-O sensor system testing in the atmosphere. Applying TQDM methods and standards to all aspects of E-O sensor system testing in the atmosphere reduces confusion and errors about sensor operational capability. Sensor development progress is measurably enhanced because the reliable historical data and information bases produced through TQDM serve as points of reference for new systems and are accessible to users. The TQDM methods and standards offer a framework from which data quality assurance can be managed, and information generated by all sources of data is made more accessible to all qualified users. Quality data assurance reduces uncertainties and confusion in all aspects of sensor-based weapons development; thus, resources will be spent more effectively. Through TQDM T&E, cost effectiveness increases for at least four major reasons:

- resources are more effectively used;
- quantitative standards measure real progress;
- sensor logistics support requirements are made clear; and
- weapons capabilities are quantified with known measures of uncertainty.

The guidelines begin with a discussion in Section [2.1](#) of the approach and concept of TQDM, including description of identifying and quantifying qualified data. The section also outlines information base development for a number of data application areas. Section [2.2](#) presents examples of test data requirements for visual image sensor tests, infrared image sensor tests, multispectral LRF tests, MMW sensor tests, the SWOE program tests, and the Smoke Week Test Program. The requirements are ranked in terms of importance and a nominally required measurement accuracy to provide an overview of the atmospheric measurement requirements for E-O sensor evaluation.

Section [2.3](#) discusses recommended methods for acquiring data for visual range, winds, absorbing gases, aerosols, precipitation, terrain signatures, humidity/temperature and refractive structure, background radiation, spectral transmittance, and surface and aloft meteorological situations. Next, Section [2.4](#) describes a process for determining and specifying measurement errors. The process includes requirements to specify RMS errors, a discussion of the impact of measurement error on sensor evaluation, and the importance of temporal and spatial averaging intervals. Section [2.5](#) discusses recommended approaches for making measured data accessible through archival databases and easily accessible information bases. The section also describes data archival formats and storage, information base generation and storage, methods of identifying and reporting data gaps, and methods of identifying and tracking future test requirements. The guidelines conclude with [Appendix A](#) through [Appendix G](#). [Appendix A](#) is a set of tables that summarize atmospheric environmental parameter requirements needed to support E-O systems testing for visual and infrared imager evaluation, LRFs, and typical ongoing DoD test programs. [Appendix B](#) through [Appendix D](#) show examples of the impact of parametric uncertainties on the probability of detection for visual and infrared imaging systems and for 1.06 μm and 10.6 μm LRFs. This illustrates the effect of measurement errors on data applications. [Appendix E](#) depicts the impact of parametric uncertainty in predicting the 1.06 μm and 10.6 μm LRF power on a designated target. [Appendix F](#) demonstrates the relative uncertainty in predicted 8 - 12 μm transmittance caused by parametric uncertainty in air temperature, relative humidity, and visual range. [Appendix G](#) illustrates the uncertainty in MMW extinction as a function of ice and liquid water precipitation temperatures.

This page intentionally left blank.

CHAPTER 2

Measurement Guidelines

This chapter provides guidelines for the methods of approach, techniques of measurement, and methods for making data accessible when performing atmospheric tests to evaluate E-O sensor performance.

2.1 Total Quality Data Management

[Figure 2-1](#) shows the data management approach now used for acquiring data in an E-O sensor atmospheric test. Data objectives are formulated as the result of perceived user needs or to provide the opportunity for T&E in a characterized environment. Experiments are designed that satisfy the data objectives and take advantage of lessons learned as the result of data analysis from past experiments. The data are acquired and archived. After archival, a minimal effort (relative to that expended acquiring the data) is performed in data evaluation on a few selected data sets. The archived data, whether qualified or not, are made available to users for atmospheric characterization, model validation (also considered evaluation), sensor design or capability specification, and military applications particularly as the data apply to operations involving weapons systems using E-O sensors. The data may also provide a point of reference for defining future experiments.

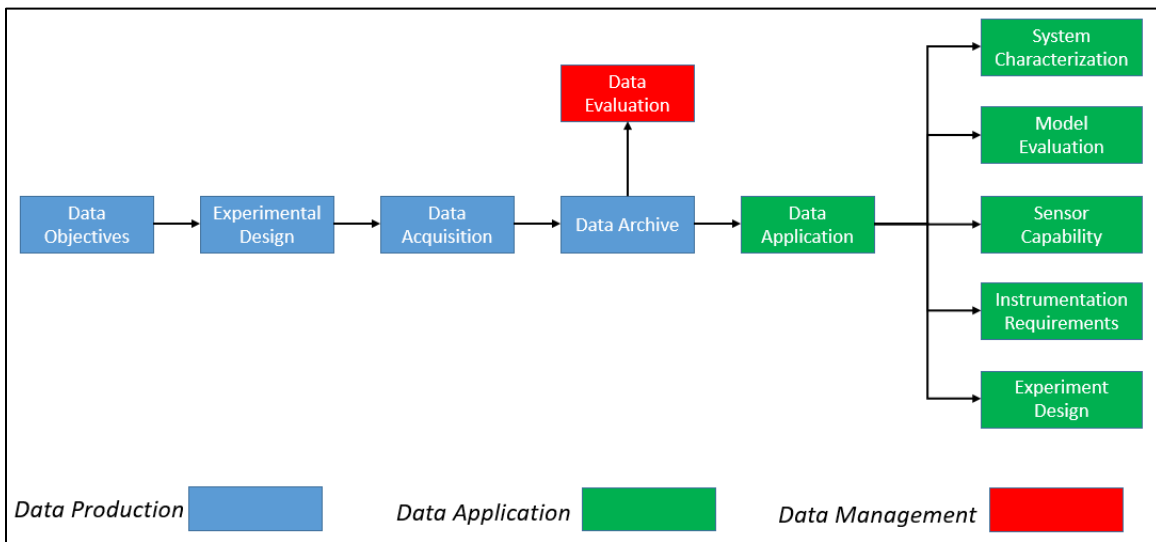


Figure 2-1. Data Management Approach Now Used for Acquiring Data in an Electro-Optical Sensor Atmospheric Test

The data generated in atmospheric E-O sensor tests and experiments are voluminous. Even after they are archived, they may still be practically inaccessible. The user, with a few notable exceptions, has neither the interest, training, time, or funds to manipulate large quantities of data to extract the information needed. It is often perceived as easier to do an additional specialized test or experiment than to work with the existing database. Consequently, improving the cost effectiveness of test data, providing ready access to the database, and developing

methods for generating relevant information from the data are as important as the original data production.

Study of the process illustrated by [Figure 2-1](#) shows that each major block in the data production and use process has an impact on the blocks preceding it. In fact, the process being addressed is a data cycle, as seen in [Figure 2-2](#), rather than as [Figure 2-1](#) presents, a linear data path. The data cycle exists because past test results and experience affect how future tests are conducted and affect the development of future models and understanding of atmospheric impacts on future sensor performance. Significant improvements in atmospheric data quality and reduction of expected problems in data applications require recognition of, and improvement in, all phases of this data cycle.

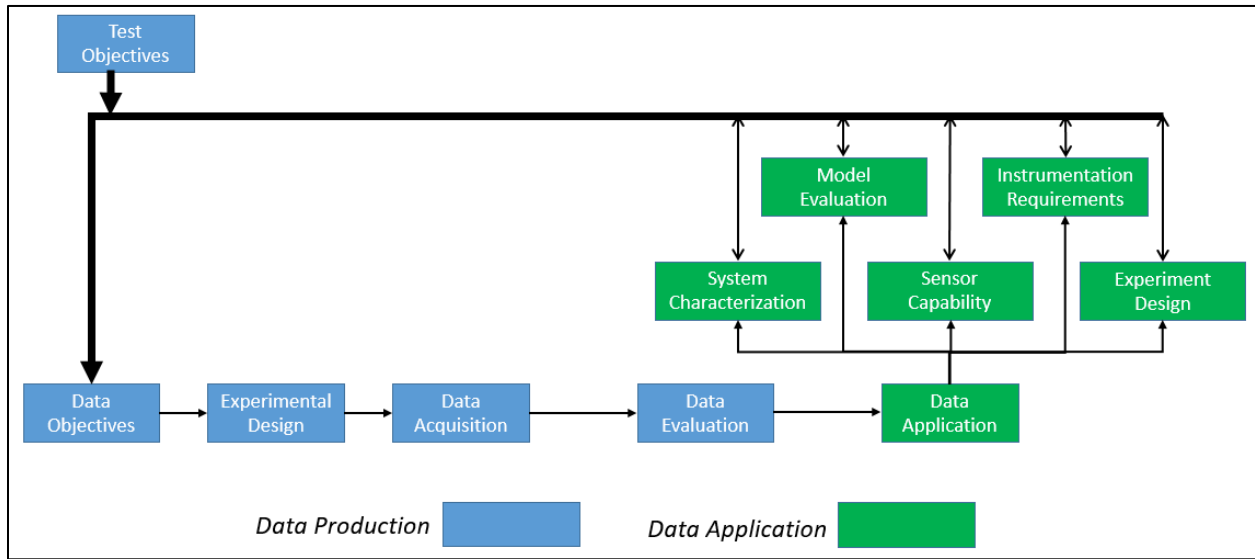


Figure 2-2. The Data Cycle with No Total Quality Data Management Operations

[Figure 2-2](#) through [Figure 2-6](#) illustrate TQDM. Comparison of [Figure 2-1](#) and [Figure 2-2](#) shows that TQDM improves or enhances all aspects of the current data path.

[Figure 2-3](#) shows that in the TQDM approach, data objectives are: produced by users who either have used information bases representing data applications and costs/benefits analysis to determine test requirements; or are generated because of new requirements input, data objectives are generated independently of the existing information base. When data objectives are defined on the basis of past test experience, the data applications information bases are used to develop required measurement standards. These standards define the minimum accuracy requirements and capabilities needed to acquire data satisfying new data objectives. Definition of measurement standards required by TQDM is driven by information base and contributes to the definition of data objectives.

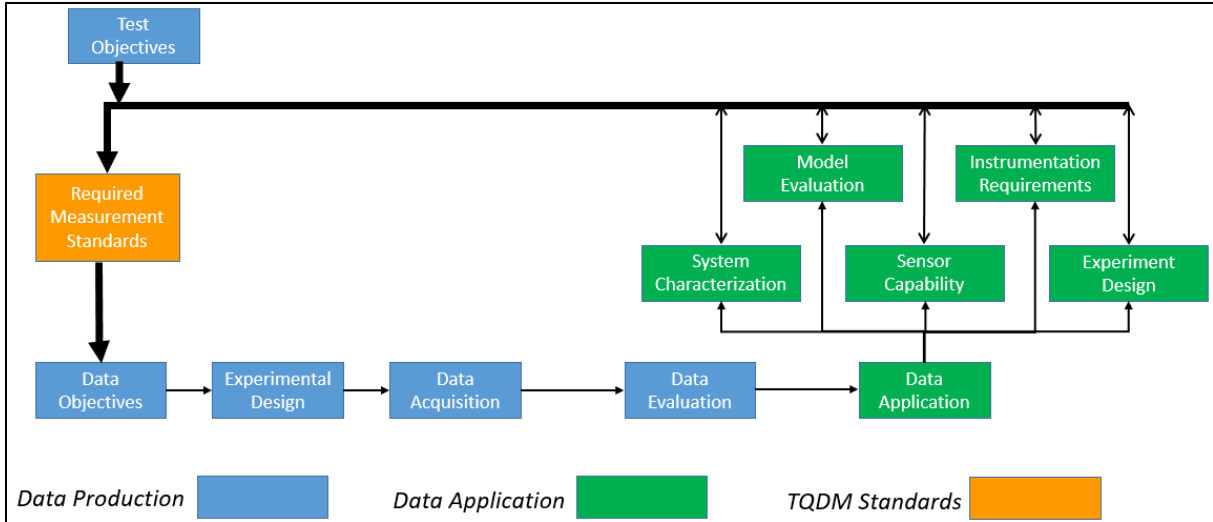


Figure 2-3. TQDM-required Measurement Standards

As in the existing data path approach (Figure 2-1), the data objectives are used to develop the experimental design. However, as noted in Figure 2-4, the TQDM approach experimental design is driven by instrument calibration requirements and built-in methods of measurement cross-checks. These factors are parametric data quality foundations. Figure 2-5 demonstrates that these factors form the basis for on-line checks as the data are acquired. Data acquisition under TQDM requires online data checks to identify extraordinary or potentially problematic data and methods of comparing data with expectations and quality-assuring supporting data. During data acquisition, the results are compared with experiment expectations that are based on the historical data and models residing in the information bases. These data checks quickly identify any unexpected measurement errors or new results. These results provide the stimulus to repeat or to obtain additional comprehensive data during the test. Thus, repeated measurements can eliminate data artifacts or reinforce unexpected results. Supporting data also are tested as they are acquired and are viewed as necessary caveats of the primary data.

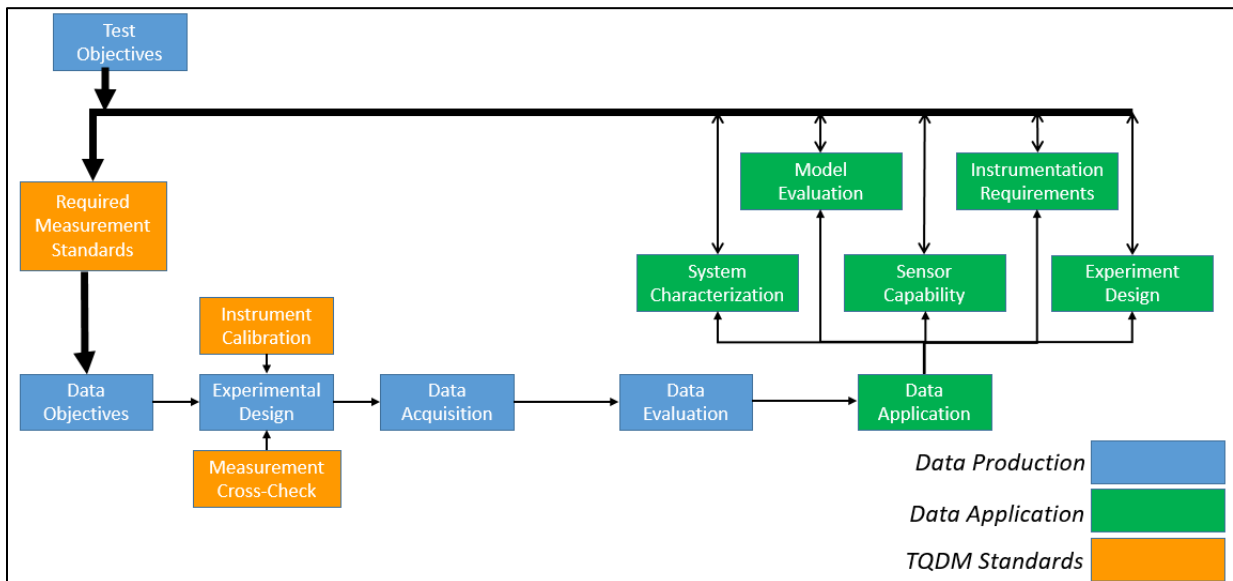


Figure 2-4. TQDM Experimental Design

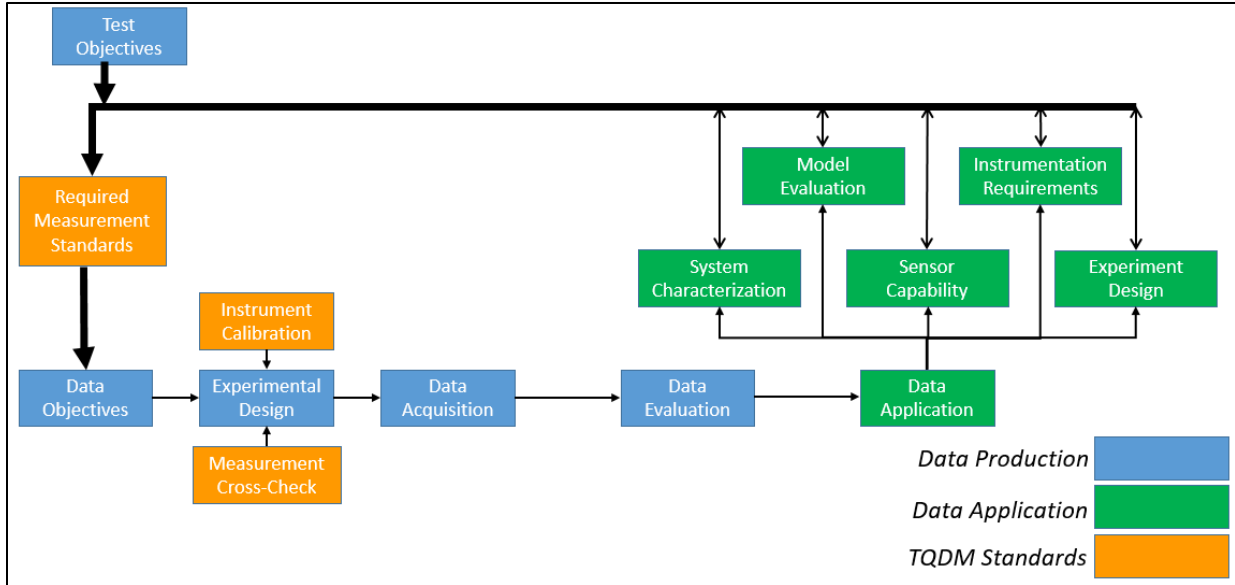


Figure 2-5. TQDM Data Acquisition

After data acquisition is complete, [Figure 2-6](#) illustrates that detailed evaluation begins in order to qualify the data. The data are specified as to application in particular information bases. A relative quality level for the data (for example, when only baseline data or data with high uncertainties are available) is assigned. The data evaluation qualifies the data for a measurement error range. Evaluation is achieved by identifying likely errors and error sources, testing for consistent results between independent measurements (planned measurement cross-checks), and comparing new data with historical data.

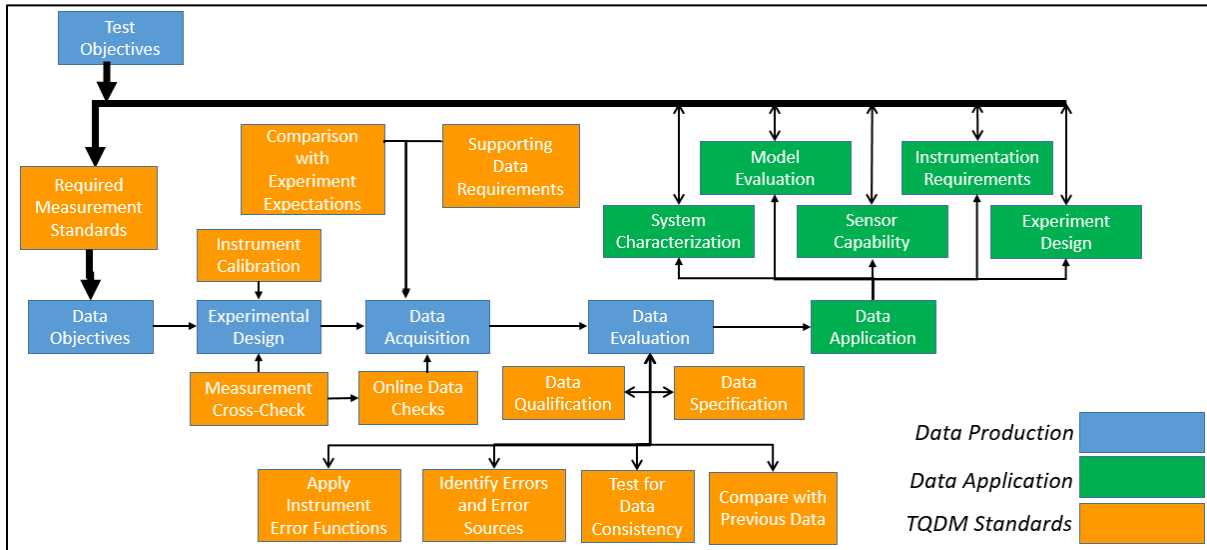


Figure 2-6. TQDM Data Evaluation

After data evaluation, the data are archived in formats that permit the qualification and specification of the data. The data are then available for data applications; these applications are also used to generate information bases. The information bases provide inputs to future data objectives and provide points of reference and information for cost/benefit analyses. Such

analyses aid planners in decisions affecting the development of new sensor or weapons systems that produce new data objectives. And the cycle begins again.

[Figure 2-7](#) illustrates the information base concept. Information bases use database structures and formats to store and make accessible the results generated using archived data produced during a sensor test. Data application results (for example, model predictions of sensor performance compared with actual measured performance) are organized and summarized in the information base. In this manner, the user does not have to deal with large quantities of data to find the information of interest. Information bases provide a key element, information access, in the data cycle. They include an evaluation system that provides methods of cost/benefit analysis, which is used to test and place in perspective the value or cost of developing new sensors or information.

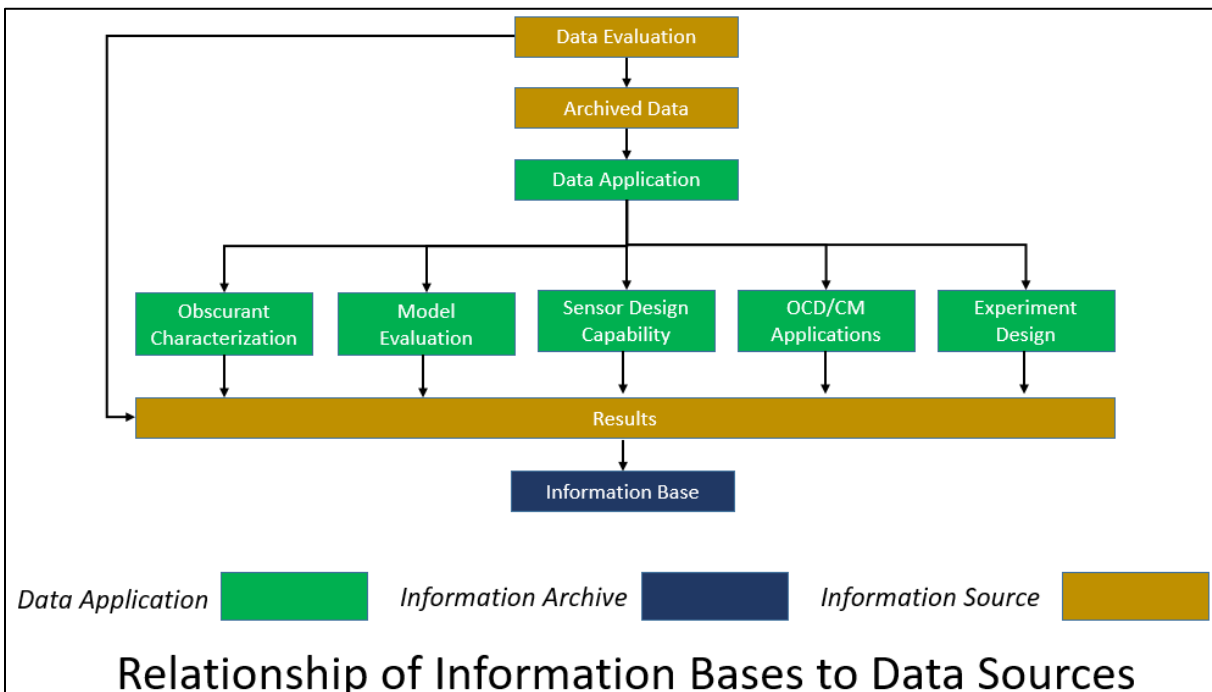


Figure 2-7. The Information Base Concept

Successful qualification of the data classes and development of atmospheric characterization information require a clear understanding of the TASS shown in [Figure 1-1](#). The TASS relationship reveals:

- atmospheres have spectral electromagnetic wave propagation and emission characteristics that depend on particular boundary conditions such as location, time of year, and synoptic meteorology;
- targets have spectrally emissive or reflective electromagnetic signatures;
- target backgrounds have spectral reflection, emission, and clutter characteristics that define target spectral contrast that meteorology directly affects through precipitation, temperature, radiation loading, and wind/evaporation drying and cooling; and

- the operating characteristics of electromagnetic wave sensors are sensitive to these factors.

All of the TASS parameters must be considered in evaluating E-O sensor performance in the atmosphere.

Databases providing data for evaluating and developing models and simulations of E-O sensor performance must present information on all aspects of the TASS parameters. As a result, TASS will be used as a general term throughout this report for TASS-related data and databases. The TASS data can be classed into four groups: atmospheric optical and meteorological data; aerosol obscuration characteristics data; target and background signature data; and sensor characteristics data.

The data groups can be related through mathematical models. Measurements for a particular data group are affected by parameters in the other groups. The analyst must be aware of this fact to separate data artifacts from reliable data and to identify and explain anomalous performance. To understand atmospheric effects on TASS linkages, measured data can be grouped into that obtained over integrated path basis scales or localized basis scales. The TASS linkages occur because the integrated path basis effects on electromagnetic wave propagation can be predicted through summations, averages, and correlation of localized basis values. Prediction of integrated path basis values from localized basis values is one method of testing mathematical models and experimental data. Integrated path basis data include multispectral transmittance, radiometric data from obscuration or targets, refractive or humidity scintillation effects, and line-of-sight crosswind distributions. Localized basis data include aerosol particle size distributions, mass extinction coefficients, and temperature and humidity turbulence characteristics.

2.1.1 TQDM Identification and Quantification of Data

This section discusses brief examples of methods for identifying and quantifying qualified data. There is a detailed discussion in RCC 382-21¹ of data quality control methods applicable to many measurements associated with testing E-O sensors in the atmosphere and supplements methods. The suggested methods in these guidelines are not new; however, their application to atmospheric measurement instruments for E-O sensor testing in the atmosphere is not routinely performed. Several side benefits are expected from the development and application of these methods. These benefits are listed below.

- Standardized methods are used to ensure qualified data. These methods can be used on existing data and in the acquisition of future data.
- Instrumentation error functions for data qualification are applied to instruments now in use. These functions allow data producers to report their data acquired with proper error bar representations.
- The degree to which various measurement methods should agree is quantified.
- Data qualification methods provide proper choices of instrument ensembles for experiments to test mathematical models with required levels of measurement accuracy.

¹ Range Commanders Council. *A Guide for Quality Control of Surface Meteorological Data*. RCC 382-21. January 2021. May be superseded by update. Retrieved 10 June 2022. Available at <https://www.trmc.osd.mil/wiki/x/DIy8Bg>.

- Levels of model and sensor simulation performance are independently established. The establishment of model and sensor simulation performance provides a baseline against which the performance of future models, simulations, and tactical decision aids can be established.

2.1.2 Developing Qualified Data

Atmospheric effects on E-O sensor performance data often are not specified with error bars. A major reason for this limitation is that instrument response functions have not been developed to produce an estimate of instrument measurement uncertainty as a function of response. By developing and applying these functions, minimum levels of uncertainty are specified for the data, and maximum accuracy values are established. Only those data within an acceptable level of uncertainty are included in a qualified data ensemble.

Data error function evaluation gives only maximum uncertainty levels for random errors. As a result, it is necessary to establish additional tests for the data to detect systematic errors and anomalous behavior. An example of these types of tests is the optical depth regression analysis using multispectral transmission data. At least three major tests for internal consistency and accuracy can be applied to transmission data using this approach.

- First, the data are tested for acceptable noise and minimum acceptable transmission levels.
- Second, broad-band data are tested against narrow-band data within the broad band (for example, determine if 90- to 95-GHz transmission is consistent with 92.5 GHz transmission).
- Third, the data are tested to determine if the Beer-Bouguer transmission law should include band averaging or multiple scatter effects. These tests can be performed through regression analysis of the logarithmic transmittances (optical depths) for any pair of spectral band transmittances along a common line of sight.²

A useful method of identifying questionable data is to compare estimates of the same parameter using independent measurements. Farmer has discussed this method in detail for a variety of aerosol measuring instruments (Farmer et al.). By computing the same parameter with data obtained by independent methods (termed “intercomparison”), data consistency is tested; data that are inconsistent can be flagged for detailed analysis and review. Results of the analysis may even call for additional experiments to determine the sources of the differences between the two data sets. It is often possible to examine integrated path basis (localized basis) data for theoretical integrated path basis (localized basis) predictions to ensure the data are consistent. In those cases where strong and consistent disagreements exist between theory and experiment, the assumptions used to develop the theory or data must be reexamined and closely reviewed.

When possible, field measurement data should be compared with laboratory data. Laboratory data typically yield reasonable parametric values for comparison with data computed using field measurements, and it is especially true when field data are obtained under stable atmospheric conditions. When large consistent differences in the data sets are found, a

² Farmer, W. M, L. Rust, M. DeAntonio, and R. Davis. “Integrated Transmissometer Modeling System (ITEMS).” In *Proceedings of the Smoke/Obscurants Symposium XII*. pp. 385-397. Aberdeen Proving Ground, 1988.

determination should be made of why the data disagree. For example, suppose the field data are reasonable and reproducible under a variety of test conditions but disagree with laboratory data. Neither data set is considered incorrect; however, a careful examination of the differences in the measurement protocols is necessary to ensure operational errors are not made. Standardized protocols, for example, for the measurement of obscurants in laboratory and field environments have evolved from such efforts.

Data that can be verified as to accuracy and relative error by the methods outlined earlier are maintained separately from data that cannot be verified but should not be thrown away. Unverified data should be categorized carefully, noting the reasons they were not evaluated for an accuracy estimate. They can be used to help identify potentially erroneous data by comparing it to the data that have been characterized as being erroneous. An explanation of the error sources should be added. The quality of data obtained in field experiments is improved steadily in this way.

A standardized data set is a natural result of the data qualification process. These data sets are used to test mathematical models and to provide descriptions of standard sensor performance. Standardized data sets are generated by forming statistical distributions of data parameters for a broad range of qualified data. The choice of parameters with which to group data may be largely arbitrary; nevertheless, after an acceptable parametric division of data is developed, statistical functions are generated to represent the individual field or laboratory experiments producing qualified data. Individual data distributions are added to produce a master distribution for the parametric set of interest. Standard deviations and mean values are computed for the data increments used in the master distribution. The master distributions include both accumulative probabilities and probability densities. This approach to the generation of standardized data sets has these advantages:

- all data that are considered consistent and reliable are used;
- data from different instruments for the same tests are grouped;
- areas where data are scarce, and where additional experiments need to be conducted, are identified;
- the range of data variance (through the generation of mean and standard deviation values for each data increment) is quantified and the statistical stability of the data is ensured; and
- personal biases of model and simulation developers in choosing and using data for model/simulation evaluation are removed.

2.1.3 Development of Information Bases

A clear perspective is needed of how a database, once measured and used for its initially intended purpose, can be used in other applications. A proper perspective for the long-term use of data developed under this and other efforts relevant to atmospheric testing of E-O sensors is the development of reference and information bases derived from archival databases. The need of many potential data users is not for data but for information derived from data. The E-O system designer cares little about the sensor line-of-sight transmission history during a field trial. For example, data important to the designer is the length of time the sensor spectral band atmospheric transmission is below the system operational threshold. There is interest in the

probability that a transmission threshold level will exist for a given set of atmospheric conditions. Model developers require standardized data sets and standardized evaluation methods for testing models. Data producers need ready reference to instrumentation error functions that can be used with their instruments. Operations analysts need ready reference to realistic performance of various E-O sensor systems in a broad range of atmospheric environments.

This section discusses several of the more important information bases that can be generated from E-O sensor system atmospheric measurement databases. The list is not exhaustive. It illustrates the types of information that will be immediately useful.

2.1.3.1 Instrumentation Error Functions

Error functions for E-O sensor system atmospheric test instrumentation form a highly useful information base. Making commonly used error functions available in an information base allows data producers to report data with error bars as the data are produced; to reduce post-test analysis time; and to provide a common data evaluation protocol for a variety of instrumentation operations. Error functions also show which operational parameters of the measurement instrument give the greatest errors. This information provides the instrument operator with guidance in identifying important error sources when data are taken. In some cases, E-O system designers can use this information to improve system response. The range of measured data applicable to mathematical model validation is clear using these functions.

2.1.3.2 Standardized Methods of Data Qualification

Development of data qualification methods provides a standard for the quality of all acquired data in E-O sensor system atmospheric testing. Such methods can be made available through an information base. Standardized data qualification methods provide field test support customers with the ability to set standards for acceptable data, and to understand data accuracy limitations. These standards can form the basis for research and development programs using qualified data for analysis, system evaluation, and model and simulation development.

2.1.3.3 Standardized Data Sets from Statistical Summaries of Qualified Data

Quantitative and qualitative standardized data set information bases are described in the following subparagraphs.

2.1.3.3.1 *Quantitative Data*

Quantitative data is defined as the value of data in the form of counts or numbers where each data set has a unique numerical value associated with it. Statistical summaries of existing data can also be generated and located in an information base to provide a standardized set of quantitative reference data. To achieve this goal, test data first are grouped into statistical summaries using qualified data. The data are sorted according to meteorological conditions and E-O sensor type evaluated during the test. Then, for example, data for a particular type of measurement are grouped to form a probability density function. The density function is interpreted as the probability that a particular value or range of values will exist for a particular set of test conditions. (Trial-to-trial and test-to-test variances will be smoothed and properly averaged in this way.)

Statistical data summaries located in an information base are viewed as the most reliable set of data available. In addition to the data probability distribution functions, analytical functions determined by curve fitting the data can be developed and included as well. Thus,

simple numeric measures (for example, moments of the distributions) can be used to characterize the data. These data will provide direct comparisons of parametric changes in E-O sensor performance for various test conditions.

2.1.3.3.2 *Qualitative Data*

Qualitative data is defined as the data that approximates and characterizes. Qualitative data can be observed and recorded. This data type is non-numerical in nature. Usually, qualitative data consists of human observer responses to targets viewed directly with the eye or with some type of imaging system, but can be relative values of conditions. Multispectral imaging systems include ultraviolet (355 nm), visual (0.4-0.7 μm), near infrared (0.7-1.1 μm), mid infrared (3-5 μm), and far infrared (8-14 μm) types. Additionally, MMW sensors (for example, systems that employ synthetic-aperture radar or side-looking radar systems) that require user interpretation are under development. While MMW imaging systems are not common, they will be a major development item in the next few years. Information bases for observer/user response data are as valuable as the responses from hardware-based sensor systems. Human responses to imager outputs are basic factors that help define sensor performance in the atmosphere. Statistical summaries of human responses to targets imaged through the atmosphere should be included in an information base. With these data, correlations are determined between quantitative atmospheric data and human responses to observed targets.

Recent use of lidar backscatter measurements have been accepted as qualitative data, in that there are no reference measurements to anchor the intensity graphics with absolute values. However, as a qualitative measurement of aerosol extinction, this measurement highly corroborates with other measures of visibility and extinction.

2.1.3.4 Model Performance for Standardized Data Sets

Many E-O sensor atmospheric performance models now exist. The E-O sensor system developers and others who rely on these models must have a clear understanding of their predictive strengths and weaknesses. Information bases that record the results of model predictions for the standardized data sets described in Subsection [2.1.3.3](#) contribute to total database dissemination. Comparison methods for quantifying model performance also are established and located in the information base. These procedures develop standards against which future models are tested and provide a standard basis for model performance improvement.

2.1.3.5 Electro-Optical System Performance Relative to Atmospheric Characteristics

This section considers examples of information bases needed to characterize E-O system performance relative to atmospheric characteristics.

2.1.3.5.1 *Electro-Optical Sensor System Target Signatures*

Effectiveness of E-O sensor systems depends on the target-background spectral contrast and angular subtense of the target to the sensor. Consequently, an information base of target-background spectral signatures assists in evaluating atmospheric impacts on E-O sensor systems. These data should represent targets such as armored fighting vehicles, airplanes, ships, and buildings for a wide range of atmospheric conditions and target/background clutter signatures.

2.1.3.5.2 Electro-Optical Sensor System Target Acquisition Envelopes

Developers of E-O sensor systems must define the conditions under which a sensor can acquire a target in atmospheres with and without aerosol counter-measures or severe aerosol backgrounds, such as low visibility hazes. Although target acquisition models are now somewhat limited, comprehensive TASS information bases help to define target acquisition envelopes. These envelopes form an effective information base that can serve a variety of purposes (such as definition of data that are lacking) to confirm the system performance envelope; comparison of different system performances under a variety of atmospheric conditions; and provision of information for the development of tactical decision aids and other models.

2.1.3.5.3 Normalized Electro-Optical Sensor Response Functions

One of the major sources of disagreement between data from the same types of electro-optical systems is that systems operating in the same band can have significantly different spectral responses. As an illustration, transmissometer measurements for the same atmospheric optical depth from two systems operating in the same spectral band, but with different spectral responses, can produce different values if the atmosphere has a significant spectral extinction structure over the spectral band. To interpret spectrally dependent data, E-O sensor spectral response data must be available. [Figure 2-8](#) illustrates the variability of optical depth at different wavelengths, driving the common practice to measure aerosol optical depth at three or more wavelengths.³ The figure shows spectral variation of the mean aerosol optical depth (AOD, τ_a) at six wavelengths, λ , from 340–870 nm in the Athens atmosphere. The linear and second order polynomial fits of $\ln \tau_a$ versus $\ln \lambda$ to the measurements are also shown.

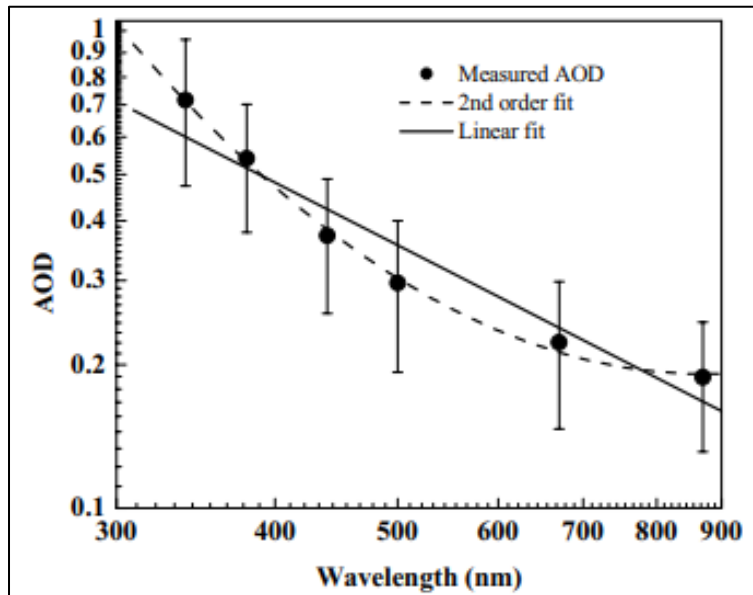


Figure 2-8. Wavelength Dependence of Aerosol Optical Depth

Another example of data in disagreement worth mentioning can be found amongst pyranometers. Class A, B, and C, ranked from best to worst performing, each can produce

³ Kaskaoutis, D.G. and H.D. Kambezidis. “Investigation into the wavelength dependence of the aerosol optical depth in the Athens area.” October 2006. In *Quarterly Journal of the Royal Meteorological Society*, V. 132 Issue 620: pp. 2217-2234.

drastically different data, as noted in [Figure 2-9](#). From Class C to Class B and from Class B to Class A, the achievable accuracy improves by a factor of 2.

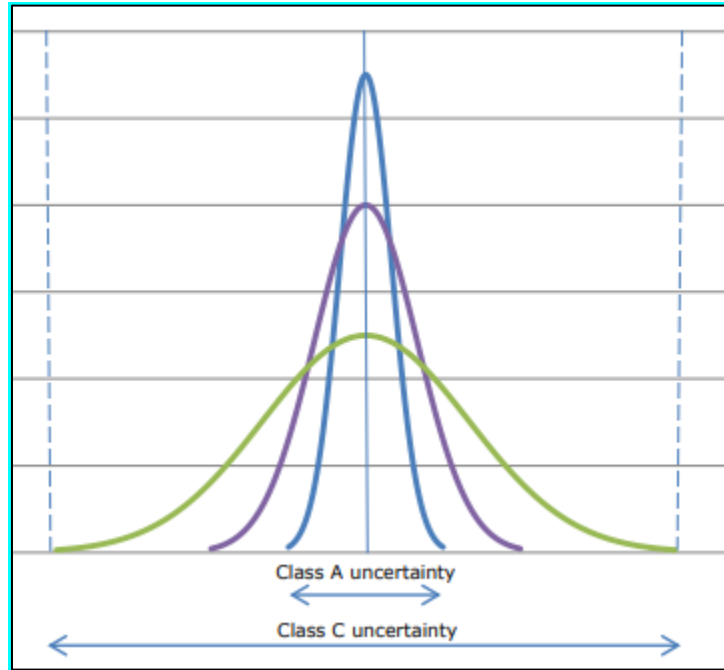


Figure 2-9. A Visual Impression of Measurement Uncertainty for Well-Maintained Instruments of Different 2018 Pyranometer Classes

Applications of E-O sensor response functions range from the tactical evaluation of systems to the evaluation of how a sensor responds to a particular environment with mathematical models. These data include both system and detector spectral response data for weapons systems and for instrumentation systems such as transmissometers and pyranometers.

2.2 Test Data Requirements

Testing E-O sensor systems in the atmosphere is driven by three basic information requirements: determining reasons for variations in observed system performance; how the system will perform under environmental conditions other than those of test conditions; and how the system will perform after it is deployed. The first information requirement is needed in case the sensor should fail to perform as anticipated, and an explanation is required for the cause of failure. The second information requirement originates because E-O sensor systems operate under a wide variety of test conditions not included in the tests. The third requirement arises because deployment is the ultimate purpose of a development program. Atmospheric tests are calibration points and validation checks for defining sensor system performance under near-realistic operating conditions. Before deployment, a sensor cannot possibly be tested under every operational condition for which it was intended. Accordingly, test results also provide an experimental measure of the capability of mathematical models to predict sensor performance under the full operational envelope of environmental conditions. If the model predictions are within acceptable error limits, it is assumed that the model contains a reasonable representation of how the sensor will perform under conditions that were not tested.

It is important for test operations to quantify atmospheric measurement errors as well as system performance. Measurement uncertainty is as important as the mean value of the measurement. Definition of measurement uncertainty ensures that models used to predict sensor performance have inputs that can specify the uncertainty in sensor performance under all intended environmental conditions and deployment scenarios for which it was intended. This section provides examples of E-O sensors tested in the atmosphere. Also presented are examples of measurement requirements for models likely to be used for predicting sensor performance in environments other than the test conditions or for deployment scenarios.

Examples of E-O sensor test applications requiring atmospheric data are (1) visual sensor target detection; (2) infrared sensor target detection; (3) LRF ranging, laser weapon effectiveness, or lidar atmospheric profiling for 0.355, 0.991, 1.06, 1.54, and 10.6 μm wavelengths; (4) MMW sensor transmission; (5) the tri-Service SWOE measurement program; (6) the U.S. Army Research Laboratory Smoke Week test program; (7) littoral warfare testing; and (8) maritime system testing. The first four applications are for specific broad- and narrow-band sensor types. The final four applications are for ongoing programs that acquire data for supporting a variety of broad- and narrow-band sensors, the seventh application is for unique test requirements at the land and sea interface, and the eighth example is open-ocean applications of the U.S. Navy.

[Table 2-1](#) provides a list of variables recommended for measurement to support examples of the above sensor types and for applications and measurements likely to be required for ongoing programs. When a parameter is used directly in the evaluation of a particular application or measurement, an x appears in the table. The applications include: (1) visual probability of detection (VISUAL PD); (2) infrared broad-band transmission (IR BRDBND TRANS); (3) infrared narrow-band transmission (IR NARROW BND TRANS); (4) infrared imager probability of detection (IR IMAGER PD); (5) visual or infrared precipitation transmission (VISUAL/IR PRECIP TRANS); (6) MMW precipitation transmission (MMW PRECIP TRANS); (7) MMW transmission (MMW TRAN); (8) LRF probability of detection (LRF PD); (9) counter-measure aerosol transport and diffusion (CM TRNSPRT AND DIFF); and (10) ultraviolet transmission (UV TRANS).

Table 2-1. Summary Atmospheric Environmental Parameters in Support of Electro-Optical Systems Testing		VISUAL PD	IR BRDBND TRANS	IR NARROW BND TRANS	IR IMAGER PD	VISUAL/IR PRECIP TRANS	MMW PRECIP TRANS	MMW TRAN	LRF PD	CM TRNSPRT AND DIFF	UV TRAN
PARAMETER											
1	Solar zenith angle	X			X					X	
2	Solar azimuth angle	X			X					X	
3	2% Contrast Visual Range	X	X	X	X	X	X	X	X	X	X

Table 2-1. Summary Atmospheric Environmental Parameters in Support of Electro-Optical Systems Testing		VISUAL PD	IR BRDBND TRANS	IR NARROW BND TRANS	IR IMAGER PD	VISUAL/IR PRECIP TRANS	MMW PRECIP TRANS	MMW TRANS	LRF PD	CM TRNSPRT AND DIFF	UV TRAN
PARAMETER											
4	Present weather	X	X	X	X	X	X	X	X	X	X
5	Cloud-free line-of-sight	X	X	X	X	X	X	X	X		X
6	Number of cloud layers	X	X	X	X	X	X	X	X		X
7	Cloud type for each layer	X	X	X	X	X	X	X	X		X
8	Cloud coverage for each layer	X	X	X	X	X	X	X	X		X
9	Base altitude of each cloud layer	X	X	X	X	X	X	X	X		X
10	Wind speed at surface				X		X	X		X	
11	Wind direction at surface				X		X	X		X	
12	Pasquill stability category				X					X	
13	Absorbing gases (other than H2O)		X	X	X		X	X			
14	Aerosol/particle index of refraction	X	X	X	X		X	X	X		X
15	Aerosol/particle size distribution	X	X	X	X	X	X	X	X	X	X
16	Aerosol/particle shape	X	X	X	X	X	X	X	X	X	X
17	Precipitation type indicator	X	X	X	X	X	X	X	X		X
18	Precipitation rate	X	X	X	X	X	X	X	X		X
19	Precipitation temperature						X	X			
20	Dew/Frost	X	X	X	X						
21	Target/background emissivity		X	X	X						
22	Relative Humidity Structure Const.						X	X			
23	State of surface	X	X	X	X					X	
24	Sea state	X	X	X	X					X	
25	Global solar radiation	X			X						
26	Diffuse sky radiation	X			X						
27	Directional sky radiation	X			X						
28	Sky-to-ground luminance ratio	X									
29	Downwelling spectral direct radiance	X			X					X	
30	Downwelling spectral diffuse irradiance	X			X					X	
31	Directional spectral sky radiance	X			X					X	
32	Spectral path transmittance	X	X	X	X	X	X	X	X		X
33	Index of refraction structure const.	X	X	X	X	X			X		X
34	Number of atmospheric layers	X	X	X	X	X	X	X	X	X	X
35	Base altitude for each atmospheric layer	X	X	X	X	X	X	X	X	X	X
36	Visibility for each atmospheric layer	X	X	X	X	X	X	X	X		X

Table 2-1. Summary Atmospheric Environmental Parameters in Support of Electro-Optical Systems Testing											
PARAMETER		VISUAL PD	IR BRDBND TRANS	IR NARROW BND TRANS	IR IMAGER PD	VISUAL/IR PRECIP TRANS	MMW PRECIP TRANS	MMW TRANS	LRF PD	CM TRNSPRT AND DIFF	UV TRAN
37	Relative humidity for each atmospheric layer		X	X	X	X	X	X	X	X	X
38	Air temperature for each atmospheric layer		X	X	X	X	X	X	X	X	X
39	Dew point temperature for each atmospheric layer		X	X	X	X	X	X	X	X	X
40	Atmospheric pressure for each atmospheric layer		X	X	X	X	X	X	X	X	X
41	Air-sea temperature difference			X					X		
42	Path-Averaged Cn2			X					X		
43	Path-Resolved Cn2			X					X		
44	Path Transmissivity			X					X		

[Table 2-1](#) lists 44 parameters, organized by blocks of related variables that are separated by a heavy line. The following discussion indicates how the parameters are used in evaluating E-O sensor performance. Path luminance is a major contributing factor to visual target contrast reduction. Parameters 1 and 2 define the position of the Sun and are used to locate the position of the brightest and most direct contributor of radiation to path illumination, target illumination, and sensor threshold sensitivity. Parameters 3-9 are used to show the directional contrast and transmittance state of the atmosphere at ground level and for slant ranges. Parameters 10-12 assist in ascertaining atmospheric transport and diffusion of atmospheric aerosols, particularly those aerosols used as passive countermeasures against E-O sensors. Parameter 13 is not applicable to visual sensor evaluations but is significant for infrared imaging systems. Aerosol parameters 14-16 play a fundamental role in describing sensor and laser weapon performance in the atmosphere because light scattered from aerosols reduces target contrast and attenuates signal level. Visual contrast reduction effects can be more significant in reducing visual probability of detection than image attenuation. Precipitation characterization established by parameters 17-19 is required to compute visual range or MMW transmission. Parameters 20 and 21 aid in defining background feature contrasts. Dew/frost are feature signatures that strongly affect target-to-background spectral contrast. Spectral emissivity is used with thermodynamic temperature measurements of target and background to estimate target thermal contrast. Target/background emissivity is of primary interest only for infrared sensor systems. Parameter 22, the relative humidity structure function, is of primary interest for MMW transmission because it is used to determine temporal fluctuations and scintillation in the transmitted beam.

Parameters 23 and 24 define the sea state environment. Parameters 25-31 characterize the illumination environment in which the sensor is tested. For visual sensors, the illumination

environment is particularly important. Spectral transmittance, parameter 32, is key to determining many of the atmospheric characteristics that limit any sensor's performance. The index of refraction structure function, parameter 33, is used to describe the limiting resolution of the imaging sensor and image scintillation or fluctuation frequency that affects laser propagation. This variable is one of the most important for ultraviolet, visual, and near-infrared band system performance. Parameters 34-40 are required for atmospheric definition in all spectral bands. Parameters 41 -44 are essential to characterize maritime laser transmission conditions.

The parameters listed in [Table 2-1](#) have been used to develop the tables in [Appendix A](#). The format of the tables is the same for all the examples of E-O sensor evaluations discussed in this guideline. Each table shows recommended dimensional units; provides the rationale for measuring the variables; suggests the averaging period for the measured parameter; defines the parameter's relative importance on a scale of 1-4 with 1 being the most important; and suggests a nominal acceptable error. Section [2.3](#) describes recommended measurement methods for the most significant variables listed in [Table 2-1](#). The subject of acceptable measurement error is discussed in detail in Section [2.4](#) where it is shown that acceptable measurement error varies strongly with specific test requirements.

The following sections provide discussions of how the measurements are applied to the example system test requirements. The discussion is intended to provide an understanding of the differences encountered in tests of different sensors and of the need to ensure comprehensive and detailed data management as determined by a TQDM approach.

2.2.1 Visual Sensor Tests

Visual sensors respond to target-to-background contrast.^{4,5} Visual sensor tests are among the more difficult to perform because so many related atmospheric factors affect object contrast and, therefore, sensor performance. Key factors affecting visual sensor performance in the atmosphere include target contrast, scattered path luminance, luminance magnitude, visual range, Sun position relative to the sensor, refractive turbulence, and target size and range. A common method for evaluating visual sensor performance is to establish the probability of target detection as a function of target, atmosphere, and sensor parameters. [Figure 2-10](#) illustrates typical probability of detection curves for eye and daysights, a starlight scope, and night vision goggles viewing targets on different backgrounds (representing different values of contrast) as a function of relative path transmittance (transmittance normalized to that for no image attenuation). This figure shows that as the target contrast increases, the relative transmittance corresponding to the 50% probability of detection decreases. Increases in target contrast mean increases in target range for 50% probability of detection, or, if range is fixed, the target is detected under much lower visual range conditions. Note that sensor probability of detection depends on sensor type as well as target contrast. It is important to keep careful records of the operational characteristics of sensors being tested.

⁴ Otto Schade. "Optical and Photoelectric Analog of the Eye." In *Journal of the Optical Society of America*, pp. 721-739. September 1956.

⁵ Alvin Schnitzler. "Image-detector model and parameters of the human visual system*." In *Journal of the Optical Society of America*, v63 n11, pp. 1357-1368. November 1973.

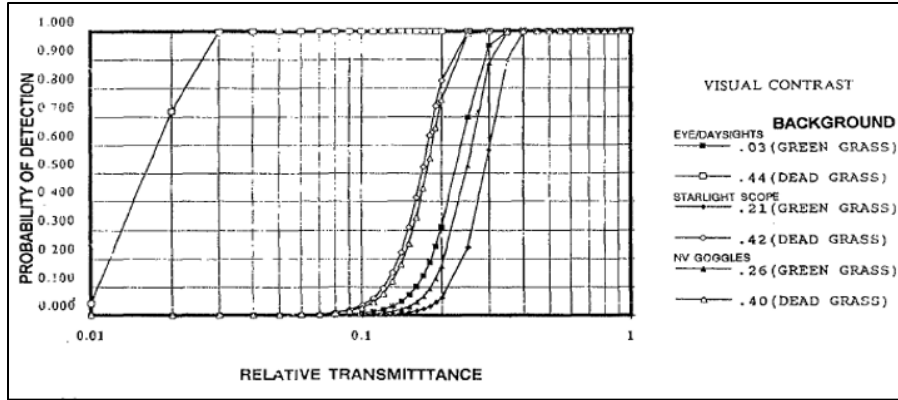


Figure 2-10. Typical Probability of Detection Curves for Visual/Near-Infrared Band Imaging Systems

[Table A-1](#) lists achievable accuracies of atmospheric parameters that may not fully support acceptable computation of the probability of target detection with a visual imaging system. As explicit computations show, this nominal value may be more or less than is required for an accurate probability of detection estimate.

2.2.2 Infrared Sensor Tests

Evaluation of imaging sensors in the 0.9-1.6 μm , 3-5 μm , and 8-14 μm spectral bands requires measurement of atmospheric parameters that affect radiometric emission and absorption of background radiation at the target and along the target path. Thus, it is important that infrared gaseous absorption be determined primarily in the water vapor and carbon dioxide bands. This absorption requires careful measurement of temperature, pressure, and humidity. There is no atmospheric visibility parameter for the infrared bands because there is no standard spectral response in the infrared as there is in the visual band. The equivalent parameter in the infrared is spectral transmittance as it applies to a particular sensor's spectral response. If sensor spectral response is assumed constant with respect to wavelength, then spectral transmittance can be computed in terms of air temperature, relative humidity, and, for specification of aerosol content, visual range.

Probability of target detection with a visual imaging system is especially difficult to determine in the infrared and is often reported in terms of target-background temperature difference, generally understood as a brightness temperature difference. This temperature difference is an equivalent temperature difference proportional to the radiometric emission and reflection difference between target and background. When the spectral emissivity (emitted radiance relative to that of a black body at the same thermodynamic temperature) of the target and background are identical, it is commonly assumed that the brightness temperature difference is directly proportional to thermodynamic temperature difference. However, target and background emissivities are rarely identical. Assuming equal target and background emissivities, when they are in fact different, can lead to errors of hundreds of percent in predicted estimates of thermal contrast. Unless target and background spectral emissivities are measured in addition to thermodynamic temperatures, the observed target-to-background thermal contrast is scene- and sensor-specific. Consequently, the test results cannot be accurately extrapolated to other targets of similar size, shape, and color in comparable background scenes.

Measurement results cannot be applied directly to similar sensors in the same spectral band unless the new sensor has the same spectral response as the tested sensor. Sensor output is an integral response to the product of all factors affecting the spectral band in which the sensor operates. These factors include spectral emissivity of the target and background, atmospheric spectral extinction, and the spectral response of the sensor optics and photodetector. If sensors are changed, even though the spectral band remains the same, the sensor output will change for the same input values because the new sensor spectral response (if different from the original sensor) weights the inputs differently. Broad-band atmospheric transmittance, for example, is sensor-specific for the same reason.

Infrared imager sensor sensitivity is often expressed in terms of minimum resolvable temperature difference (MRTD); however, MRTD is sensitive to the magnitude of the radiometric energy input, making sensor performance sensitive to the square of the line-of-sight transmittance. Thus, it is nearly impossible to separate sensor response characteristics, target-background thermal contrast, and atmospheric effects in the evaluation of sensor performance in the atmosphere. Atmospheric testing must ensure that all significant variables relative to sensor performance are acquired.

[Figure 2-11](#) illustrates the effects of target thermal contrast and atmospheric transmittance on the probability of detection of a tank target set against a grass-covered background. Note that thermal contrast varies strongly as a function of time of day (the primary source of background temperature is the Sun). Transmittance is normalized to that for no atmospheric attenuation. [Table A-2](#) defines the parametric characteristics that should be determined in atmospheric evaluation of infrared imaging systems in the context of 50% probability of detection. Key factors affecting infrared imager tests in the atmosphere are spectral transmittance in relation to sensor spectral response, air temperature, relative humidity, visual range, thermodynamic temperatures for target and background, spectral emissivities for target and background, sensor spectral response and radiometric sensitivity, and target range and size.

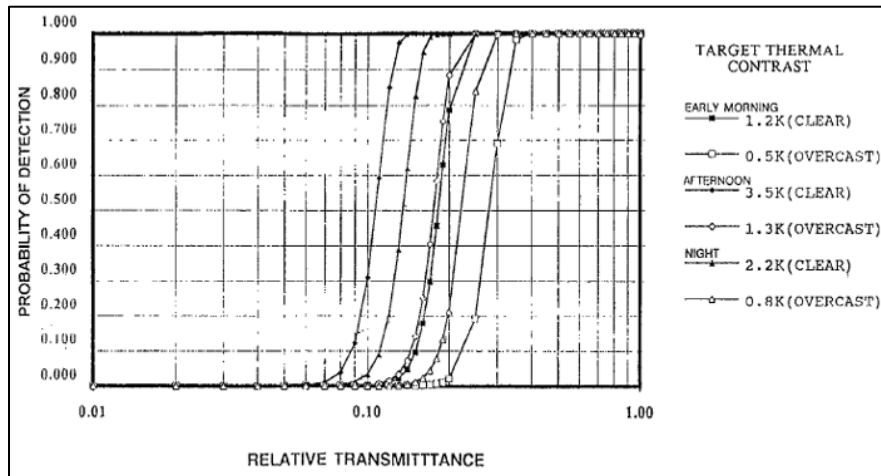


Figure 2-11. Example of 8-4 μm Band FLIR Probability of Detection of a Tank on a Grass Background as a Function of Time of Day

2.2.3 Laser Range Finder Tests

The narrow operating spectral band and its spectrum location determine the most significant atmospheric factors affecting LRF performance. The most common military LRF

systems operate at 1.06, 1.54, or 10.6 μm wavelengths. The performance of those systems operating in the near-infrared (1.06 and 1.54 μm) is most sensitive to attenuation by atmospheric aerosols and refractive turbulence. The 10.6 μm system is most sensitive to attenuation by gaseous absorption and, hence, to air density, temperature, pressure, and humidity. It is not nearly as sensitive to refractive turbulence as the near-infrared systems. All three systems are sensitive to the magnitude of background radiation, because sensor detector signal-to-noise is affected. The LRF system response is determined by target spectral reflectivity rather than target-to-background contrast.

[Figure 2-12](#) illustrates the probability of successful ranging for a 1.06 μm LRF for 20 km of visual range, 3% target reflectivity, no refractive turbulence, and no background radiation as a function of target range and relative transmittance through a smoke screen. The figure shows that the 50% probability of successful ranging is a sensitive function of target range and transmittance through the smoke screen. It is particularly important to accurately measure transmittance between target and sensor for these systems. [Table A-3](#) lists the atmospheric parameters that should be measured for 1.06, 1.54, and 10.6 μm LRF systems in the context of probability of successful ranging. As with broad-band E-O systems, it is important that the operating characteristics of the LRF system under test be recorded so that the atmospheric and target parameters be applicable to other systems.

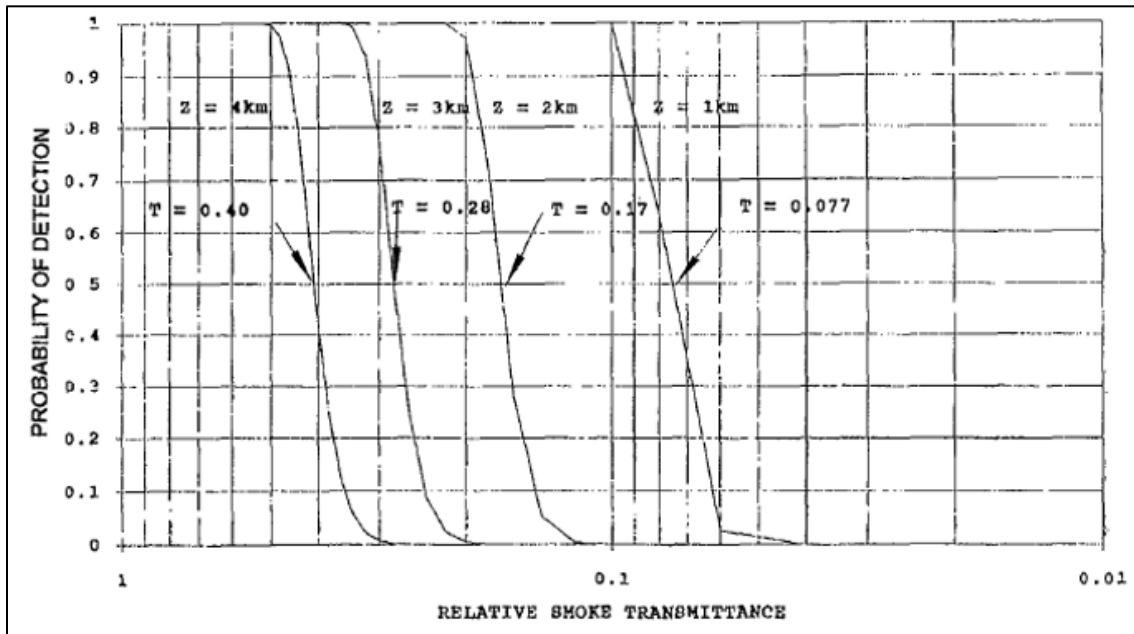


Figure 2-12. Example Probability of Successful Ranging

2.2.4 High-Energy Laser Power Effectiveness

The nature of HEL effectiveness as a weapon relies on the beam maintaining its coherence over long distances, to create sufficient energy in a small area that will result in thermal damage to threat components. The laser beam can be affected by system variables such as jitter and wander, but it can also be substantially corrupted by atmospheric effects. The primary effects of the atmosphere on laser are atmospheric extinction due to aerosols and optical turbulence due to fluctuating refractivity conditions, most notably due to temperature and humidity gradients, as described in [Equation 2-1](#). Aerosol extinction is a combination of

molecular absorption and the various forms of scattering: Rayleigh, Mie, and geometric. Optical turbulence primarily causes a dispersion of the laser beam, reducing its intensity due to rapidly changing refraction structure along the laser path through the atmosphere.

$$C_N^2 = \left(\frac{A_T C_T}{T}\right)^2 + \left(\frac{A_Q C_Q}{Q}\right)^2 + 2 \frac{A_T C_T}{T} \frac{A_Q C_Q}{Q} \quad \text{Equation 2-1}$$

Refraction due to vertical temperature gradients and lensing can also be significant factors, especially at low altitudes over solar heated land areas or evaporative duct conditions in a maritime area. Due to the high variability of water content in the atmosphere and its influence on both the absorption factor and aerosol particle growth, humidity is also a major parameter that should be characterized during laser tests.

Other effectiveness factors such as jitter and wander are system-specific issues with laser performance compared to strongly influenced by the atmosphere.

2.2.5 Millimeter Wave Sensor Tests

The MMW sensor systems are much less sensitive than visual or infrared systems to attenuation resulting from normally occurring atmospheric particulates or refractive turbulence. The MMW systems are particularly sensitive to radiometric absorption by liquid water and water vapor. Thus, MMW transmission is a sensitive function of air temperature, pressure, and humidity. While insensitive to refractive index turbulence, this spectral band is particularly sensitive to relative humidity turbulence, which is proportional to refractive index turbulence. In [Equation 2-1](#), C_N , C_T , and C_Q are so-called structure functions for refractive index, temperature, and humidity fluctuations because of atmospheric turbulence. A_T and A_Q are constants that are wavelength-dependent. As wavelength increases, A_T decreases and A_Q increases. The cross-correlation between temperature and humidity effects is represented by the last term in [Equation 2-1](#). This term plays a particularly important role in defining turbulence effects on MMW propagation when there is high variability in temperature and humidity along the propagation path. At the shorter wavelengths, temperature effects are dominant, while at the longer wavelengths, humidity effects dominate. The end result is that refractive turbulence effects can be as strong for MMW propagation as those at the shorter wavelengths but for entirely different reasons. The shorter wavelengths undergo scintillation because temperature fluctuations of the air refract the transmitted beam. The longer wavelengths undergo scintillation because humidity varies, causing fluctuations in transmitted beam absorption.

Target and background signatures are sensitive to dew, frost, and the liquid water content in snow cover, precipitation, and clouds; therefore, background and target emissivity become as important in the millimeter wavelength band as in the infrared bands. Precipitation temperature is a uniquely important parameter for this spectral band (even though it can be neglected in other bands) because spectral absorption is temperature-dependent and changes drastically between ice and water.

The characterization of natural hydrometeor effects on electromagnetic wave propagation in the MMW and microwave bands is critical in atmospheric evaluation of these sensors. For example, polarization used to increase the information transmitting capacity of MMW systems is affected by the orientation of raindrops. Falling raindrops are shaped like oblate spheroids that become canted at particular angles by surface and aloft winds. The canting angle affects communication channel leakage in both horizontal ground level and vertical satellite transmission paths. Snow crystal preferred orientation effects at high altitudes are commonly

observed as rings around the moon. These orientations also occur near the surface and can strongly affect sensor performance. Particle orientation is driven by background winds and turbulence and must be measured accurately with high spatial and temporal resolution. Thus, atmospheric testing of MMW sensor systems requires greater attention to details relevant to natural hydrometers than the visual and infrared systems. [Table A-4](#) provides a summary of the parameters needed for measurement as a function of MMW transmission characterization.

2.2.6 Test Programs

The E-O sensor atmospheric test programs share many common features and data requirements regardless of which DoD agency is testing the sensor. The common thread is the type of sensor being tested. The following sections illustrate E-O test program data requirements by discussing Army, joint DoD agency, and general Navy/Marine littoral warfare testing programs.

2.2.6.1 SWOE Test Program

The SWOE program started in 1989 and is sponsored by the U.S. Army Corps of Engineers (the lead Service), the individual Services, and the Joint Test and Evaluation program of the Office of the Director for Test, Systems Engineering and Evaluation, Office of the Secretary of Defense. The SWOE is intended to develop, validate, and demonstrate the capability of an integrated process to handle complex ground target signatures and worldwide operating environment effects. This process will provide the DOD smart weapons and aided target recognition developers with reliable methods to integrate measurement, information base, modeling, and scene rendering techniques for complex environments. The SWOE measurements are intended as basic inputs for “first principles” models that predict ground target image characteristics in multispectral sensors, meaning that environmental measurements must be of the highest possible quality and sampled at a rate that provides averaging for effective signal-to-noise improvement and avoidance of aliasing effects. [Table A-5](#) provides a summary of the parameters required by SWOE first principles imaging models. The SWOE Report 92-8⁶ should be consulted for more detailed programmatic information.

2.2.6.2 Smoke Week Test Program

The Smoke Week test program is intended to provide weapons systems E-O sensor developers a characterized environment in which to evaluate sensor performance against smoke and obscurant countermeasures. A Smoke Week test requires measurement of target signatures; atmospheric characteristics including the attenuation and transport and diffusion characteristics of smoke and obscurant countermeasures; and the performance of the sensor during the countermeasure event. These tests include multispectral imaging systems, multiwavelength LRFs and designators, MMW systems, and smokes and obscurants developed to counter the effectiveness of these systems against realistic targets. Smoke and obscurant tests are among the most dynamic events encountered in E-O sensor testing in the atmosphere and are among the most challenging. Sampling periods may be 10 Hz or higher for atmospheric transmission and for sensor response measurements with averaging periods that run to seconds or tens of seconds. The steepness of the probability of detection curves shown in [Figure 2-10](#), [Figure 2-11](#), and [Figure 2-12](#) suggests that data accuracy needs to be high to properly qualify sensor performance.

⁶ J.P. Welsh. *Smart Weapons Operability Enhancement (SWOE) Program Joint Test and Evaluation Program Test Design*. SWOE Report 92-5. June 1992. Retrieved 10 June 2022. Available at <https://apps.dtic.mil/sti/pdfs/ADA289660.pdf>.

[Table A-6](#) shows the parameters typically acquired in Smoke Week tests. The STC Technical Report 2094⁷ and Technical Report SMK-001-90⁸ are sample documents describing these test programs.

2.2.6.3 Littoral Warfare Testing

Littoral warfare testing requires that E-O sensors be tested in the atmosphere at the land-sea interface where there are strong diurnal meteorological effects and atmospheric variables that can change rapidly and often. Sensor performance can be significantly different for the same propagation path when transmitted from a land- or a sea-based platform because atmospheric aerosol loading and refractive index structure constants can be drastically different between sea surface propagation and land propagation. Thus, testing E-O sensors in a littoral environment is complex and challenging. Littoral testing requires that data be acquired at high rates, that detailed measurements be made along the propagation path over land and sea, and that the sensor be evaluated for operation from either end of the propagation path. In many cases, there is little or no historical data to support this testing, and instrumentation to support measurements made only over the ground are likely to be highly limited in operational applicability over a land-sea interface or open-ocean. [Table A-7](#) shows the parameters that require measurement in a littoral test program.

2.2.6.4 Navy Laser Atmospheric Measurements: CABLE/TRAX-West

The Navy has a strong interest in characterizing the atmosphere over the ocean to determine effects on HEL performance in the maritime environment. Performance of HEL systems can be dramatically different in the ocean scenarios, primarily due to the heavy aerosols at low altitude but also to boundary-height increases in optical turbulence. To most optimally evaluate the conditions, lidar systems have been developed that can emulate the slant paths and wavelength-specific extinction conditions that HEL systems will experience. Atmospheric testing requires careful consideration of the rapid temporal changes that can occur on the very structure being measured. Some participating sensors operate at the speed of light, some require integration time, and some others require flight time. These different factors drive the actual capability to conduct valid measurements of any particular parameter. Testing was conducted in accordance with the general goals below.

- Measure the same atmosphere, at the same time, with all applicable sensors.
- Collect multiple measurements at each geometric point of interest.
- Correlate the sensor bias to a properly located NIST-traceable truth sensor.
- Minimize variables that contribute to non-maritime atmospheric factors.
- Evaluate associated atmospheric features using a NIST-traceable sensor.
- Emphasize vertical profile, boundary height conditions.

⁷ Science and Technology Corporation. *Indirect Fire Battlefield Obscurants Test (Smoke Week VII) July 15-26, 1985, Fort Sill, OK*. STC-TR-2094. 1 February 1986. Retrieved 10 June 2022. Available to personnel from U.S. Government agencies only at <https://search.dtic.mil>.

⁸ Kennedy, B. W., B. A. Locke, W. M. Farmer, W. G. Klimek, and F. E. Perron, "Joint U.S.-Canadian obscuration analysis for smokes in snow (Smoke Week XI), Final Report: Part I," Report No. SMK-001-90, Project Manager, Smoke/Obscurants, Aberdeen Proving Ground, MD (April 1990). This document is classified unclassified/limited.

- Dwell at longer intervals on each vector, to improve accuracy while accepting some loss of temporal registration.

[Table A-8](#) shows the parameters that require measurement in a maritime HEL test program and other E-O programs.

2.3 Recommended Measurement Methods

This section discusses recommended measurement methods for the parameters required to characterize E-O sensor performance in the atmosphere for the types of sensors and tests discussed in Section [2.2](#). These recommendations are intended to be guidelines that will help the user ask the test customer the proper TQDM-related questions to ensure that sufficient data are acquired, that the data are of sufficient accuracy for the sensor test, and that the data will be of sufficient quality to be used with assurance in future applications.

2.3.1 Visual Range (Visibility)

Visual range, or visibility, is a shorthand specification for atmospheric contrast transmittance when the sensor is assumed to be the human eye. In meteorology, visibility is a measure of the distance at which an object or light can be clearly discerned. It is one of the most misapplied, misunderstood, and incorrectly measured parameters in field evaluation of E-O sensors. Visual range is a function of atmospheric attenuation; absolute magnitude of background illumination; scatter and absorption of background illumination along the observation path; target contrast without path attenuation and path illumination effects; and sensor contrast threshold. The difference between daytime visibility and nighttime visibility definitions illustrates the subjective, pilot-focused nature of the visual range measurement: the former determines the distance at which a dark object can be discerned against a white or sky background, whereas the night visibility is measured with a light source against a dark background. Some subjective aspects can be reduced by describing visibility in terms of meteorological optical range, which is represented solely by the daytime scenario reflected in the daytime Koschmieder model, compared to the nighttime Allard model.

Definitions of terms relative to visual range vary throughout the literature. Definitions that are assumed for these guidelines are commonly used in atmospheric testing of E-O sensors. Contrast is defined as the difference between maximum and minimum target luminance divided by the background luminance.⁹ Visual range is the distance at which an object with unit target contrast can be detected with a 50% probability of detection. It is important that the telephotometer used to measure contrast have a photopic spectral response, which is defined as the eye response of the cones in the retina and occurs after the eyes have become adapted to a field luminance equal to or greater than about 3 candles/m².¹⁰ Photopic spectral response peaks around 560 nm and falls to 10% of the peak at about 470 nm for the short wavelength and 685 nm for the long wavelength ranges of the spectrum.

Path luminance is often expressed in terms of the ratio of horizon sky (S) to background luminance (G): the sky-to-ground ratio. In the special case where the sky-to-ground ratio is 1, the

⁹ G. J. Burton. "Transformation of Visual Target Acquisition Data Between Different Meteorological and Optical Sight Parameters: A Simple Method." In *Applied Optics*, V22 Issue 11, pp. 1679-1683. 1983.

¹⁰ Radio Corporation of America. *Electro-optics handbook: a compendium of useful information and technical data*. Harrison, N.J., 1968, p. 5-3.

contrast transmission (ratio of zero path contrast to observed contrast) is identical to radiometric transmission described by the Beer-Bouguer law. The visual range is then computed by assuming some contrast detection threshold limit and solving the Beer-Bouguer transmission equation for the range equivalent to an atmospheric attenuation value expressed in terms of the volume extinction coefficient, which is the so-called Koschmieder law. Values of the contrast detection threshold commonly assumed for the Koschmieder relationship are 0.02 or 0.05. Note that care needs to be taken to avoid the Sun Corridor during visibility measurements, the area just below the Sun location where strong spectral and diffuse reflections can obscure dark contrast targets.

Unfortunately, the sky-to-ground ratio is rarely 1 and is sensitive to path orientation relative to Sun position. Thus, a visual range estimate using Koschmieder's relationship is often in error. The simplified relationship developed by Koschmieder that relates the visual range and the extinction coefficient is given by [Equation 2-2](#).

$$Lv = \frac{3.912}{ext} \quad \text{Equation 2-2}$$

where Lv is the distance at which a black object is just barely visible.¹¹ [Equation 2-2](#) is based on the following assumptions.

- a. The background behind the target is uniform.
- b. The object is black.
- c. An observer can detect a contrast of 0.02.
- d. The ratio of air light to extinction is constant over the path of sight.

The assumption that human observation can achieve a detection contrast of 0.02 frequently is ambitious, as there are many subjective aspects to detecting a target and even the detection threshold is often confused with the identification threshold. Thus, the World Meteorological Organization and the National Weather Service have adopted a 5% (0.05) contrast threshold as the standard to determine atmospheric visibility conditions. This assumption changes the Koschmieder equation to [Equation 2-3](#).

$$Lv = \frac{2.996}{ext} \quad \text{Equation 2-3}$$

The significant variation of these two formulas applied to convert the visual range to extinction coefficient is in the realm of fairly short-range visibility conditions, since this relationship follows the Junge Power Law. Fortunately, these are also the conditions where observers have substantial visibility markers at their disposal, and the majority of visiometer sensors are designed to be optimized; so even though there can be a difference in the two calculations, the overall uncertainty should achieve a usable value.

While the Koschmieder relationship is useful as a first approximation for determining visual range, many situations exist in which the results are only qualitative. [Figure 2-13](#) shows

¹¹ Fred Nicodemus. *Self-Study Manual on Optical Radiation Measurements*. NBS Technical Note 910-8. Washington: National Bureau of Standards, 1985.

how the line-of-sight path direction can easily produce wide variations in the sky-to-ground ratio. [Figure 2-14](#) quantitatively illustrates the impact of this problem; it also plots observable visual range relative to that predicted by Koschmieder's relationship for a 0.02 contrast detection threshold. Koschmieder's law gives the observable visual range when the sky-to-ground ratio is 1. When the sky-to-ground ratio is less than 1 (for example, snow-covered ground under overcast sky as shown in [Figure 2-13](#)), the visual range is greater than predicted; the visual range is less than predicted when the sky-to-ground ratio is greater than 1. The magnitude of the incorrect estimate depends on the contrast detection threshold that, in the Koschmieder relationship, is assumed to be 0.02 or 0.05. Ultimately, the magnitude of the environmental illumination determines the contrast detection threshold. The contrast sensitivity of the human eye depends on the magnitude of object illuminance. The theoretical contrast detection threshold (for a bright sunlit background) for a 50% probability of detection is roughly an order of magnitude smaller than the Koschmieder values (Kennedy et al., 1990). Thus, to obtain an accurate value of visual range, the following parameters must be measured:

- a. absolute magnitude of the target-background luminance (used to determine limiting contrast threshold of human eye for 50% probability of detection);
- b. radiometric transmittance of the atmosphere for photopic eye spectral response;
- c. horizon sky luminance immediately above the target (required for sky-to-ground ratio);
- d. background luminance around the target (required for sky-to-ground ratio);
- e. near target contrast (negligible path effects) (required for contrast ratio); and
- f. target contrast at desired range (required for contrast ratio).

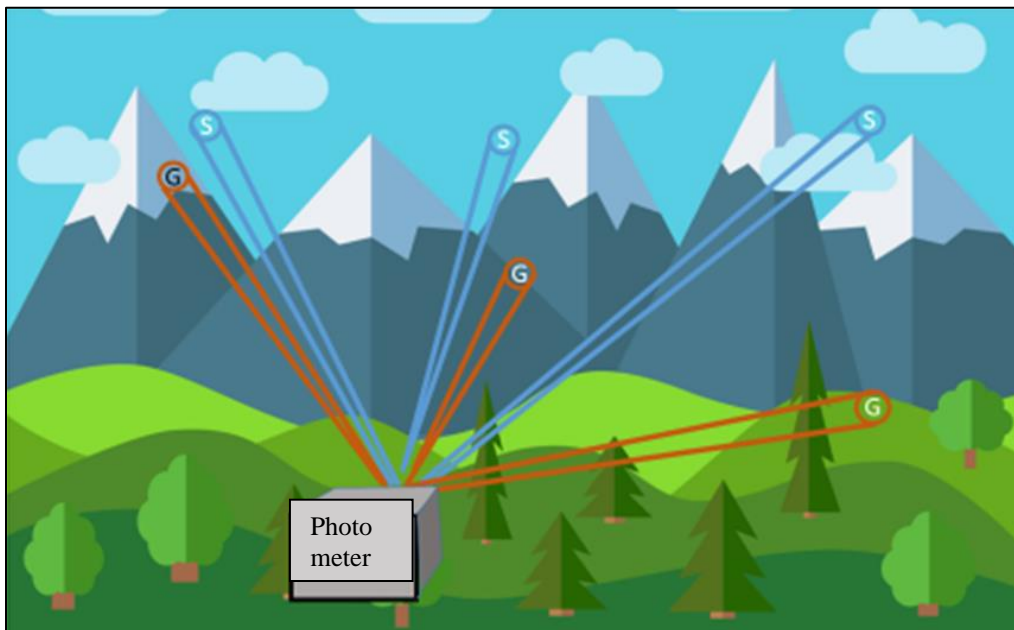


Figure 2-13. Illustration of the Dependence of the Sky (S)-to-Ground (G) Illuminance Ratio on Viewing Direction

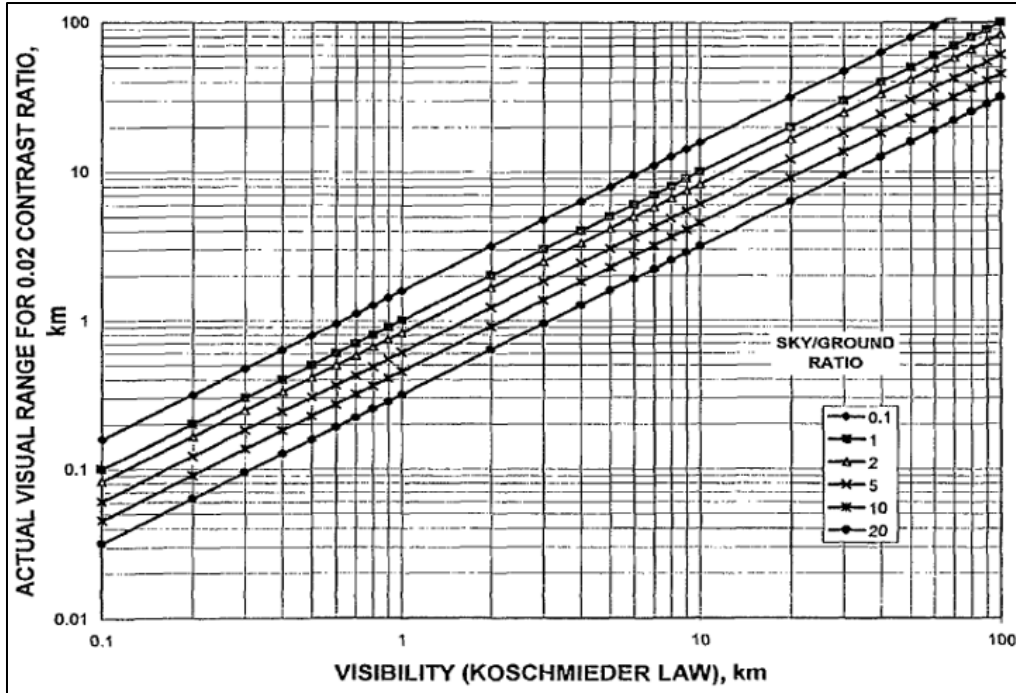


Figure 2-14. The Effect of Sky-to-Ground Ratio on Visual Range

Radiometric transmittance must be measured near the line of sight to the target but with the transmissometer source outside the field of view of the telephotometer used to measure sky-to-ground ratio to avoid biases in background illumination created with the artificial transmissometer source. The spectral response of the transmissometer must include the source characteristics as well as the optical system transmittance, the photopic filter, and the response of the photodetector. Radiometric transmittance is computed by normalizing the measured radiometer output obtained for the desired range to that for a nonattenuating atmosphere. The normalization must include the effects of source divergence and transmitter beam homogeneity for the two different measurement ranges.

Transmissometer and telephotometer calibration should follow the NIST standards that define methods for measuring instrument spectral response and operational characteristics of calibration lamps (Nicodemus, 1985). Attention must also be given to contrast targets. Normal aging and “weathering” cause target contrast to decrease. Environments with high atmospheric dust concentrations or precipitation levels affect target contrasts at much higher rates (daily changes may be notable) than those where these values are small because the target collects ambient dusts and aerosols to which it is exposed. Thus, contrast targets operating in low visual range environments need to be calibrated much more often than those operating in high visual ranges to compensate for increased collection of dust and other aerosols on the target surface.

Short-range visimeters have become popular, and translate a virtual point measurement of forward scatter or backscatter light detections into an extrapolation of meteorological optical range typically up to 30 km using back-scatter or forward-scatter optical sensor detections. The latest models advertise visibility calculations to 100 km. The visimeters have been replacing high-maintenance transmissometers at airfields for many years, and require little calibration or maintenance. Note that these are adjusted to relate to pilot visual range, and emphasize daytime visibility in the 600-800 nm region of the visual spectrum.

2.3.1.1 Solar Position

Solar position is most easily determined by an accurate survey of measurement position on the Earth's surface and measurement of time and date with respect to local time or UTC time. Equations for computing Sun position are available in the Smithsonian Meteorological Tables List (1958). Computer programs in spreadsheet format are available that specify solar position within fractions of a minute given latitude, longitude, and time of day and date. Accurate solar position specification relative to a line of sight requires an accurate site survey of all instrumentation locations and an accurate record of local time. The associated Sun Corridor can vary greatly with solar position and Earth surface cover. Most Sun Corridor measurements are qualitative in nature using human observer or photographic documentation.

2.3.1.2 Cloud Cover

Cloud cover is an estimate of the fraction of the sky contributing to ground-level illumination through direct illumination and indirectly through diffuse illumination filtered through clouds. For quantitative computations, it is useful to specify the cloud cover in terms of sky hemisphere sectors that subtend equal solid angles to a ground-level observer. Once the number of sectors is chosen, their midpoint locations (denoted by a subscript i) can be computed.¹² The result is:

$$\phi = (i - 1) \frac{\pi}{m} \quad \text{azimuth} \quad \text{Equation 2-4}$$

$$\cos \theta = 1 - \frac{2i-1}{2n} \quad \text{zenith} \quad \text{Equation 2-5}$$

where m is the desired number of azimuth sectors and n is the number of zenith sectors. By choosing a sufficient number of azimuth and zenith sectors, cloud cover can be specified to as high or as low a precision as necessary.

Cloud cover can be recorded with a camera (video or film) using a fish eye lens and analyzed after a test is complete; however, if such a measurement is performed, the lens must be calibrated in terms of its solid angle projection onto the flat surface of the recording medium. An automated technique such as this is much preferred to manual observations, which are labor-intensive and low in accuracy. Newer all-sky cloud cover sensors such as the Reuniwatt SkyInsight can automatically calculate the percentage of sky cover.

Specification of cloud characteristics is particularly crucial for E-O testing of airborne sensors. Cloud characteristics range from size to concentrations of water and ice to types and distributions of particles. The details of these characteristics encompass a large body of literature and ongoing research that are beyond the scope of these guidelines. Excellent sources of information on this subject are given in Pruppacher and Klett¹³ and in Oguchi.¹⁴

¹² U.S. Army Atmospheric Sciences Laboratory. *Interim SWOE Site Characterization Handbook*. SWOE Report 91-14. May 1991. Available to DoD personnel and contractors at <https://search.dtic.mil/>.

¹³ Pruppacher, H.R. and J.D. Klett. *Microphysics of Clouds and Precipitation*. Dordrecht: Springer Science + Business Media, 2010.

¹⁴ T. Oguchi. "Electromagnetic wave propagation and scattering in rain and other hydrometeors." In *Proceedings of the IEEE*, V. 71, Issue 9, September 1983.

2.3.2 Wind

Wind is a fundamental parameter that affects aerosol and precipitation transport and diffusion, the spread of transmitted beam energy, and target signatures (in the thermal infrared). It is a highly dynamic vector phenomenon and can vary strongly as a function of surface position and time. It is important the three orthogonal vector components of wind be measured at a sampling frequency that does not alias the descriptive statistics for each velocity component and the potential for obtaining aliased results be controlled by using proper data filters or averaging methods. Often it is important or useful for one of the orthogonal wind components to be oriented along the line of sight. The mean and standard deviations for each wind velocity component are required. The number of measurements per component for a statistically stable value depends on the turbulence intensity; the number of spatial points measured depends on stability of the atmosphere required for evaluation of the sensor system and how the data will be applied in its analysis.

A useful rule of thumb for the number of measurements, N , for example, to be averaged in a single point sample for a required coefficient of variation, C , is:

$$N = \left(\frac{\sigma/\mu}{C} \right)^2 \quad \text{Equation 2-6}$$

where σ/μ is the turbulent intensity (standard deviation/mean speed). As an example in the application of [Equation 2-6](#), assume a 95% confidence level is required for the data mean (the coefficient of variation is 0.05). A 20% turbulence intensity then requires that 16 data points must be sampled to ensure a 95% confidence level in the computed mean. The rule of thumb given by RCC 382-21 is a simplification of a complicated problem having many features. Refer to 382-21 for additional details on sampling requirements for meteorological instrumentation and data quality control.

The location of wind measurement stations in a test grid depends on the type of E-O sensor being evaluated and the data application. For example, in the thermal infrared bands, target-background thermal contrast observable with a forward-looking infrared (FLIR) depends on wind speed (particularly for low values of thermal contrast) because target and background thermodynamic temperatures are affected by background winds. Thus, a measurement station should be within at least one wind speed correlation length of the target. A correlation length is the distance over which two similar measurements (for example, wind speed or scintillation) can be sampled and expected to produce correlations better than 0.36. Image resolution depends on refractive turbulence effects that are an integrated path result. Wind speed variations, in this case, are important down the line of sight and must be measured with a closely spaced meteorological sensor array or with a scintillometer. On the other hand, when laser systems are evaluated, correlation lengths have a different impact on test results. For example, LRF target reflectivity is not directly affected by wind or temperature as is a thermal contrast signature, but the amount of power illuminating the target is affected by scintillation. The scintillation can be represented by a turbulence scale length distribution that is a measure of turbulence eddy sizes and represents a length over which scintillation effects can be correlated. The scintillation description is frequently termed the refractive structure function, C_n^2 , which has measurable parameters

primarily influenced by the temperature structure function and by a smaller amount by the humidity structure function. The refractive structure function is expressed by Tatarski¹⁵ as:

$$C_n^2 \approx 2.8M^2L_0^{\frac{4}{3}} \quad \text{Equation 2-7}$$

Where M is the dimensionless refractive index of the atmosphere based on changes in density over distance calculated by Equation 2-8 and L₀ is the outer scale of turbulence measured in meters.

$$M(h) = N(h) + 157h \text{ (M-units)} \quad \text{Equation 2-8}$$

Relating [Equation 2-7](#) to the outer scale determined by atmospheric conditions and noting that $L_0 \sim K_{3/2}\epsilon$, [Equation 2-7](#) becomes:

$$C_n^2 = b\epsilon^{-\frac{1}{3}}K_H \left(\frac{\partial n}{\partial z} \right)^2 \quad \text{Equation 2-9}$$

Where the outer scale of turbulence value has been replaced with the following values: b (this has the value 3.2 and is the Obukhov-Corrsin constant)^{16,17,18,19}; ϵ (the energy dissipation rate); and K_H (the turbulent exchange coefficient for heat diffusion).²⁰ The fraction $\frac{\partial n}{\partial z}$ is the vertical gradient of the index of refraction, n.²¹ Approximations based on the correlation of Tatarski to commonly measured atmospheric factors yields equations such as Roddier²² as:

$$C_n^2(z) = \left(\frac{80 \times 10^{-6}p}{\vartheta^2} \right)^2 C_{\vartheta}^2(z) \quad \text{Equation 2-10}$$

Where p is atmospheric pressure and ϑ is potential air temperature, which includes the covariance factors from humidity. The value 80 in the formula can vary from 82.9 at 0.3 microns to 77.5 at 10 microns. It is customary to use 79 for the 0.5 micron normalized visible wavelength since C_n^2 varies by several orders of magnitude. The potential temperature can be further broken into its temperature and humidity components as:

¹⁵ V. I. Tatarski. *Wave propagation in a turbulent medium*. Mineola: Dover Publications, 2017.

¹⁶ H. A. Panovsky. "The Structure Constant for the Index of Refraction in Relation to the Gradient of Index of Refraction in the Surface Layer." In *Journal of Geophysical Research*, V73, I18, pp. 6047-6049. 15 September 1968.

¹⁷ J. C. Wyngaard. "On Surface-Layer Turbulence." In *Workshop on Micrometeorology*, American Meteorological Society, Boston, 1973, pp. 101-149.

¹⁸ Edgar Andreas. "Estimating C_n^2 over Snow and Sea Ice from Meteorological Data." In *Journal of the Optical Society of America A*. V5, I4, pp. 481-195. 1 April 1988.

¹⁹ R. J. Hill. "Implications of Monin-Obukhov Similarity Theory for Scalar Quantities." In *Journal of the Atmospheric Sciences*. V46, I14, pp. 2236-2244. 15 July 1989.

²⁰ Businger, J. A., J. C. Wyngaard, Y. Izumi, and E. F. Bradley. "Flux-Profile Relationships in the Atmospheric Surface Layer." In *Journal of the Atmospheric Sciences*, V28, I2, pp. 181-189. 1 March 1971.

²¹ Rachele, H. and Arnold Tunick. *Estimating Cn2, Ct2, Cq2, and Cq2 During Unstable Atmospheric Conditions*. U.S. Army Laboratory Command, Atmospheric Sciences Laboratory. TR-0299, White Sands Missile Range, NM 88002-5501, August 1991.

²² F. Roddier. "The Effects of Atmospheric Turbulence in Optical Astronomy." In *Progress in Optics*, V19, pp. 281-376. 1981.

$$C_n^2 = \frac{A_T^2}{\bar{T}_a^2} C_{T^2} + \frac{A_q^2}{\bar{q}^2} C_{q^2} + 2 \frac{A_T A_q}{\bar{T}_a \bar{q}} C_{T_q} \quad \text{Equation 2-11}$$

The Rytov number is a fundamental scaling parameter for laser propagation through atmospheric turbulence. Rytov numbers greater than 0.2 are generally considered to be strong scintillation. A Rytov number of 0 would indicate no turbulence, thus no scintillation of the beam.²³ For a spherical wave, Rytov is directly related to the refractivity structure function by:

$$Ry = 0.124 \cdot (2\pi/\lambda)^{7/6} \cdot L^{11/6} \cdot C_n^2. \quad \text{Equation 2-12}^{24}$$

A third way of expressing optical turbulence is by the traditional astronomer's value called the Fried Parameter, annotated as r_0 (verbally expressed as “arr-nought”). The value of r_0 , typically expressed in mm, is the maximum diameter of a telescope optic sized such that its diffraction-limited resolution equals the “seeing” resolution, the largest telescope aperture that can be used without observing scintillation. The well-known Kolmogorov turbulence model describes the shape of the atmospheric long-exposure point spread function, and many other phenomena, by this single parameter r_0 . This effects-based measurement of scintillation can be converted to an atmospheric measurement with somewhat linear results by [Equation 2-13](#).

$$r_0 = \left[0.423 k^2 \int_{\text{Path}} C_n^2(z') dz' \right]^{-3/5} \quad \text{Equation 2-13}$$

Typical values of r_0 with variations of outer turbulence scale L are illustrated in [Figure 2-15](#), based on the similar value of The Ratio of Seeing (ϵ_0). The atmospheric seeing is set to the Paranal standard value of 0.83 arcsecond at 0.5 μm .

²³ “Rytov number”, Wikipedia, last modified 17 March 2016, https://en.wikipedia.org/wiki/Rytov_number.

²⁴ Farrell, T., D. Dixon, L. Heflinger, S. Klyza, and K. Triebes. “Low-Cost Experiment to Measure Optical Turbulence Between Two Buildings.” In *Journal of Directed Energy*, V. 2, no. 4, pp. 297-311. Fall 2007.

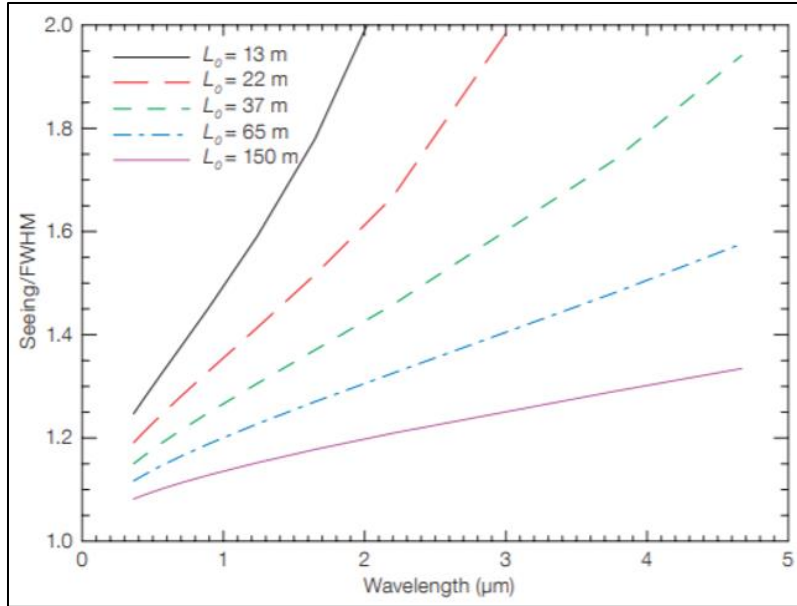


Figure 2-15. Ratio of Seeing ϵ_0 to Full Width Half Maximum ($\epsilon_{\nu K}$) as a Function of the Wavelength for Several Values of L_0

Wind speed within a correlation length of the target is not critical for LRF target characterization; however, scintillation characterization in terms of turbulence scale length distributions down the line of sight is required to specify LRF and HEL performance. Wind speed, measured in three dimensions with sonic anemometers, can also derive a sonic temperature structure function at high enough speeds to derive optical turbulence. The sonic temperature would also be influenced by the humidity structure function, so this factor is captured by a 3D sonic anemometer as well. There are recent studies intimating that the wind structure function, if captured accurately enough and at a high data rate, can also correlate to the refractivity structure function. The minimum 3D wind direction sample rate generally accepted is 20 Hz, but 80 Hz is considered optimum. There have been recent experiments with 10-Hz sonic anemometers that show acceptable performance at a minimum wind speed of 2 to 3 m/s. Note that the wind speed variation values measured are used to derive the temperature structure function, used in the above equations to determine C_n^2 .

Spatial separation of wind measurement stations for a particular level of acceptable error depends on atmospheric stability and the orientation of the sensor line of sight with respect to the wind vector. For lines of sight perpendicular to the wind vector and for flat terrain, it is normally assumed (and often erroneously) that the wind speeds are relatively uniform down the line of sight. The correlation functions depend on surface roughness and the height above ground level at which the measurements are to be made, that is, the sensor line of sight.

For example, rough estimates of the integral length scales (the distance over which turbulence spectra energy remains correlated to a value of 0.36 or better) over level terrain in the direction of the wind vector are about 10.3 z (z is the line-of-sight height). Perpendicular to the wind vector, it is about 7.5 z ; vertically, it is 0.5 z ; and for the mean direction it is 8.4 z for a “C”

or “D” Pasquill atmospheric stability category.^{25,26} These estimates show that if an LRF or HEL line of sight is 2 m above ground level and perpendicular to the wind direction, a parallel line of sight sensor such as a scintillometer must be within 20.6 m of the laser line of sight in the upwind or downwind direction and within 1 m of height if there is to be correlation of the measurements with the response of the LRF to turbulence effects.

2.3.2.1 Wind Speed and Direction at Surface

Horizontal wind components measured at the meteorological stations in the sampling array are collected to interpolate between spatial measurement points to simulate the horizontal variation of the wind field. Near-surface mean wind speeds can be measured reasonably with mechanical anemometers (cup or propeller). According to Lyons and Scott, these should be “...accurate within 0.2 m/s 5% of the wind speed, with a start speed of less than 0.5 m/s, and a distance constant (63% recovery) of less than 5 m. Wind vanes should have a resolution of 1° and an accuracy of 5°. Delay distance (50% recovery) must be less than 5 m with a damping ratio of greater than 0.4. Sixty or more samples will estimate hourly means to within 5-10%. Sample averaging time should be 1-5 s with a response time of no more than 1 second. At least 360 samples are required to estimate the hourly deviation within 5-10%.” (Lyons et al.)

2.3.2.2 Winds Aloft and Mixing Layer Height

Winds aloft are determined using tower-mounted anemometers and vanes, pilot balloons, radiosondes, acoustic sounders, radar profilers, and rocketsondes. Global positioning technology added to pilot balloons and small rocketsondes provides spatial resolution capability of ± 2 -3 m. This capability provides measurement of high-altitude wind characteristics that is commensurate with measurements made on towers, to 33 km altitudes and beyond.

The height of the mixing layer is a fundamental parameter in characterizing the stability of the atmosphere. Atmospheric stability, for example, is used to define transport and diffusion parameters for E-O sensor passive countermeasures such as smokes and obscurants or for specifying maximum acceptable line-of-sight separation. This height can be detected by observing rapid changes in temperature gradient or wind shear using continuous monostatic and Doppler acoustic sounders that measure two-way acoustic propagation time. These data are normally correlated with tethered sonde or airborne sensors. Acoustic sounders normally have spatial resolutions of about 30 m with a useful range of about 50-600 m above ground level. Resolutions of 1.5-3 m can be obtained by using pulsed laser systems (for example, lidar or the visioceilometer developed by the U.S. Army) that detect scatter from aerosols that concentrate in the mixing layer. The frequency modulation/continuous wave radar that detects backscatter from changes in relative humidity associated with the mixing layer height offers the potential for all-weather operation, high spatial and temporal resolution, and sufficient accuracy. Modern wind profilers can be optimized for boundary height measurements, such as the 915M wavelength that can determine wind speeds to 1 m/s and 5° azimuth, down to range bins as small as 60 meters.

²⁵ Kader, B. A., A. M. Yaglom, and S. L. Zubkovskii. “Spatial Correlation Functions of Surface-Layer Atmospheric Turbulence in Neutral Stratification.” Chapter in *Boundary Layer Studies and Applications*, pp. 233-249. Dordrecht: Kluwer Academic, 1989.

²⁶ Lyons, T. J. and W. D. Scott. *Principles of air pollution meteorology*. London: Belhaven, 1990.

2.3.2.3 Atmospheric Stability

Atmospheric stability is often expressed in terms of A-F Pasquill stability categories (SWOE Report 91-14). Atmospheric stability can be computed from the vertical temperature gradient, wind direction fluctuations, sensible heat flux, wind speed, and surface roughness, or empirically derived from global solar radiation, wind speed, dry bulb temperature, and optical scintillation.^{27,28} Measurement of atmospheric stability using temperature gradients requires at least 0.1 °C accuracy and 0.02 °C resolution. The temperature probe should have at least 63% recovery in 1 minute for these kinds of measurements. Higher sampling rates (0.1 Hz) with thin film probes are highly desirable. Accuracy and resolution requirements of these measurements are highest for wind speeds of 1-3 m/s measured at a 10-m height and for sensible heat fluxes less than about 60 W/m² (Sutherland, et al.). This conceptual method begins to fail for very low wind speeds and quiescent conditions punctuated by intermittent turbulence.

2.3.3 Absorbing Gases

Atmospheric gases that impact E-O system performance are primarily water vapor, ozone, carbon dioxide, carbon monoxide, and nitrogen oxide. Absorption by these gases occurs near the 3-5 and 8-14 μm bands. Absorption by ozone is negligible near sea level. For millimeter radio waves, the main components of molecular absorption are oxygen at 63 GHz and at 22 GHz due to water vapor. [Figure 2-16](#) shows the common absorption features of the atmosphere for visual and infrared wavelengths.

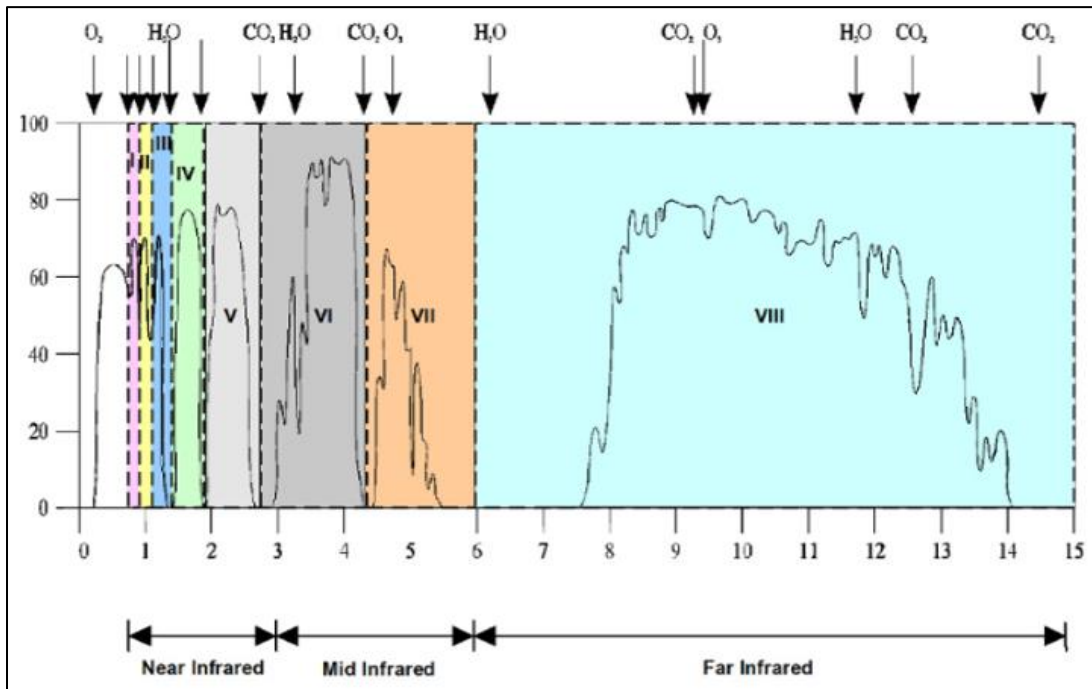


Figure 2-16. Sea-Level Transmittance over an 1820 m Horizontal Path

²⁷ Sutherland, R. A., F. Hansen, and W. Bach. "A Quantitative Method for Estimating Pasquill Stability Class from Windspeed and Sensible Heat Flux Density." In *Boundary Layer Meteorology*, V. 37, N. 4, pp. 357-369. 1996.

²⁸ Edgar Andreas. "Atmospheric Stability from Scintillation Measurements." In *Applied Optics*, V. 27, Issue 11, pp. 2241-2246. June 1988.

Nearly all E-O sensors have been designed to operate in spectral bands that avoid the effects of gaseous absorption on the transmitted radiation; however, some HEL wavelengths (for example 3.8 μm) are impacted by gaseous absorption requiring a measurement of the absorption coefficient. This measurement is best accomplished by using a calibrated Fourier-transform spectrometer (FTS) of at least 2 cm⁻¹ resolution viewing a black body source at a range (typically 300 m) that provides acceptable sensitivity. The spectrometer line of sight should be within a crosswind correlation length of the E-O system line of sight. However, the empirical molecular absorption spectrum is highly stable at lower altitudes, which has been successfully modelled by programs such as MODTRAN. A basic estimation of the absorptive extinction has been developed by Elder and Strong, later modified by Langer to determine infrared absorption τ_{ai} based on accurate measures of relative humidity:²⁹

$$\tau_{ai} = e^{-A_i\sqrt{w}}, \text{ for } w < w_i \quad \text{Equation 2-14}$$

$$\tau_{ai} = k_i \left(\frac{W_i}{W} \right)^{\beta_i}, \text{ for } w > w_i \quad \text{Equation 2-15}$$

where A_i , k_i , β_i , and w_i are constant whose values for each atmospheric window are listed in [Table 2-2](#).

Table 2-2. Constants to be used in Equations 2-10 and 2-11				
Window \ Constants	A_i	k_i	β_i	w_i
I	0.0305	0.800	0.112	54
II	0.0363	0.765	0.134	54
III	0.1303	0.830	0.093	2.0
IV	0.211	0.802	0.111	1.1
V	0.350	0.814	0.1035	0.35
VI	0.373	0.827	0.095	0.26
VII	0.3598	0.784	0.122	0.165

Point sensors also can be used to specify absorbing gas concentrations. The sensors require a grid network having at least correlation-length spacing. Protocol for the reliable sensor operation is well-developed and available from the Environmental Protection Agency.^{30,31,32}

2.3.4 Aerosols

Aerosols are a fundamental component affecting atmospheric transmission. In concentrations exceeding several hundred per cubic centimeter, aerosols significantly impact

²⁹ Sabatini, R. and M. Richardson. "New techniques for laser beam atmospheric extinction measurements from manned and unmanned aerospace vehicles." In *Central European Journal of Engineering*, 3, pp. 11-35. 2013.

³⁰ Smith, F. and A. C. Nelson. *Guidelines for development of a quality assurance program, reference method for continuous measurement of carbon monoxide in the atmosphere*. Springfield, VA: National Technical Information Service, 1973.

³¹ J. J. Wesolowski et al. *Evaluation of the proposed ambient air monitoring equivalent and reference methods*. Springfield: National Technical Information Service, 1974.

³² W. C. Eaton. *Use of the Flame Photometric Detector Method for Measurement of Sulfur Dioxide in Ambient Air: a Technical Assistance Document*. Research Triangle Park: Environmental Protection Agency, 1978.

E-O sensor-based weapons systems. Aerosol particle sizes are assumed to be sufficiently small that, once airborne, the particles remain so, meaning that aerosol particle sizes of materials found in the atmosphere typically are less than 10 μm in diameter. Particles larger than 10 μm rapidly fall out of the atmosphere unless atmospheric conditions are uncommon, for example, during the production of water fogs. In such a case, particles as large as 100 μm in diameter can remain airborne for times much longer than would otherwise be possible. Particles that are too large to remain airborne are considered precipitation. The next section discusses means of characterizing and measuring precipitation.

Two types of aerosol diameters are frequently measured: the aerodynamic diameter and the optical diameter. The aerodynamic diameter is proportional to particle physical size and specific gravity. This diameter is used to compute the ability of a particle to follow an air flow. Aerodynamic diameter is of interest for removal rates and when particle drag is significant as in wind tunnel simulations. Instruments used to measure aerodynamic diameter normally express the diameter as the product of physical diameter and square root of particle specific gravity (assumed to be one unless better information is available). The optical diameter is proportional to physical size and optical refractive and absorptive characteristics. Optical particle counters that relate scatter magnitude to particle diameter express particle diameter as equivalent to that for a calibration particle material (often polystyrene latex) and diameter or in terms of true diameter when the refractive indices of the particle material are known. Optical particle counters are normally used for atmospheric aerosol measurements because they can count particles at high rates (thousands per second) and because an optical measurement is meaningful for an E-O. Both aerodynamic and optical particle-sizing systems assume the measured particles are spherical, which is rarely the case. Hence, it is important to understand that the measured size is an equivalent diameter in accord with the response function of the instrument.

Aerodynamic particle measurement systems use active sampling. Optical particle counters use active or passive sampling systems. Active samplers draw a sample of the aerosol into the measurement system. Passive samplers allow the aerosol to drift through the measurement system as transported by atmospheric winds. Active samplers are commonly found in field applications; however, they must be used with care to ensure that the aerosol is sampled isokinetically. Isokinetic sampling is achieved when the sampling tube inlet pressure is adjusted such that flow streamlines passing around the sampling tube inlet are not perturbed. If the inlet pressure is too high, the streamlines are pulled into the inlet, effectively increasing the inlet sampling area and producing aerosol concentration measurements that are higher than the true value. If the inlet pressure is too low, the streamlines are diverted away from the inlet and the aerosol concentration measurements are lower than the true value.

An optical particle counter for atmospheric measurements should be able to measure number densities as high as $10^5/\text{cm}^3$ and detect particles as small as 0.3 μm in diameter and as large as 10 μm . If the counter uses active sampling, the system should be capable of sampling isokinetically by pointing the sampling head into the wind and adjusting the dynamic pressure for a range of wind speeds between 1 and 8 m/s. Because there are no standard aerosols, it is important that aerosol data acquired with an optical counter be compared with other independent measurements to at least determine data consistency between measured variables such as particle size distributions and mass concentrations obtained with filter samplers.

The number of aerosol counters required for a line of sight depends on the relative variance of the size distribution along the line of sight and the desired coefficient of variation

(see [Equation 2-6](#)). If the relative variance for the particle size distribution is large, an integrated path measurement utilizing multispectral transmittances from which the size distribution is inferred using an inversion algorithm is a more cost-effective approach than employing a large network of individual particle sizing systems.

2.3.5 Aerosol Speciation

The type of particle causing the aerosol extinction is sometimes important to determine what kind of atmospheric phenomena are occurring in the region. For example, the strong signal of brown carbon from a nearby forest fire in a littoral environment may require a certain discounting of the realism of the atmosphere. Identification of the actual species is currently performed by association to the size of the particles. More precise instrumentation may be deployed to determine the quantities of each major species of aerosol being detected by deployed particle counters. Aerosol origins include sea salt spray, volcanic duct, forest fires and human wood burning, petroleum combustion, desert sandstorms, pollen, and agricultural plowing.

2.3.6 Precipitation

Precipitation is commonly considered to include all forms of water that fall out of the atmosphere. For precipitation to occur, the equivalent aerodynamic particle diameter must be about 10 μm or larger. Measurements of precipitation include those for precipitation type, rate (or mass concentration), and temperature. These characteristics are addressed in the discussions that follow. Precipitation measurements are particularly important for sensor systems that operate in the MMW spectral bands where attenuation because of liquid water is particularly strong. When precipitation is frozen, attenuation at MMW frequencies is significantly less than that for liquid water. Thus, radar systems can distinguish between so-called wet snow (strong return when the snow is a mixture of ice and liquid water) and dry snow (weak return because the snow is virtually all ice).

Extinction and backscatter of MMW are strongly dependent on precipitation particle shape. Temperature, wind speed versus height, and precipitation forms are particularly important parameters needed to quantify MMW transmission characteristics through precipitation. Even raindrops become distorted into oblate spheroids that have their axes of symmetry canted in proportion to horizontal wind velocities. The raindrop canting angle affects the transmittance characteristics of polarized MMW radar; therefore, wind speeds and wind speed profiles are also important parameters in specifying MMW transmission through rain ([Table 2-1](#)).

Schemes for classifying frozen precipitation shapes are common and should be used as a matter of record. For example, snow and sleet types have been separated into the following category shapes.³³

- | | | | | |
|-------------|------------|----------------------|-----------------------|----------|
| 1. plates | 3. columns | 5. spatial dendrites | 7. irregular crystals | 9. sleet |
| 2. stellars | 4. needles | 6. capped columns | 8. graupel | 10. hail |

2.3.6.1 Precipitation Type

Precipitation type falls into three general categories: liquid water, frozen water, and liquid and frozen water mixtures. Liquid water precipitation ranges in size from tens of micrometers to raindrops about 10 mm in diameter. Above 10 mm in diameter the drops become aerodynamically unstable and break up. Raindrops greater than about 240 μm in diameter begin

³³ Schaefer, V. J. and J. A. Day. *A Field Guide to the Atmosphere*. Boston: Houghton Mifflin, 1998.

to deviate from spherical shapes. Air resistance forces the drops into oblate spheroidal shapes that have their axis of symmetry tilted by winds through which they fall (Oguchi, 1983). The size distribution of raindrops is typically multimodal. It is not unusual for three or more modes to exist. Normally, most raindrop sizes are less than 1 mm in diameter.

Frozen precipitation includes snow, sleet, graupel, and hail. Snow has a wide variety of shapes. Sleet differs from snow in that sleet does not have the well-organized crystalline structure observable in snow. Hail stones are spheroidal rigid spheres ranging in size from millimeters to several centimeters in diameter.

Many forms of frozen precipitation appear as a mixture of solid and liquid water. Snow may be “dry” or “wet” depending on the relative amount of liquid water present. Sleet is often a combination of frozen and liquid water. The surface of hail is often a thin layer of liquid water. The ratio of frozen to liquid water depends on the precipitation form for the air temperature and humidity distribution through which the precipitation falls and the terminal velocity of the precipitation.

Instruments that measure precipitation particle size and shape must use methods that can accommodate nonspherical particles and particles that are significantly larger than aerosol particles. For example, snow comes in a wide range of shapes, as does sleet. Thus, instruments that record images of the precipitation such as photographic or holographic cameras are often used for research types of measurements. Indirect means of inferring precipitation particle size and shapes include the use of polarized radars (Oguchi, 1983).

It is common practice to measure frozen precipitation in terms of equivalent liquid water content. A device for these types of measurements has been developed by the Canadian Defense Research Establishment, Val Cartier, and the U.S. Army Corp of Engineers Cold Regions Research and Engineering Laboratory.³⁴ Number densities of precipitation particles are much lower than aerosols, but because of their increased sizes, they typically have much higher mass concentrations.

2.3.6.2 Precipitation Rate

Precipitation rate is a commonly used integral measure of mass concentration per unit time (particle flux) delivered by the precipitation source. The precipitation rate for any particle form can be expressed in the form of an equivalent rain rate (Oguchi,). The rain rate in mm/hr is

$$R = 4.8\pi \cdot 10^{-3} \cdot \int_0^{a_{max}} v(a) a^3 n(a) da \quad \text{Equation 2-16}$$

where $v(a)$ is the terminal velocity in m/s, a is the drop radius in millimeters, and a_{max} is the maximum radius in the number density at size a per size increment, $n(a)$. For precipitation that is not liquid drops, [Equation 2-16](#) shows the precipitation rate is affected by the mass distribution $a^3 n(a)$ of the precipitation, most commonly modelled by the Marshall-Palmer Distribution³⁵ expressed as $N(D)$, which is a truncated gamma function, and the particle terminal velocity (a strong function of particle shape). It is common practice to relate radar attenuation

³⁴ James Lancombe. “A Technique for Measuring the Mass Concentration of Falling Snow.” In *Optical Engineering for Cold Environments*, V. 0414, pp. 17-28.

³⁵ Marshall, J. S. and W. M. Palmer. “The distribution of raindrops with size.” In *Journal of Meteorology*, ed. 5, pp. 165-166. August 1948.

and cross section to rain rate in the form expressed by [Equation 2-16](#). The attenuation is approximately:

$$A \text{ (db/km)} = \kappa R^\gamma \quad \text{Equation 2-17}$$

The rain rate or its equivalent correlates uniquely with particular radar frequencies and precipitation types. The constants κ and γ are unique for each radar frequency. [Equation 2-16](#) and [Equation 2-17](#) illustrate the need for accurate precipitation measurements down the propagation line of sight or from a properly spaced network of sensors that can detect the type of precipitation as well as its rate.

2.3.6.3 Precipitation Temperature

Because the complex dielectric constant of water at MMW frequencies is a function of temperature, it is important to determine the precipitation temperature.³⁶ The complex dielectric constant is a major parameter that determines MMW attenuation propagation characteristics. Liquid water is strongly absorbing at MMW frequencies; ice is nearly transparent. Changes of fractions of a degree near 0 °C can affect the attenuation characteristics of precipitation by orders of magnitude. This is the reason for the so-called ‘bright-band’ radar effect for wet snow, which has a significant liquid water content. The precipitation temperature must be the true thermodynamic temperature rather than an equivalent brightness temperature such as might be produced by a FLIR measurement.

2.3.7 Terrain Signatures

Terrain signatures are one of the major backgrounds against which E-O sensors must detect targets. Atmospheric conditions affect the terrain signature in visual, infrared, and MMW bands. Dew and frost, for example, provide a much brighter background against which to detect targets than dry vegetation. Moist soil has a different infrared emissivity than dry soil. Further, the amount of water vapor and other absorbing gases in the atmosphere can radically affect the observed terrain spectral signature at long distances. Although terrain signatures are not explicitly related to atmospheric characteristics, the interaction of terrain signatures with atmospheric characteristics affects the performance of E-O sensors. Thus, this section briefly discusses atmospheric effects on terrain signatures, with the view that evaluation of E-O sensor performance in the atmosphere can require measurement of these parameters as supporting data.

2.3.7.1 Dew and Frost

Dew and frost increase the reflectivity or emissivity of background terrain. Dew is more likely to produce nearly specular reflections of background radiation, whereas frost has a higher magnitude diffuse reflection component in the visual band. In the thermal infrared bands, dew in droplet form reflects sky radiation, which appears much cooler than normal terrain signatures. Frost specular reflection in the thermal infrared band will have a similar effect. In the MMW bands, dew will be highly reflective because of the liquid water component, whereas frost reflectivity will depend mainly on the small fraction of liquid water present in the frost. The frozen component contributes relatively little signal return.

Meteorological parameters used to characterize dew and frost include the temperature and relative humidity conditions under which they are formed and the temperature of

³⁶ Matthew N. O. Sadiku. “Refractive Index of Snow at Microwave Frequencies.” In *Applied Optics* V. 24, Issue 4, 15 February 1985. pp. 572-575.

background terrain on which they condense. For electro-optical sensor testing, it is important that the background visual luminance and infrared radiance magnitudes be measured in the direction of the sensor as well as the target-to-background contrast. At times when dew and frost are significant factors in scene characterization, background lighting and the dew and frost level changes rapidly. Consequently, it is important that the characterization data be sampled at rates as high as possible with 10-point running averages used to smooth the data and that averages of the data be made over times in which the mean value of the measured parameter is stationary.

2.3.7.2 Target/Background Emissivities

Emissivity is defined as the ratio of spectral radiance emitted by an object to that of a perfect black body at the same temperature. Most previous field tests and analyses have assumed that the emissivity of backgrounds and targets were identical, had a value near that of a blackbody (0.98 - 1.0), and were independent of wavelength (a so-called graybody). These assumptions allow radiance differences between targets and backgrounds observed with 3-5 and 8-14 μm band FLIRs to be expressed in terms of apparent temperature differences between targets and backgrounds because the radiometric difference is linearly proportional to thermodynamic temperature difference. As a result, FLIR performance and response specifications are often given in terms such as MRTD. This approach has resulted in much confusion and test data that are highly limited in the scope of their applicability to other scenarios. For example, the MRTD is a function of the absolute magnitude of the source radiance for which it was developed. Different calibration source magnitudes yield different MRTD response values. It is possible (and may often occur) that a radiometric difference can be observed between target and background when both objects have identical thermodynamic temperatures because spectral emissivities between target and background are not equal. The assumption that thermodynamic temperature difference between target and background is nearly the same or linearly proportional to the brightness temperature or radiometric temperature difference leads to major differences between predictions and observations. A rule of thumb is that a 1% change in emissivity corresponds to a half degree change in brightness temperature difference.^{37,38} Thus, a target moved to a slightly different background from those of the test conditions, but operating under identical meteorological and thermodynamic conditions, could have a significantly different radiometric contrast that affects the performance envelope of the sensor under test. If emissivity varies with wavelength, sensor radiometric response is the integral product of emissivity and sensor spectral response. This means extrapolation of sensor performance among sensors operating in the same spectral band, but with different sensor spectral responses, is nonlinear. Sensor performance extrapolation in this case can be estimated accurately only with a response inversion algorithm.

Similar considerations apply to tests where the sensor background is sky or sea. The magnitude of background infrared radiation for sky backgrounds is typically less than that for terrain backgrounds. A sky background with clouds can fluctuate strongly as a function of Sun position relative to sensor line of sight and terrain reflectivity. Both solar and terrain reflectivity contribute to cloud illumination. To first order, terrain reflectivity is 1 - spectral emissivity. Thus, cloud radiation indirectly depends on emissivity from the terrain supplying radiation to the

³⁷ William Wolf. "Differences in Radiance: Relative Effects of Temperature Changes and Emissivity Changes." In *Applied Optics* V. 14, Issue 8, 1 August 1975. pp. 1937-1939.

³⁸ W. Michael Farmer. "Analysis of Emissivity Effects on Target Detection Through Smokes/Obscurants." In *Optical Engineering* V. 30, November 1991. pp. 1701-1708.

ground-illuminated cloud. Over water surfaces, the surface emissivity (1 - spectral reflectivity) and reflectivity depend on the angle of incidence of the incident radiation on wave surfaces. Surface roughness, or sea state, which defines the distribution of wave reflecting angles, plays a major role in the thermal contrast background.³⁹ At the land-sea interface where terrain and water wave emissivity and reflectivity must be considered simultaneously, detailed spectral measurements and specification of water and terrain conditions are required. The signature database for the land-sea interface is limited and is undergoing major development.

It is important to determine the spectral emissivity of the target and target background in order to ensure that meteorological and target signature data for E-O systems operating in the infrared bands are consistent between measurements over similar types of background. There is no standard method for the measurement of emissivity. A recommended method for determining emissivity is to measure the bidirectional reflectance distribution function (BRDF). The emissivity is taken to be (1-BRDF). The BRDF is the variation of reflected radiance (power projected per unit projected area per unit solid angle) per unit variation of incident irradiance for given polarization states of source and receiver. Spectral resolution for emissivity measurements should be at least 4 cm^{-1} .

2.3.8 Humidity and Temperature Structure Constants

Most atmospheric effects on E-O sensor performance depend on differences in optical paths rather than absolute values of optical paths. The notable exceptions are radars where absolute path lengths are critical. Spatial statistics of random atmospheric variable differences for index of refraction, humidity, or temperature are often given in terms of structure functions rather than autocovariance or autocorrelation functions. Structure functions are typically defined as the ensemble average of the square of the difference between the variable measured at two spatial locations. If the random process producing the parameter is isotropic, the structure function is a function only of the absolute distance between the measurement points. In the atmosphere, solar heating produces kinetic energy over scale sizes that range from meters to global sizes. Near the Earth's surface, kinetic energy leaves the air by frictional generation of heat over scales that range from a few millimeters to a few meters. This phenomenon is called the inertial sub range. Over this range, the structure functions are proportional to the separation distance raised to the $2/3$ power. The constant of proportionality is the structure constant. Structure constants are functions of height above ground, wavelength, and transmission path length. For homogeneous turbulence, structure constants are proportional to correlation lengths for index of refraction, relative humidity, and temperature.^{40,41,42}

The index of refraction structure functions is used to compute such factors as laser beam spread through a turbulent atmosphere as a function of wavelength and path length and refraction. Optical turbulence primarily affects sensors in the visual and infrared wavelength bands. It has relatively little impact on MMW and microwave frequencies; however, the MMW

³⁹ Miriam Sidran. "Broadband Reflectance and Emissivity of Specular and Rough Water Surfaces." In *Applied Optics*, V. 20, Issue 18, 15 September 1981. pp. 3176-3183.

⁴⁰ Ochs, G. R. and Ting-I Wang. "Finite Aperture Optical Scintillometer for..." In *Applied Optics*, V. 17, Issue 23, 1 December 1978. pp. 3774-3778.

⁴¹ Churnside, J. H., Richard J. Lataitis, and Robert S. Lawrence. "Localized Measurements of Refractive Turbulence Using Spatial Filtering of Scintillations." In *Applied Optics*, V. 27, Issue 11, 1 June 1988. pp. 2199-2213.

⁴² Biloft, Christopher A. and Rick D. Wald. *Dugway Optical Climatology Study*. DPG # DPG-FR-89-711. Available at <https://apps.dtic.mil/sti/citations/ADA220136>.

bands are affected by water vapor absorption, which is a function of relative humidity and temperature fluctuations caused by atmospheric turbulence. Thus, the primary structure constants of interest for MMW propagation are those for temperature and relative humidity. The index of refraction structure constants can be measured with path-integrating instruments such as those developed by the National Oceanic and Atmospheric Administration (Ochs and Wang 1978, Churnside et al., 1988). These instruments are preferred over techniques using point measurements obtained by, for example, measuring the temperature structure constant with sets of thermometers, then computing the index of refraction structure constant. The integrated path instruments are preferred because of the likely variation of the structure constants along the measurement path. The structure constants represent integrated path conditions and should be measured accordingly. Similar considerations apply for the effects of turbulence on MMW propagation; however, MMW-equivalent scintillometers are not common. Most structure constant measurements for temperature and relative humidity are made with networks of point sensors. Values of the cross correlations between temperature and absolute humidity are assumed to provide the necessary structure constants for evaluating the effects of turbulence on MMW propagation. Included in this technique is the Bulk Method of calculating near-surface turbulence over the ocean developed by Naval Postgraduate School, Monterey. The Bulk Method evaluates the air-sea temperature difference using the following semi-empirical model to compare the air-sea temperature difference with expected optical turbulence values, as illustrated in [Figure 2-17](#). The bulk C_n^2 estimates were computed for wind speed = 5 m/s, sea temperature = 16 °C, height above the surface = 5 m, and wavelength = 3.8 μm.

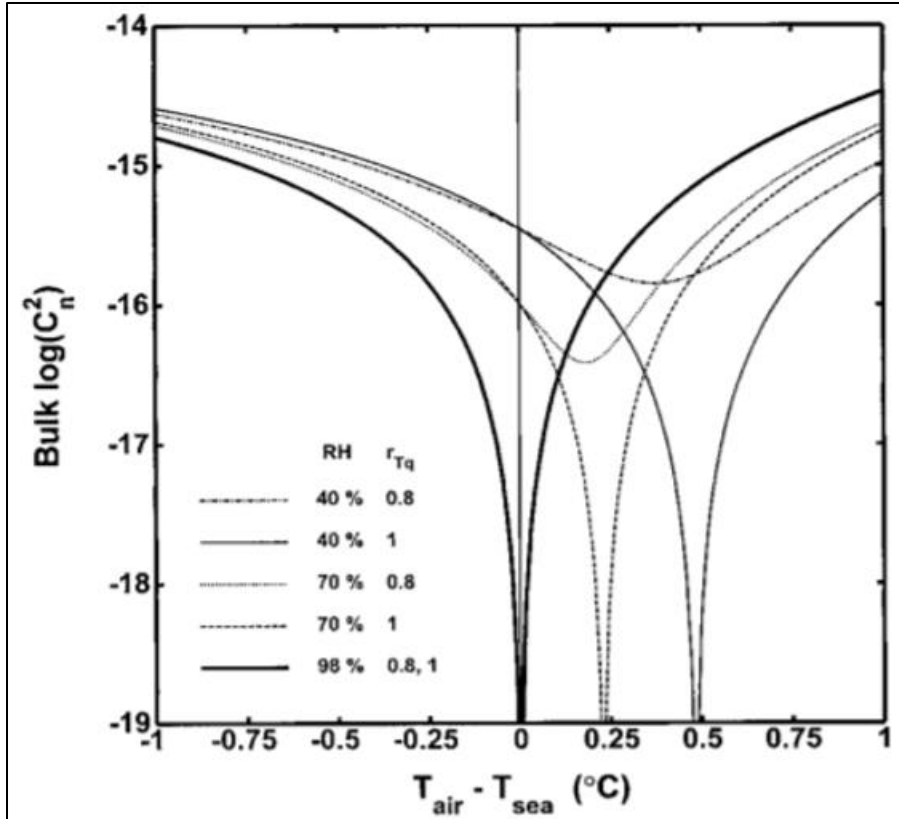


Figure 2-17. Bulk Log Estimates for Different Values of Relative Humidity (RH) and Temperature-specific Humidity Correlation Coefficient (r_{Tq}) as Indicated, vs. Air-Sea Temperature Difference⁴³

Unfortunately, these data may not agree well with similarity theory predictions (Biltoft and Wald, Cook and Burk⁴⁴). The Monin-Obukhov similarity theory in fluid mechanics hypothesizes that nondimensionalized properties of a flow are universal functions of a stability parameter. The theory is reasonably accurate for some atmospheric variables, but not for potential refractivity (Cook and Burk). The assumption that refraction effects can be treated with similarity theory by assuming temperature and humidity variations are always coherent is commonly used because some models can be greatly simplified (Andreas⁴⁵ and Rachele and Tunick). In some applications, the assumption of a temperature-humidity coherence value of 1.0 leads to the unrealistic result that the structure constant for refractive index approaches 0 for MMW propagation (Biltoft and Wald, Rachele and Tunick).

2.3.9 Sea State

Sea-state specification is necessary to estimate sea target background. The World Meteorological Organization sea-state scale should be employed to define sea state in commonly

⁴³ Frederickson, P. A., K. L. Davidson, C. R. Zeisse, and C. S. Bendall. "Estimating the Refractive Index Structure Parameter (C_n^2) over the Ocean Using Bulk Methods". In *Journal of Applied Meteorology*, Vol. 39, pp. 1770-1783. October 2000.

⁴⁴ Cook, J. and Stephen Burk. "Potential Refractivity as a Similarity Variable." *Boundary Layer Meteorology*, 58, pp 151-159, 1992.

⁴⁵ Edgar Andreas. "Using Scintillation at Two Wavelengths to Measure Path-Averaged Heat Fluxes in Free Convection." *Boundary Layer Meteorology*, 54, pp 167-182, 1991.

accepted terms. The specification of sea state is particularly important for evaluation of imaging systems in the visible and infrared bands. Depending on sea state, radiation specularly or diffusely reflected or emitted from the surface can be polarized. Computation of reflection or emission from wind-driven waves assumes that the surface consists of many plane facets having various slopes and large dimensions relative to the wavelength of the radiation. Therefore, it is necessary to define the size, tilt, and orientation of the wave facets relative to the wind vector and to measure the wind vector to characterize the sea state. If it is not possible to directly measure wave facet size, tilt, and orientation, the measurement of the wind vector can be used with the probability distribution developed by Cox and Munk to predict facet tilt and orientation angles (Sidran, 1981). Sensor performance can be radically affected by the polarization of the background radiation. It is important that the polarization properties of the radiation be determined if the E-O sensor under test is polarization-sensitive.

Note that sea state, especially wind-driven seas, can have significant effect on aerosols and energy flux in the maritime environment. The influence of sea spray on the surface heat and moisture exchange peaks during times of greatest difference between air and sea temperatures. When air temperature is low, sea spray-sensible heat flux can be nearly as great as the spray-latent heat flux at high latitudes. In addition, sea spray enhances the air/sea enthalpy flux during high winds as a result of temperature and humidity redistribution in the marine boundary layer. Sea spray droplets injected into the air thermally equilibrate ~1% of their mass. This leads to the addition of sensible heat to the atmosphere prior to ocean reentry, enhancing their potential for significant enthalpy input.

2.3.10 Background Radiation

One of the most difficult tasks in evaluating E-O sensor performance in the atmosphere is the measurement of the background radiation budget. Radiation sources include the Sun, moon, stars, reflection and emission from terrain, clouds, and atmospheric scatter from all sources. Each source has spectral structure and a magnitude that can vary with time of day and location, the most notable being the Sun corridor of energy reflection from the ground or ocean. If the spectral response of the E-O sensor under test is not constant over the spectral operating band, it is important to spectroscopically measure the spectral content of the background radiation. If the sensor response is spectrally constant, then it is proper to measure only the integral value of the background radiation with a calibrated broad-band sensor. Direct and diffuse radiation in the visual band (0.4-0.7 μm) and near-infrared (0.7 – 2.8 μm) are typically measured with a pyrhelimeter and pyranometer. Diffuse infrared irradiance in the 3-20 μm band is measured with a pyrgeometer. A radiometer that uses a circularly variable filter is typically used to measure spectral radiance and irradiance, especially in the thermal infrared bands where spectral resolution is low. An FTS can be used to provide high-resolution spectral measurements in the 2-14 μm band. Photographic imagery can provide a qualitative measure of the relative intensities of background radiation, when data are collected at the wavelength of interest. The following subsections discuss the characteristics of the various sources of atmospheric radiation.

2.3.10.1 Global Irradiance

Global irradiance is the total radiant flux density incident on the Earth's surface from the totality of the upward hemisphere. It includes radiation contributions from the Sun and sky. It is also referred to as global radiation, insolation, or solar radiation.

2.3.10.2 Diffuse Global Radiation

Global irradiance is often considered to be formed of direct radiation (from the Sun only) and diffuse radiation (from the sky only). The diffuse global radiation is the integral of the sky radiance, R_{sky} , over the entire upward hemisphere excluding the Sun (SWOE Report 91-14).

$$E_{sky} = \int_{2\pi} R_{sky} \cos\theta d\Omega \quad \text{Equation 2-18}$$

θ is the solar zenith angle measured from the vertical and $d\Omega$ is the differential increment of sky solid angle centered about θ that contributes to the diffuse global radiation observed at a point on the surface. The global irradiance is found by adding the solar beam irradiance to the diffuse sky component.

$$E_{global} = E_{sky} + E_{sun} \cos(\theta_{zn}) \quad \text{Equation 2-19}$$

Where E_{sun} is the solar beam irradiance and θ_{zn} is the solar zenith angle.

2.3.10.3 Directional Sky Radiation

Isopleths (constant contours) of diffuse sky irradiance are spatially variable and change with time as the Sun changes position in the sky. Near the Sun, the isopleths are circular. As the angle from the Sun increases, the isopleth circular symmetry is quickly changed to paths that encompass the entire upward hemisphere. For air-to-ground or ground-to-air E-O sensor applications, it is important to specify the sky or solar beam radiation within the sensor's field of view. This radiation level determines in part the sensor signal-to-noise ratio. By determining the sky radiation isopleths at which the sensor is pointed, sensor performance can be decided over the range of zenith and azimuth angles encompassing the isopleths that are less than or equal in magnitude to the isopleths. A spectral radiometer mounted on a tracking theodolite is typically used to measure sky isopleths.

Aerosol optical depth (AOD), or aerosol optical thickness is a measurement of aerosols distributed within a column of air from the instrument to the top of the atmosphere. Common aerosols include, but are not limited to, urban haze, smoke particles, dust, and sea salt. On a clear day (that is, with no clouds obstructing the path from the photometer to the Sun) AOD can be measured with a Sun photometer. The photometer measures solar irradiance at the location of the photometer that is used to compute dimensionless AOD values. The Sun photometer can measure solar irradiance at different wavelengths that will affect the AOD value. Shorter wavelengths will increase AOD values. Since AOD correlates to overall path transmissivity, it plays an important role in determining the effectiveness of laser weapons, and can be used to provide a reference level of optical thickness to improve the accuracy of lidar extinction measurements.

2.3.10.4 Sky-Ground Luminance Ratio

Luminance is radiance weighted by the wavelength according to the spectral response of the human eye. The sky-ground luminance ratio (often called sky-ground ratio) is the ratio of horizon sky luminance immediately above the target to the ground-level luminance surrounding the target. The luminances are measured with a telephotometer using a photopic filter to ensure proper spectral response for the measurement. [Figure 2-14](#) illustrates the potential sources of

variation of the sky-ground luminance ratio in a single scene. It is important that the lines of sight for this measurement are commensurate with the E-O sensor view of the target. Not only does ground-level luminance vary greatly, but horizon-sky luminance is a strong function of Sun position. As previously stated, a major application of the sky-ground luminance ratio is computation of visual range, as discussed in Subsection [2.3.1](#).

2.3.10.5 Downwelling Spectral Direct Radiation

The downwelling spectral direct radiation is spectrally resolved direct solar radiation. It is the same measurement described in Subsection [2.3.10.1](#), except that the input radiation is spectrally resolved. Such data are required to compare different sensors operating in the same spectral band and to model scene images from first principles. Spectrometer resolution required for these measurements varies with the application for which the data are intended. The resolution can vary for the infrared bands from 4 cm^{-1} , for applications where aerosol scatter and precipitation have significant impact on the radiation reaching the surface from the Sun, to 16 cm^{-1} or larger, when band averages are the primary concern for sensors such as FLIRs. For visual to near-infrared bands, spectral resolution of the order 100 angstroms is sufficient. The magnitude and spectral content of this radiation are highly variable and dynamic because the solar radiation moves through an air mass that has a wide diurnal range. The sampling frequency of the measurement spectrometer must be at a rate sufficient to ensure that co-added measured spectra are obtained through essentially the same air mass. It is normal practice to improve measured spectrum signal-to-noise ratio by co-adding repeated spectral measurements. If N spectra are co-added, the signal-to-noise ratio will increase by \sqrt{N} .

2.3.10.6 Downwelling Spectral Diffuse Radiation

Downwelling spectral diffuse radiation is spectrally resolved sky radiation incident at the surface. It is the same measurement described in Subsection [2.3.10.2](#), except that the input radiation is spectrally resolved. This measurement is made for the same reasons as those for the direct radiation. The same spectrometers, spectral resolution, and sampling rates are used for these measurements as for those of the direct measurements.

2.3.10.7 Directional Spectral Sky Radiation

Directional spectral sky radiation is represented by isopleths of the type described in Subsection [2.3.10.3](#), except that the isopleth is spectrally resolved for the spectral band considered. Alternatively, narrow-band filters can be used to generate narrow-band isopleths rather than those for a broad band. Narrow-band isopleths can be different from those of the broad band, which are much more dependent on measurement radiometer characteristics. Broad-band isopleths are weighted by the spectral response of the radiometer used to make the observation, the spectral distribution of energy within the band, and the spectral scattering characteristics for the atmosphere.

2.3.11 Spectral Transmittance

Spectral transmittance is a fundamental radiometric measurement for narrow- or broad-band E-O sensor systems. A transmittance measurement is said to be narrow-band if $\beta(\lambda)$, the atmospheric extinction as a function of wavelength, is constant in the interval λ_1, λ_2 , and the atmospheric transmittance can be brought outside the integral representing band averaged transmittance (see [Equation 2-20](#)).

$$\tau = \frac{I}{I_0} = \frac{\int_{\lambda_1}^{\lambda_2} e^{-\beta(\lambda)Z} \Phi d\lambda}{\int_{\lambda_1}^{\lambda_2} \Phi(\lambda) d\lambda} \quad \text{Equation 2-20}$$

The measurement is broad-band if the atmospheric transmission containing $\beta(\lambda)$ must be kept under the integral because of significant variations in transmittance between λ_1, λ_2 . Narrow-band transmittance is typically measured using a laser for the source or a narrow-band filter to reject background illumination, thereby increasing the dynamic range of the measurement. Narrow-band measurements are normally used to quantify performance of laser systems. Broad-band measurements are normally made using high-temperature (1000-1500 °C) blackbody sources with outputs collimated to a few milliradians of divergence. A broad-band receiver is either a single passband system or a spectrometer that performs a series of narrow-band measurements across the band. Broad-band E-O sensors such as FLIRs operate in a single passband. A spectroscopic measurement is required of transmittance across the passband of the sensor in order to accurately interpret E-O system performance. The FTSs are especially appropriate for this task because they produce high resolution and have the highest throughput and fastest spectral acquisition for any spectrometer operating in the 2-14 μm band. A circularly variable filter radiometer, while having much lower resolution capabilities than an FTS, can be configured to measure bands in the visible through 14 μm band at 1-2 Hz rates.

A transmittance measurement is made with a known radiation source and a radiometer viewing the source. The purpose of spectral transmittance data is to determine the attenuation as a function of wavelength, which is used to determine target probability of detection. To obtain meaningful results, the transmittance source must either have the same spectral content as the target, or must be calibrated such that equivalent transmittances for low-temperature target radiation and a high-temperature transmissometer source can be computed. For example, transmissometer sources are often blackbodies that operate at temperatures between 1000-1500 °C (1273-1773 K). This source transmittance is applied to sensors operating against tank targets that are less than 30 °C. Even if the tank is a perfect blackbody (which it is not) like the radiometer source, the difference in temperatures means that the transmissometer source and tank spectral irradiance characteristics are widely different. Transmittance measured with a radiometer observing a high-temperature source can be much different than that for a FLIR observing the low-temperature tank even though the radiometer and FLIR are measuring and observing commensurate lines of sight and are operating in the same spectral band. This effect is illustrated by [Figure 2-18](#) and [Figure 2-19](#). The 3-5 μm blackbody spectral distributions for a 1500 °C (1773 K) transmissometer source and 27 °C (300 K) target are depicted in [Figure 2-18](#), which also shows the hot radiometer source has a different spectral structure than the cool target. The spectral radiance increases nearly two orders of magnitude between 3 and 5 μm . For the same spectral band, the transmissometer source spectral radiance decreases by about 50%. [Figure 2-19](#) shows source and target transmittance through a water fog as a function of concentration length expressed as the product of the fog Sauter mean particle diameter, D_{32} in micrometers and the water density, ρ_0 , and ratio, Z/V of transmission distance for the radiometer and target sources, Z , relative to visual range, V . [Figure 2-19](#) clearly shows the major differences in transmittance between the two sources. These results show, for example, that if the high-temperature transmissometer source yields a transmittance of 1%, the actual target transmittance is about 5%. If the probability of detection was 50% at 1% transmittance, the target is more likely to be seen than is predicted by the high-temperature source transmissometer measurement.

When a transmittance measurement is made to support E-O sensor evaluation in the atmosphere, it is important to express the measured transmittance in terms of the sensor-to-target transmittance that actually occurs. The transformation is possible provided the spectral content of the transmissometer source and target and spectral response of the transmissometer radiometer and sensor are known in addition to the directly measured transmittance.⁴⁶

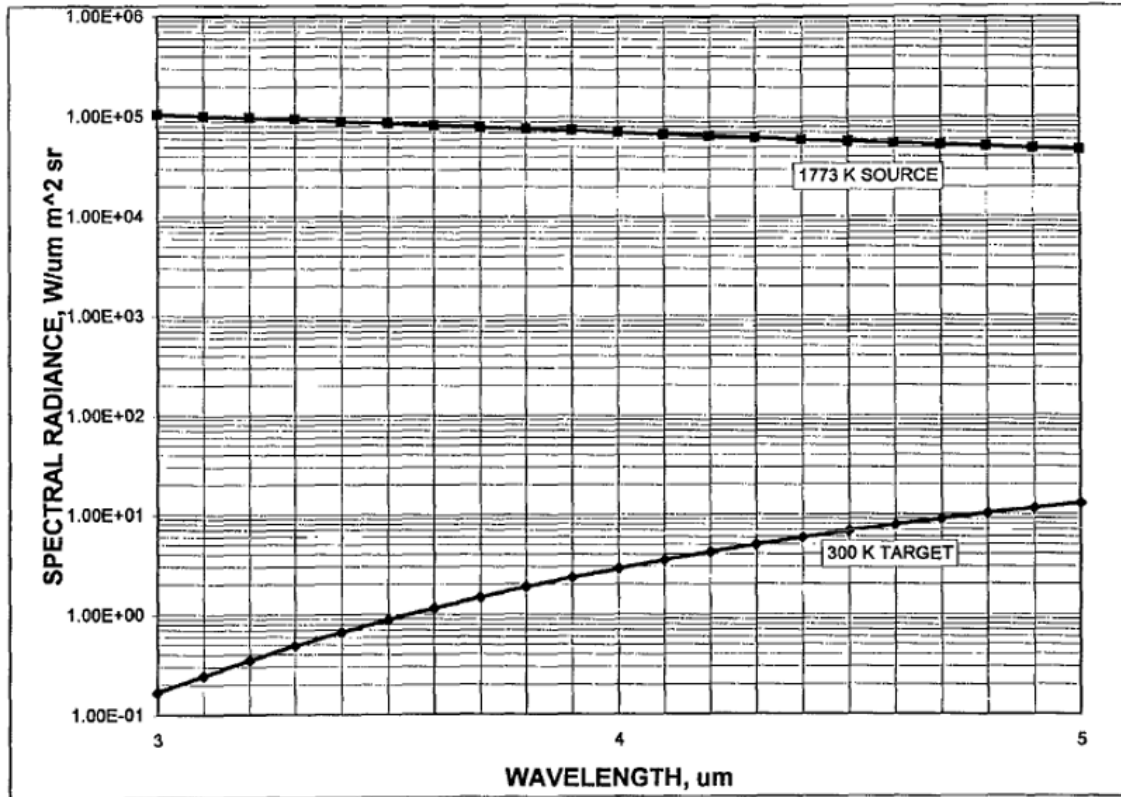


Figure 2-18. 3-5 μm Band Spectral Irradiance Distributions for a 27 °C (300 K) Blackbody Target and 1500 °C (1773 K) Blackbody Radiometric Source

⁴⁶ Farmer, W. M. and Roger Davis. "Computation of Broad Spectral Band Electro-Optical System Transmittance Response Characteristics to Military Smokes/Obscurants Using Field Test Data from Transmissometer System Measurements." Technical Report AMCPM-SMK-CT-011-89. In *Proceedings of the Smoke/Obscurants Symposium XIII*, pp. 259-273, Aberdeen Proving Ground, MD 21005, 1989.

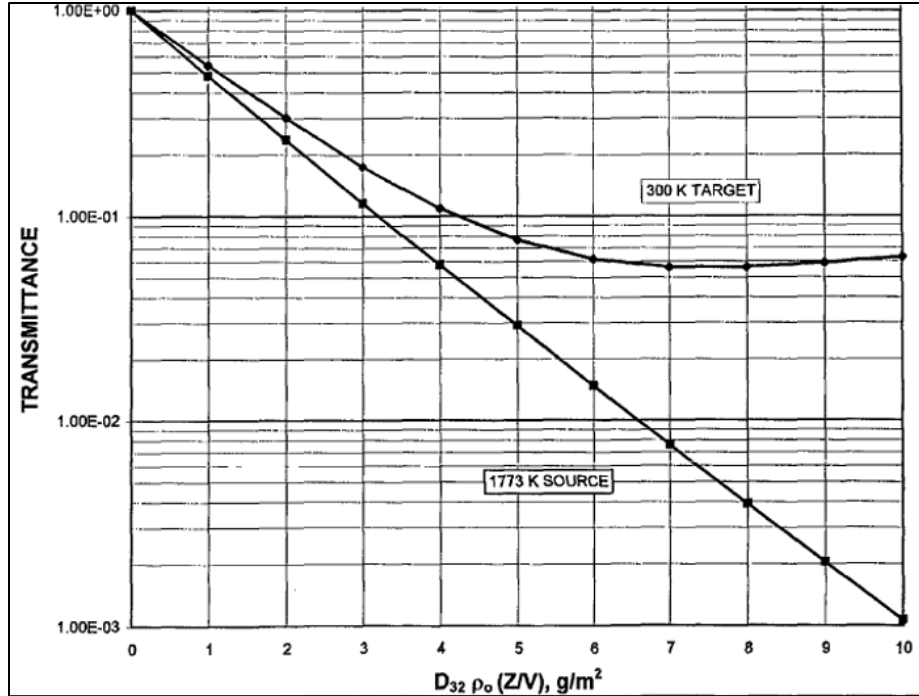


Figure 2-19. 3-5 μm Transmittance to a 27 °C (300 K) Blackbody Target or a 1500 °C (1773 K) Radiometric Source

There are two broad categories of transmittance measurement made to support E-O sensor testing in the atmosphere: absolute transmittance and relative transmittance. In each of these categories either a narrow-band or broad-band transmittance measurement is made. To clarify the significance of these classifications, consider the equation representing the transmittance process. Equation 2-20 calculates transmittance. $\beta(\lambda)$ is the atmospheric extinction, $\Phi(\lambda)$ is the source and radiometer spectral response, λ_1, λ_2 are the limits of the spectral band over which the transmittance is measured, I_1 is the integrated source irradiance magnitude at the aperture of the radiometer, and I_0 is the integrated source radiance magnitude for zero pathlength. Z is the distance between the transmitter and receiver.

Absolute transmittance is measured by determining absolute values for I_1 and I_0 . If the source is perfectly collimated, $I = I_0$. However, normal optical divergence spreads the transmitted radiation beam, and if the spatial distribution of the beam is not uniform, it can be significantly different than at the zero path length measurement at the source. Furthermore, refractive turbulence, depending on the magnitude of the refractive index structure constant, C_n^2 and wavelength will spread the beam over an area larger than normal optical divergence. Thus, an absolute transmittance measurement is extremely difficult and rarely attempted, except with highly collimated sources that produce spatially uniform beams transmitted to large-aperture radiometers of sufficient size to fully collect radiances that are spread and modulated spatially and temporally by refractive turbulence. Absolute transmittance measurements are required to

verify that models such as MODTRAN or FASCODE define the performance envelope of a sensor or define the aerosol or gaseous content of the atmosphere.^{47,48}

Relative transmittance is much easier to measure than absolute transmittance. Relative transmittance is obtained by normalizing the measured radiance from the source by the radiance measured for a particular path situation, rather than for the zero path source radiance. For example, relative transmittance is used to quantify the attenuation resulting from smokes/obscurants in a sensor line of sight relative to that of clear air. Thus, the transmittance with smokes/obscurants in the sensor line of sight is measured relative to the transmittance when none are present. This measurement yields a measure of the concentration length (the product of mean concentration and transmission path length) and extinction properties of the smokes/obscurants in the sensor line of sight. Relative transmittance measurements define and detect changes to a reference atmosphere.

2.3.12 Index of Refraction Structure Constant

The index of refraction structure constant (see Subsection [2.3.8](#) for a definition of refraction structure constant) can be computed from the correlation of integrated path variations between parallel transmitted beams (the principle behind the optical scintillometer [Ochs and Wang, Churnside et al.]), derived from noise signals on optical systems, or from the correlation of vertically separated relative temperature or humidity sensors. Of the three, the integrated path optical scintillometer such as the Scintec BLS900 produces the most well-established measurements and is universally used. There is a known source of bias to the scintillometer measurements in that they are center-weighted, which can be exploited as a feature to minimize contributions from the end stations, if unwanted. For example, obtaining a maritime measurement across a bay is ideally suited to exploit the center biased measurements of scintillometers.

There are other systems being developed to achieve measurements of the refraction structure constant. The most established is the Differential Image Motion Monitor (DIMM) technique, which collects measurements of multiple light sources to compare rapid relative motion. The results of this comparison can be modeled to fit representative optical turbulence conditions. There is a known source of bias from the product that the path average value is strongly weighted toward the aperture. This can be exploited as a feature to capture near-field optical turbulence contributions that can be much larger than the path average turbulence.

In comparison, the Delayed Tilt Anisoplanatism (DELTA) Imaging Path Turbulence Monitor, PM-02-600 from MZA, has been introduced to the commercial market and appears to offer even higher quality measurements than the dual-beam scintillometer or DIMM telescope. This system provides basic strength of turbulence (C_n^2) and bounds on variation of C_n^2 over the path with somewhat reduced sensitivity near the target end of the path. In addition to C_n^2 , the system measures standard propagation parameters such as r_0 , Rytov number, isoplanatic angle, transverse wind speeds, and the Greenwood and Tyler frequencies. The DELTA system is placed at one end of the path, with a target or object with multiple trackable features on the opposite

⁴⁷ Ridgway, W.L., R.A. Moose, and A.C. Cogley. *Atmospheric Transmittance/Radiance Computer Code FASCOD2*. AFGL-TR-82-0395. October 1982. Retrieved 10 June 2022. Available at <https://apps.dtic.mil/sti/pdfs/ADA130241.pdf>.

⁴⁸ Clough, S.A., F.X. Kneizys, L.S. Rothman, and W.O. Gallery. "Atmospheric Spectral Transmittance and Radiance: FASCOD1B." In *Proceedings Volume 0277, Atmospheric Transmission*, 28 July 1981.

end. Depending on the size of the target and the optics on the telescope, a measured path length of ½ to 3 kilometers can be achieved. Data is formatted for use with ATMTools propagation analysis and WaveTrain wave-optics simulation. This device now is undergoing extensive evaluation by the Services. [Figure 2-20](#) illustrates the concept of operations for the DELTA.

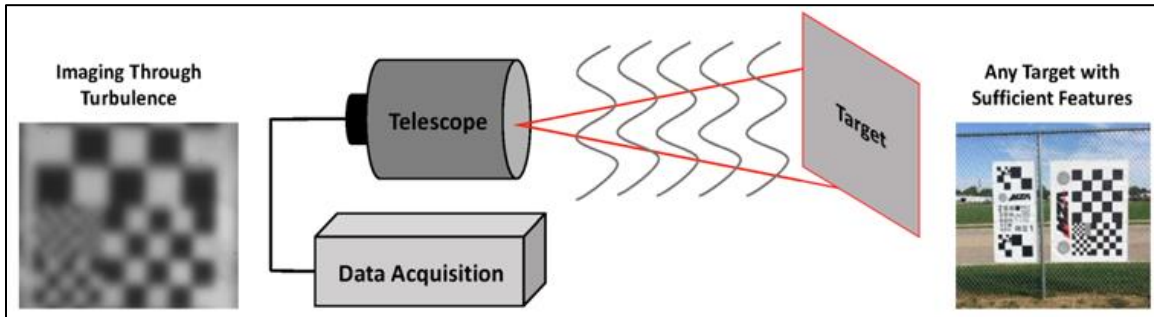


Figure 2-20. MZA DELTA Concept of Operations

Similar devices are being developed to extract range-resolved measurements from a DIMM technique using lidar that will eliminate the need to install a downrange target or light source. Other techniques to directly measure the refraction structure include using a Shack-Hartmann wavefront sensor, which requires a laser to transmit energy into its sensor. MZA has also developed a dual-ended optical turbulence sensor-transmitter system called Path-Resolved Optical Profiler System (PROPS) that is a wavefront sensor-based profiler that can use light-emitting diodes at short distance or laser at longer distance. The PROPS gives better path resolution and can collect data at longer ranges than what the DELTA imaging solution provides.

The boldest innovation is work using lidars to collect Raman shifts of reflected laser energy that correlates temperature, humidity, and wind structure measurements to provide range-resolved optical turbulence calculations that are calibratable to NIST standards. These new lidar systems have not yet reached production status.

Note that at very low altitudes over the ocean where the Services are most concerned, many of the above techniques fail due to haze or noise induced by wave activity. This region is being attempted by small unmanned drones carrying point sensors such as sonic anemometers. Another technique to measure the refraction in this region is to use the Bulk Method, an empirical model (see Subsection [2.3.8](#) for a definition of the Bulk Method). This technique uses the air-sea temperature difference to determine the bulk optical turbulence at very low altitudes, in both stable and unstable conditions.

2.3.13 Surface and Aloft Meteorological Situation

The T&E of E-O weapons systems requires careful specification of the atmospheric envelope for operations. Variables such as the mixing layer height are key to determining atmospheric transport and diffusion, forecasting precipitation and turbulence, estimating likely aerosol content, and defining radiative transfer characteristics pertinent to sensor operation.

2.3.13.1 Surface Meteorological Measurements

Surface meteorological characteristics are normally determined by networks of meteorological sensors. For example, the Army has developed a portable network system that is one of the most advanced and useful for surface meteorological measurements. The Surface Atmospheric Measuring System consists of solar-powered remote field data collection platforms

and a centrally located acquisition control unit (ACU). The data collection platforms consist of a 10-meter mast on which several meteorological sensors are mounted including wind speed, wind direction, temperature, pressure, relative humidity, solar radiation, precipitation, and soil moisture. Other sensors can be attached to the system to measure visibility, cloud height, and inversion. The system can log and store any analog or pulse signal from other measurement devices such as those designed to measure atmospheric gases or particulates. As the sensors are measuring the atmospheric variables, the data are processed and stored in a data logger and removable media. Periodically (5 to 30 minutes), each station is interrogated through a radio link by the ACU and the data set transferred to the ACU computer for storage and archiving. Reports are generated for use as required. These reports include, but are not limited to, current data from each station and the last 24-hour data from individual stations.

When a sensor test encompasses a relatively small uniform terrain area, several well-instrumented meteorological towers may be used instead of a large network of sensors. Meteorological towers can be configured in many ways to meet the requirements of the user. A complete station situated in a remote area typically includes a 2- to 10-meter mast on which the temperature, wind, pressure, humidity, and other sensors are mounted. Other instruments such as rain gauges and visibility devices are located adjacent to the mast. A meteorological tower erected to support a specific field test will have instrumentation at several heights. For example, a 10-meter tower will have sensors at the 2- and 10-meter positions. Sensors used will depend on the project requirements and equipment availability. In many cases, there are likely to be several towers ranging from 2- to 32-meter height.

Sensor selection for a meteorological tower depends on test data requirements and desired derivative information. For example, if information on the transport direction of an aerosol cloud is required, a wind vane with a speed threshold of about 0.5 m/s is all that is required. If the objective is the measurement of turbulent flow characteristics, a threshold of about 0.1 m/s is needed. In this case, a sensor such as a 3D sonic anemometer coupled with hot wire temperature sensors can supply the necessary information. In any case, the characteristics of each sensor must be known. Information such as accuracy, range of sensitivity, threshold sensitivity, and resolution are used to describe these characteristics. Sensor electrical parameters such as signal output voltage, frequency range, and signal type are important, so the data acquisition system can be tailored to the device. Physical characteristics such as environmental limitations, size, weight, and ruggedness are important to the operator. The selection of sensors, therefore, depends on specific test requirements.

Data collection procedures are similar for towers and remote weather stations. They differ only in the number of channels that are needed, the rate at which the sensors are sampled, and the manner in which the data are transmitted to the recording device. A remote station might monitor 5 to 10 sensors. It may use either a self-contained removable media or transmit data periodically over a radio or telephone link to a central recording facility. A meteorological tower, on the other hand, might have dozens of sensors that are sampled periodically and the data recorded and transmitted via a modem and hard wire to a computer. In both cases, the sensor signals are sent to a data logger where they are processed and digitized. A commonly used data logger accepts sensor signals from either analog or pulse sources. Analog instrument outputs might include temperature, pressure, relative humidity, or solar radiation. Pulse sources include sensors such as wind speed (as measured with a propeller) or precipitation as measured with a

rain gauge from a tipping bucket. A well-designed data logger will accept up to 16 single-ended or 8 differential measurement analog sensors and 4 pulse output sensors.

A well-designed data logger makes voltage measurements by integrating the input signal for a fixed time and then holding the integrated value for the analog-to-digital conversion. Fast and slow integration times should be available. A typical logger digitizing rate for meteorological data is typically one per second. Data are typically averaged by the logger for 1- or 15-minute output periods. The logger is programmed to output the sensor data in engineering units.

Two output formats are typically available: one for analog recording (for example, on removable media) and the other is RS-232 or RS-485 for transmission via radio or telephone modem to a computer for data storage. The final output can then be stored on a computer disk or other internal memory storage.

2.3.13.2 Aloft Meteorological Measurements

Aloft meteorological measurements can be divided into those attained using sensors that operate remotely, and those attained using sensors that are carried aloft and relay data back to a ground level recorder. Examples of remote meteorological sensors include the laser Doppler velocimeter (LDV), sodar, ultra-high frequency (UHF) wind profilers, and radar acoustic sounding systems. Examples of systems that carry sensors aloft include balloon sondes and rocketsondes.

The LDVs are mobile remote wind sensing systems that use laser technology to make wind measurements at altitudes ranging from 5 to 1000 meters. Typical LDV systems use continuous wave carbon dioxide laser sources operating at a wavelength of 10.6 μm . The light is sent through output optics and deflected into the atmosphere via a rotating deflector, causing the laser beam to scan the atmosphere conically. The measured velocity component is along the beam axis. To determine a three-dimensional velocity component set, the beam is swept about a preset conical half angle (for example, 45°) at rates of several hertz. Light scattered from the measurement volume (that increases with transmission range) is collected by an optical receiver and processed to detect the Doppler frequency shifts. For each complete beam scan, Doppler shifts in the backscattered signals received from several hundred sampling volumes around the circular path are processed to obtain a mean 3D wind field. Each wind field measurement is time tagged and reported in both graphic and tabular form to include date, site, orthogonal wind components, wind speed, wind direction, and altitude at which the measurement was made. The LDV systems also detect boundary layer altitudes through signal magnitude. At the boundary layer, aerosol concentration decreases sharply. The LDV signal magnitude depends on the square root of aerosol number density. Thus, at the boundary layer, LDV signal magnitude suffers a noticeable reduction. The LDV systems are expensive but not uncommon at test ranges. They represent a major advance in the ability to routinely and continuously sample aloft boundary layer winds remotely.

The sodars measure wind speed, direction, and echo intensity as a function of altitude. The sodar functions like a pulsed radar, but instead of an electromagnetic wave, it emits an acoustic wave. Unlike an electromagnetic wave, acoustic signal propagation varies as a function of atmospheric temperature. A series of acoustic waves propagating outward through the atmosphere are partially reflected back to the antenna as a continuous echo train because of small-scale temperature fluctuations along the pulse path. Altitude is derived from the

propagation rate (speed of sound), the elapsed time of the round trip, and the angular cosine of the antenna.

Wind speed is derived from the Doppler shift encountered by the pulse in a dynamic turbulent structure. Thermal turbulence is derived from the amplitude of the received signal. The sodars transmit acoustic signals with one vertical and two tilted beams. Typically, data are collected between 50 and 1000 meters height depending on instrument design.

The UHF wind profiler measures horizontal and vertical wind as a function of altitude. A UHF pulse Doppler radar operating at a frequency of 915 or 924 MHz transmits signals at an angle of 15° from the vertical in north-south and east-west directions. The radial wind velocity, determined from Doppler shifted backscattered signal returns from turbulent atmospheric cells, is measured and converted to horizontal wind components and vertical wind speed. The opposed transmission directions can be in any direction, provided the orientation with respect to true north is known.

The Radio Acoustic Sounding System (RASS) measures temperature profiles in the lower troposphere. The RASS functions as an auxiliary system by emitting a 2 kHz acoustic signal along with the 915 MHz UHF wind profiler. The zenith pointing radar and high-intensity acoustic signals are transmitted simultaneously. Backscatter occurs over the altitude range where the radar and acoustic beams overlap. Doppler processing of the backscattered signal yields an acoustic velocity profile that is then converted to a virtual temperature profile after the effects of air motion are minimized.

State-of-the-art tethered systems measure temperature, pressure, wet bulb depression, wind speed, and wind direction as a function of altitude and elapsed time. The measurements are made using a radiosonde attached to a tethered, helium-filled balloon. For example, a well-designed tethered system consists of a winch powered by a 12-Vdc battery or commercial power, a tether line, a radiosonde powered by a 9-Vdc dry cell, the balloon, and a data acquisition system. The sonde transmits at a radio frequency of 402-406 MHz and is attached to a carriage mounted below the balloon. The balloon is designed to align itself and the sonde into the wind. The horizontal wind direction is measured with a magnetic compass inside the sonde, and the wind speed is measured by a three-cup anemometer attached to the sonde. The altitude of the sonde above ground level is computed from the output of an aneroid temperature-compensated pressure sensor. Profiles of the atmosphere can be made to approximately 800 meters altitude. Maximum attainable altitude is limited by the length of the tether line deployed, air traffic concerns, and wind speed. Higher wind speeds cause the balloon to be carried out to greater horizontal distances, thus reducing the maximum achievable altitude. Temperature can be measured from the tethered sonde with a precision matched bead thermistor, and the relative humidity can be derived from a wet bulb temperature depression measurement also using a precision matched thermistor. Data from the sonde can be telemetered to a ground-based receiving station that decodes the data, and generates online graphics for real-time analysis, then stores the data on computer disk or removable media for future processing and analysis.

Aloft meteorological measurements to higher altitudes are accomplished with rawinsondes and rocketsondes. A state-of-the-art rawinsonde set measures temperature, pressure, relative humidity, wind speed, and wind direction from the surface to 30 km altitude. It is common for many sondes to derive pressure from other recorded atmospheric conditions. Using humidity and temperature profiles, atmospheric pressure at the height of the sonde can be

derived by using the Global Positioning System (GPS) height difference between the sonde and sonde launch site along with initial ground station measurements. A commercially available system uses a free-flight balloon with attached radiosonde, which performs the in-situ measurement of temperature, pressure, and relative humidity. It is common for many sondes to derive pressure from other recorded atmospheric conditions. Using humidity and temperature profiles, atmospheric pressure at the height of the sonde can be derived by using the GPS height difference between the sonde and sonde launch site along with ground station pressure. The differential position, coupled with the pressure-height measurement, permits the calculation of wind speed and direction as a function of altitude. All data are transmitted to a ground receiving and processing station via a 403 MHz radio link.

A modification of the radiosonde technique is to use coupled sensors or multiple radiosondes separated by a one-meter boom to collect the temperature structure function at high data rates. This technique, commonly called a thermosonde, provides a vertical depiction of the optical turbulence after calculation, typically using the following formula derived from Tatarski (2017):

$$C_n^2 = \left(\frac{79 * 10^{-6} * P}{T^2} \right)^2 * C_t^2 \quad \text{Equation 2-21}$$

A second technique used with free-flight balloons employs a radio theodolite for balloon tracking. This system measures atmospheric temperature, pressure, relative humidity, wind speed, and wind direction. A commercially available radio theodolite system consists of a helium-filled free-flight balloon with an attached radiosonde, a pedestal-mounted tracking antenna, and a receiving station to decode, process, and store data. The theodolite antenna automatically tracks the radiosonde transmitter on the free-floating balloon and measures the pedestal azimuth and elevation angles. The system can track the transmitter for up to 150 km slant range distance with direct line of sight. The altitude of the sonde above ground level is computed from an onboard pressure transducer. The spatial position of the sonde is computed from the azimuth, elevation, and altitude data, and the wind speed and direction are computed from the differential position as a function of time. Temperature is measured using a bead thermistor, and relative humidity is detected with a carbon hygistor. The sonde data are transmitted via 402-406 MHz or 1680 MHz radio frequency to the radio theodolite receiver and then to the recording and processing system. A computer performs preliminary processing, generates a quick-look report, and stores the data on removable media for future processing and analysis.

A commercially developed small rocketsonde system makes possible the very rapid measurement of aloft meteorological parameters. This rocketsonde uses a model rocket to carry precision temperature/humidity and pressure probes aloft. A unique satellite GPS gives the rocket coordinates continuously with an error of less than 1.5 m. Information from the onboard instruments is telemetered to a ground station that acquires and displays the data using a personal computer.

2.3.14 Air Temperature, Humidity, and Pressure

Air temperature, humidity, and pressure are fundamental parameters required to characterize the performance of virtually any E-O sensor in the atmospheric boundary layer. Major advances have been made during the past 10 years in the ability to measure these

parameters. Thin film technology makes available instruments having fast response and sensitivity. For example, an RH sensor that uses a 2 μm thick polymer film has a 0-100% RH range for operating temperature between -40 and $+60$ $^{\circ}\text{C}$, a 0.5 second response time, and is accurate to $\pm 2\%$ at 25 $^{\circ}\text{C}$. A barometer covering a range of 1100 to 600 mb (-700 to 4200 m altitude) with an accuracy of ± 0.5 mb and a resolution of 0.1 mb (1 m altitude) is operable at temperatures between -25 and $+50$ $^{\circ}\text{C}$.

Accuracy and resolution requirements for these measurements will depend on the ultimate use of the data in evaluating E-O sensor performance. As is shown in the next section, instrument accuracy and resolution of fundamental parameters are major contributors to the error associated with the characterization of the tested sensor.

2.4 Test Data Evaluation

Test data evaluation is one of the most important and the least applied areas in E-O sensor atmospheric T&E. Test data evaluation procedures define data quality and reliability. Using these procedures, data can be assigned a relative measurement error, and the uncertainty of sensor performance or model being evaluated can be quantified. In this section, methods to evaluate and assign measurement errors are reviewed. The impact of measurement error on sensor performance is then considered through examples for a visual and infrared imaging system and for LRF system performance. It is shown that production of a prescribed instrument accuracy can be insufficient for sensor evaluation requirements or may be too restrictive. In conducting experimental evaluations of sensor performance, the test engineer and the system developer must have a clear understanding of the measurement accuracy required to achieve an acceptable evaluation of system performance.

2.4.1 RMS Errors

Since it is impossible to test the sensor under every possible field condition, it is assumed all sensors use a model to predict performance under most meteorological conditions, and the objective of the T&E process is a calibration check on the reliability of the model relative to actual sensor performance. It is further assumed the model is a “perfect” physical representation of the sensor. Considering only the effects of accuracy of input parameters on prediction capability, three questions are addressed that must be answered to evaluate sensor model performance prediction capability.

- a. What are the effects of model input uncertainty on model prediction uncertainty?
- b. What are the major parameters that affect model prediction uncertainty?
- c. How accurate must input data be for a required level of model prediction?

To provide answers to these questions, the following assumptions are made.

- a. Measured model inputs are independently determined.
- b. Each parametric uncertainty is a small fraction of the value of the corresponding observed variable.

- c. Positive and negative errors are equally likely to occur.
- d. The RMS error represents measured uncertainty.

This section considers the computation of RMS error for evaluating the effects of the quality of experimental data on specifying sensor capability.

Assume a function $f(x_i)$, where x_i represents the defining parameters of the function. The RMS error of $f(x_i)$ is shown in [Equation 2-22](#).

$$\sqrt{(\langle \delta f(x_i) \rangle)^2} = \left[\sum_{i=1}^N \left(\frac{\partial f(x_i)}{\partial x_i} \delta x_i \right)^2 \right]^{1/2} \quad \text{Equation 2-22}$$

If Gaussian statistics are assumed (the errors are random), then δx_i is the standard deviation evaluated at the mean value of x_i , $\langle x_i \rangle$, and the probability of exceeding the RMS error is 31.73% and the probable error is 0.6745 times the RMS error.⁴⁹ Thus, the functional error components may be treated as a vector with components that are computed according to

$$\delta f(x_i) = \frac{\partial f(x_i)}{\partial x_i} \delta x_i \quad \text{Equation 2-23}$$

The relative error for each functional component is

$$\frac{\delta f(x_i)}{f(x_i)} = \frac{1}{f(x_i)} \frac{\partial f(x_i)}{\partial x_i} \delta x_i. \quad \text{Equation 2-24}$$

Therefore, the RMS relative error is

$$\sqrt{\left(\frac{\delta f(x_i)}{f(x_i)} \right)^2} = \frac{\pm 1}{F(x_i)} \left[\sum_{i=1}^N \left(x_i \frac{\partial f(x_i)}{\partial x_i} \frac{\delta x_i}{x_i} \right)^2 \right]^{1/2} \quad \text{Equation 2-25}$$

If $f(x_i)$ represents an E-O sensor performance model, and x_i are the functional parameters affecting sensor performance, the relative uncertainty in model performance can be evaluated by (1) computing first derivatives of model performance with respect to the functional parameters; (2) measuring the parameter x_i and its corresponding relative error, $\frac{\delta x_i}{x_i}$; and (3) using the results in [Equation 2-25](#). Note that if x_i is itself determined by a set of independent measurements, say y_i , then [Equation 2-25](#) is applied to find the resulting error for the parameter by replacing $f(x_i)$ with x_i , and x_i with y_i .

The use of [Equation 2-25](#) requires test planning that will allow the functional parameters to be measured enough times to compute a reliable standard deviation for the measurement, and the measurement must be completed under conditions where the mean value of the parameter is constant (statistically stable). As is shown in the next subsections, when this information is not provided with the measured data, little is actually known about sensor performance. As [Equation 2-23](#) to [Equation 2-25](#) show, the relative RMS uncertainty in the function of interest is

⁴⁹ R. T. Birge. "The Propagation of Errors." In *The American Physics Teacher*, V. 7, No.6, pp. 351-357. December 1939.

proportional to the differential change in the function with respect to the change in the measured variable. The error in extrapolated values, therefore, depends on the slope of the function at the extrapolated point for which the data are acquired. If the functional slope is less than 1, the effect of data errors at the measured point decreases at the extrapolated point. If the functional slope is greater than 1, the effect of data errors at the measured point increases at the extrapolated point. It is important in determining acceptable data error limits to understand the application of the data and to specify the measured data error and precision.

2.4.2 Impact of Measurement Error on Sensor Evaluation

To illustrate the impact of measurement errors on sensor evaluation, measurements for three sensor types are considered in the subsections that follow. First, the probability of successful target detection and ranging is considered for visual and infrared imaging systems, and the probability of successful ranging for 1.06 and 10.6 μm wavelength laser systems is considered. Examples of meteorological effects on the relative uncertainty of atmospheric transmission for broad-band infrared and narrow-band MMW systems are then considered. The effects of spatial and temporal sampling intervals are then considered in the context of point sensor sampling networks and other meteorological variables.

2.4.2.1 Target Detection and Ranging

[Table 2-1](#) provides a summary of the atmospheric environmental measurements required to evaluate E-O systems used to detect, recognize, or range targets. Relative measurement errors for selected sensor examples have been used to compute the relative uncertainty in the corresponding sensor function. This illustrates the impact of measurement errors in the evaluation of E-O sensors performing these functions. The examples are

- relative uncertainty in visual 50% probability of detection;
- relative uncertainty in infrared (thermal bands) 50% probability of detection;
- relative uncertainty in 1.06 and 10.6 μm laser wavelength probability of successful ranging;
- relative uncertainty in 1.06 and 10.6 μm laser wavelength laser power on target;
- relative uncertainty in broad band infrared transmission; and
- relative uncertainty in MMW extinction and transmission.

The results of the computations are presented in [Appendix B](#) through [Appendix G](#), which show the relative uncertainty of sensor performance as functions of key measurements affecting sensor response. The relative errors chosen for inputs into the models used to compute the results are arbitrarily chosen but are reasonable and attainable values.

Results of the sensor performance relative uncertainty computations shown in [Appendix B](#) through [Appendix G](#) clearly demonstrate that a single acceptable error value for a measurement does not provide sufficient guidance for the accuracy of sensor evaluation measurement. Suppose, for example, that determination of the visual 50% probability of detection ([Figure B-1](#)) was required for the sensor under evaluation. Assume further that for the chosen target-to-background scenario, the relative transmittance required for 50% probability of detection is such that relative (to a nonattenuating atmosphere) atmospheric transmittance needs

to be 0.5. In this case, if the sky-to-ground ratio is 20 (sky much brighter than the ground), the relative uncertainty in 50% probability of detection is about 6.5% even though relative uncertainties in target inherent contrast, sky-to-ground ratio, and relative transmittance to the target are all 10%. However, if the sky-to-ground ratio is about 1, then the relative uncertainty in 50% probability of detection is about 40% for the same relative measurement uncertainties when the sky-to-ground ratio was 20. It is important to choose acceptable measurement error levels on the basis of how accurately sensor performance must be quantified.

As the figures in [Appendix B](#) through [Appendix G](#) are examined, it should become clear that the TASS relationships discussed in Section [2.1](#) are evident. For example, the thermal band 50% probability of detection relative uncertainty shown in [Appendix C](#) depends on the FLIR MRTD relative uncertainty, while the 50% probability of successful ranging depends on the transmitter aperture diameter, pulse width, number of range gates, and the relative uncertainty in measured atmospheric parameters. Sensor operating characteristics contribute to the definition of the accuracy required for parameters used to characterize the atmosphere. The test engineer should keep an accurate log of the operating characteristics of the sensor under test.

2.4.2.2 Broad- and Narrow-Band Transmission

A second set of examples has been computed to illustrate the impact of atmospheric measurement uncertainty on quantifying sensor performance, broad-band infrared transmission, and narrow-band MMW transmission relative uncertainty. The computations have been developed as functions of relative uncertainty in input parameters required by empirical transmission models. The infrared broad-band transmission was computed using a model developed by Analytics, Inc. in 1985.⁵⁰

The MMW transmittance was computed using the Beer-Bouguer transmission law and extinction cross-section computations were made using the complex dielectric constant for water and ice as a function of temperature given by Sadiku. The results of these computations are given in [Appendix D](#). Results similar to those observed for the probabilities of detection and ranging in the previous section are shown in [Appendix D](#) and serve to reinforce conclusions concerning required measurement accuracy.

2.4.3 Temporal and Spatial Averaging Intervals

How data will be averaged temporally and spatially to evaluate E-O sensor performance is a major issue that must be addressed during test design and used as a guiding principle during data acquisition and analysis. There are numerous references that describe protocols to follow in determining measurement sensor spacing in a sensor network and data acquisition rates to ensure statistically stable data and data that can have specified accuracy and relative uncertainty (Lyons and Scott, Noll and Miller⁵¹, Munn⁵², and Gandin⁵³). These references should be consulted when networks are used. A guiding principle should be to use path-integrated measurement techniques along the same line of sight as the sensor under test whenever possible. The measurement line of

⁵⁰ Analytics, Inc. "Camouflage Effectiveness Evaluation System." Technical Memorandum 1900-03. Prepared for the U.S. Army Engineer Waterways Experiment Station, Vicksburg, MS, 1985.

⁵¹ Noll, K. and T. Miller. *Air Monitoring Survey Design*. Ann Arbor: Ann Arbor Science Publishers, January 1977.

⁵² R. E. Munn. "Urban Meteorology: Some Selected Topics." In *Bulletin of the American Meteorological Society*, V. 54, I. 2, pp. 90-93. February 1973.

⁵³ L. S. Gandin. *Objective Analysis of Meteorological Fields*. Jerusalem: Israel Program for Scientific Translation, 1965.

sight should be within at least one correlation length (see Subsection [2.3.7](#)) of test article line of sight. It should be sampled at least twice as fast as the highest frequency of the phenomena measured. If point sensors are used along the line of sight, each sensor should be within a correlation length of the other. Note that the size of the correlation length may vary down the line of sight and can easily be a function of atmospheric conditions. Tests designed under consideration of particular atmospheric conditions must be reconsidered in terms of point sensor placement when factors affecting correlation length change.

Whenever possible and reasonable, statistical regression and probability distribution analysis of the data should be used to produce mean values and standard deviations that can be understood in terms of sensor performance without resorting to explicitly computing parametric averages. For example, regression of visible range against logarithmic infrared transmission should yield (for constant air temperature and relative humidity) a nearly linear relationship with a slope proportional to the extinction characteristics of the intervening atmosphere. The best fit line to the data is the mean value of the measurements and does not directly average the data temporally or spatially. The resulting correlation coefficient is proportional to the standard deviations of both sets of data. The data analysis performed in this way automatically yields the extra dividends of defining the atmospheric extinction properties, providing a relationship between the infrared transmission and visible range can be checked by other experimental and theoretical means, and providing analytical relationships can be used directly in the evaluation of the E-O sensor. All are achieved without directly performing temporal or spatial averages of the data. Data averaging should be approached with the intent of extracting as much information about the sensor evaluation and data itself as possible.

2.5 Data and Information Bases

A key factor in test design and data evaluation is data and information accessibility. From the beginning of test design and planning, how the data will be archived and used must be considered both directly for the sensor evaluation and for potential future applications. Digital data acquisition is standard practice. Software for relational digital databases is common and sufficiently standardized that data can be imported and exported easily among systems. Therefore, it is taken as axiomatic that although there are still analog instruments and recording systems in use, the data will be in digital form and will be archived in database formats.

Test design and planning should identify the database in which the test data will be archived. By identifying the database, requisite formats for variable measurements already included in the database are available to guide data acquisition formats. In the case where no archival database can be identified prior to the test, the data should as a minimum be formatted in ASCII code.

In following subsections, a clear distinction is drawn between databases and information bases. Databases are defined as archival records of qualified parametric measurements and documentation to support their use and interpretation (for example, specification of accuracy, instrument used in the measurement, and synoptic acquisition conditions). Information bases are archived records of results obtained with the data. These results might include, for example, analysis reports with the data used in the report, model predictions using measured parameters as inputs, results of data analysis that yield regression relationships, or characteristic E-O sensor

responses for the ranges of parameters covered in the database. Database and information base recommendations to support E-O sensor T&E are addressed next.

2.5.1 Data Archival Formats and Storage

The most popular form of digitized data media for field applications is removable media that can hold several megabytes of data through disk compression programs. Blocked records with a header containing data and supporting information should be used for archived data. The header should contain all information pertinent to the test with the exception of drawings and photographs. In facilities where CD-ROM or removable media can be written and read, drawings, weather charts, maps, and photographs should be included as a normal part of the data file. The header information should include at least the following information.

- a. date of the measurement
- b. time basis (UTC, local)
- c. test facility
- d. reports in which the measurements are used
- e. primary author
- f. classification
- g. point of contact for the measurements
- h. lead sponsoring agency
- i. test range weather (meteorological and specific line of sight)
- j. types and kinds of meteorological observations (requirement sources and specific applications)
- k. data validity concerns (cross-checks as data were acquired)
- l. target configurations (contrasts, dynamic characteristics, locations)
- m. number and types of measurement sensors
- n. sensor response characteristics (dynamic range, response time, calibration history and method, accuracy capability with caveats)
- o. definition of least significant digit in data
- p. data averaging interval as appropriate
- q. site survey (locations of instrumentation to include height above ground, targets, and significant terrain features, located with ± 0.5 m uncertainty)

- r. test variables measured (formats, units, applications, method of cross-checks)
- s. sample of data record with “plain English” interpretation

Archived data should be qualified and organized according to:

- a. measurements specifying the same parameter located by a common file reference in a common format and in chronological order;
- b. SI units or powers of 10 variations; and
- c. mean values of measured quantities over time periods commensurate with statistically stable data (10 minutes running average for meteorological, 1 minute running average for SWOE data, 1 second for smokes/obscurants), standard deviations, regression or statistical distribution summaries and correlation coefficients, and when networks are used to provide line-of-sight predictions, the prediction or interpolation algorithm employed for interpreting the data.

2.5.2 Information Base Generation and Storage

Information bases typically reside in the same physical location as the archived data; however, it is accessible independently and is referenced and identified as the information base for the archived data. The information base contains a directory of content files, a help file, and all the tools (word processors, spreadsheets, graphics software, models used as analysis tools, and project planners/schedulers) necessary to access and use the information that is archived in any of the information manipulation formats. It should be clear that information bases are a direct result of test customer feedback to the data production source. To produce total quality data, the producer must have a clear understanding of how data are used. Storing customer applications with identification of the data the customer used and how the data were manipulated for the analysis or evaluation provides a logical repository of all information pertinent to the sensor and provides a historical data basis for improvement in future testing.

2.5.3 Identifying and Reporting Data Gaps

It is a fiscal and physical impossibility to test an E-O sensor or HEL system under all meteorological conditions of its operating envelope. It is important that an information base be maintained identifying gaps in the data and information base pertinent to sensor performance or evaluation requirements. As new tests are designed, it is possible to include within the test framework opportunities to secure data that are otherwise overlooked for lack of identification of requirements. Maintenance of an information base that identifies the range limits and application limitations of previously acquired data provides a clear picture of standard test needs, extraordinary test requirements, and acquired data limitations.

2.5.4 Identifying and Tracking Future Test Requirements

An information base identifying developmental items and their projected test schedules assists in planning test range usage and projecting hardware requirements. This tracking system need not be complicated. Commercially available project tracking software is sufficient to provide the guidance needed for planning and future test design to pursue TQDM.

This page intentionally left blank.

APPENDIX A

Summary of Atmospheric Environmental Parameter Requirements in Support of Electro-Optical Systems Testing

A.1 Purpose

These tables were prepared with the cooperation and assistance of the RCC Meteorology Group Subcommittee for Electro-Optics to provide an overview of the test variables and parameters needed to evaluate E-O sensors in the atmosphere.

A.2 Scope

Seven types of tests, in two categories, are presented. The first test category covers generic tests for imaging systems, LRFs, and MMW sensors. The second test category involves specific ongoing test programs that normally include E-O sensors operating in the atmosphere. These tests are for:

- a. visual image sensors,
- b. infrared image sensors,
- c. LRFs and HEL weapons,
- d. MMW sensors,
- e. the SWOE program,
- f. the Smoke Week test program, and
- g. littoral warfare test programs.

As many as 40 variables are listed in the tables. The variables are ranked in importance on a scale of 1 to 3. A rank of 1 is considered fundamental to the specification of sensor performance and must be measured for determination of sensor performance. A rank of 2 shows that the variable is desirable and perhaps fundamentally necessary if sensor performance in scenarios not covered by test conditions is to be determined. A rank of 3 indicates the variable is of secondary importance for directly evaluating sensor performance, but is likely to provide information to help explain anomalous sensor performance.

Guidelines for Atmospheric Measurements in Support of Electro-Optical Systems Testing
RCC 356-22 August 2022

Table A-1. Summary Atmospheric Environmental Parameters in Support of Electro-Optical Visual Image Detection Testing

Parameter	Units	Parameter Rationale	VISUAL DETECTION			
			Averaging Period, Min	Importance	Acceptable Error	
1	Solar zenith angle	deg	Direct radiance source position	10	1	2 deg
2	Solar azimuth angle	deg	Direct radiance source position	10	1	10 deg
3	2% Contract Visual Range	km	Environment characterization	10	1	10%
4	Present weather		Environment characterization	10	1	
5	Cloud-free line-of-sight	km/direction	Environment characterization	10	1	10%
6	Number of cloud layers		Atmospheric definition	10	1	
7	Cloud type for each layer		Absorption, amounts of scattering	10	1	
8	Cloud coverage for each layer	%	Downwelling irradiance level	10	1	5%
9	Base altitude of each cloud layer	km	Downwelling irradiance level	10	1	0.05 km
10	Wind speed at surface	knots	Feature signatures, transmittance calculation, dust-airborne particulate concentrations, feature directional reflectance	2	1	5%
11	Wind direction at surface	deg	Feature signatures, dust-airborne particulate concentrations	2	1	5 deg
12	Pasquill stability category	A-F	Atmospheric definition	60	2	
13	Absorbing gages (other than H ₂ O)		Transmittance calculation	NA	NA	
14	Aerosol/particle index of refraction		Transmittance calculation	1	1	
15	Aerosol/particle size distribution	number/um	Transmittance calculation	1	1	
16	Aerosol/particle shape		Transmittance calculation	1	1	
17	Precipitation type indicator		Transmittance calculation	10	1	
18	Precipitation rate	mm/hr	Feature signatures	2	1	20%
19	Precipitation temperature	°C	Transmittance calculation	10	3	1 °C
20	Dew/Frost		Feature/background signatures, MMW transmission	10	1	
21	Target/background emissivity		Feature signatures	NA	NA	
22	Relative Humidity Structure Const.	m**--2/3	Beamspread/Scintillation	NA	NA	
23	State of surface		Environment characterization	60	2	
24	Sea state		Environment characterization	10	2	
25	Global solar radiation	W/cm**2	Solar insolation analysis	2	1	5-10%
26	Diffuse sky radiation	W/cm**2	Thermal radiation exchange analysis	2	1	5-10%
27	Directional sky radiation	W/cm**2	Scattered/reflected sky radiation	2	1	5-10%
28	Sky-to-ground luminance ratio		Thermal radiation exchange analysis	10		
			Scattered/reflected sky radiation			
			Cloud distribution level			
			Visual range estimation			

Guidelines for Atmospheric Measurements in Support of Electro-Optical Systems Testing
RCC 356-22 August 2022

Table A-1. Summary Atmospheric Environmental Parameters in Support of Electro-Optical Visual Image Detection Testing						
Parameter	Units	Parameter Rationale	VISUAL DETECTION			
			Averaging Period, Min	Importance	Acceptable Error	
29	Downwelling spectral direct radiance	W/cm**2-um	Feature signatures	10	1	5-10%
30	Downwelling spectral diffuse irradiance	W/cm**2-um	Feature signatures	10	1	5-10%
31	Directional spectral sky radiance	W/cm**2-um-er	Thermal radiation exchange analysis Scattered/reflected sky radiation Cloud distribution level	10	1	5-10%
32	Spectral path transmittance		Apparent feature and background signatures	0.50	1	5%
33	Index of refraction structure const.	m**2-2/3	Image resolution/beamsread/scintillation	2	1	
34	Number of atmospheric layers		Atmospheric definition	60	2	
35	Base altitude for each atmospheric layer	km	Atmospheric definition	60	2	0.05 km
36	Visibility for each atmospheric layer	km	Transmittance calculation Downwelling irradiance level	60	2	10%
37	Relative humidity for each atmospheric layer	%	Transmittance calculation Downwelling irradiance level	60	2	10%
38	Air temperature for each atmospheric layer	°C	Feature signatures Transmittance calculation	60	2	1 °C
39	Dew point temperature for each atmospheric layer	°C	Humidity calculation Rain temperature calculation	60	2	1 °C
40	Atmospheric pressure for each atmospheric layer	mbar	Transmittance calculation Downwelling irradiance level	60	2	10%

Guidelines for Atmospheric Measurements in Support of Electro-Optical Systems Testing
RCC 356-22 August 2022

Table A-2. Summary Atmospheric Environmental Parameters in Support of Electro-Optical Infrared Image Detection Testing					
Parameter	Units	Parameter Rationale	INFRARED IMAGE DETECTION		
			Averaging Period, Min	Importance	Acceptable Error
1 Solar zenith angle	deg	Direct radiance source position	10	1	2 deg
2 Solar azimuth angle	deg	Direct radiance source position	10	1	10 deg
3 2% Contract Visual Range	km	Environment characterization	10	1	10%
4 Present weather		Environment characterization	10	1	
5 Cloud-free line-of-sight	km/direction	Environment characterization	10	1	10%
6 Number of cloud layers		Atmospheric definition	10	1	
7 Cloud type for each layer		Absorption, amounts of scattering	10	1	
8 Cloud coverage for each layer	%	Downwelling irradiance level	10	1	5%
9 Base altitude of each cloud layer	km	Downwelling irradiance level	10	1	0.05 km
10 Wind speed at surface	knots	Feature signatures, transmittance calculation, dust-airborne particulate concentrations, feature directional reflectance	2	1	5%
11 Wind direction at surface	deg	Feature signatures, dust-airborne particulate concentrations	2	1	5 deg
12 Pasquill stability category	A-F	Atmospheric definition	60	2	
13 Absorbing gages (other than H2O)		Transmittance calculation	10	1	
14 Aerosol/particle index of refraction		Transmittance calculation	1	1	
15 Aerosol/particle size distribution	number/um	Transmittance calculation	1	1	
16 Aerosol/particle shape		Transmittance calculation	1	1	
17 Precipitation type indicator		Transmittance calculation	10	1	
18 Precipitation rate	mm/hr	Feature signatures	2	1	20%
19 Precipitation temperature	°C	Feature/background signatures, MMW transmission	10	3	1 °C
20 Dew/Frost		Feature signatures	10	1	
21 Target/background emissivity		Feature signatures	NA	1	
22 Relative Humidity Structure Const.	m**-2/3	Beamsread/Scintillation	2	2	
23 State of surface		Environment characterization	60	2	
24 Sea state		Environment characterization	10	2	
25 Global solar radiation	W/cm**2	Solar insolation analysis	2	1	5-10%
26 Diffuse sky radiation	W/cm**2	Thermal radiation exchange analysis	2	1	5-10%
27 Directional sky radiation	W/cm**2	Scattered/reflected sky radiation	2	1	5-10%
		Thermal radiation exchange analysis			
		Scattered/reflected sky radiation			
28 Sky-to-ground luminance ratio		Cloud distribution level	10		
		Visual range estimation			
29 Downwelling spectral direct radiance	W/cm**2-um	Feature signatures	10	1	5-10%

Guidelines for Atmospheric Measurements in Support of Electro-Optical Systems Testing
RCC 356-22 August 2022

Table A-2. Summary Atmospheric Environmental Parameters in Support of Electro-Optical Infrared Image Detection Testing						
Parameter	Units	Parameter Rationale	INFRARED IMAGE DETECTION			
			Averaging Period, Min	Importance	Acceptable Error	
30 Downwelling spectral diffuse irradiance	W/cm**2-um	Feature signatures	10	1	5-10%	
31 Directional spectral sky radiance	W/cm**2-um-er	Thermal radiation exchange analysis Scattered/reflected sky radiation Cloud distribution level	10	1	5-10%	
32 Spectral path transmittance		Apparent feature and background signatures	5-10	1	5%	
33 Index of refraction structure const.	m**-2/3	Image resolution/beamspread/scintillation	2	1		
34 Number of atmospheric layers		Atmospheric definition	10	2		
35 Base altitude for each atmospheric layer	km	Atmospheric definition	10	2	0.05 km	
36 Visibility for each atmospheric layer	km	Transmittance calculation Downwelling irradiance level	10	1	10%	
37 Relative humidity for each atmospheric layer	%	Transmittance calculation Downwelling irradiance level	10	1	10%	
38 Air temperature for each atmospheric layer	°C	Feature signatures Transmittance calculation	10	1	1 °C	
39 Dew point temperature for each atmospheric layer	°C	Humidity calculation Rain temperature calculation	10	1	1 °C	
40 Atmospheric pressure for each atmospheric layer	mbar	Transmittance calculation Downwelling irradiance level	10	1	10%	

Guidelines for Atmospheric Measurements in Support of Electro-Optical Systems Testing
RCC 356-22 August 2022

Table A-3. Summary Atmospheric Environmental Parameters in Support of Electro-Optical Rangefinder/Designator Testing									
Parameter	Units	Parameter Rationale	Averaging Period, Min	SUCCESSFUL LRF RANGING					
				Importance			Acceptable Error		
				1.06	1.54	10.6	1.06	1.54	10.6
1 Solar zenith angle	deg	Direct radiance source position	10	3	3	3	2	2	2
2 Solar azimuth angle	deg	Direct radiance source position	10	3	3	3	10	10	10
3 2% Contract Visual Range	km	Environment characterization	10	1	1	1	10%	10%	10%
4 Present weather		Environment characterization	10	1	1	1	10%	10%	10%
5 Cloud-free line-of-sight	km/direction	Environment characterization	10	1	1	1	0.05	0.05	0.05
6 Number of cloud layers		Atmospheric definition	10	2	2	2			
7 Cloud type for each layer		Absorption, amounts of scattering	10	1	1	1			
8 Cloud coverage for each layer	%	Downwelling irradiance level	10	3	3	3			
9 Base altitude of each cloud layer	km	Downwelling irradiance level	10	3	3	3			
10 Wind speed at surface	knots	Feature signatures, transmittance calculation, dust-airborne particulate concentrations, feature directional reflectance	2	1	1	1	5%	5%	10%
11 Wind direction at surface	deg	Feature signatures, dust-airborne particulate concentrations	2	1	1	1	10%	10%	10%
12 Pasquill stability category	A-F	Atmospheric definition	60	2	2	2			
13 Absorbing gages (other than H2O)		Transmittance calculation	10	3	3	1	NA	NA	5%
14 Aerosol/particle index of refraction		Transmittance calculation	1	1	1	1			
15 Aerosol/particle size distribution	number/um	Transmittance calculation	1	1	1	1			
16 Aerosol/particle shape		Transmittance calculation	1	1	1	1			
17 Precipitation type indicator		Transmittance calculation	10	1	1	1			
18 Precipitation rate	mm/hr	Feature signatures	2	1	1	1	10%	10%	10%
19 Precipitation temperature	°C	Feature/background signatures, MMW transmission	10	3	3	3			
20 Dew/Frost		Feature signatures	10	1	1	1			
21 Target/background emissivity		Feature signatures	NA	3	3	3			
22 Relative Humidity Structure Const.	m**-2/3	Beamspread/Scintillation	2	3	3	3			
23 State of surface		Environment characterization	60	2	2	2			
24 Sea state		Environment characterization	10	2	2	2			
25 Global solar radiation	W/cm**2	Solar insolation analysis	2	3	3	3	5-10%	5-10%	5-10%
26 Diffuse sky radiation	W/cm**2	Thermal radiation exchange analysis	2	3	3	3	5-10%	5-10%	5-10%
27 Directional sky radiation	W/cm**2	Scattered/reflected sky radiation							
		Thermal radiation exchange analysis	2	3	3	3	5-10%	5-10%	5-10%
		Scattered/reflected sky radiation							
		Cloud distribution level							
28 Sky-to-ground luminance ratio		Visual range estimation	10	3	3	3			
29 Downwelling spectral direct radiance	W/cm**2-um	Feature signatures	10	3	3	3	5-10%	5-10%	5-10%

Guidelines for Atmospheric Measurements in Support of Electro-Optical Systems Testing
RCC 356-22 August 2022

Table A-3. Summary Atmospheric Environmental Parameters in Support of Electro-Optical Rangefinder/Designator Testing									
Parameter	Units	Parameter Rationale	Averaging Period, Min	SUCCESSFUL LRF RANGING					
				Importance			Acceptable Error		
				1.06	1.54	10.6	1.06	1.54	10.6
30 Downwelling spectral diffuse irradiance	W/cm**2-um	Feature signatures	10	3	3	3	5-10%	5-10%	5-10%
31 Directional spectral sky radiance	W/cm**2-um-er	Thermal radiation exchange analysis Scattered/reflected sky radiation Cloud distribution level	10	3	3	3	5-10%	5-10%	5-10%
32 Spectral path transmittance		Apparent feature and background signatures	5-10	1	1	1	0.5		
33 Index of refraction structure const.	m**-2/3	Image resolution/beamspread/scintillation	2	1	1	2			
34 Number of atmospheric layers		Atmospheric definition	10	1	1	1			
35 Base altitude for each atmospheric layer	km	Atmospheric definition	10	1	1	1	0.05 km	0.05 km	0.05 km
36 Visibility for each atmospheric layer	km	Transmittance calculation Downwelling irradiance level	10	1	1	1	10%	10%	10%
37 Relative humidity for each atmospheric layer	%	Transmittance calculation Downwelling irradiance level	10	2	2	1	10%	10%	10%
38 Air temperature for each atmospheric layer	°C	Feature signatures Transmittance calculation	10	2	2	1	1	1	0.5
39 Dew point temperature for each atmospheric layer	°C	Humidity calculation Rain temperature calculation	10	2	2	1	1	1	0.5
40 Atmospheric pressure for each atmospheric layer	mbar	Transmittance calculation Downwelling irradiance level	10	2	2	1	10%	10%	0.5

Guidelines for Atmospheric Measurements in Support of Electro-Optical Systems Testing
RCC 356-22 August 2022

Table A-4. Summary Atmospheric Environmental Parameters in Support of Millimeter Wave Transmission Testing

Parameter	Units	Parameter Rationale	INFRARED IMAGE DETECTION		
			Averaging Period, Min	Importance	Acceptable Error
1 Solar zenith angle	deg	Direct radiance source position	10	2	2 deg
2 Solar azimuth angle	deg	Direct radiance source position	10	2	10 deg
3 2% Contract Visual Range	km	Environment characterization	10	2	10%
4 Present weather		Environment characterization	10	1	
5 Cloud-free line-of-sight	km/direction	Environment characterization	10	2	10%
6 Number of cloud layers		Atmospheric definition	10	1	
7 Cloud type for each layer		Absorption, amounts of scattering	10	1	
8 Cloud coverage for each layer	%	Downwelling irradiance level	10	1	5%
9 Base altitude of each cloud layer	km	Downwelling irradiance level	10	1	0.05 km
10 Wind speed at surface	knots	Feature signatures, transmittance calculation, dust-airborne particulate concentrations, feature directional reflectance	2	1	5%
11 Wind direction at surface	deg	Feature signatures, dust-airborne particulate concentrations	2	1	5 deg
12 Pasquill stability category	A-F	Atmospheric definition	60	2	
13 Absorbing gages (other than H2O)		Transmittance calculation	10	1	
14 Aerosol/particle index of refraction		Transmittance calculation	1	1	
15 Aerosol/particle size distribution	number/um	Transmittance calculation	1	1	
16 Aerosol/particle shape		Transmittance calculation	1	1	
17 Precipitation type indicator		Transmittance calculation	10	1	
18 Precipitation rate	mm/hr	Feature signatures	2	1	20%
19 Precipitation temperature	°C	Feature/background signatures, MMW transmission	10	1	1 °C
20 Dew/Frost		Feature signatures	10	1	
21 Target/background emissivity		Feature signatures	60	1	
22 Relative Humidity Structure Const.	m**-2/3	Beamsread/Scintillation	2	2	
23 State of surface		Environment characterization	60	2	
24 Sea state		Environment characterization	10	2	
25 Global solar radiation	W/cm**2	Solar insolation analysis	2	2	5-10%
26 Diffuse sky radiation	W/cm**2	Thermal radiation exchange analysis Scattered/reflected sky radiation	2	2	5-10%
27 Directional sky radiation	W/cm**2	Thermal radiation exchange analysis Scattered/reflected sky radiation	2	2	5-10%
28 Sky-to-ground luminance ratio		Cloud distribution level Visual range estimation			
29 Downwelling spectral direct radiance	W/cm**2-um	Feature signatures	10	2	5-10%

Guidelines for Atmospheric Measurements in Support of Electro-Optical Systems Testing
RCC 356-22 August 2022

Table A-4. Summary Atmospheric Environmental Parameters in Support of Millimeter Wave Transmission Testing

Parameter	Units	Parameter Rationale	INFRARED IMAGE DETECTION		
			Averaging Period, Min	Importance	Acceptable Error
30 Downwelling spectral diffuse irradiance	W/cm**2-um	Feature signatures	10	2	5-10%
31 Directional spectral sky radiance	W/cm**2-um-er	Thermal radiation exchange analysis Scattered/reflected sky radiation Cloud distribution level	10	2	5-10%
32 Spectral path transmittance		Apparent feature and background signatures	5-10	1	5%
33 Index of refraction structure const.	m**-2/3	Image resolution/beamsread/scintillation	2	2	
34 Number of atmospheric layers		Atmospheric definition	60	2	
35 Base altitude for each atmospheric layer	km	Atmospheric definition	60	2	0.05 km
36 Visibility for each atmospheric layer	km	Transmittance calculation Downwelling irradiance level	60	2	10%
37 Relative humidity for each atmospheric layer	%	Transmittance calculation Downwelling irradiance level	60	2	10%
38 Air temperature for each atmospheric layer	°C	Feature signatures Transmittance calculation	60	2	1 °C
39 Dew point temperature for each atmospheric layer	°C	Humidity calculation Rain temperature calculation	60	2	1 °C
40 Atmospheric pressure for each atmospheric layer	mbar	Transmittance calculation Downwelling irradiance level	60	2	10%

Guidelines for Atmospheric Measurements in Support of Electro-Optical Systems Testing
RCC 356-22 August 2022

Table A-5. Summary Atmospheric Environmental Parameters in Support of SWOE Program Electro-Optical Systems Simulations

Parameter	Units	Parameter Rationale	SWOE PROGRAM		
			Averaging Period, Min	Importance	Acceptable Error
1 Solar zenith angle	deg	Direct radiance source position	10	2	2 deg
2 Solar azimuth angle	deg	Direct radiance source position	10	2	10 deg
3 Visibility	km	Environment characterization	10	1	10%
4 Present weather		Environment characterization	10	1	
5 Cloud-free line-of-sight	km/direction	Environment characterization	10	1	10%
6 Number of cloud layers		Atmospheric definition	10	1	
7 Cloud type for each layer		Absorption, amounts of scattering	10	1	
8 Cloud coverage for each layer	%	Downwelling irradiance level	10	1	5%
9 Base altitude of each cloud layer	km	Downwelling irradiance level	10	1	0.05 km
10 Wind speed at surface	knots	Feature signatures, transmittance calculation, dust-airborne particulate concentrations, feature directional reflectance	2	1	5%
11 Wind direction at surface	deg	Feature signatures, dust-airborne particulate concentrations	2	1	5 deg
12 Pasquill stability category	A-F	Atmospheric definition	60	2	
13 Precipitation type indicator		Transmittance calculation Feature signatures	10	1	
14 Precipitation rate	mm/hr	Transmittance calculation	2	1	20%
15 Precipitation temperature	°C	Feature/background signatures, MMW Transmission	10	2	1 °C
16 Dew/Frost		Feature signatures	10	1	
17 Scintillation		Laser beamspread	2	2	
18 State of surface		Environment characterization	60	2	
19 Sea state		Environment characterization	10	2	
20 Global solar radiation	W/cm**2	Solar insolation analysis	2	1	5-10%
21 Diffuse sky radiation	W/cm**2	Thermal radiation exchange analysis Scattered/reflected sky radiation	2		5-10%
22 Directional sky radiation	W/cm**2	Thermal radiation exchange analysis Scattered/reflected sky radiation	2	1	5-10%
23 Downwelling spectral direct radiance	W/cm**2-um	Cloud distribution level Feature signatures	10	2	5-10%
24 Downwelling spectral diffuse irradiance	W/cm**2-um	Feature signatures	10	2	5-10%
25 Directional spectral sky radiance	W/cm**2-um-er	Thermal radiation exchange analysis Scattered/reflected sky radiation Cloud distribution level	10	2	5-10%
26 Atmospheric spectral path transmittance		Apparent feature and background signatures	5-10	1	5%

Guidelines for Atmospheric Measurements in Support of Electro-Optical Systems Testing
RCC 356-22 August 2022

Table A-5. Summary Atmospheric Environmental Parameters in Support of SWOE Program Electro-Optical Systems Simulations

Parameter	Units	Parameter Rationale	SWOE PROGRAM		
			Averaging Period, Min	Importance	Acceptable Error
27 Turbulence (optical)		Image recognition	2	2	
28 Number of atmospheric layers		Atmospheric definition	60	2	
29 Base altitude for each atmospheric layer	km	Atmospheric definition	60	2	0.05 km
30 Visibility for each atmospheric layer	km	Transmittance calculation Downwelling irradiance level	60	2	10%
31 Relative humidity for each atmospheric layer	%	Transmittance calculation Downwelling irradiance level	60	2	10%
32 Air temperature for each atmospheric layer	°C	Feature signatures Transmittance calculation	60	2	1 °C
33 Dew point temperature for each atmospheric layer	°C	Humidity calculation Rain temperature calculation	60	2	1 °C
34 Atmospheric pressure for each atmospheric layer	mbar	Transmittance calculation Downwelling irradiance level	60	2	10%

Guidelines for Atmospheric Measurements in Support of Electro-Optical Systems Testing
RCC 356-22 August 2022

Table A-6. Summary Atmospheric Environmental Parameters in Support of Smoke Week Test Program Electro-Optical Systems Testing

Parameter	Units	Parameter Rationale	SMOKE WEEK TEST REQUIREMENTS		
			Averaging Period, Min	Importance	Acceptable Error
1 Solar zenith angle	deg	Direct radiance source position	10	1	2 deg
2 Solar azimuth angle	deg	Direct radiance source position	10	1	10 deg
3 2% Contract Visual Range	km	Environment characterization	10	1	10%
4 Present weather		Environment characterization	10	1	
5 Cloud-free line-of-sight	km/direction	Environment characterization	10	1	10%
6 Number of cloud layers		Atmospheric definition	10	1	
7 Cloud type for each layer		Absorption, amounts of scattering	10	1	
8 Cloud coverage for each layer	%	Downwelling irradiance level	10	1	5%
9 Base altitude of each cloud layer	km	Downwelling irradiance level	10	1	0.05 km
10 Wind speed at surface	knots	Feature signatures, transmittance calculation, dust-airborne particulate concentrations, feature directional reflectance	1	1	5%
11 Wind direction at surface	deg	Feature signatures, dust-airborne particulate concentrations	1	1	5 deg
12 Pasquill stability category	A-F	Atmospheric definition	5	1	
13 Absorbing gages (other than H2O)		Transmittance calculation	10	2	
14 Aerosol/particle index of refraction		Transmittance calculation	1	1	
15 Aerosol/particle size distribution	number/um	Transmittance calculation	1	1	
16 Aerosol/particle shape		Transmittance calculation	1	1	
17 Precipitation type indicator		Transmittance calculation	2	1	
18 Precipitation rate	mm/hr	Feature signatures			
19 Precipitation temperature	°C	Transmittance calculation	2	1	20%
		Feature/background signatures, MMW transmission	2	1	1 °C
20 Dew/Frost		Feature signatures	10	1	
21 Target/background emissivity		Feature signatures	NA	1	
22 Relative Humidity Structure Const.	m**-2/3	Beamsread/Scintillation	2	1	
23 State of surface		Environment characterization	60	3	
24 Sea state		Environment characterization	10	3	
25 Global solar radiation	W/cm**2	Solar insolation analysis	2	1	5-10%
26 Diffuse sky radiation	W/cm**2	Thermal radiation exchange analysis	2		5-10%
		Scattered/reflected sky radiation			
27 Directional sky radiation	W/cm**2	Thermal radiation exchange analysis	2	1	5-10%
		Scattered/reflected sky radiation			
		Cloud distribution level			
28 Sky-to-ground luminance ratio		Visual range estimation			
29 Downwelling spectral direct radiance	W/cm**2-um	Feature signatures	5	1	5-10%

Guidelines for Atmospheric Measurements in Support of Electro-Optical Systems Testing
RCC 356-22 August 2022

Table A-6. Summary Atmospheric Environmental Parameters in Support of Smoke Week Test Program Electro-Optical Systems Testing

Parameter	Units	Parameter Rationale	SMOKE WEEK TEST REQUIREMENTS		
			Averaging Period, Min	Importance	Acceptable Error
30 Downwelling spectral diffuse irradiance	W/cm**2-um	Feature signatures	5	1	5-10%
31 Directional spectral sky radiance	W/cm**2-um-er	Thermal radiation exchange analysis Scattered/reflected sky radiation Cloud distribution level	5	1	5-10%
32 Spectral path transmittance		Apparent feature and background signatures	5-10	1	5%
33 Index of refraction structure const.	m**-2/3	Image resolution/beamsread/scintillation	2	1	
34 Number of atmospheric layers		Atmospheric definition	60	2	
35 Base altitude for each atmospheric layer	km	Atmospheric definition	60	2	0.05 km
36 Visibility for each atmospheric layer	km	Transmittance calculation Downwelling irradiance level	60	2	10%
37 Relative humidity for each atmospheric layer	%	Transmittance calculation Downwelling irradiance level	60	2	10%
38 Air temperature for each atmospheric layer	°C	Feature signatures Transmittance calculation	60	2	1 °C
39 Dew point temperature for each atmospheric layer	°C	Humidity calculation Rain temperature calculation	60	2	1 °C
40 Atmospheric pressure for each atmospheric layer	mbar	Transmittance calculation Downwelling irradiance level	60	2	10%

Guidelines for Atmospheric Measurements in Support of Electro-Optical Systems Testing
RCC 356-22 August 2022

Table A-7. Summary Atmospheric Environmental Parameters in Support of Littoral Warfare Test Program Electro-Optical Systems Testing

Parameter	Units	Parameter Rationale	LITTORAL WARFARE TEST REQUIREMENTS		
			Averaging Period, Min	Importance	Acceptable Error
1 Solar zenith angle	deg	Direct radiance source position	10	1	2 deg
2 Solar azimuth angle	deg	Direct radiance source position	10	1	10 deg
3 2% Contrast Visual Range	km	Environment characterization	10	1	5%
4 Present weather		Environment characterization	10	1	
5 Cloud-free line-of-sight	km/direction	Environment characterization	10	1	5%
6 Number of cloud layers		Atmospheric definition	10	1	
7 Cloud type for each layer		Absorption, amounts of scattering	10	1	
8 Cloud coverage for each layer	%	Downwelling irradiance level	10	1	5%
9 Base altitude of each cloud layer	km	Downwelling irradiance level	10	1	0.05 km
10 Wind speed at surface	knots	Feature signatures, transmittance calculation, dust-airborne particulate concentrations, feature directional reflectance	1	1	5%
11 Wind direction at surface	deg	Feature signatures, dust-airborne particulate concentrations	1	1	5 deg
12 Pasquill stability category	A-F	Atmospheric definition	5	1	
13 Absorbing gages (other than H2O)		Transmittance calculation	10	2	
14 Aerosol/particle index of refraction		Transmittance calculation	1	1	
15 Aerosol/particle size distribution	number/um	Transmittance calculation	1	1	
16 Aerosol/particle shape		Transmittance calculation	1	1	
17 Precipitation type indicator		Transmittance calculation	2	1	
18 Precipitation rate	mm/hr	Feature signatures	2	1	20%
19 Precipitation temperature	°C	Transmittance calculation	2	1	20%
20 Dew/Frost		Feature/background signatures, MMW transmission	2	1	1 °C
21 Target/background emissivity		Feature signatures	10	1	
22 Relative Humidity Structure Const.	m**-2/3	Feature signatures	NA	1	
23 State of surface		Beamsread/Scintillation	2	1	
24 Sea state		Environment characterization	60	1	
25 Global solar radiation	W/cm**2	Environment characterization	10	1	
26 Diffuse sky radiation	W/cm**2	Solar insolation analysis	2	1	5-10%
27 Directional sky radiation	W/cm**2	Thermal radiation exchange analysis	2	1	5-10%
28 Sky-to-ground luminance ratio		Scattered/reflected sky radiation	2	1	5-10%
29 Downwelling spectral direct radiance	W/cm**2-um	Thermal radiation exchange analysis	2	1	5-10%
		Scattered/reflected sky radiation	2	1	5-10%
		Cloud distribution level	2	1	5-10%
		Visual range estimation	2	1	5-10%
		Feature signatures	5	1	5-10%

Guidelines for Atmospheric Measurements in Support of Electro-Optical Systems Testing
RCC 356-22 August 2022

Table A-7. Summary Atmospheric Environmental Parameters in Support of Littoral Warfare Test Program Electro-Optical Systems Testing						
Parameter	Units	Parameter Rationale	LITTORAL WARFARE TEST REQUIREMENTS			
			Averaging Period, Min	Importance	Acceptable Error	
30 Downwelling spectral diffuse irradiance	W/cm**2-um	Feature signatures	5	1	5-10%	
31 Directional spectral sky radiance	W/cm**2-um-er	Thermal radiation exchange analysis Scattered/reflected sky radiation Cloud distribution level	5	1	5-10%	
32 Spectral path transmittance		Apparent feature and background signatures	5-10	1	5%	
33 Index of refraction structure const.	m**-2/3	Image resolution/beamsread/scintillation	2	1		
34 Number of atmospheric layers		Atmospheric definition	60	1		
35 Base altitude for each atmospheric layer	km	Atmospheric definition	60	1	0.05 km	
36 Visibility for each atmospheric layer	km	Transmittance calculation Downwelling irradiance level	60	1	10%	
37 Relative humidity for each atmospheric layer	%	Transmittance calculation Downwelling irradiance level	60	1	10%	
38 Air temperature for each atmospheric layer	°C	Feature signatures Transmittance calculation	60	1	1 °C	
39 Dew point temperature for each atmospheric layer	°C	Humidity calculation Rain temperature calculation	60	1	1 °C	
40 Atmospheric pressure for each atmospheric layer	mbar	Transmittance calculation Downwelling irradiance level	60	1	10%	

Guidelines for Atmospheric Measurements in Support of Electro-Optical Systems Testing
RCC 356-22 August 2022

Table A-8. Summary Atmospheric Environmental Parameters in Support of Maritime Warfare Test Program Electro-Optical Systems Testing

Parameter	Units	Parameter Rationale	LITTORAL WARFARE TEST REQUIREMENTS		
			Averaging Period, Min	Importance	Acceptable Error
1 Solar zenith angle	deg	Direct radiance source position	10	1	2 deg
2 Solar azimuth angle	deg	Direct radiance source position	10	1	10 deg
3 2% Contrast Visual Range	km	Environment characterization	1	1	5%
4 Present weather		Environment characterization	10	1	
5 Cloud-free line-of-sight	km/direction	Environment characterization	10	1	5%
6 Number of cloud layers		Atmospheric definition	10	1	
7 Cloud type for each layer		Absorption, amounts of scattering	10	1	
8 Cloud coverage for each layer	%	Downwelling irradiance level	10	1	5%
9 Base altitude of each cloud layer	km	Downwelling irradiance level	10	1	0.05 km
10 Wind speed at surface	knots	Feature signatures, transmittance calculation, dust-airborne particulate concentrations, feature directional reflectance	1	1	5%
11 Wind direction at surface	deg	Feature signatures, dust-airborne particulate concentrations	1	1	5 deg
12 Pasquill stability category	A-F	Atmospheric definition	5	1	
13 Absorbing gages (other than H2O)		Transmittance calculation	10	2	
14 Aerosol/particle index of refraction		Transmittance calculation	1	1	
15 Aerosol/particle size distribution	number/um	Transmittance calculation	1	1	
16 Aerosol/particle shape		Transmittance calculation	1	1	
17 Precipitation type indicator		Transmittance calculation	2	1	
18 Precipitation rate	mm/hr	Feature signatures			
19 Precipitation temperature	°C	Transmittance calculation	2	1	20%
		Feature/background signatures, MMW transmission	2	1	1 °C
20 Dew/Frost		Feature signatures	10	1	
21 Target/background emissivity		Feature signatures	NA	1	
22 Relative Humidity Structure Const.	m**-2/3	Beamspread/Scintillation	2	1	
23 State of surface		Environment characterization	60	1	
24 Sea state		Environment characterization	5	1	
25 Global solar radiation	W/cm**2	Solar insolation analysis	2	1	5-10%
26 Diffuse sky radiation	W/cm**2	Thermal radiation exchange analysis	2		5-10%
		Scattered/reflected sky radiation			
27 Directional sky radiation	W/cm**2	Thermal radiation exchange analysis	2	1	5-10%
		Scattered/reflected sky radiation			
		Cloud distribution level			
28 Sky-to-ground luminance ratio		Visual range estimation			
29 Downwelling spectral direct radiance	W/cm**2-um	Feature signatures	5	1	5-10%

Guidelines for Atmospheric Measurements in Support of Electro-Optical Systems Testing
RCC 356-22 August 2022

Table A-8. Summary Atmospheric Environmental Parameters in Support of Maritime Warfare Test Program Electro-Optical Systems Testing

Parameter	Units	Parameter Rationale	LITTORAL WARFARE TEST REQUIREMENTS		
			Averaging Period, Min	Importance	Acceptable Error
30 Downwelling spectral diffuse irradiance	W/cm**2-um	Feature signatures	5	1	5-10%
31 Directional spectral sky radiance	W/cm**2-um-er	Thermal radiation exchange analysis Scattered/reflected sky radiation Cloud distribution level	5	1	5-10%
32 Spectral path transmittance		Apparent feature and background signatures	5-10	1	5%
33 Index of refraction structure const.	m**-2/3	Image resolution/beamsread/scintillation	2	1	
34 Number of atmospheric layers		Atmospheric definition	60	1	
35 Base altitude for each atmospheric layer	km	Atmospheric definition	60	1	0.05 km
36 Visibility for each atmospheric layer	km	Transmittance calculation Downwelling irradiance level	60	1	10%
37 Relative humidity for each atmospheric layer	%	Transmittance calculation Downwelling irradiance level	60	1	10%
38 Air temperature for each atmospheric layer	°C	Feature signatures Transmittance calculation	60	1	1 °C
39 Dew point temperature for each atmospheric layer	°C	Humidity calculation Rain temperature calculation	60	1	1 °C
40 Atmospheric pressure for each atmospheric layer	mbar	Transmittance calculation Downwelling irradiance level	60	1	10%

This page intentionally left blank.

APPENDIX B

Relative Uncertainty in Visual 50% Probability of Detection

B.1 Purpose

This appendix demonstrates the impact of meteorologic measurement uncertainty on the evaluation of visual imaging sensors.

B.2 Scope

The 50% probability of detection is taken as the data application. The primary parameters affecting probability of detection with a visual imager are the inherent contrast of the target, the contrast threshold of the sensor, relative (to no attenuation) atmospheric transmittance, target range and size, visual and sensor response to contrast, and path luminance, which is defined in terms of the ratio of sky illuminance to background illuminance. Figure B-1 shows the relative uncertainty in the 50% probability of detection as a function of relative atmospheric transmittance for selected values of the sky-to-ground ratio. A sky-to-ground ratio of 1 corresponds to the Koschmieder transmittance for visual range. Figure B-1 can be interpreted as defining the transmittance required to reduce target probability of detection to 50% for a fixed ratio of inherent target contrast to threshold contrast. As the inherent contrast approaches the threshold contrast, less attenuation (higher levels of transmittance) is required to reduce the probability of detection. As the inherent contrast increases relative threshold contrast, increased attenuation (lower values of transmittance) is required to reduce the probability of detection. Figure B-2 shows information similar to that in figure B-1 except that the relative transmission axis has been written in terms of the ratio of target to visual range. Figure B-3, Figure B-4, and Figure B-5 show the impact of sky-to-ground ratio for a range of inherent contrast to threshold contrast values.

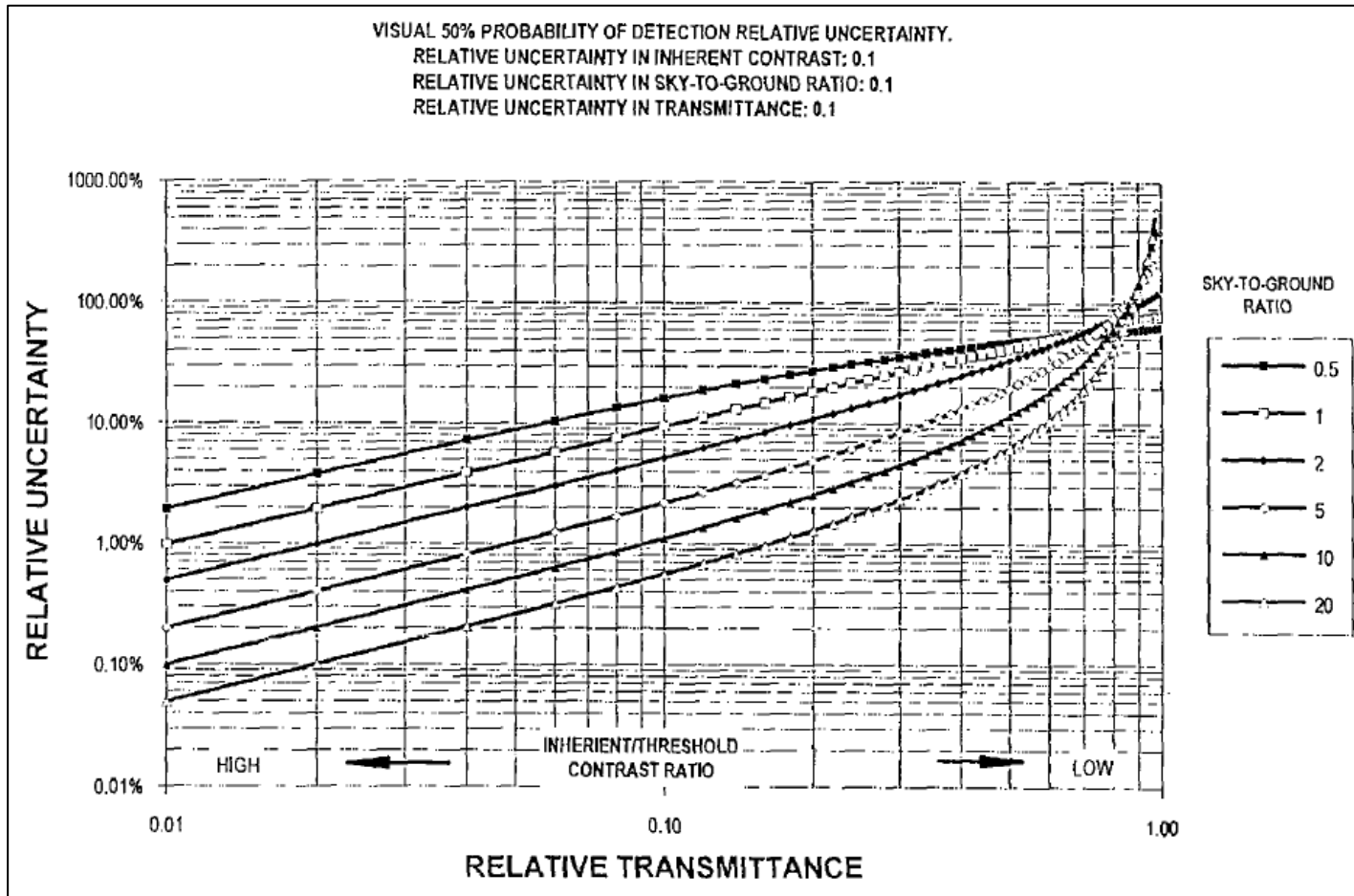


Figure B-1. Relative Uncertainty in Visual 50% Probability of Detection as a Function of Atmospheric Transmittance and Sky-to-Ground Ratio

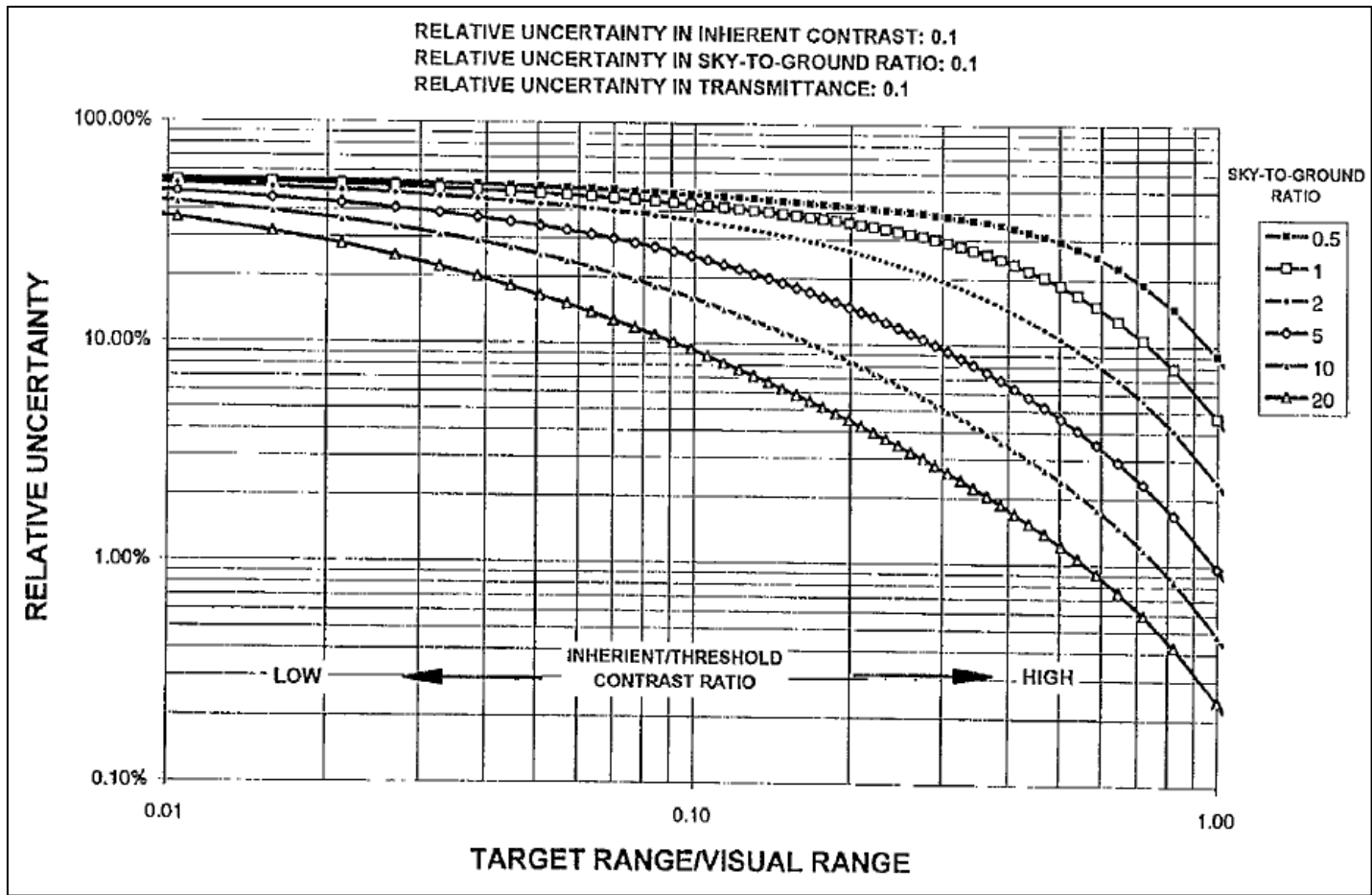


Figure B-2. Relative Uncertainty in Visual 50% Probability of Detection as a Function of Target Range to Visual Range Ratio and Sky-to-Ground Illumance Ratio

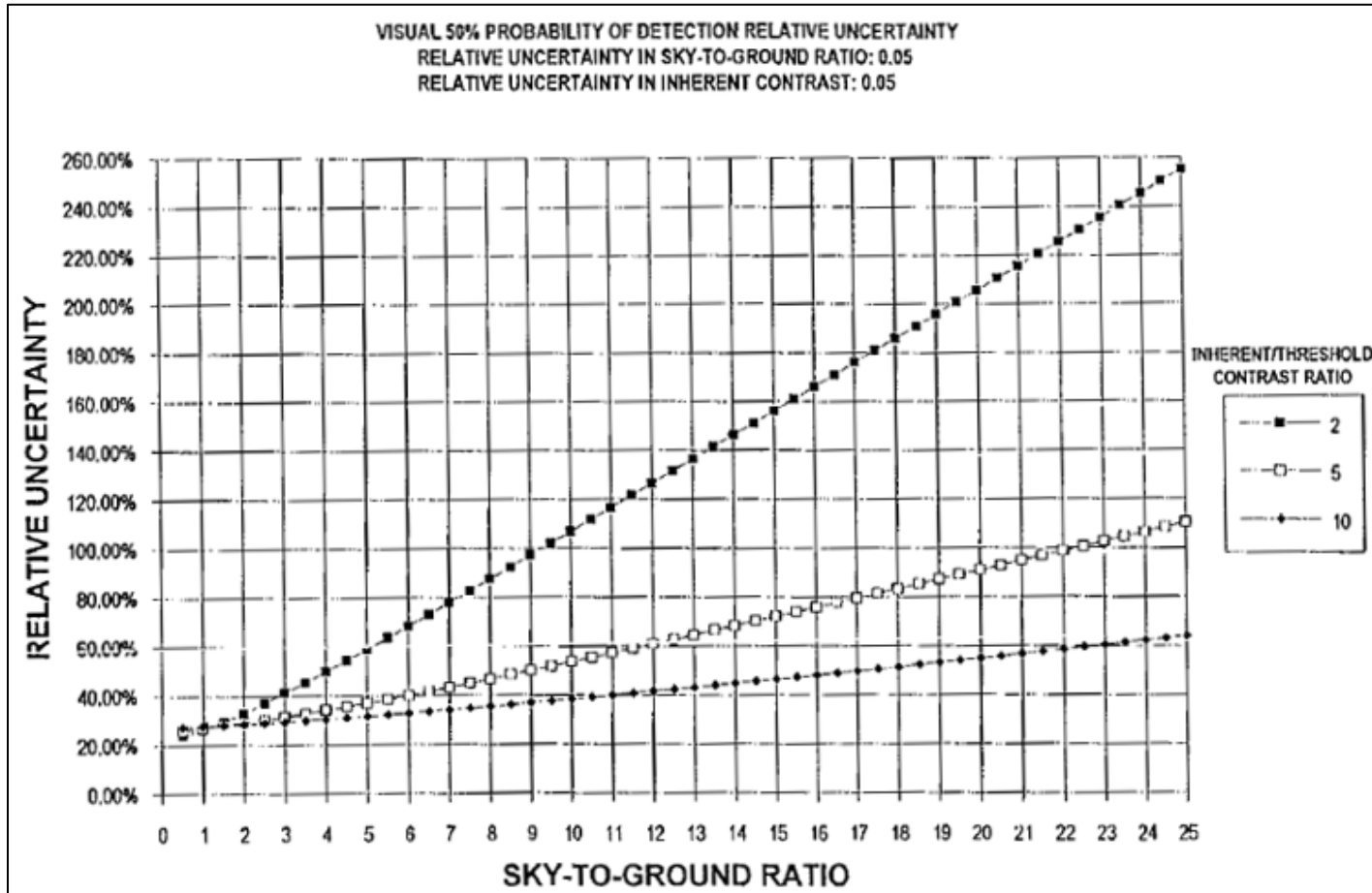
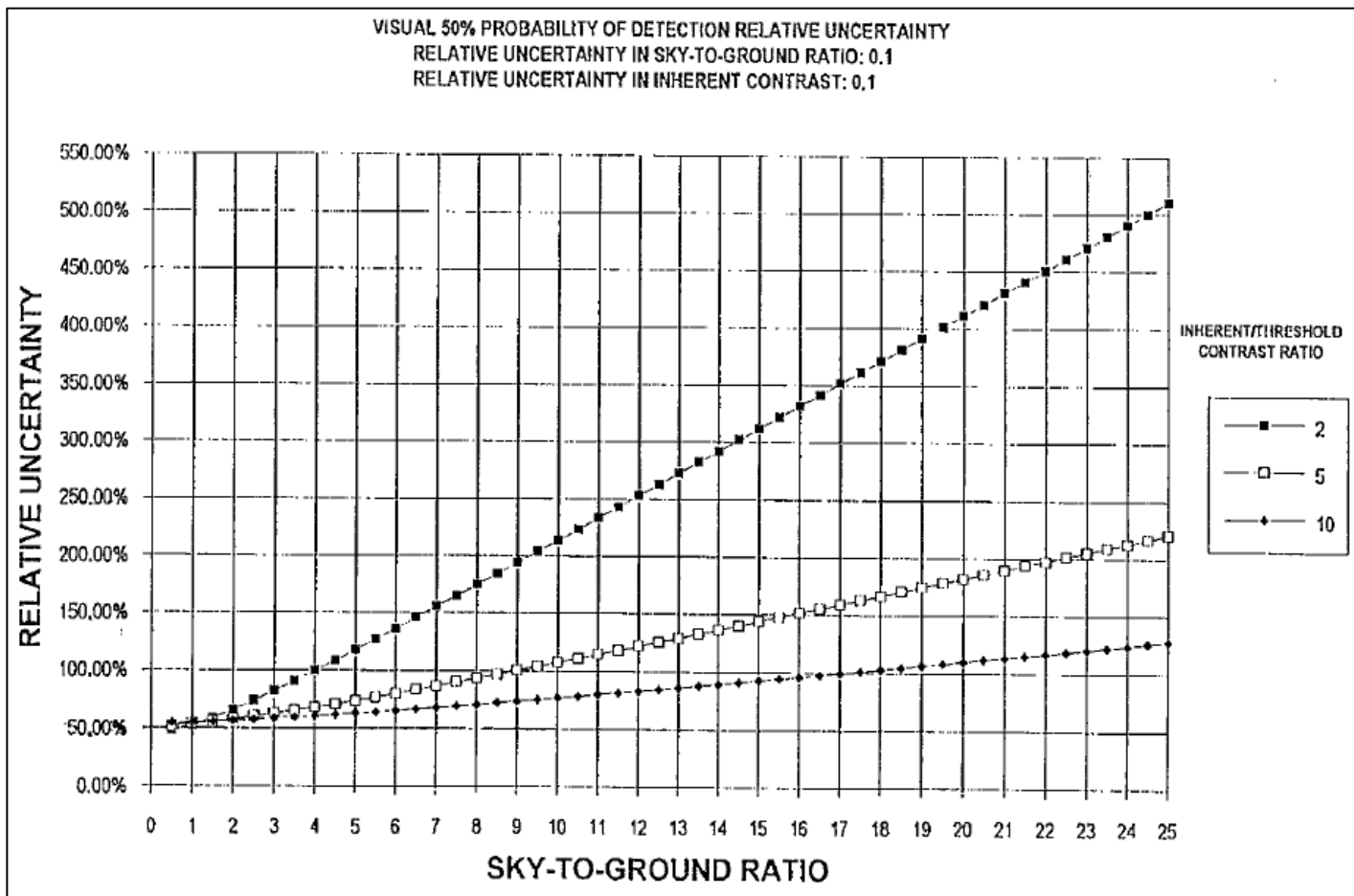


Figure B-3. Relative Uncertainty in Visual 50% Probability of Detection as a Function of and Sky-to-Ground Ratio for Increasing Target Contrast Relative to Threshold Contrast for 5% Uncertainty in Inherent Contrast and Sky-to-Ground Ratio



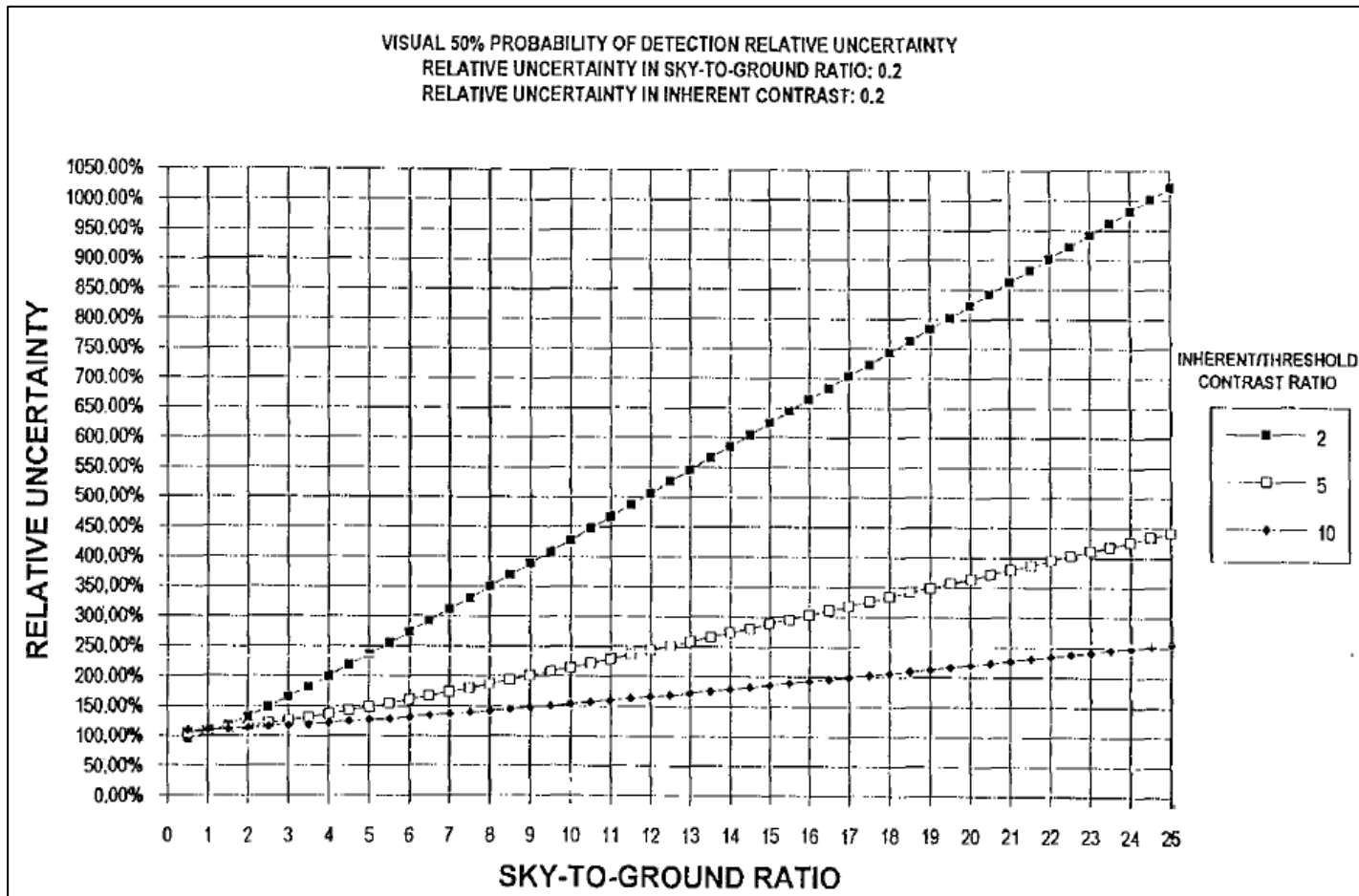


Figure B-4. Relative Uncertainty in Visual 50% Probability of Detection as a Function of and Sky-to-Ground Ratio for Increasing Target Contrast Relative to Threshold Contrast for 10% Uncertainty in Inherent Contrast and Sky-to-Ground Ratio

APPENDIX C

Relative Uncertainty in Infrared (Thermal Bands) 50% Probability of Detection

C.1 Purpose

This appendix demonstrates the impact of meteorologic measurement uncertainty on the evaluation of infrared imaging sensors.

C.2 Scope

The 50% probability of detection for an 8-12 μm band FLIR is taken as the data application. The primary parameters affecting the probability of detection are the target-background thermal contrast, the absolute magnitude of the thermal irradiance (which is a function of thermodynamic temperature), target size and range, atmospheric attenuation, target and background spectral emissivities, and the MRTD of the sensor. Figure C-1 shows the relative uncertainty in the 50% probability of detection as a function of atmospheric transmittance for selected target ranges.

The transmittance can be interpreted as the transmittance required to reduce target probability of detection to 50% for a fixed ratio of target-to-background thermal contrast to MRTD that is the infrared analog to that shown in Appendix B for Figure B-1. The MRTD is assumed to be that for a commonly used military FLIR. Figure C-2 shows the variation in relative uncertainty as a function of background temperature. Figure C-3 plots the relative uncertainty in brightness temperature as a function of uncertainty in thermodynamic temperature difference for selected values of relative uncertainty in the target/background emissivity ratio.

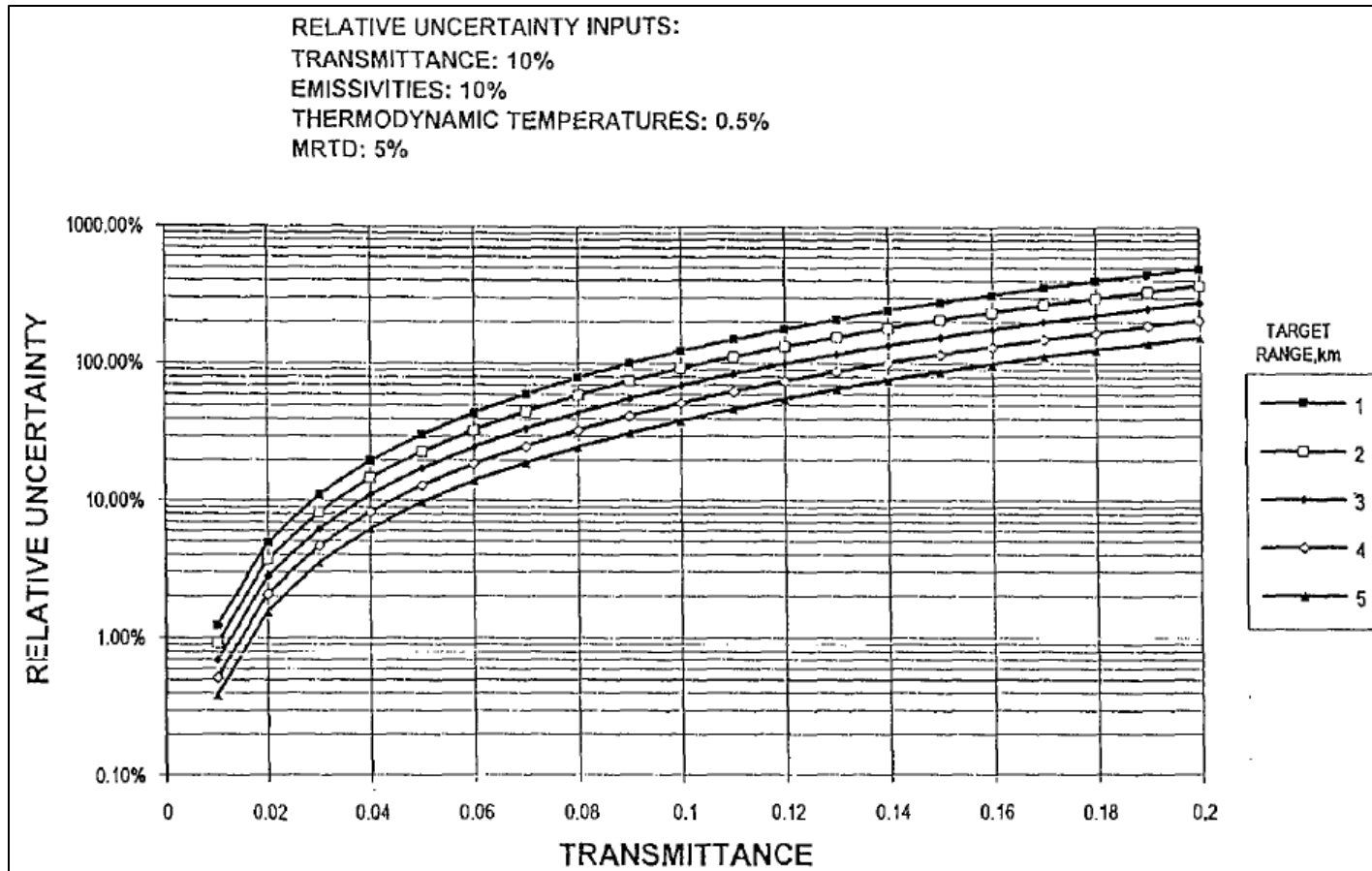


Figure C-1. Relative Uncertainty in 8-12 μm Band 50% Probability of Detection as a Function of Relative Transmittance and Increasing Target Range for 27 $^{\circ}\text{C}$ Ambient Temperature, 3 K Target-to-Background Thermal Contrast, and 0.98 Target Emissivity, and 0.9 Background Emissivity

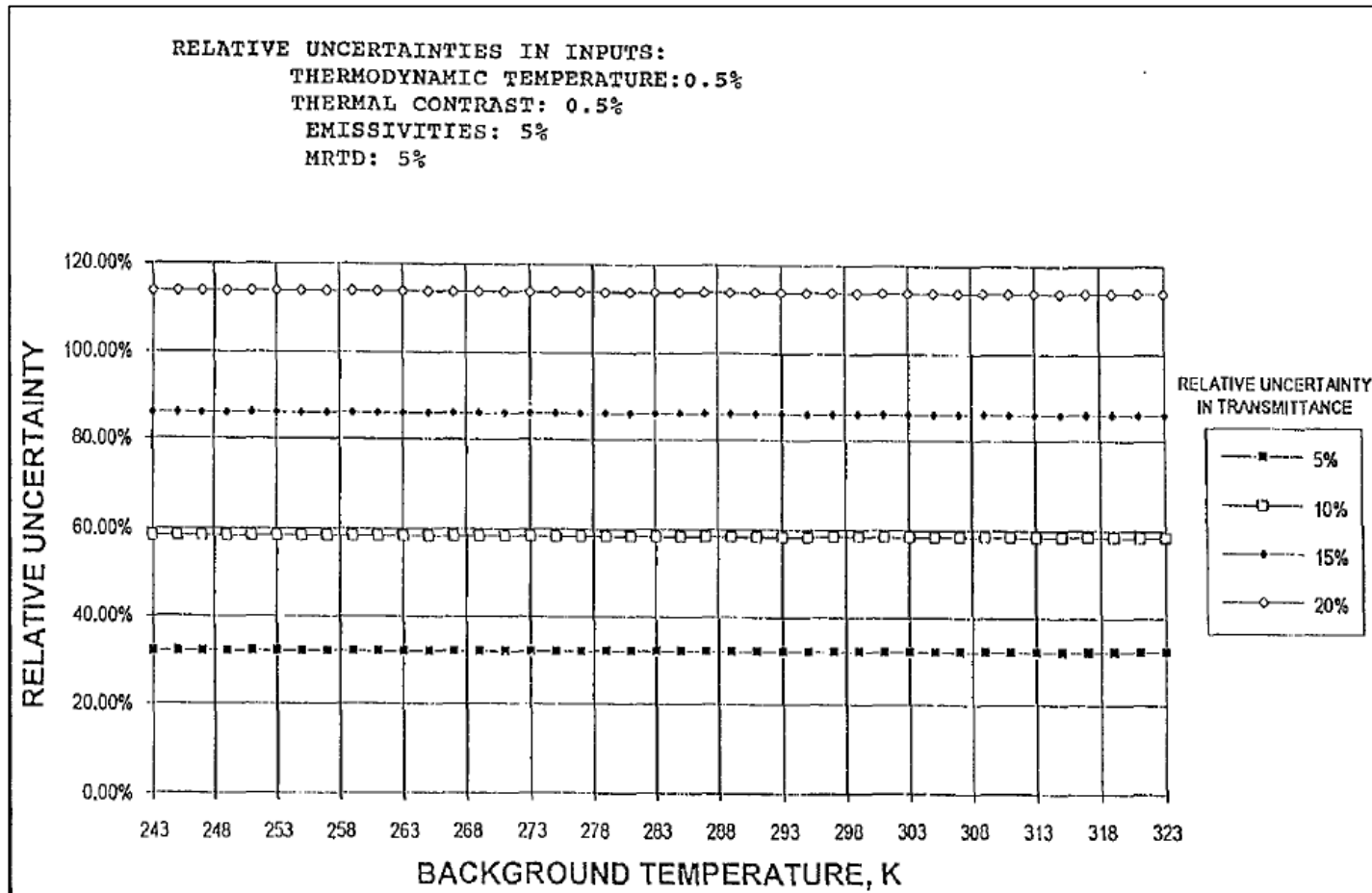


Figure C-2. Relative Uncertainty in 8-12 μm Band 50% Probability of Detection as a Function of Ambient Temperature and Increasing Relative Uncertainty in Transmittance of 27 $^{\circ}\text{C}$ Ambient Temperature, 3 K Target-to-Background Thermal Contrast, and 0.98 Target Emissivity, and 0.9 Background Emissivity

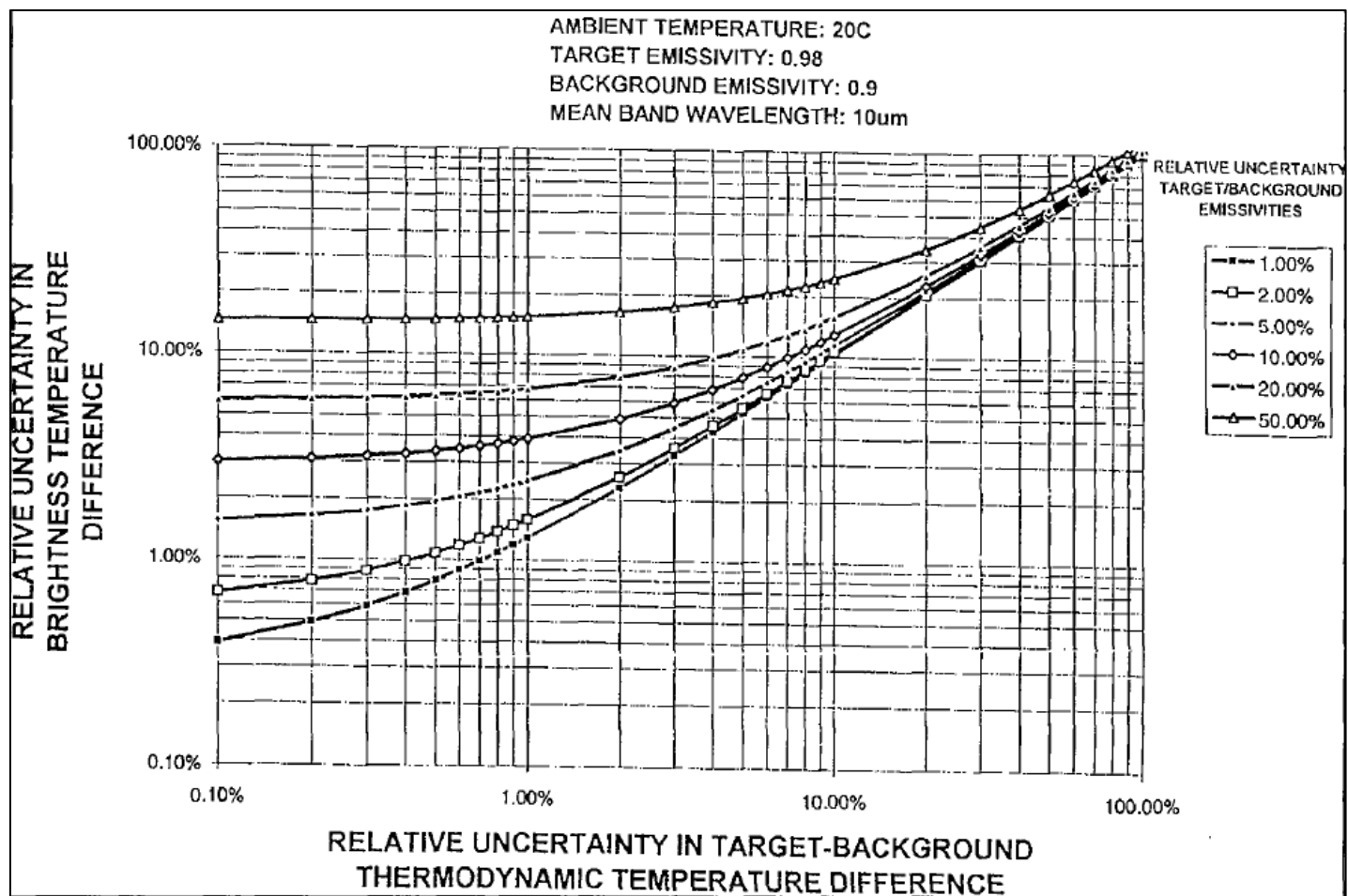


Figure C-3. Relative Uncertainty in 8-12 μm Band Brightness Temperature Difference as a Function of Relative Uncertainty in Target-to-Background Thermodynamic Temperature Difference for Values of Relative Uncertainty in the Ratio of Target-to-Background Emissivities

APPENDIX D

Relative Uncertainty in 1.06 and 10.6 μm Laser Wavelength Probability of Successful Ranging

D.1 Purpose

This appendix demonstrates the impact of meteorologic measurement uncertainty on the evaluation of LRFs/designators.

D.2 Scope

The 50% probability of successful ranging for 1.06 and 10.6 μm laser wavelengths is taken as the data application. Once the system operating characteristics (laser power, pulse width, number of range gates, transmitter beam size, and receiver aperture diameter) are established, the primary atmospheric factors affecting LRF performance are refractive turbulence and relative transmittance. Figures D-1 to D-8 show the relative uncertainty in successful ranging as a function the index of refraction structure constant for an LRF that has operating parameters normally found in military systems. The apparent plot discontinuities in figures D-1 to D-4 for 1.06 μm LRF wavelengths arise because of changes in the equations for the Strehl ratio when the inner turbulence scale exceeds three times the transmitting aperture size. Note that the refractive turbulence has a much stronger effect at the shorter wavelength than for the longer wavelength.

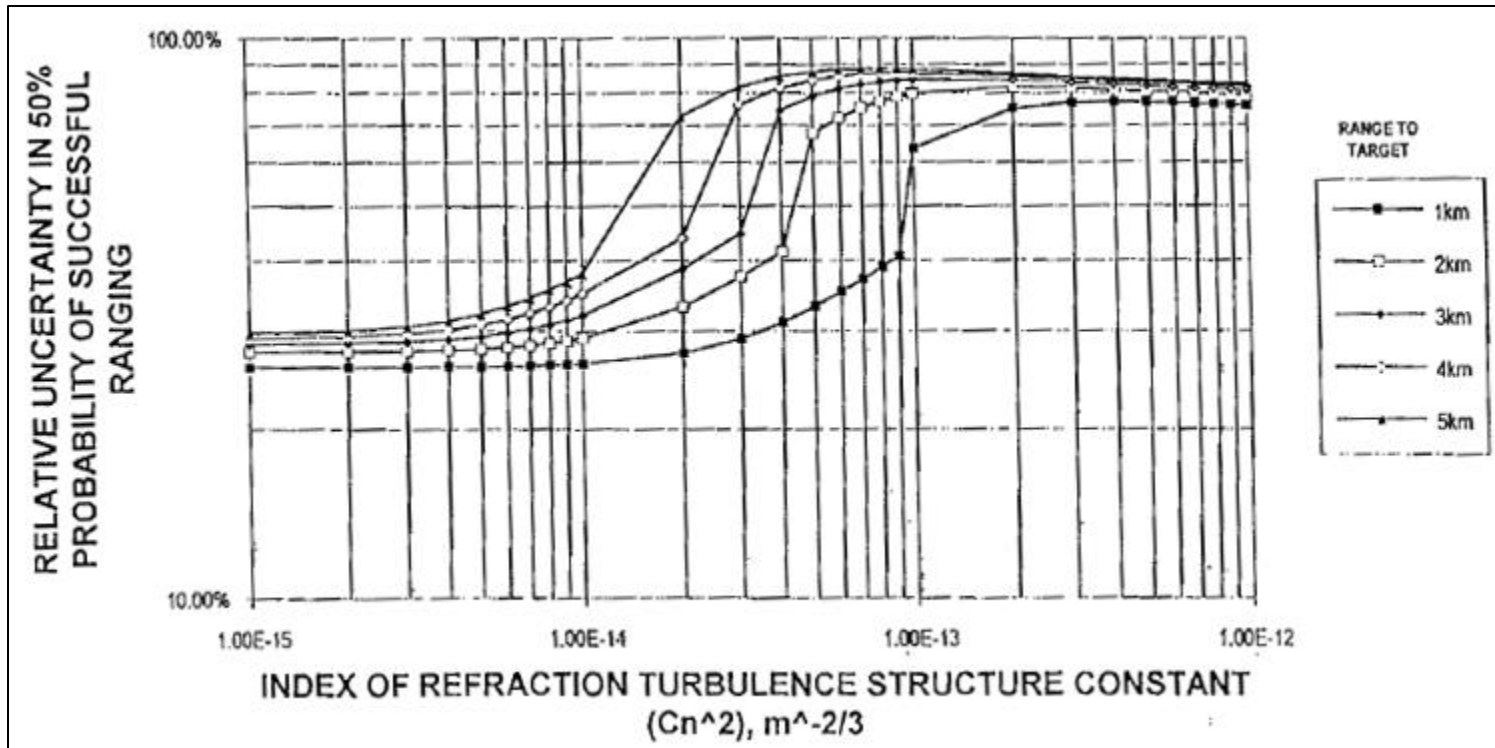


Figure D-1. Relative Uncertainty in 50% Probability of Successful Ranging for a 1.06 μm Wavelength LRF with 7-cm Diameter Circular Aperture as a Function of Refractive Index Turbulence Structure Constant, C_n^2 , and Range to Target for 10% Relative Uncertainty in C_n^2 and 5% Relative Uncertainty in Transmission

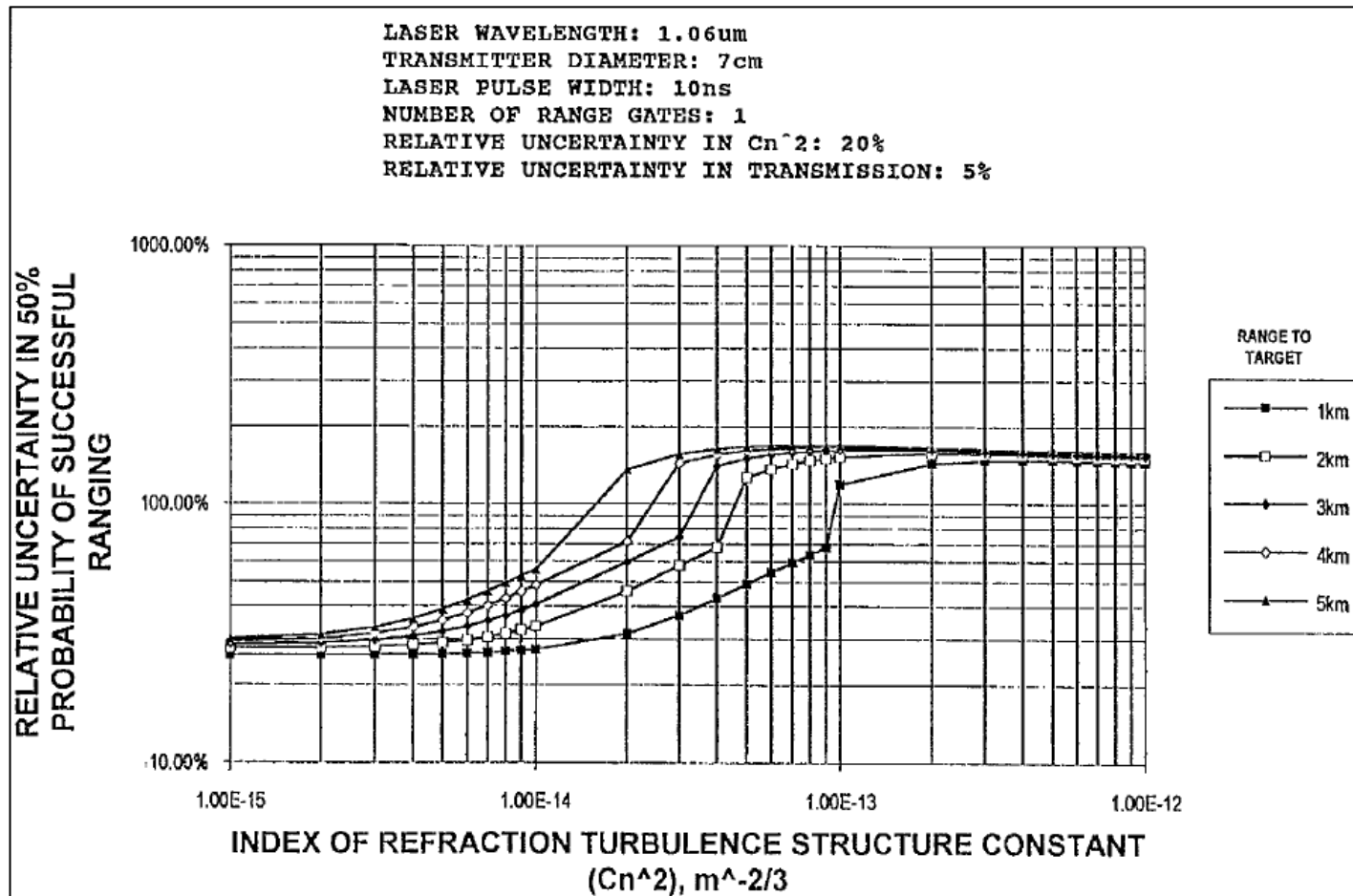


Figure D-2. Relative Uncertainty in 50% Probability of Successful Ranging for a 1.06 μm Wavelength LRF with 7-cm Diameter Circular Aperture as a Function of Refractive Index Turbulence Structure Constant, C_n^2 , and Range to Target for 20% Relative Uncertainty in C_n^2 and 5% Relative Uncertainty in Transmission

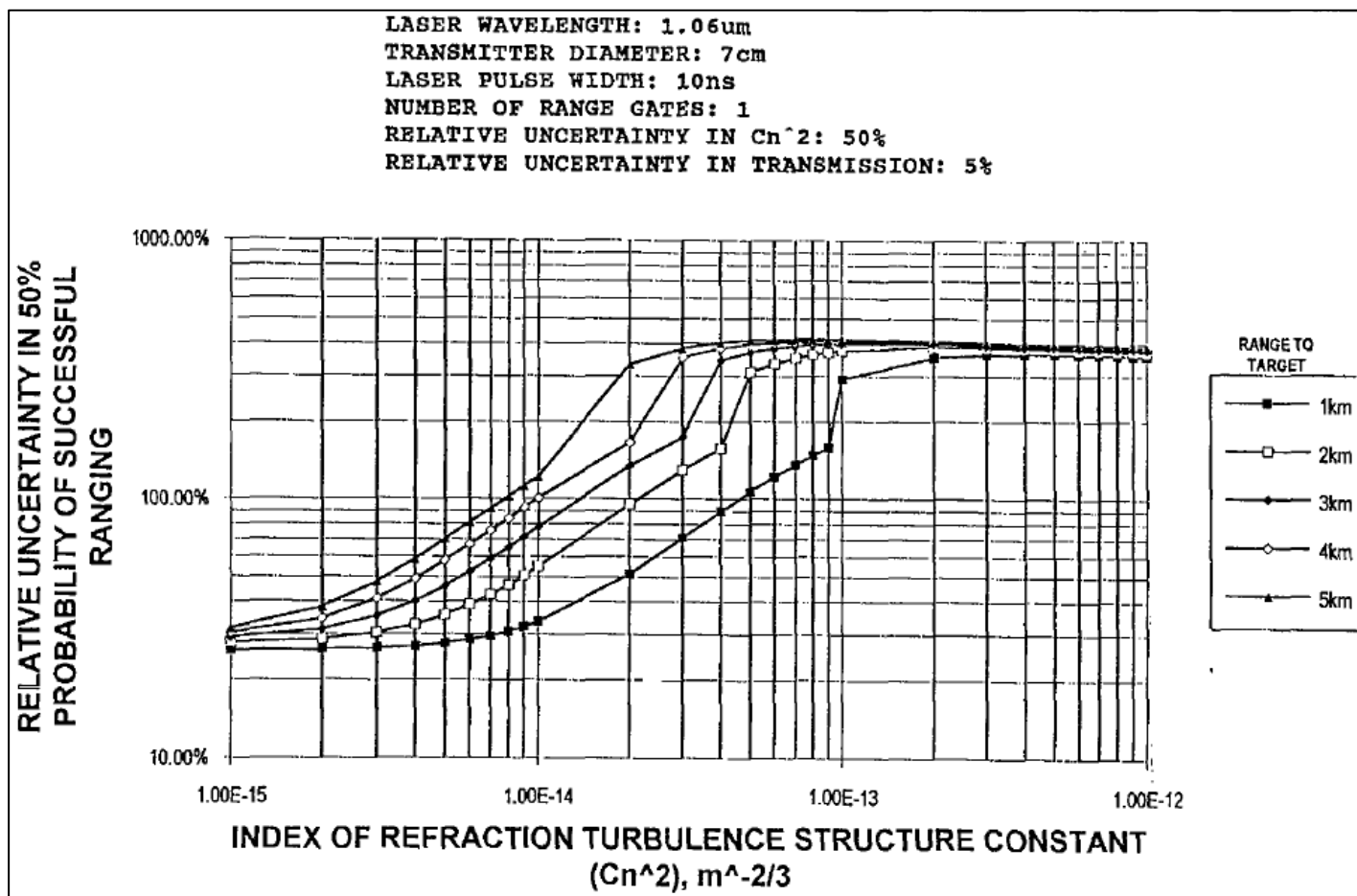


Figure D-3. Relative Uncertainty in 50% Probability of Successful Ranging for a 1.06 μm Wavelength LRF with 7-cm Diameter Circular Aperture as a Function of Refractive Index Turbulence Structure Constant, C_n^2 , and Range to Target for 50% Relative Uncertainty in C_n^2 and 5% Relative Uncertainty in Transmission

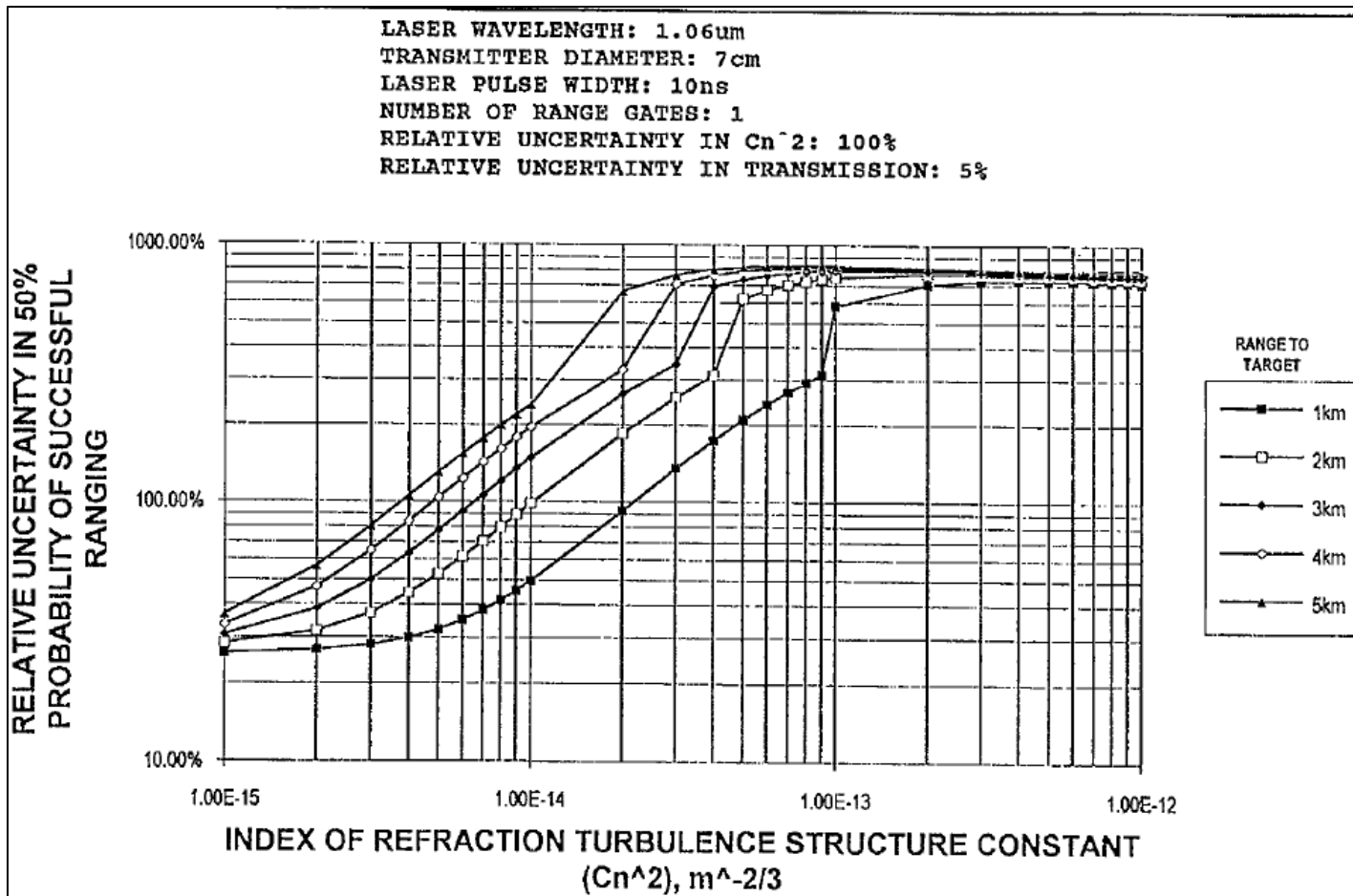


Figure D-4. Relative Uncertainty in 50% Probability of Successful Ranging for a 1.06 μm Wavelength LRF with 7-cm Diameter Circular Aperture as a Function of Refractive Index Turbulence Structure Constant, C_n^2 , and Range to Target for 100% Relative Uncertainty in C_n^2 and 5% Relative Uncertainty in Transmission

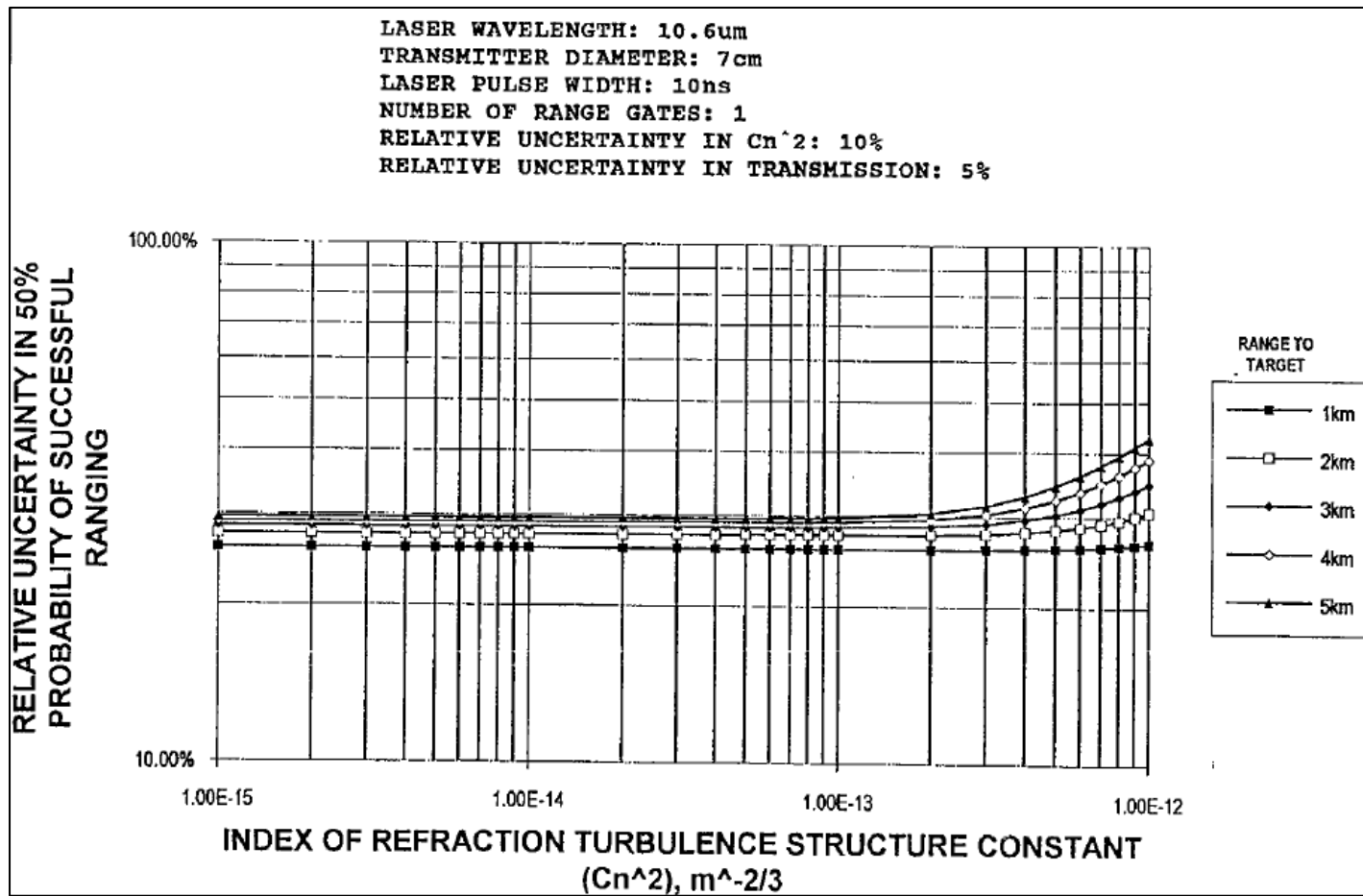


Figure D-5. Relative Uncertainty in 50% Probability of Successful Ranging for a 1.06 μm Wavelength LRF with 7-cm Diameter Circular Aperture as a Function of Refractive Index Turbulence Structure Constant, C_n^2 , and Range to Target for 10% Relative Uncertainty in C_n^2 and 5% Relative Uncertainty in Transmission

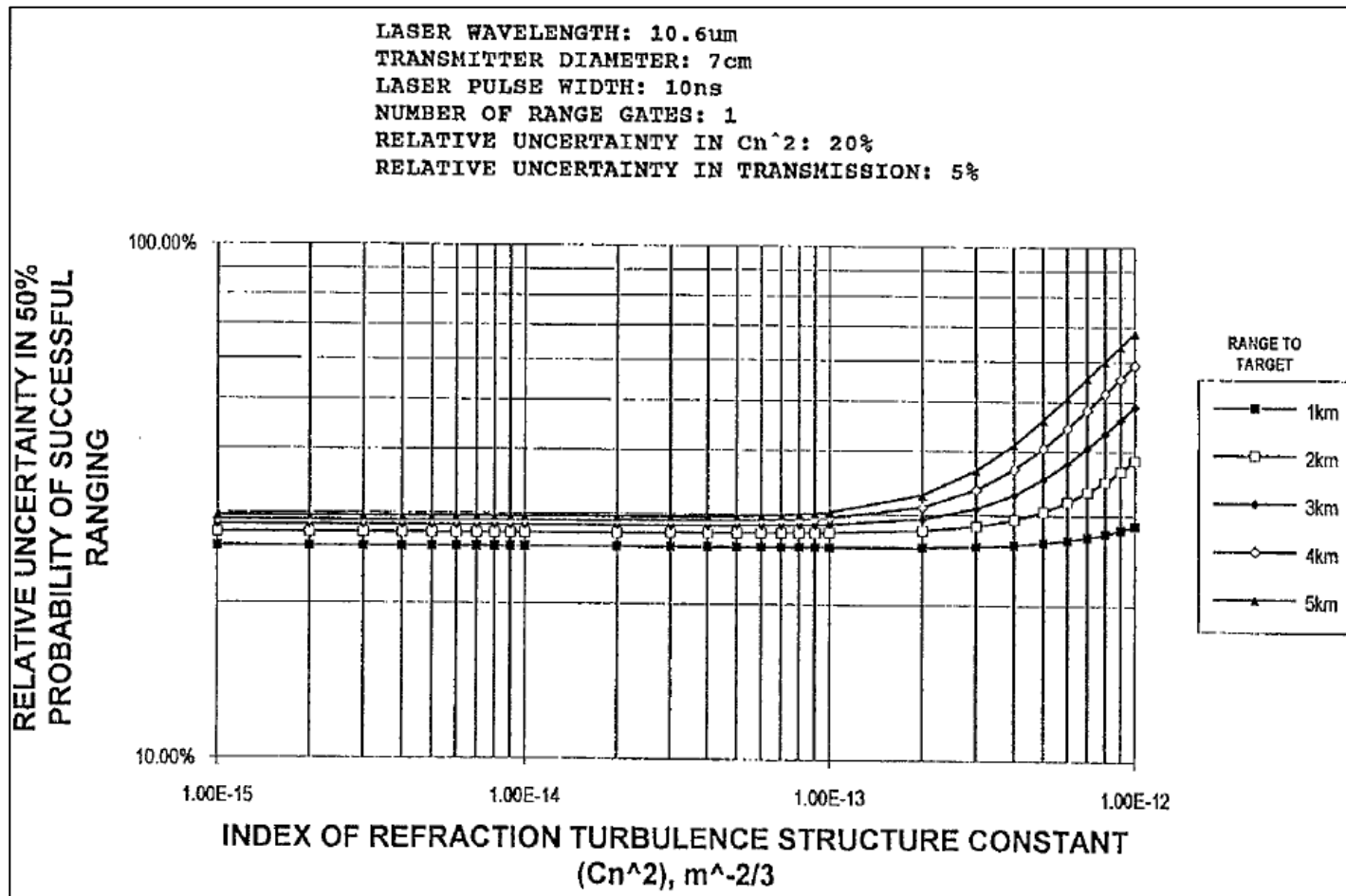


Figure D-6. Relative Uncertainty in 50% Probability of Successful Ranging for a 10.6 μ m Wavelength LRF with 7-cm Diameter Circular Aperture as a Function of Refractive Index Turbulence Structure Constant, C_n^2 , and Range to Target for 20% Relative Uncertainty in C_n^2 and 5% Relative Uncertainty in Transmission

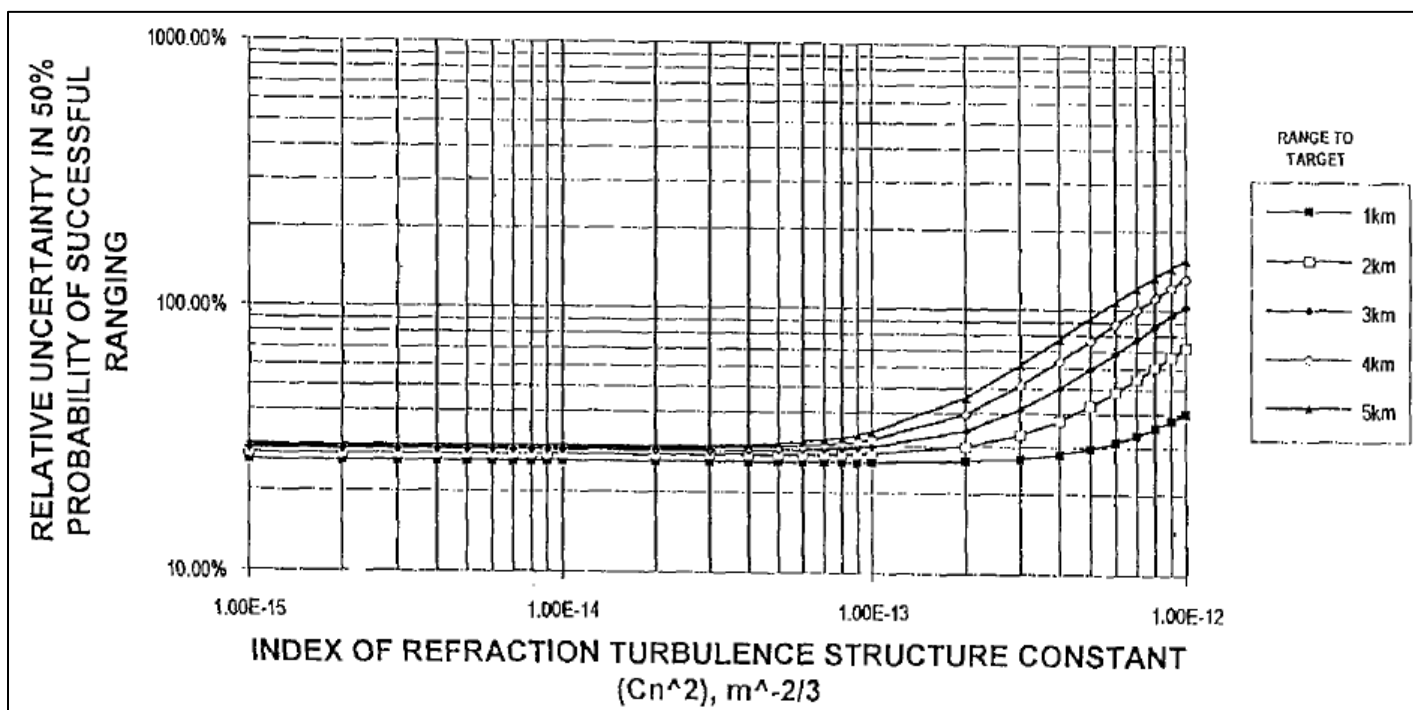


Figure D-7. Relative Uncertainty in 50% Probability of Successful Ranging for a 10.6 μm Wavelength LRF with 7-cm Diameter Circular Aperture as a Function of Refractive Index Turbulence Structure Constant, C_n^2 , and Range to Target for 50% Relative Uncertainty in C_n^2 and 5% Relative Uncertainty in Transmission

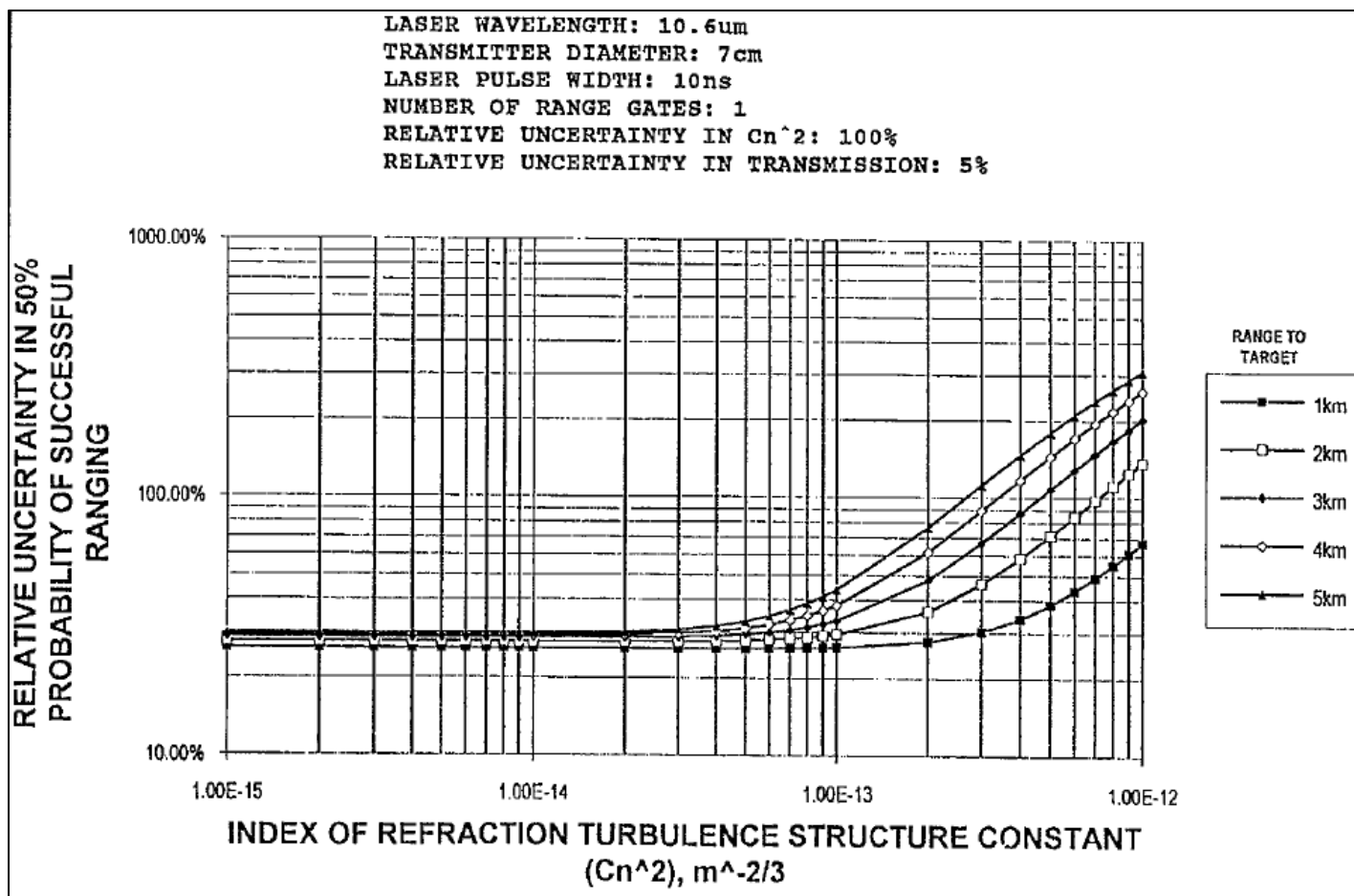


Figure D-8. Relative Uncertainty in 50% Probability of Successful Ranging for a 10.6 μm Wavelength LRF with 7-cm Diameter Circular Aperture as a Function of Refractive Index Turbulence Structure Constant, C_n^2 , and Range to Target for 100% Relative Uncertainty in C_n^2 and 5% Relative Uncertainty in Transmission

This page intentionally left blank.

APPENDIX E

Relative Uncertainty in 1.06 and 10.6 μm Laser Wavelength Laser Power, on Target

E.1 Purpose

This appendix demonstrates the impact of meteorologic measurement uncertainty on the evaluation of the amount of power that directed energy devices such as LRFs and designators can deliver to a target.

E.2 Scope

A major effect of refractive turbulence on directed energy devices such as LRFs is to spread the transmitted beam to a size much greater than predicted by diffraction limited design performance. As a result, target illumination may decrease because the incident beam overfills the target, signal return is decreased because less power is delivered to the target, and mean target reflectivity is reduced because the entire target is involved in the signal return.

The relative uncertainty in power delivered to a target through a turbulent atmosphere is a major contributor to the relative uncertainty in the probability of successful ranging as illustrated in [Appendix D](#). The results presented here are applicable to any E-O directed energy device as long as propagation is linear (atmospheric thermal heating and blooming effects are not considered).

Transmission of 1.06 and 10.6 μm wavelength radiation is considered here as function of target range and relative uncertainty in the index of refraction turbulence structure constant.

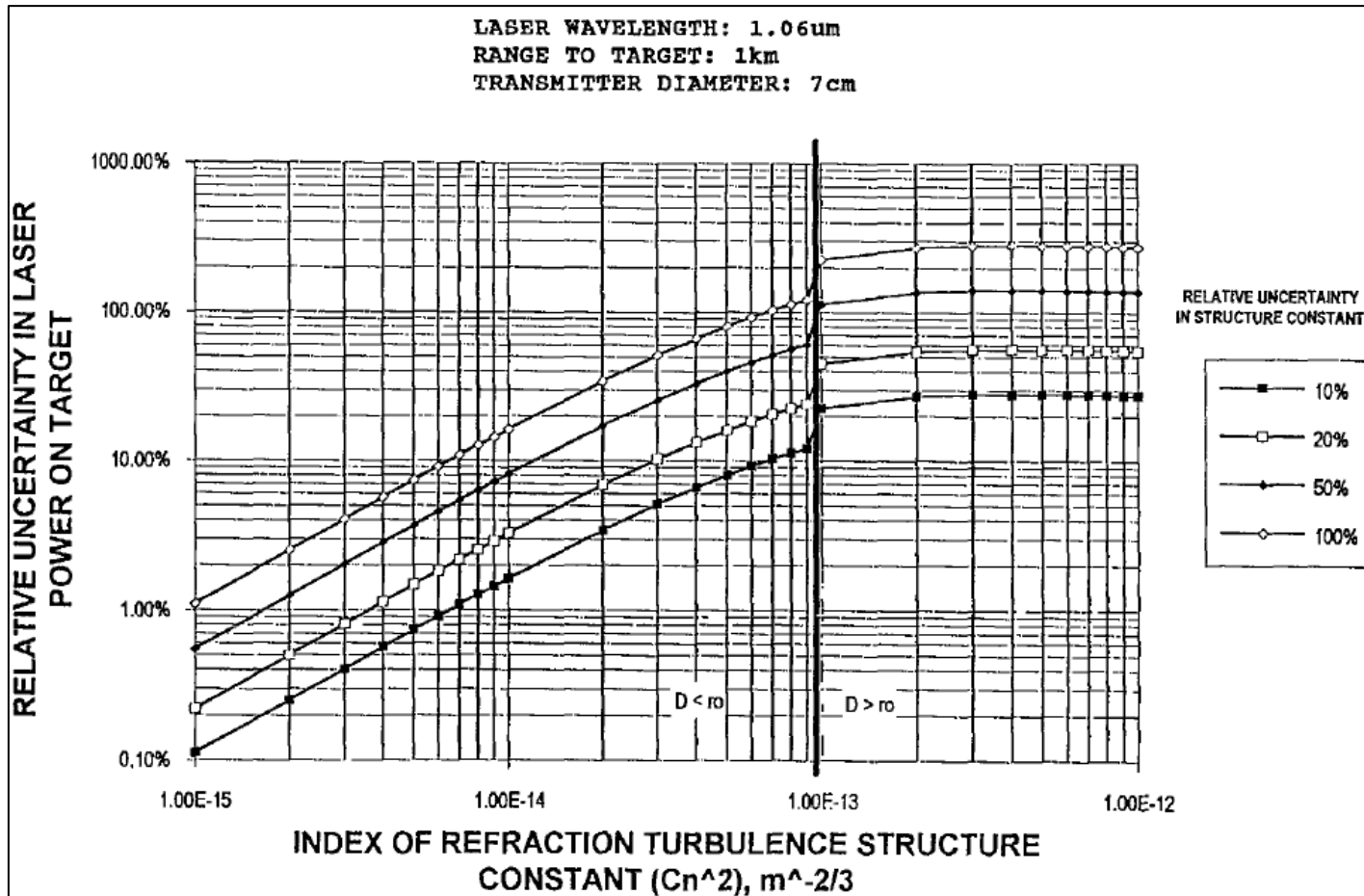


Figure E-1. Relative Uncertainty in 1.06 μm Wavelength Power Delivered to a Target for a 7-cm Transmitter Aperture Diameter and 1-km Target Range as a Function of Index of Refraction Structure Constant and Selected Relative Uncertainties in the Structure Constant

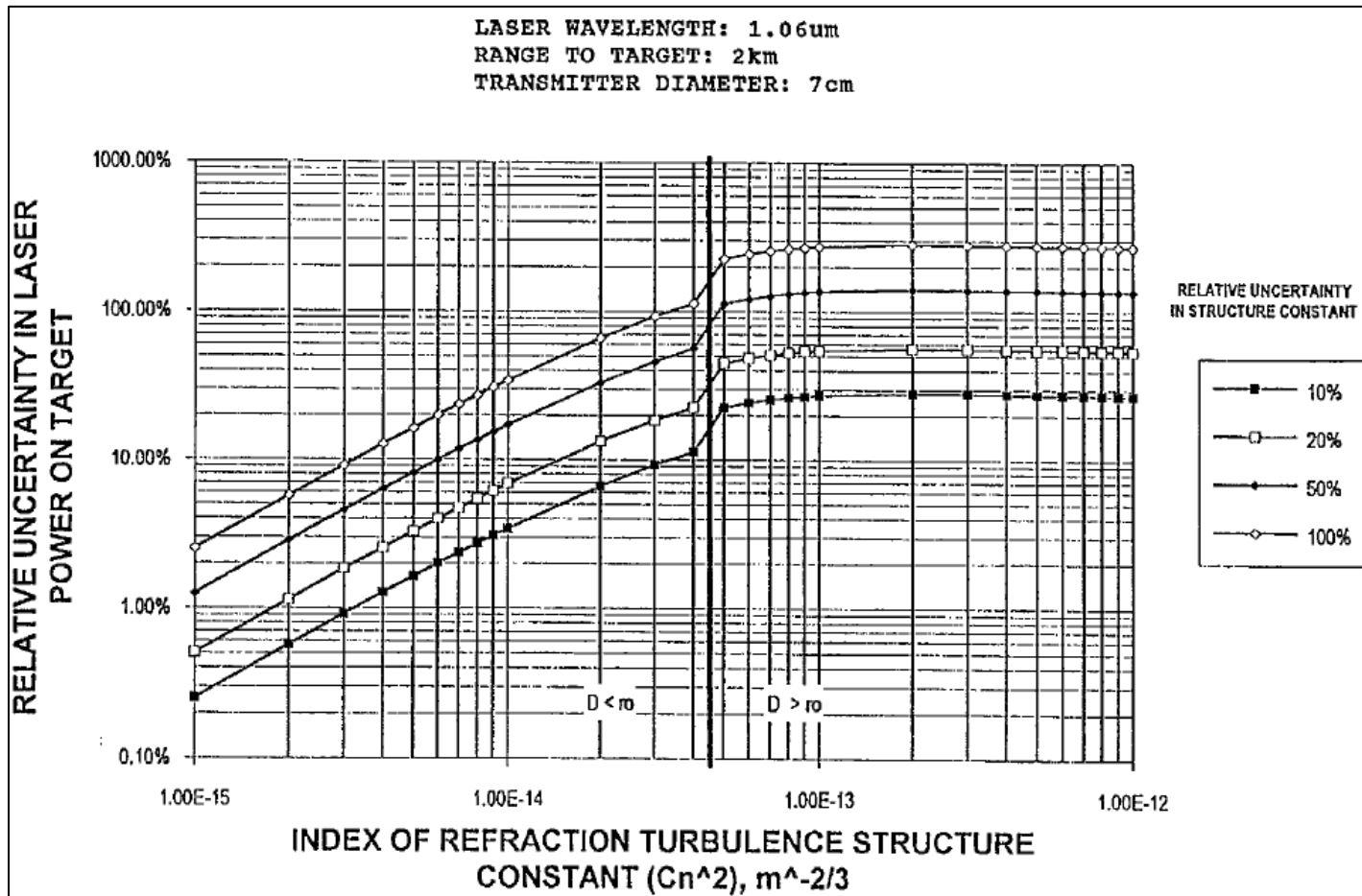


Figure E-2. Relative Uncertainty in 1.06 μ m Wavelength Power Delivered to a Target for a 7-cm Transmitter Aperture Diameter and 2-km Target Range as a Function of Index of Refraction Structure Constant and Selected Relative Uncertainties in the Structure Constant

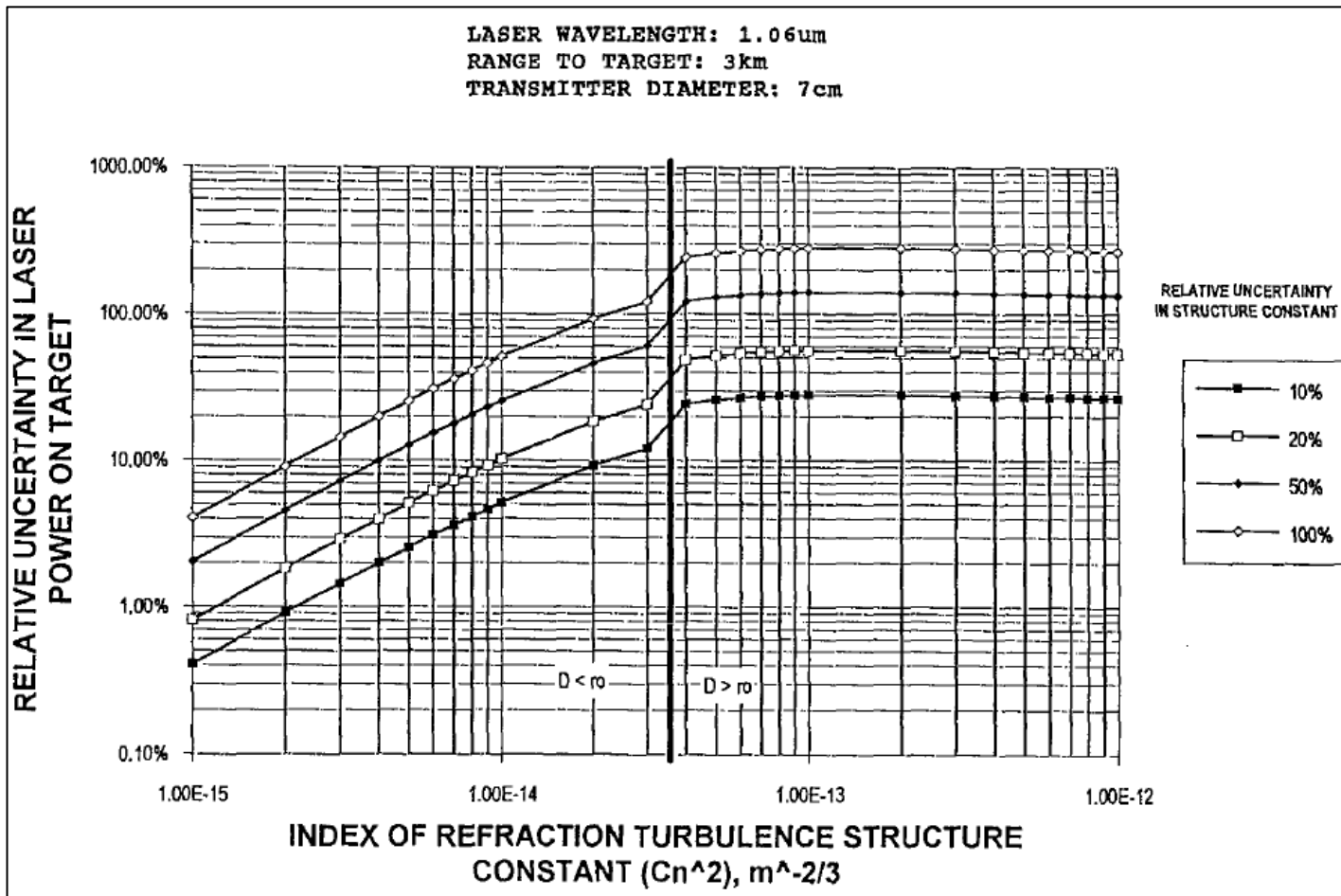


Figure E-3. Relative Uncertainty in 1.06 μ m Wavelength Power Delivered to a Target for a 7-cm Transmitter Aperture Diameter and 3-km Target Range as a Function of Index of Refraction Structure Constant and Selected Relative Uncertainties in the Structure Constant

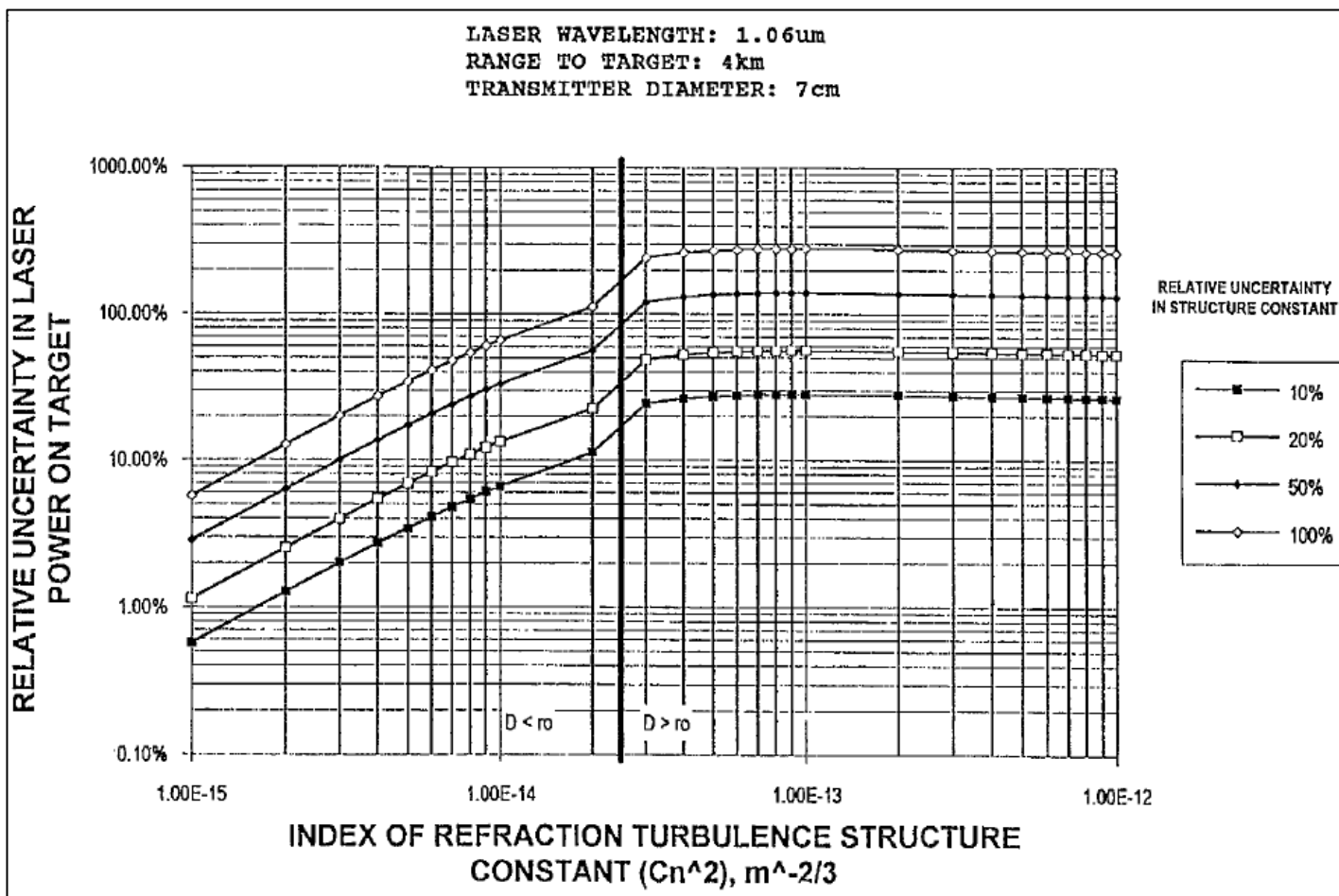


Figure E-4. Relative Uncertainty in 1.06 μ m Wavelength Power Delivered to a Target for a 7-cm Transmitter Aperture Diameter and 4-km Target Range as a Function of Index of Refraction Structure Constant and Selected Relative Uncertainties in the Structure Constant

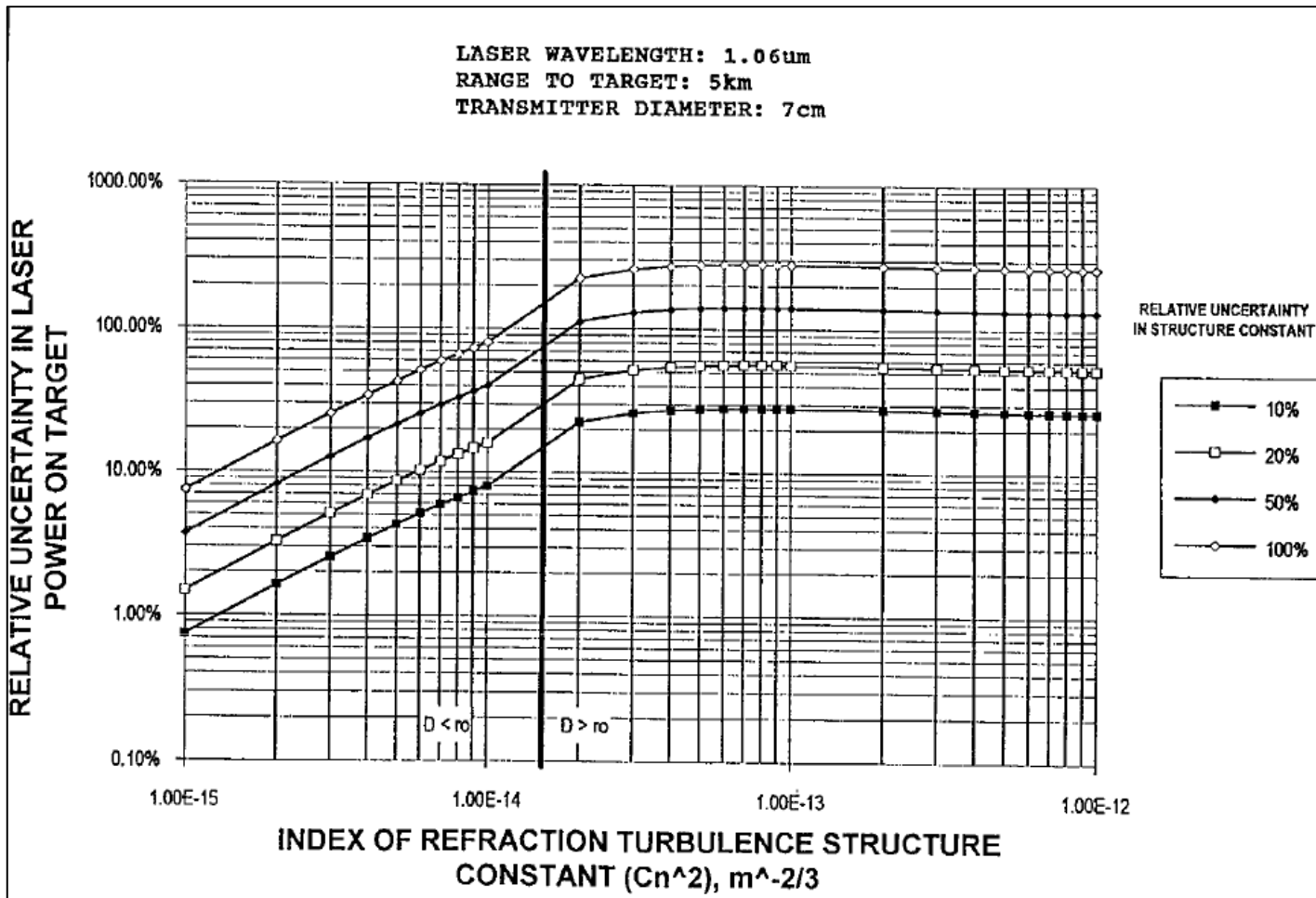


Figure E-5. Relative Uncertainty in 1.06 μm Wavelength Power Delivered to a Target for a 7-cm Transmitter Aperture Diameter and 5-km Target Range as a Function of Index of Refraction Structure Constant and Selected Relative Uncertainties in the Structure Constant

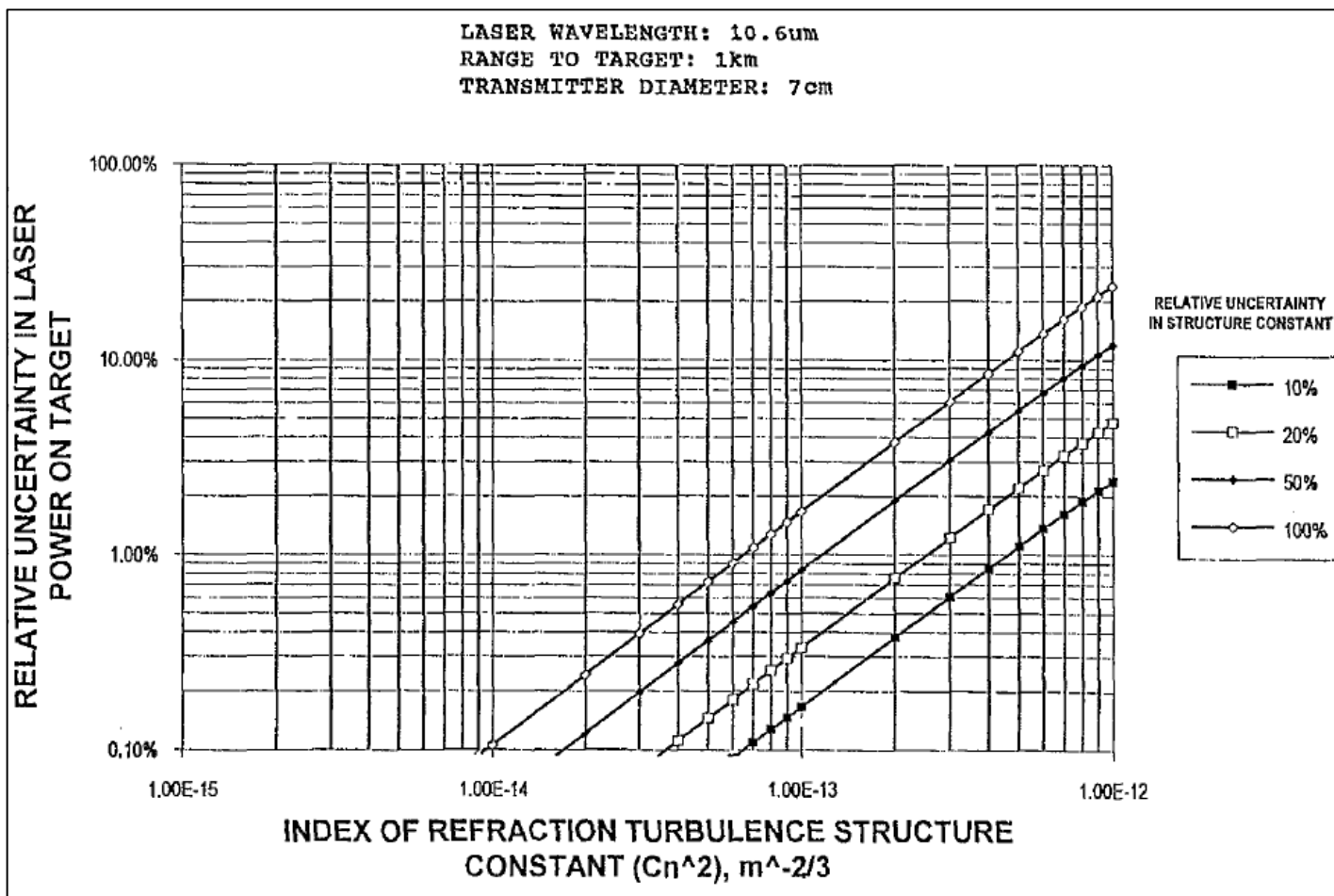


Figure E-6. Relative Uncertainty in 10.6 μ m Wavelength Power Delivered to a Target for a 7-cm Transmitter Aperture Diameter and 1-km Target Range as a Function of Index of Refraction Structure Constant and Selected Relative Uncertainties in the Structure Constant

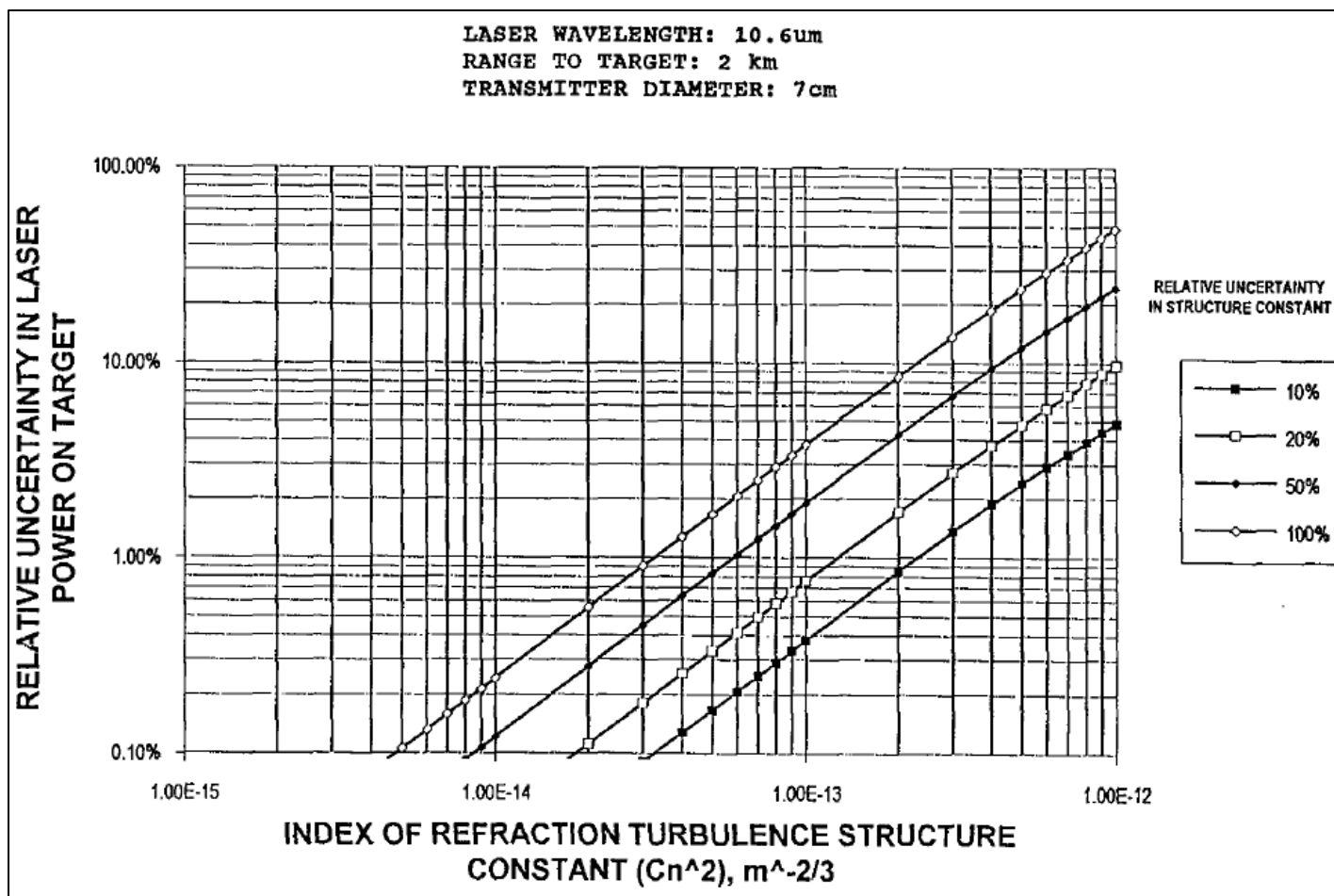


Figure E-7. Relative Uncertainty in 10.6 μ m Wavelength Power Delivered to a Target for a 7-cm Transmitter Aperture Diameter and 2-km Target Range as a Function of Index of Refraction Structure Constant and Selected Relative Uncertainties in the Structure Constant

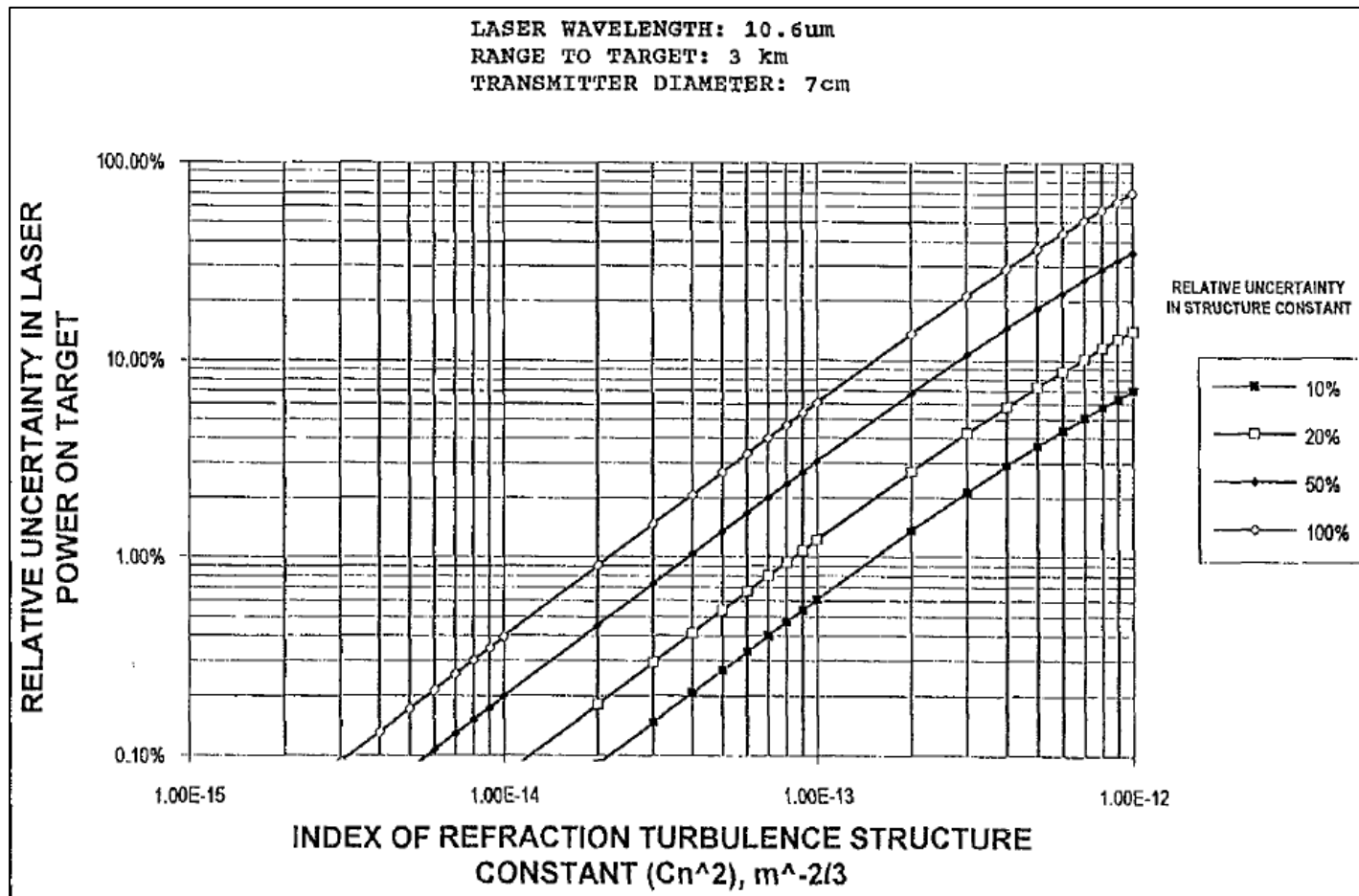


Figure E-8. Relative Uncertainty in 10.6 μ m Wavelength Power Delivered to a Target for a 7-cm Transmitter Aperture Diameter and 3-km Target Range as a Function of Index of Refraction Structure Constant and Selected Relative Uncertainties in the Structure Constant

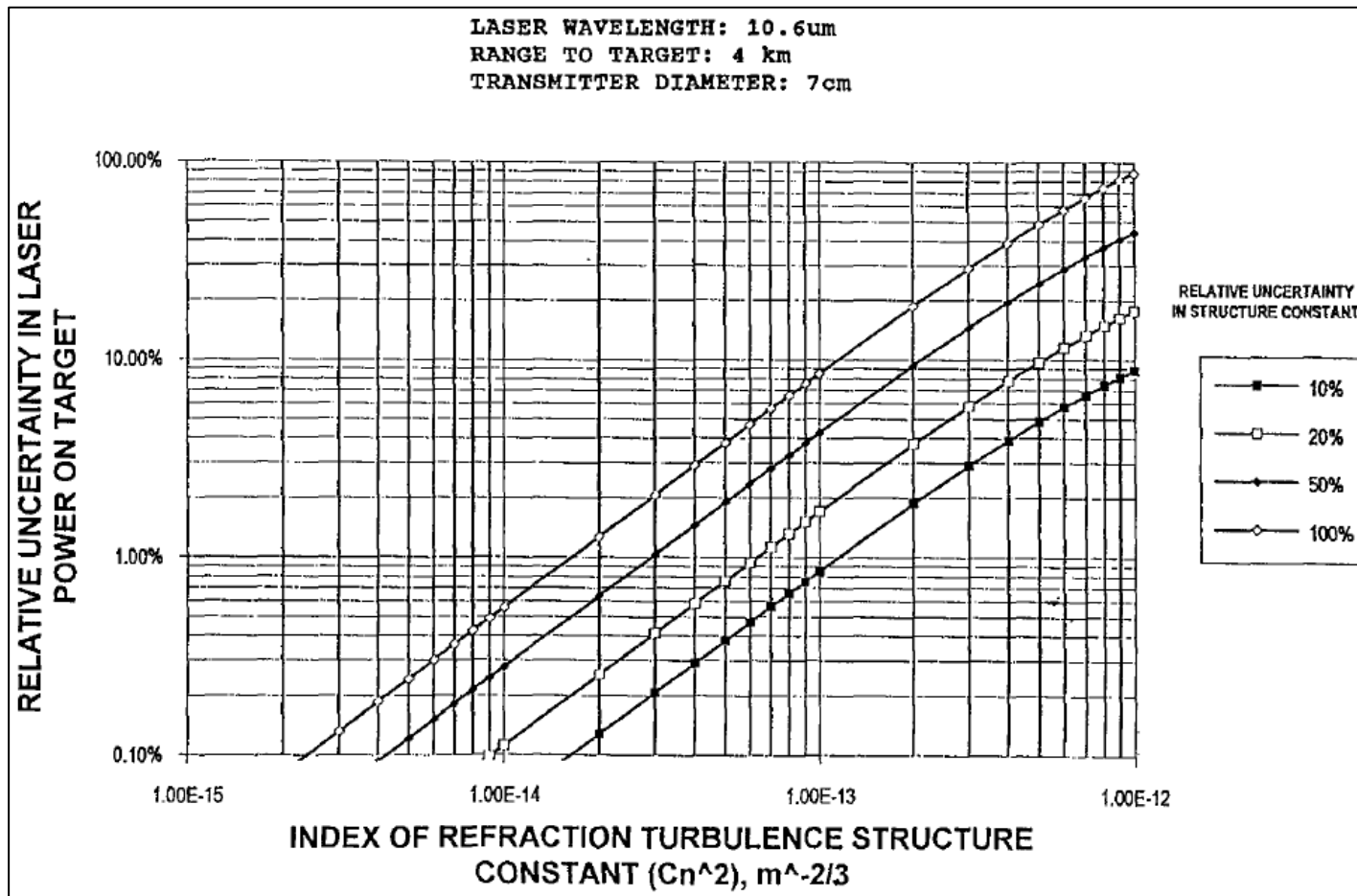


Figure E-9. Relative Uncertainty in 10.6 μ m Wavelength Power Delivered to a Target for a 7-cm Transmitter Aperture Diameter and 4-km Target Range as a Function of Index of Refraction Structure Constant and Selected Relative Uncertainties in the Structure Constant

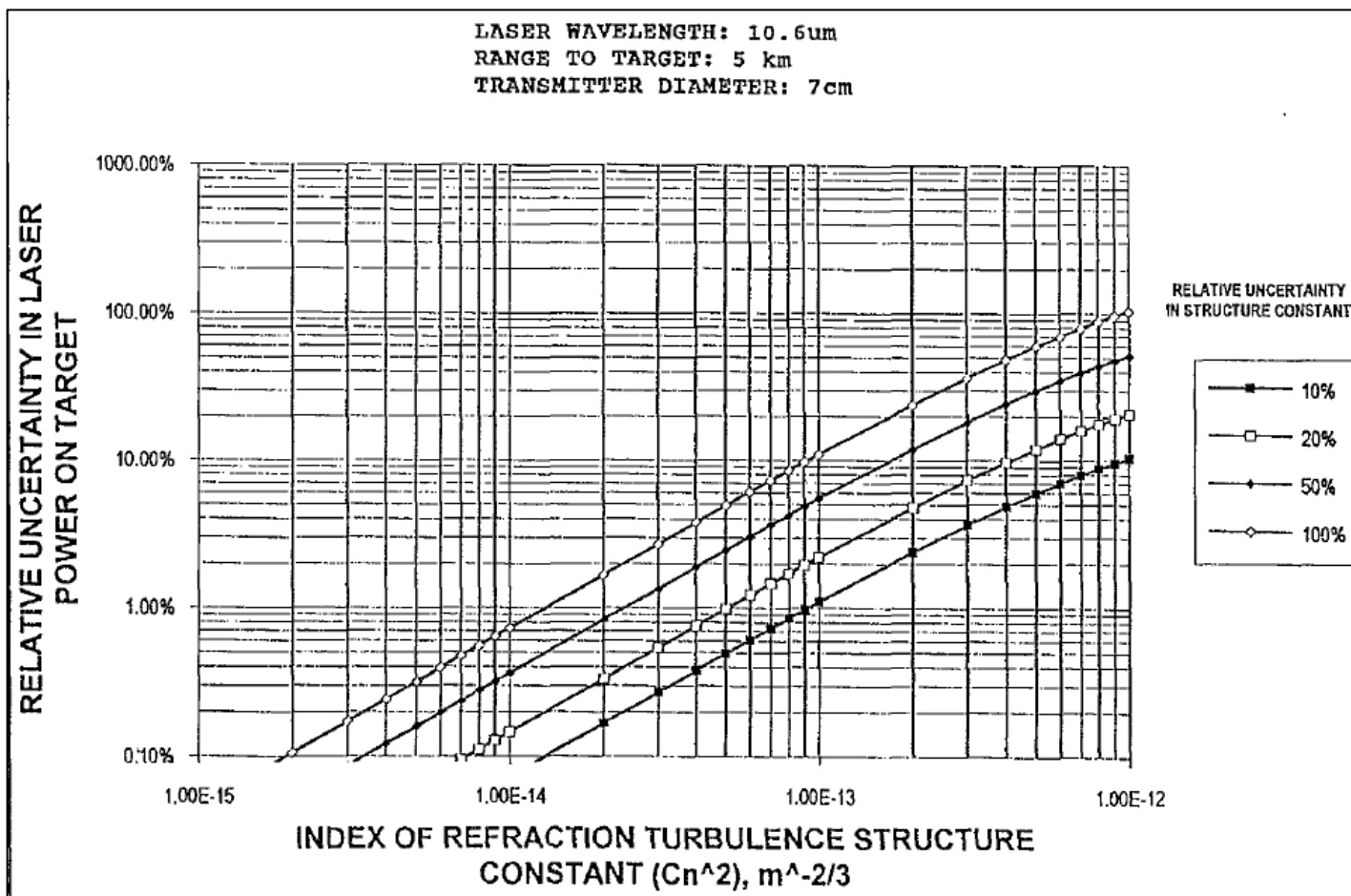


Figure E-10. Relative Uncertainty in 10.6 μ m Wavelength Power Delivered to a Target for a 7-cm Transmitter Aperture Diameter and 5-km Target Range as a Function of Index of Refraction Structure Constant and Selected Relative Uncertainties in the Structure Constant

This page intentionally left blank.

APPENDIX F

Relative Uncertainty in 8-12 μm Transmittance because of Air Temperature, Relative Humidity, and Visual Range

F.1 Purpose

This appendix demonstrates the impact of meteorologic measurement uncertainty on the evaluation of the 8-12 μm band irradiance transmitted in the atmosphere.

F.2 Scope

Water vapor and aerosol scattering are the primary mechanisms for extinction of 8-12 μm band irradiance in the atmosphere. The 8-12 μm band is the primary operational band for E-O sensors that are used as night vision devices or to extend operational capability in atmospheric hazes. The meteorologic parameters used to characterize extinction are air temperature, relative humidity, and visual range. Results can also be applied to directed energy sensor evaluation. [Figure F-1](#) plots the relative (no extinction) 8-12 μm band irradiance transmittance as a function of slant range for selected values of visual range (a measure of aerosol loading) and air temperature of 20 °C and relative humidity of 80% (a measure of water vapor content). [Figure F-2](#) fixes the aerosol content at a visual range of 4 km and varies the water vapor content for a fixed relative humidity by plotting selected values of air temperature. [Figure F-3](#) through [Figure F-12](#) plot the relative uncertainty in transmittance as a function of slant range for selected atmospheric conditions by individually considering the relative uncertainty contributions of temperature, relative humidity, visibility, and the RMS sum of the contributions. All analysis presented here assumes the spectral response of the thermal imager is independent of wavelength.

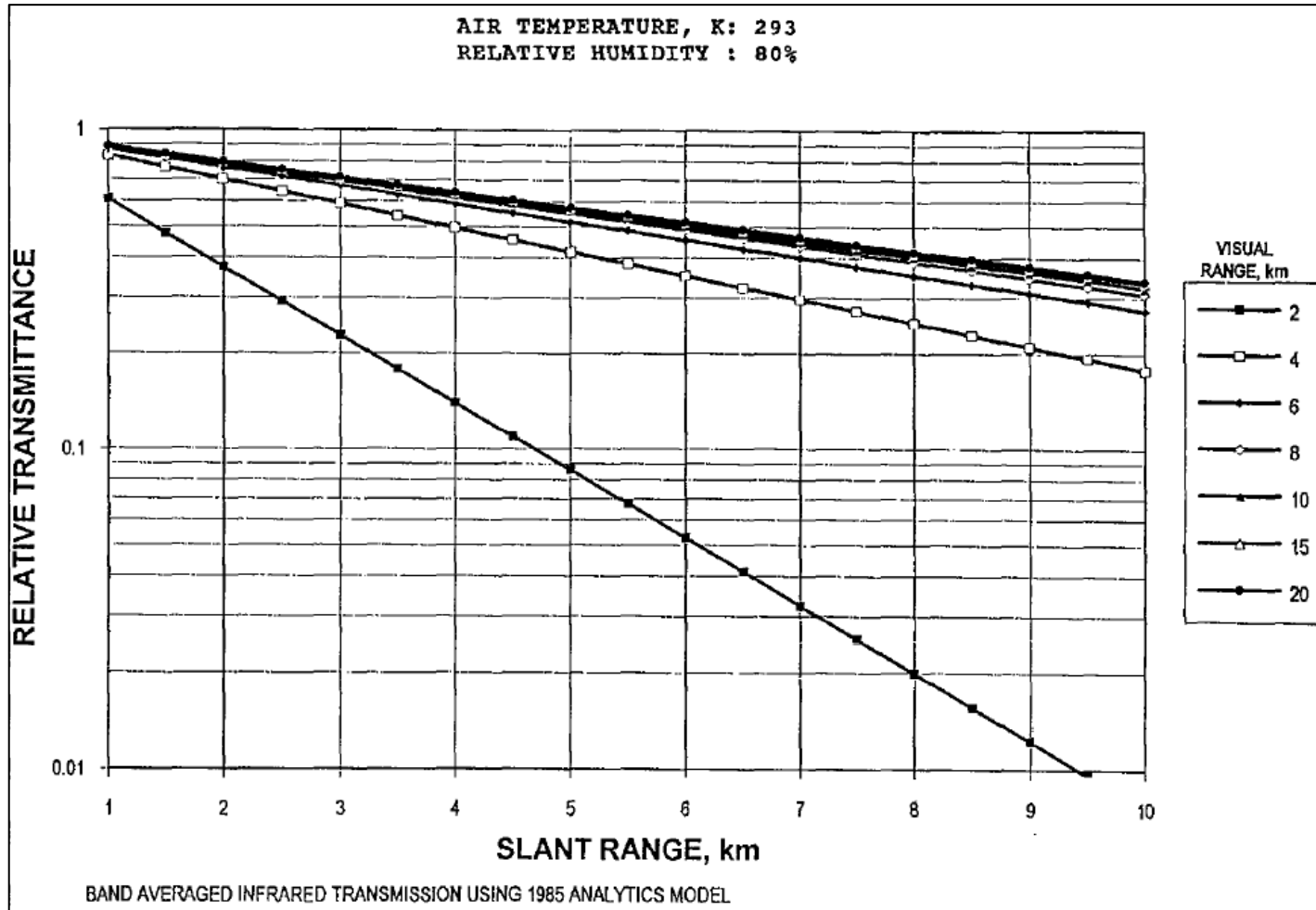


Figure F-1. The 8-12 μm Band Averaged Transmittance as a Function of Slant Range for a 20 °C Air Temperature and 80% Relative Humidity and Selected Visual Range

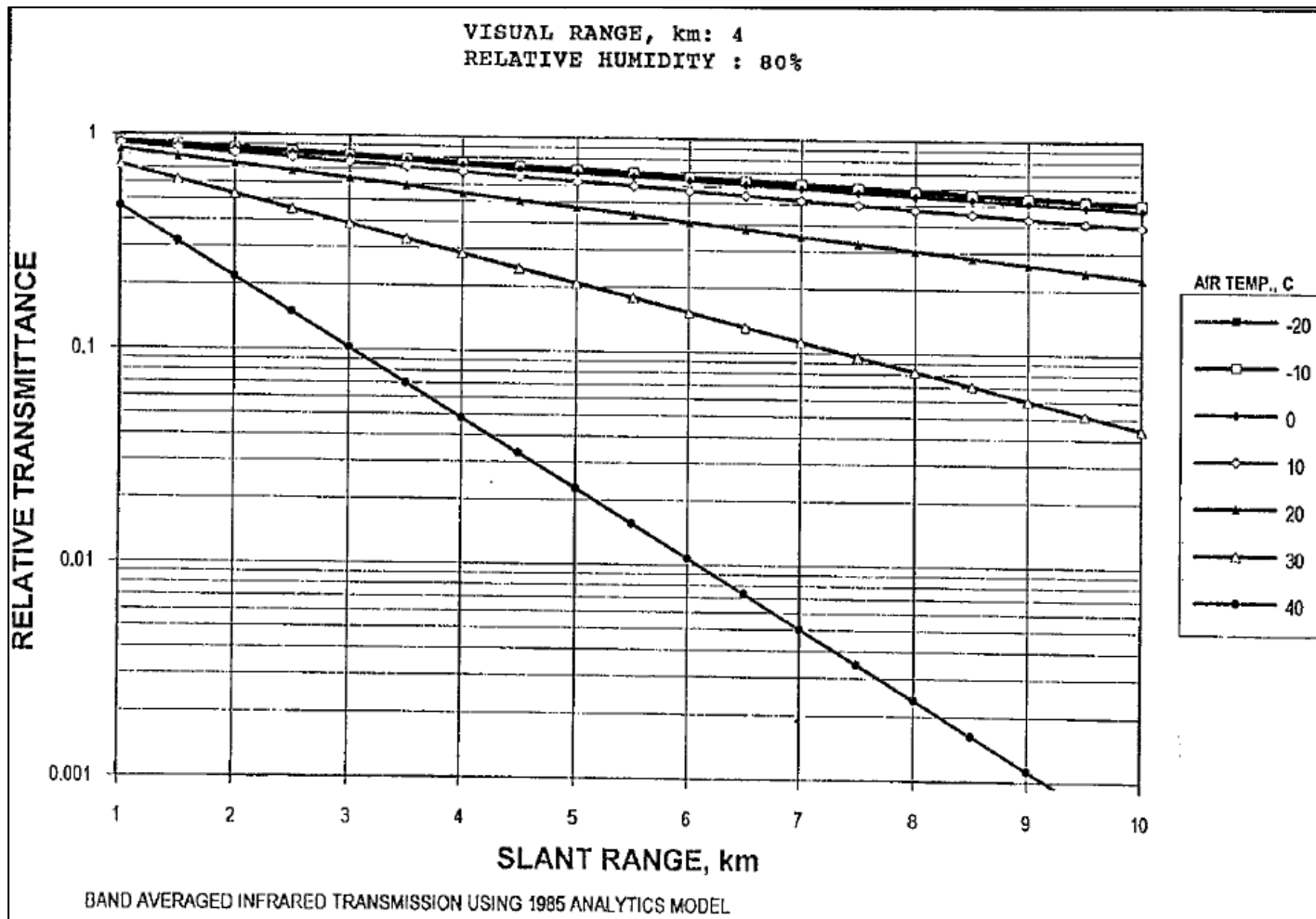


Figure F-2. The 8-12 μm Band Averaged Transmittance as a Function of Slant Range for 80% Relative Humidity, 4 km Visual Range, and Selected Air Temperatures

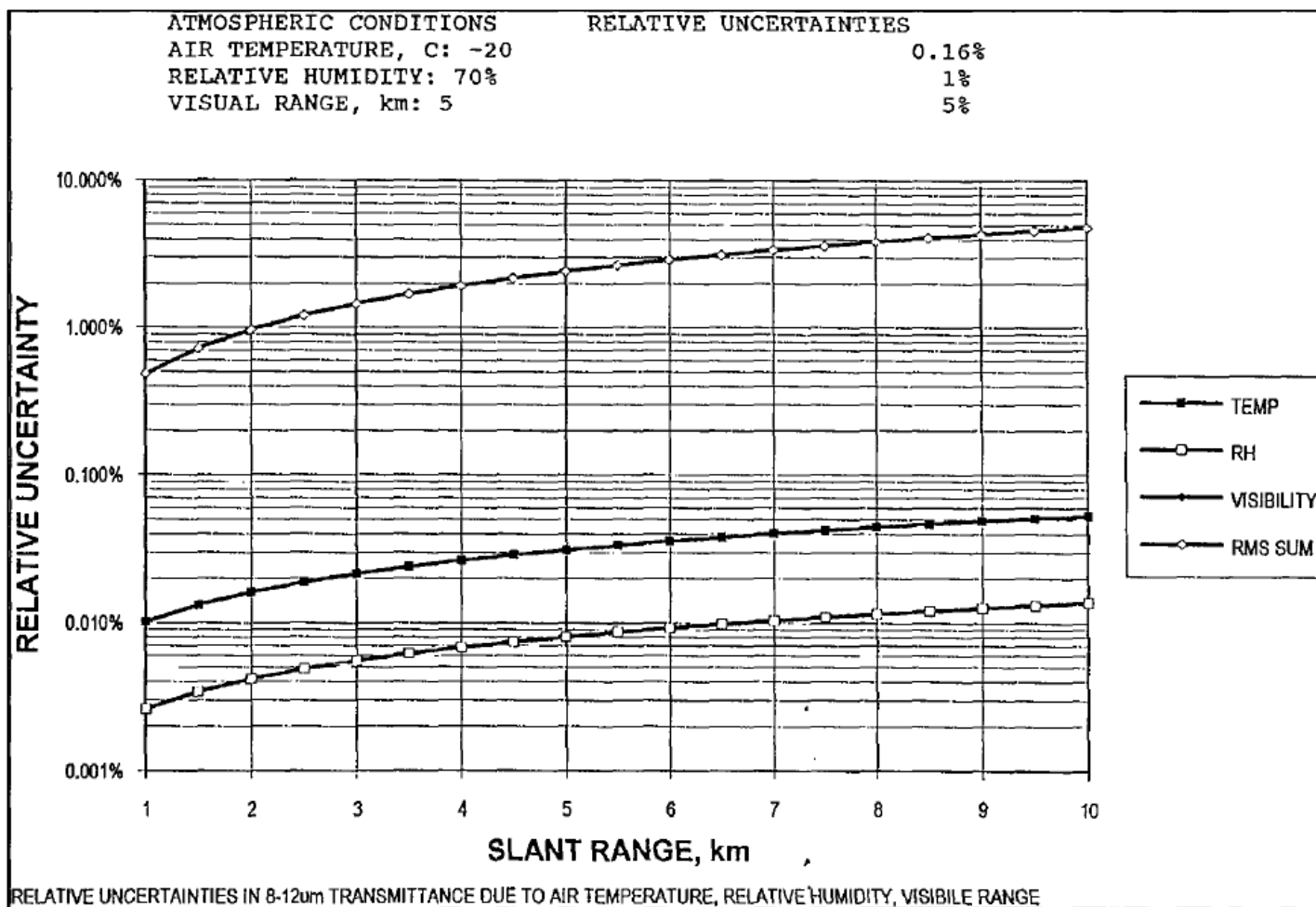


Figure F-3. Relative Uncertainty in 8-12 μ m Band Averaged Transmittance as a Function of Slant Range for -20°C Air Temperature, 70% Relative Humidity, and 5 km Visual Range. Relative Uncertainty in Air Temperature is 0.16%, Relative Humidity is 5%, and Visual Range is 5%.

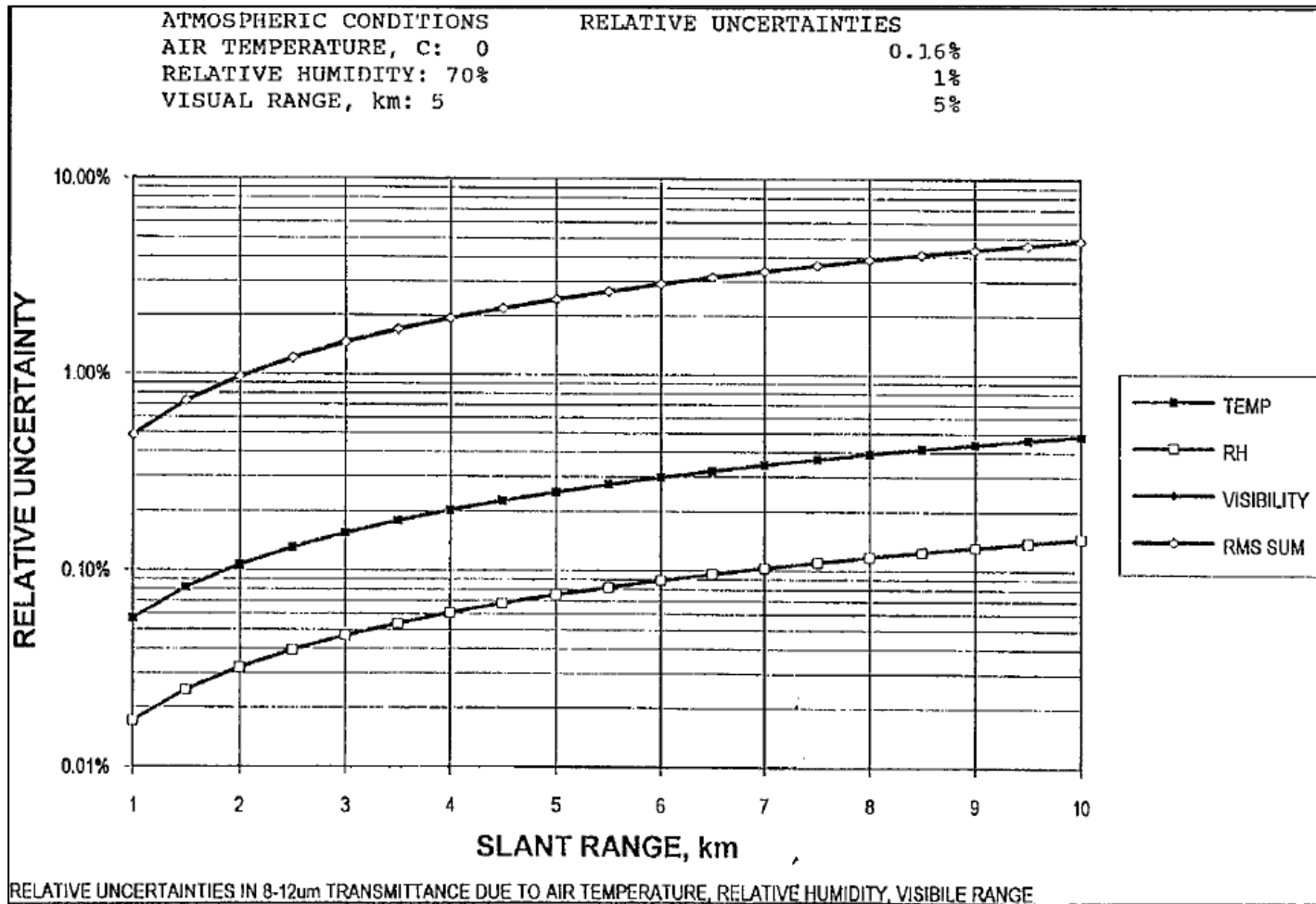


Figure F-4. Relative Uncertainty in 8-12 μ m Band Averaged Transmittance as a Function of Slant Range for 0 °C Air Temperature, 70% Relative Humidity, and 5 km Visual Range. Relative Uncertainty in Air Temperature is 0.16%, Relative Humidity is 5%, and Visual Range is 5%.

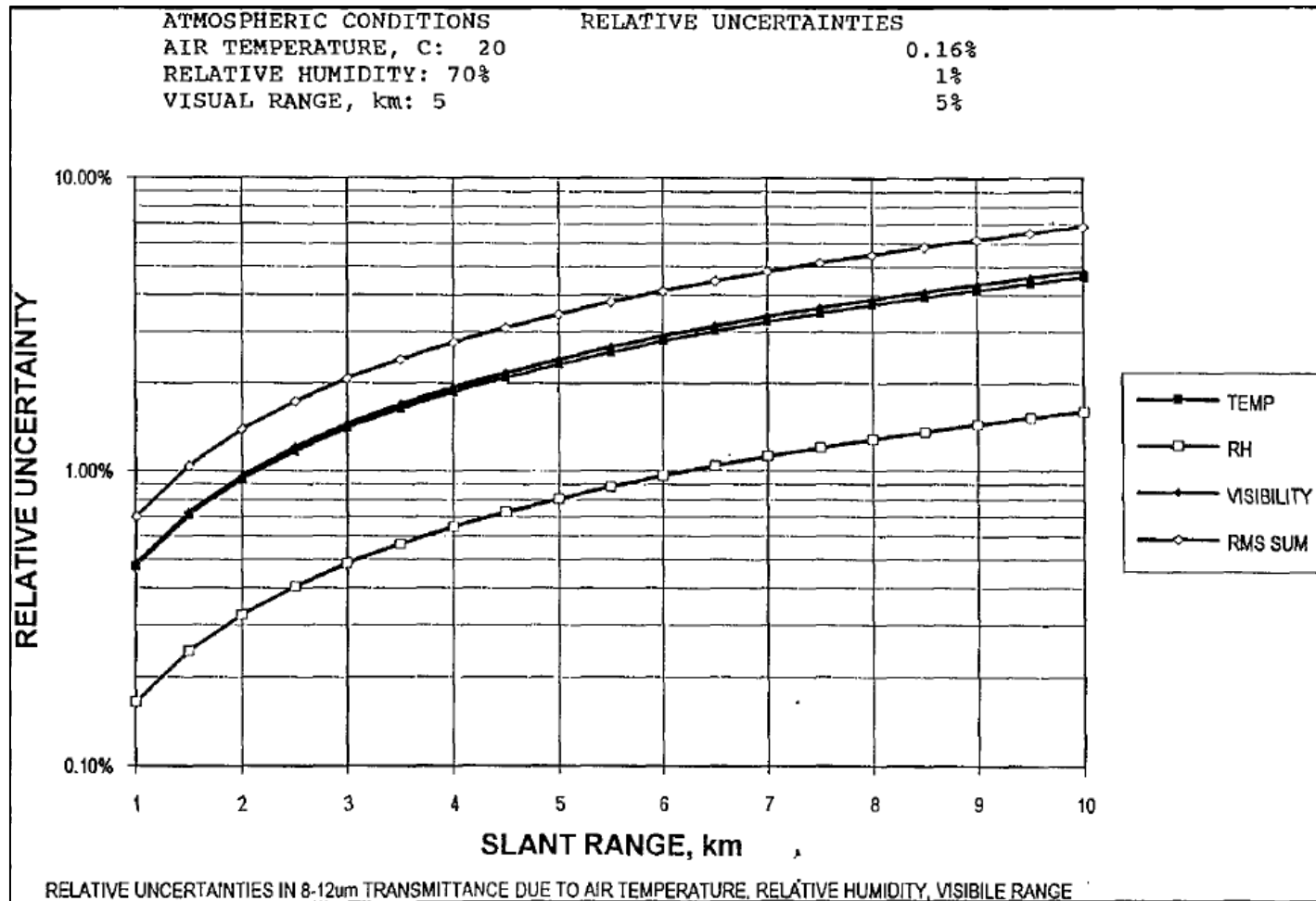


Figure F-5. Relative Uncertainty in 8-12 μ m Band Averaged Transmittance as a Function of Slant Range for 20 °C Air Temperature, 70% Relative Humidity, and 5 km Visual Range. Relative Uncertainty in Air Temperature is 0.16%, Relative Humidity is 5%, and Visual Range is 5%.

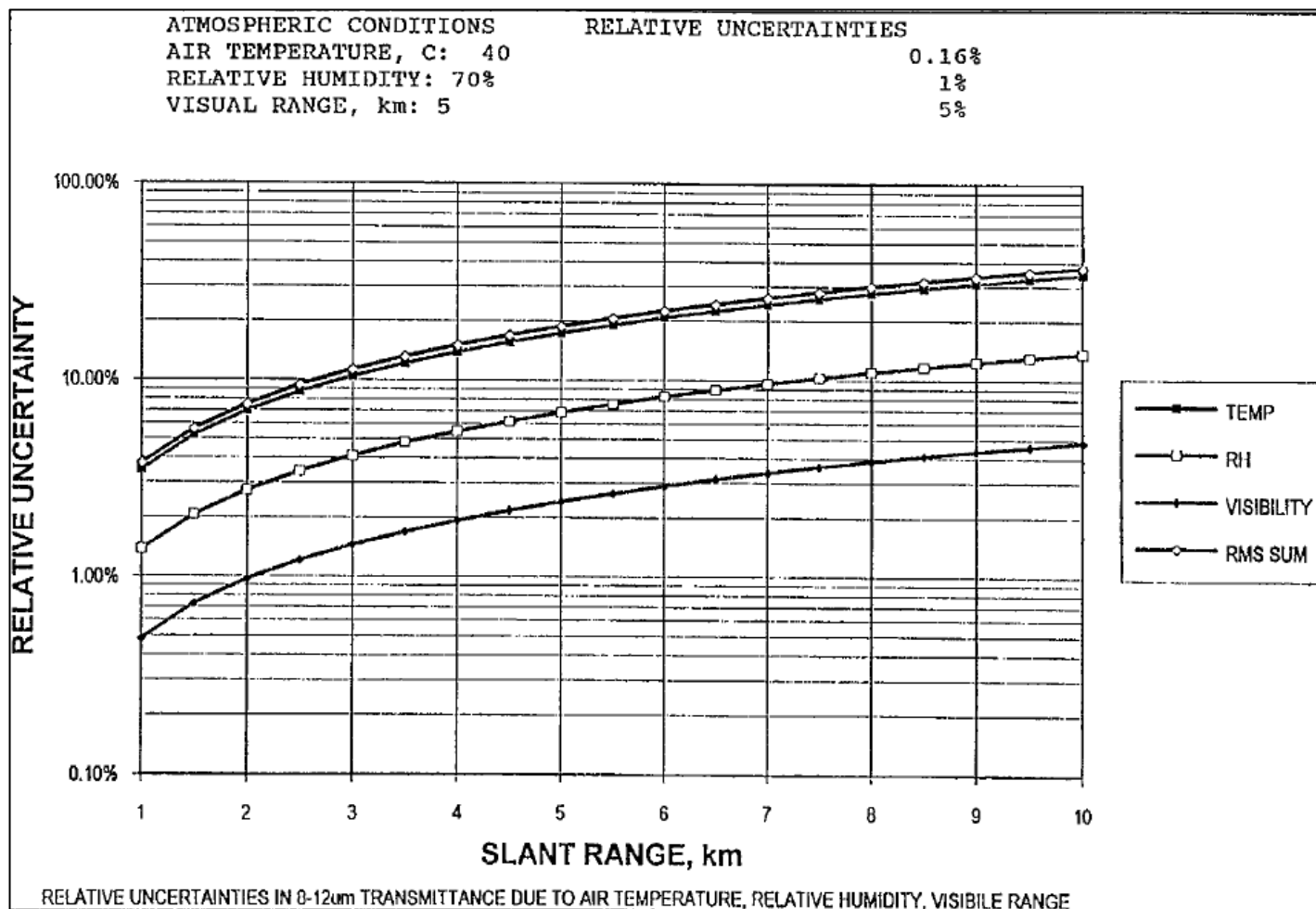


Figure F-6. Relative Uncertainty in 8-12 μ m Band Averaged Transmittance as a Function of Slant Range for 40 °C Air Temperature, 70% Relative Humidity, and 5 km Visual Range. Relative Uncertainty in Air Temperature is 0.16%, Relative Humidity is 5%, and Visual Range is 5%.

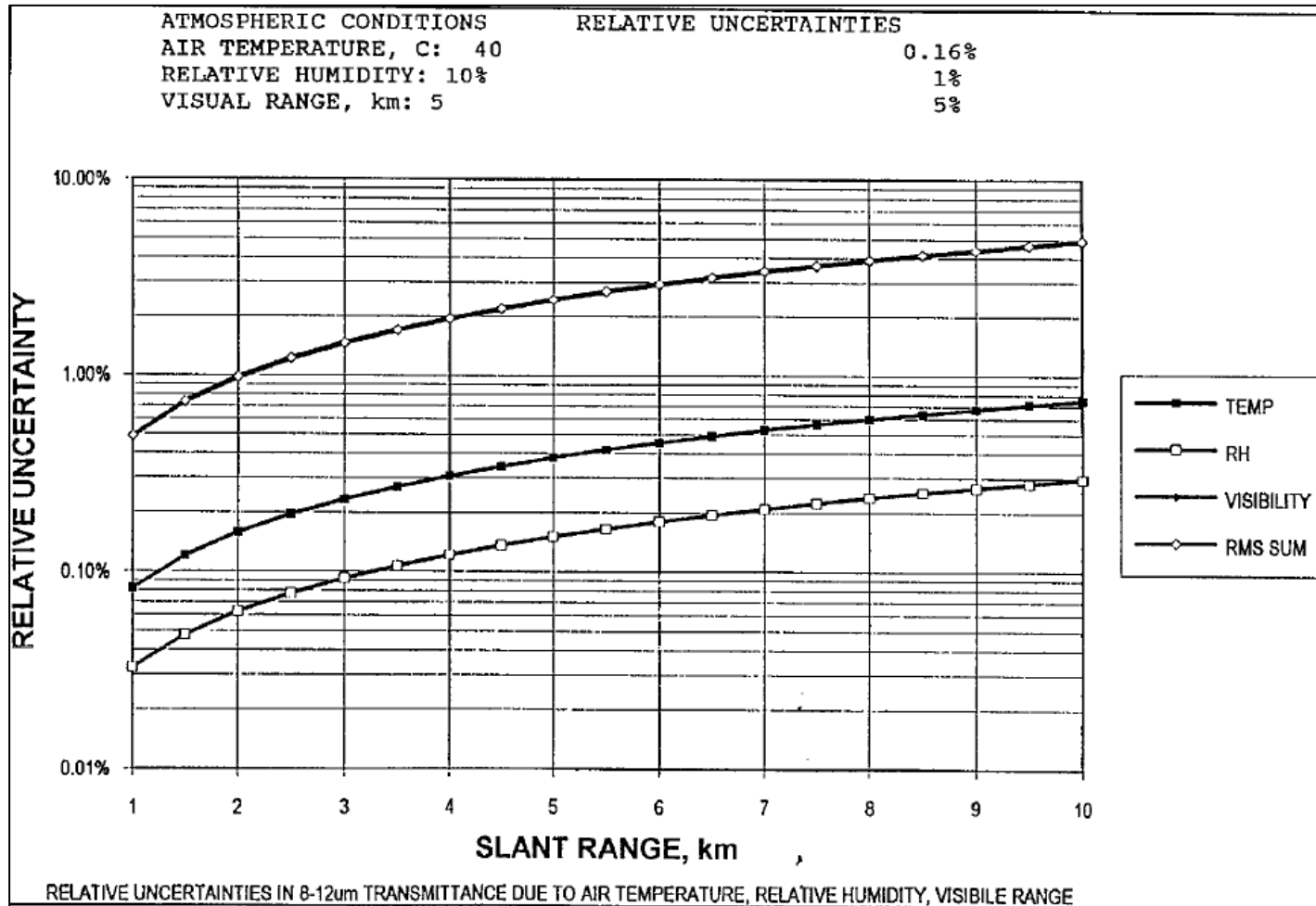


Figure F-7 Relative Uncertainty in 8-12 μ m Band Averaged Transmittance as a Function of Slant Range for 40 °C Air Temperature, 10% Relative Humidity, and 5 km Visual Range. Relative Uncertainty in Air Temperature is 0.16%, Relative Humidity is 5%, and Visual Range is 5%.

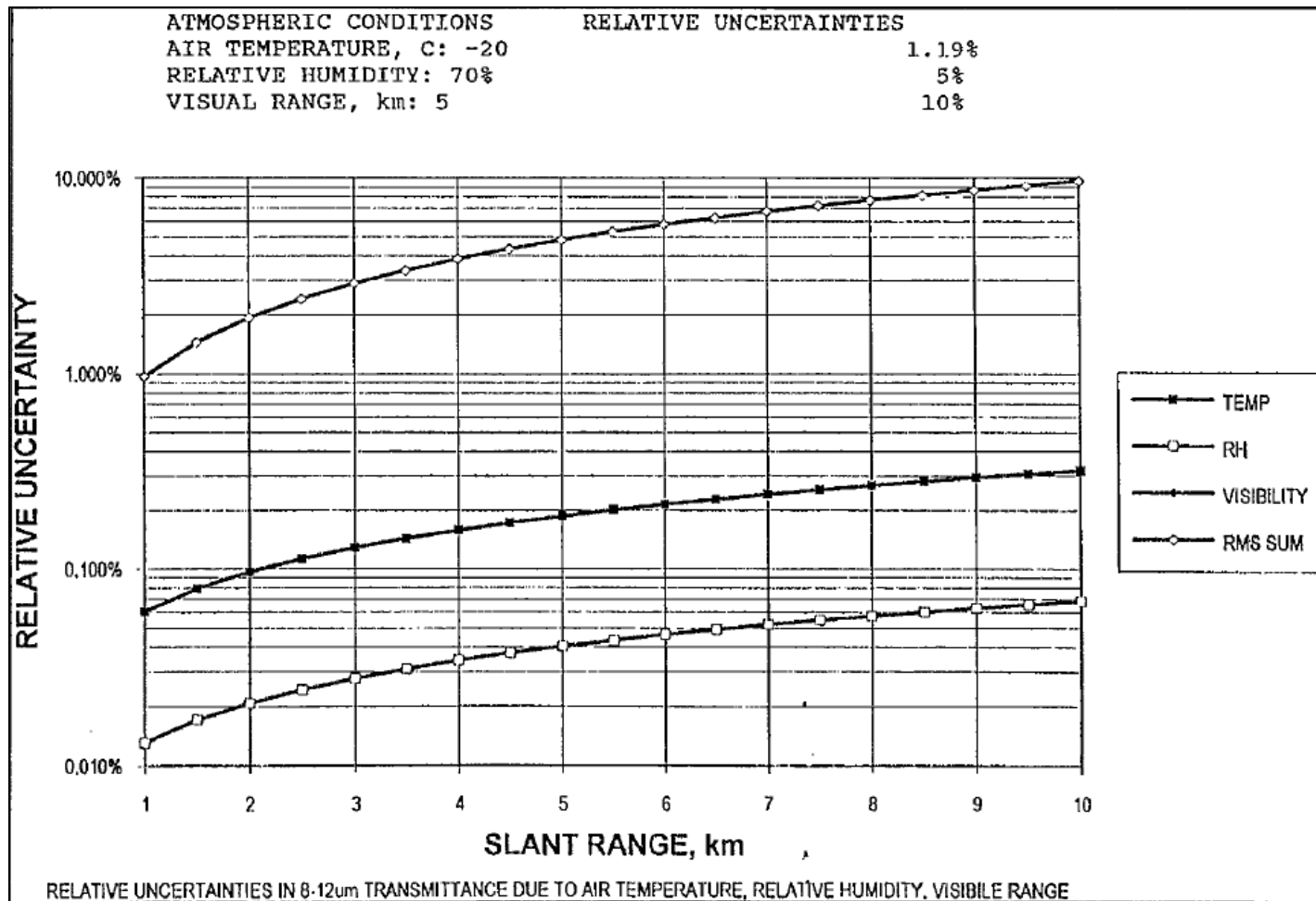


Figure F-8. Relative Uncertainty in 8-12 μ m Band Averaged Transmittance as a Function of Slant Range for -20°C Air Temperature, 70% Relative Humidity, and 5 km Visual Range. Relative Uncertainty in Air Temperature is 1.19%, Relative Humidity is 5%, and Visual Range is 10%.

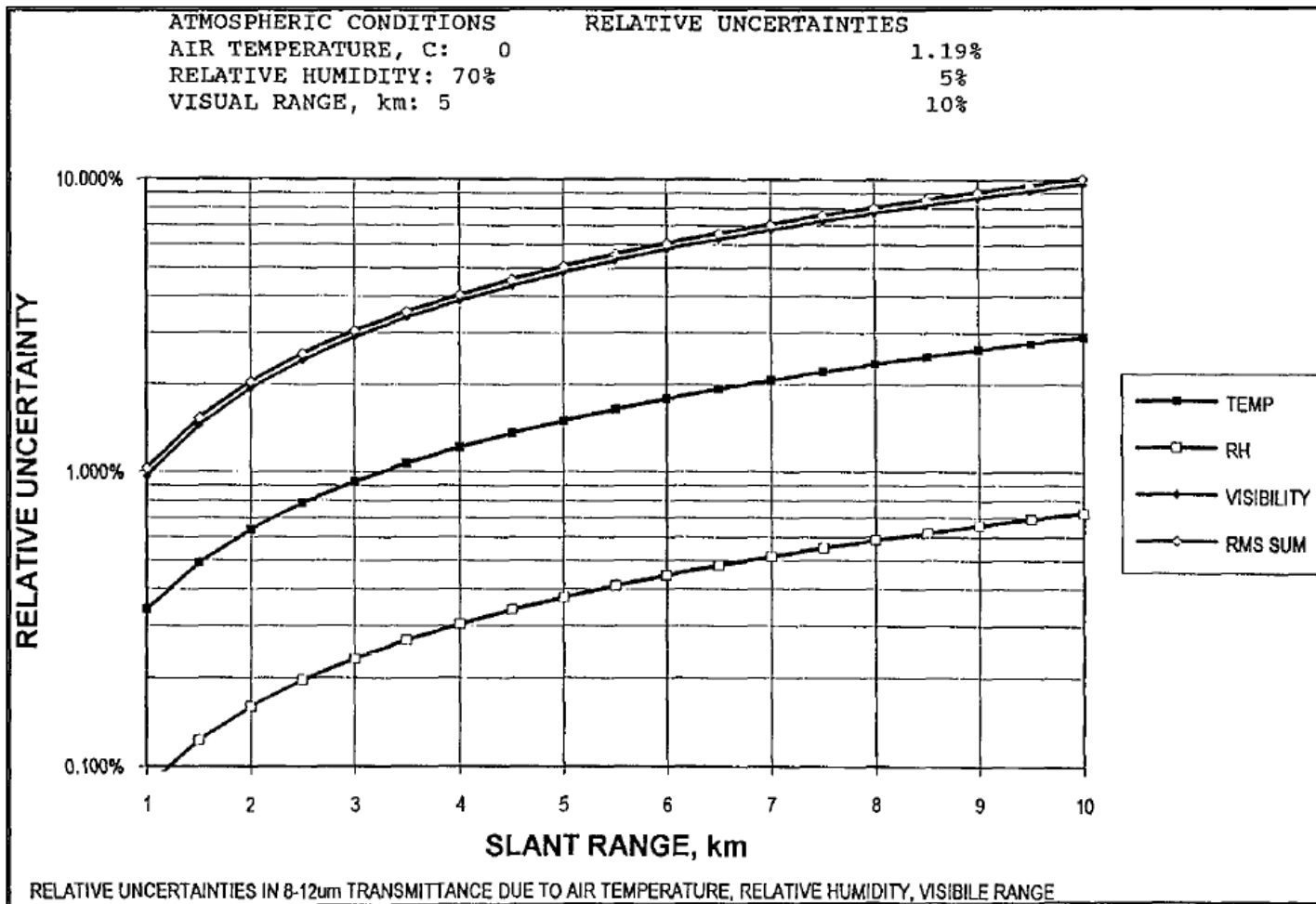


Figure F-9. Relative Uncertainty in 8-12 μ m Band Averaged Transmittance as a Function of Slant Range for 0 °C Air Temperature, 70% Relative Humidity, and 5 km Visual Range. Relative Uncertainty in Air Temperature is 1.19%, Relative Humidity is 5%, and Visual Range is 10%.

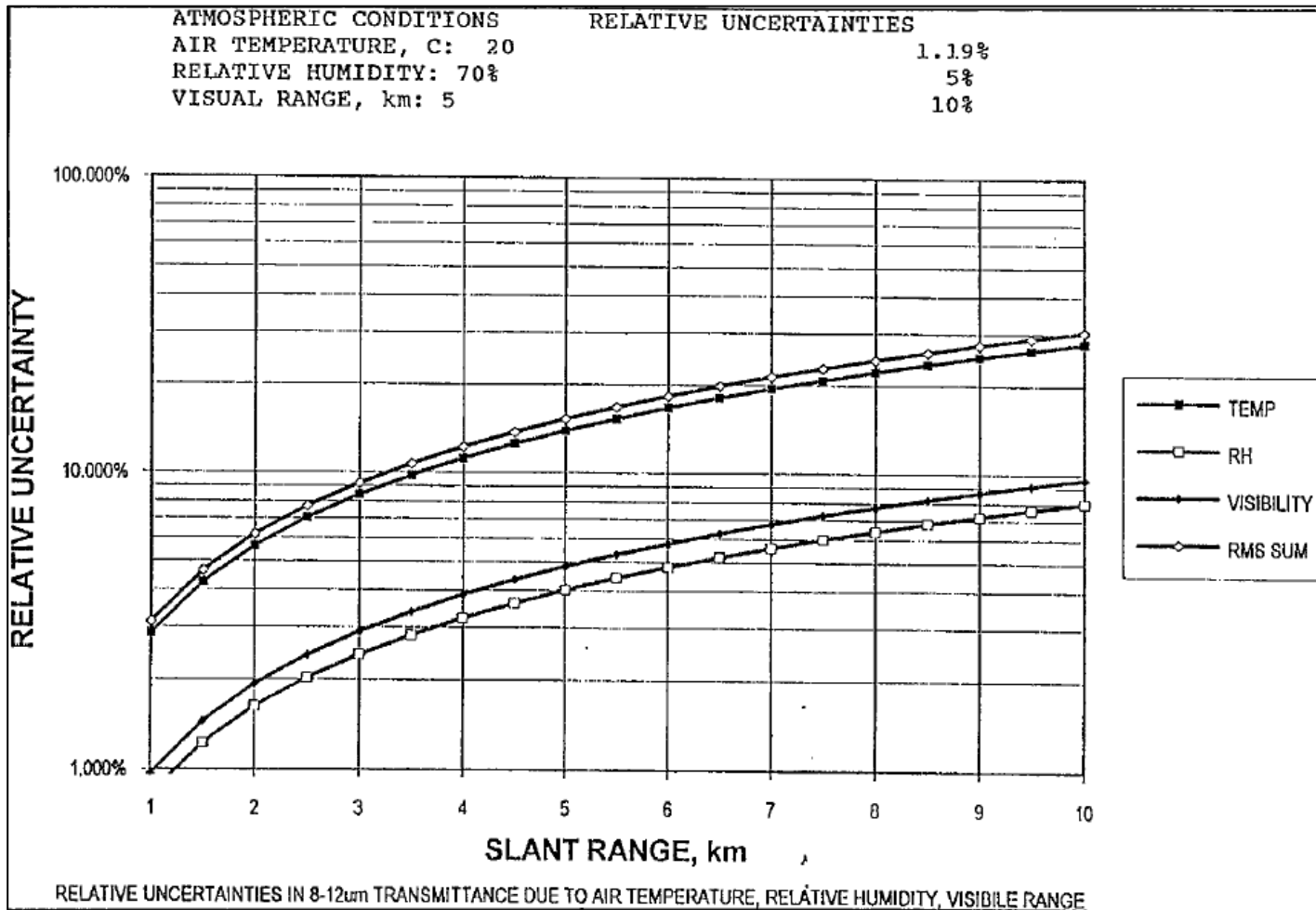


Figure F-10. Relative Uncertainty in 8-12 μ m Band Averaged Transmittance as a Function of Slant Range for 20 °C Air Temperature, 70% Relative Humidity, and 5 km Visual Range. Relative Uncertainty in Air Temperature is 1.19%, Relative Humidity is 5%, and Visual Range is 10%.

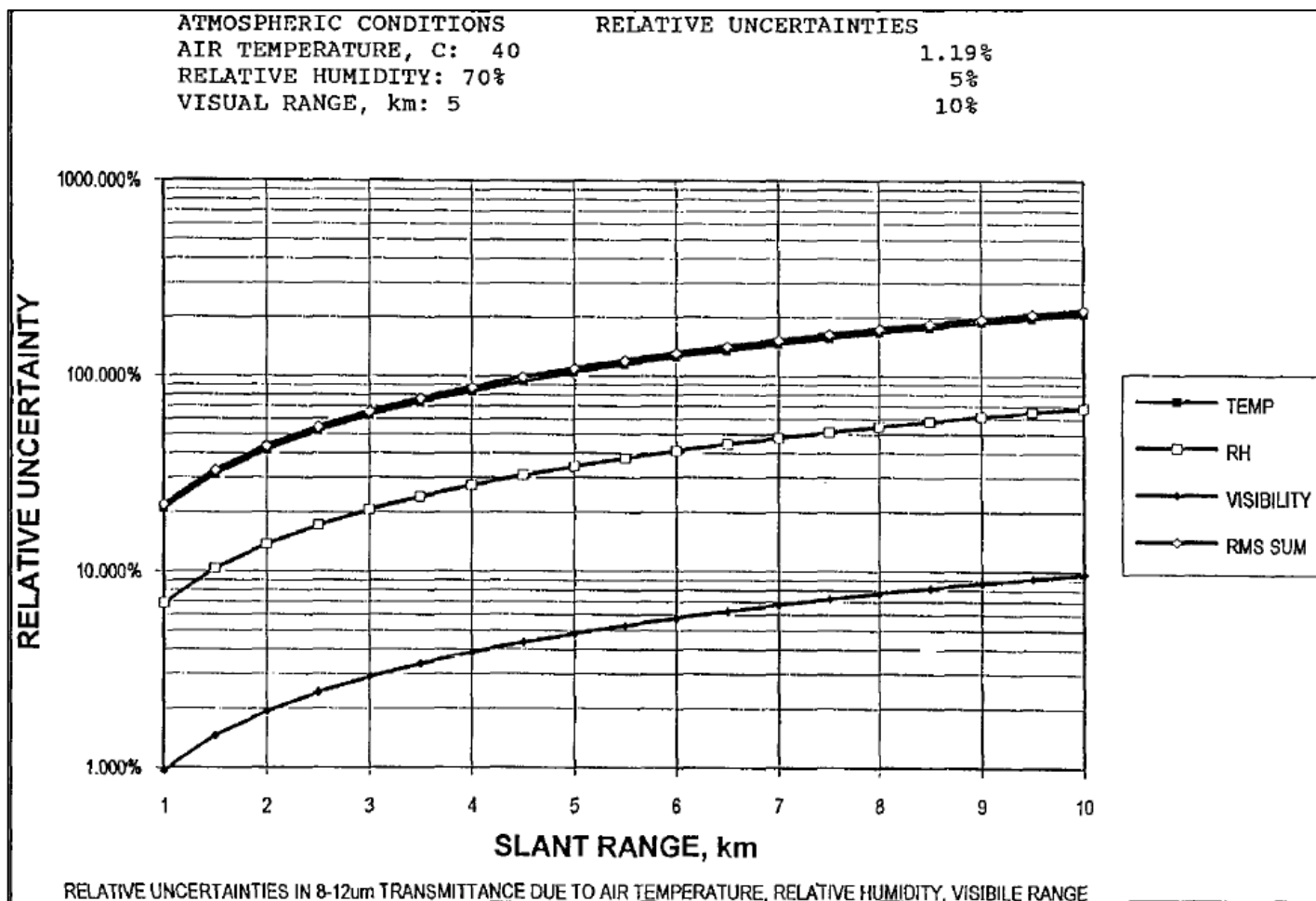


Figure F-11. Relative Uncertainty in 8-12 μm Band Averaged Transmittance as a Function of Slant Range for 40 °C Air Temperature, 70% Relative Humidity, and 5 km Visual Range. Relative Uncertainty in Air Temperature is 1.19%, Relative Humidity is 5%, and Visual Range is 10%.

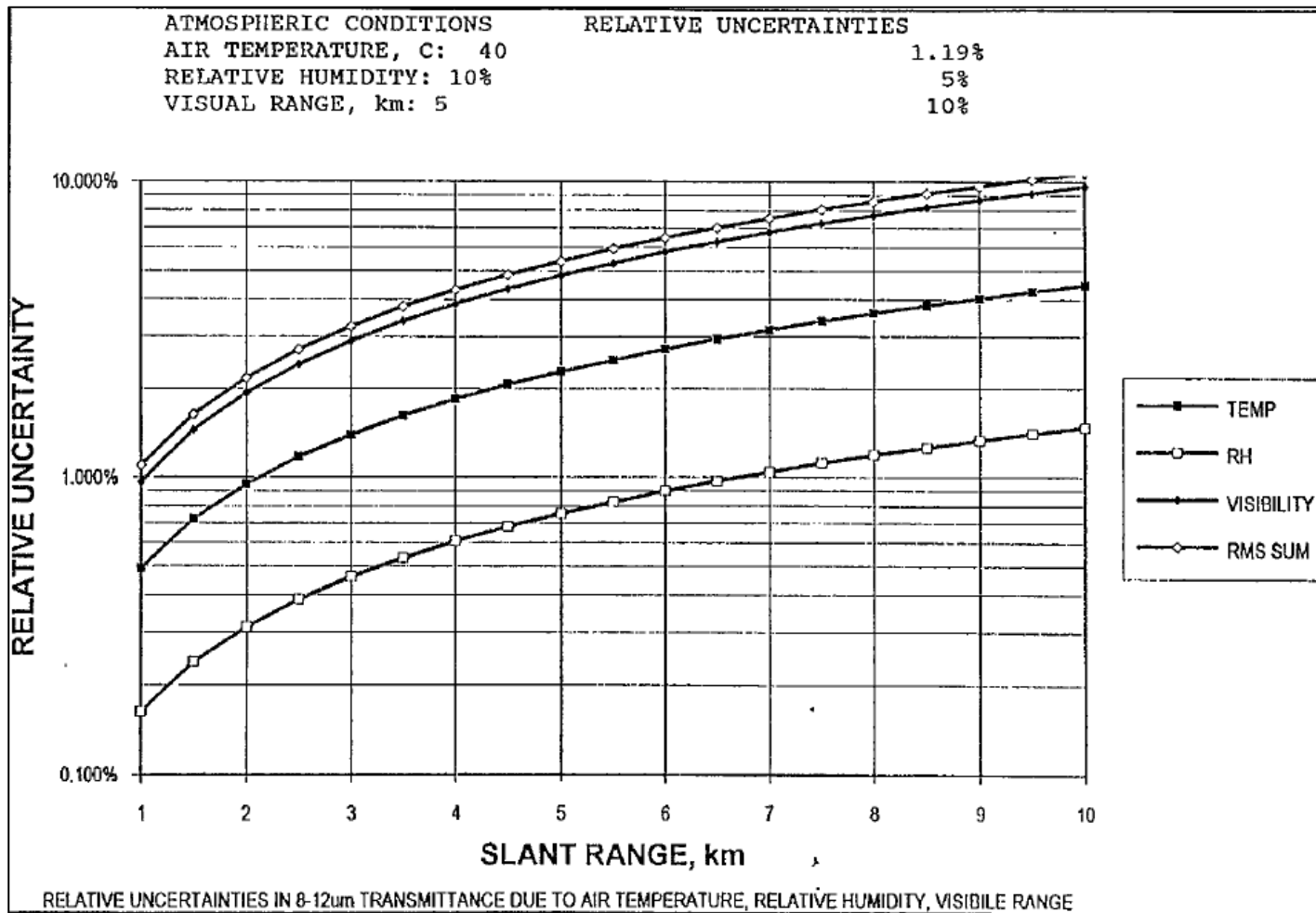


Figure F-12. Relative Uncertainty in 8-12 μ m Band Averaged Transmittance as a Function of Slant Range for 40 °C Air Temperature, 10% Relative Humidity, and 5 km Visual Range. Relative Uncertainty in Air Temperature is 1.19%, Relative Humidity is 5%, and Visual Range is 10%.

This page intentionally left blank.

APPENDIX G

Relative Uncertainty in Millimeter Wave Extinction and Transmittance Parameters as a Function of Ice and Liquid Water Precipitation Temperatures

G.1 Purpose

This appendix demonstrates the impact of meteorologic measurement uncertainty on the evaluation of MMW extinction as a function of ice and liquid water precipitation temperature.

G.2 Scope

The temperatures of water and ice affect the dielectric constant used to compute MMW extinction. The Debye model of the dielectric constants for water and ice have been used to compute the relative uncertainty in parametric values associated with MMW transmission.

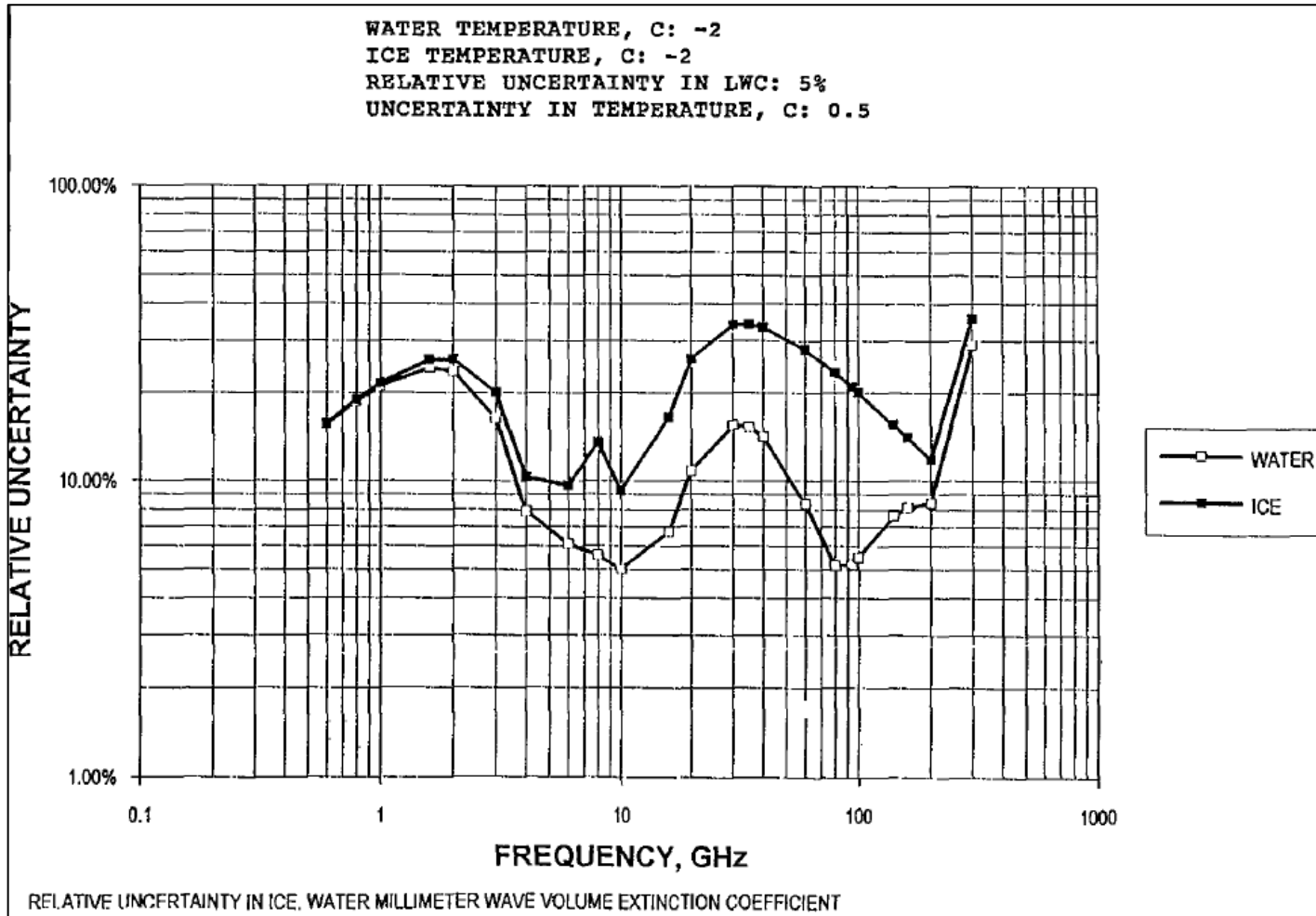


Figure G-1. Relative Uncertainty in the Volume Extinction Coefficients as a Function of Frequency for Ice and Water for Precipitation Temperatures of $-2\text{ }^{\circ}\text{C}$ for Ice and $-2\text{ }^{\circ}\text{C}$ for Water, a $0.5\text{ }^{\circ}\text{C}$ Uncertainty in Temperature, and a 5% Uncertainty in Liquid Water Content

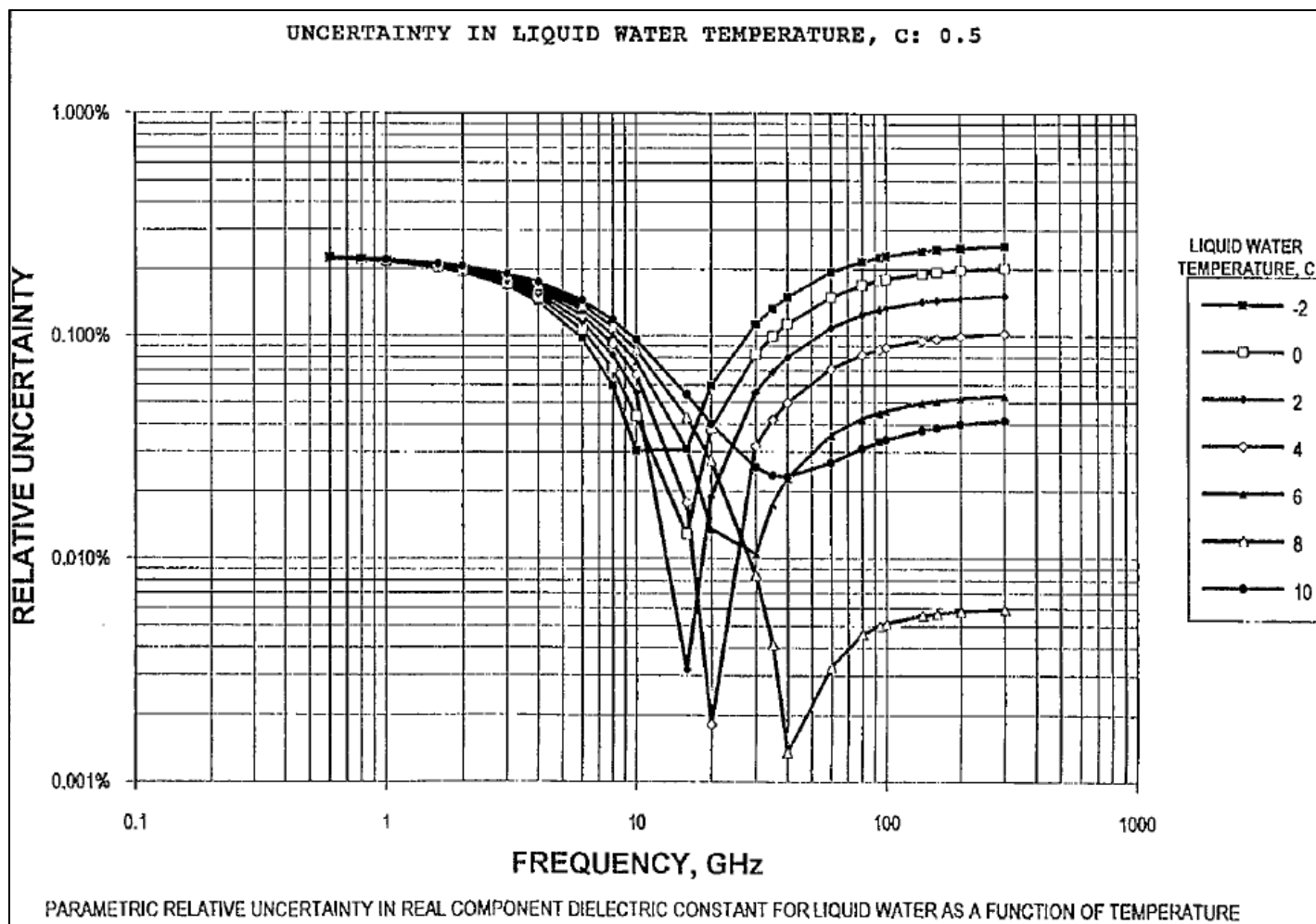


Figure G-2. Relative Uncertainty in the Real Component of the Dielectric Constant as a Function of Frequency and Liquid Water Temperature for a 0.5 °C Uncertainty

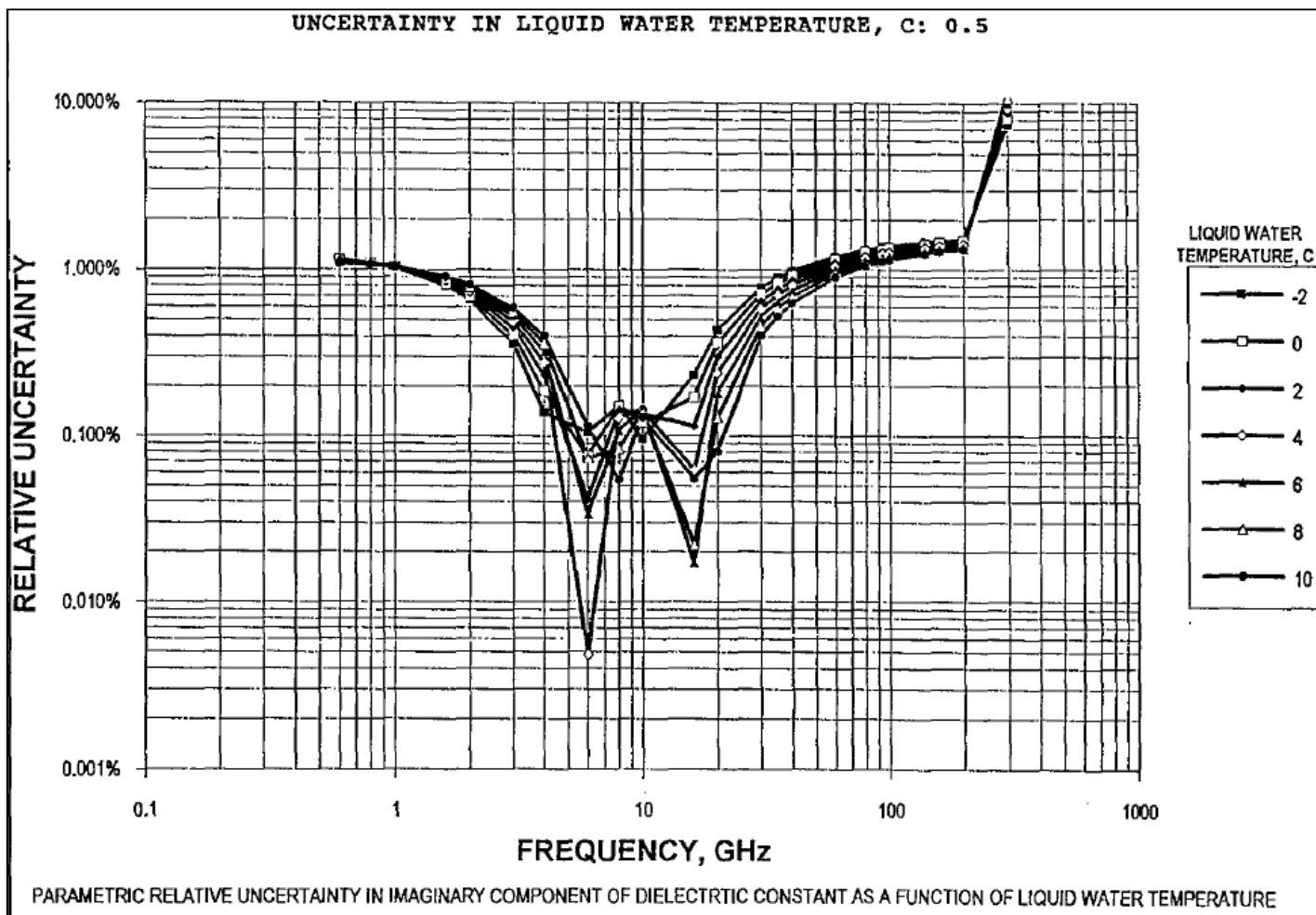


Figure G-3. Relative Uncertainty in the Imaginary Component of the Dielectric Constant as a Function of Frequency and Liquid Water Temperature for a 0.5 °C Uncertainty

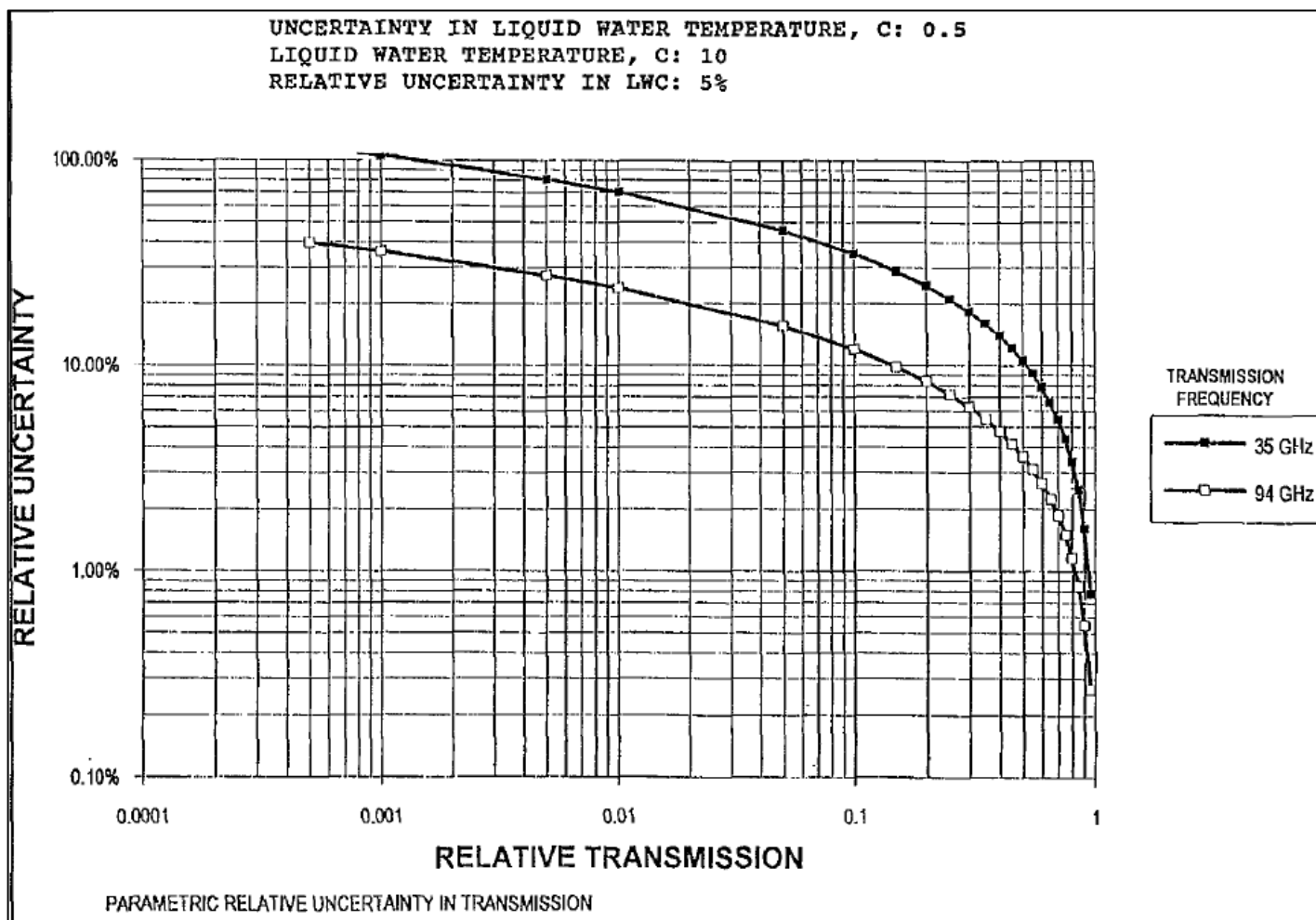


Figure G-4. Relative Uncertainty in Relative Transmission (With Respect to no Extinction) for 35 GHz and 95 GHz MMW Propagation for a 0.5 °C Uncertainty in Liquid Water Content Temperature, 10 °C Temperature, and 5% Relative Uncertainty in Liquid Water Content

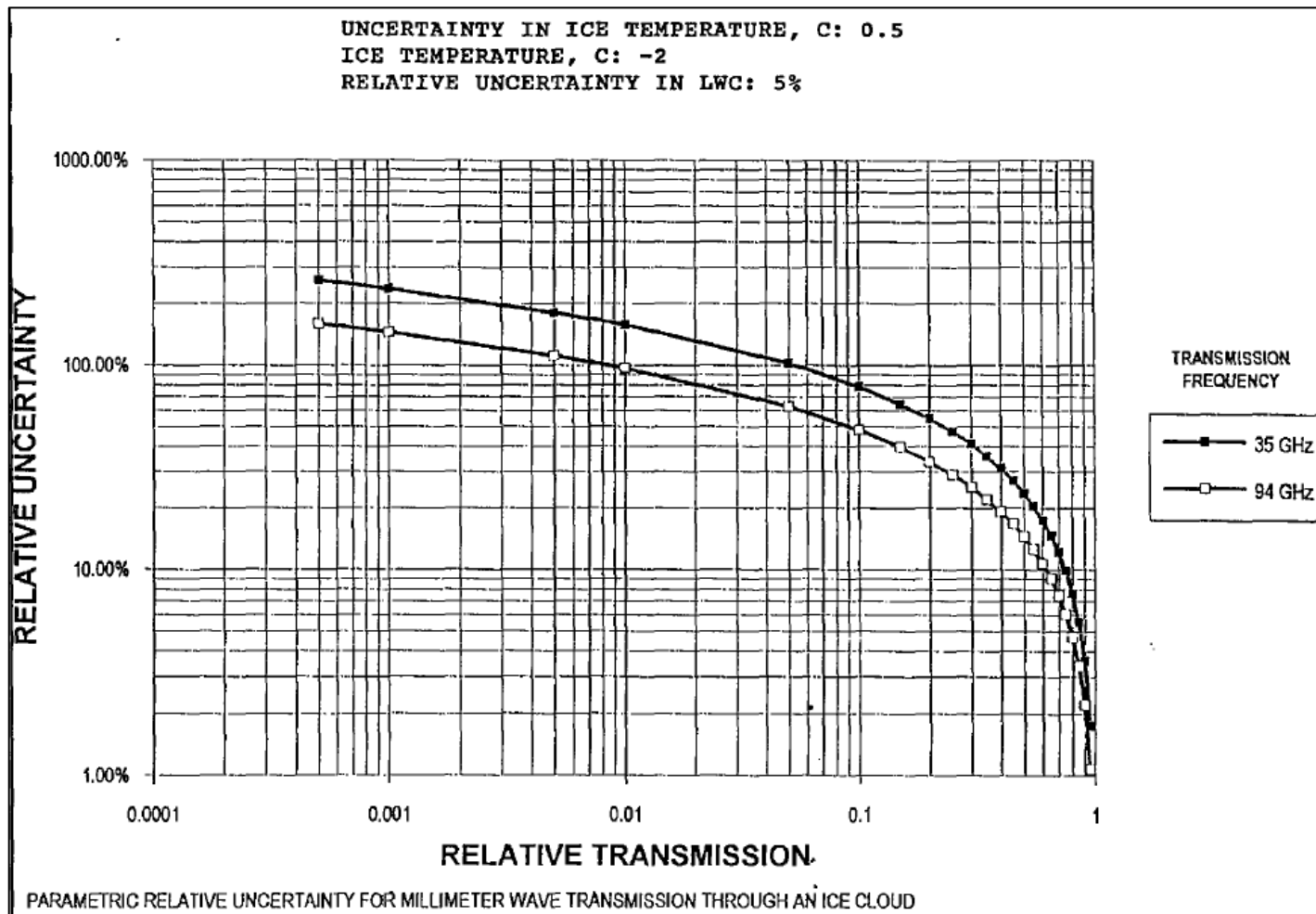


Figure G-5. Relative Uncertainty in Relative Transmission (With Respect to no Extinction) for 35 GHz and 95 GHz MMW Propagation for a 0.5 °C Uncertainty in Liquid Water Content Temperature, -2 °C Temperature, and 5% Relative Uncertainty in Liquid Water Content

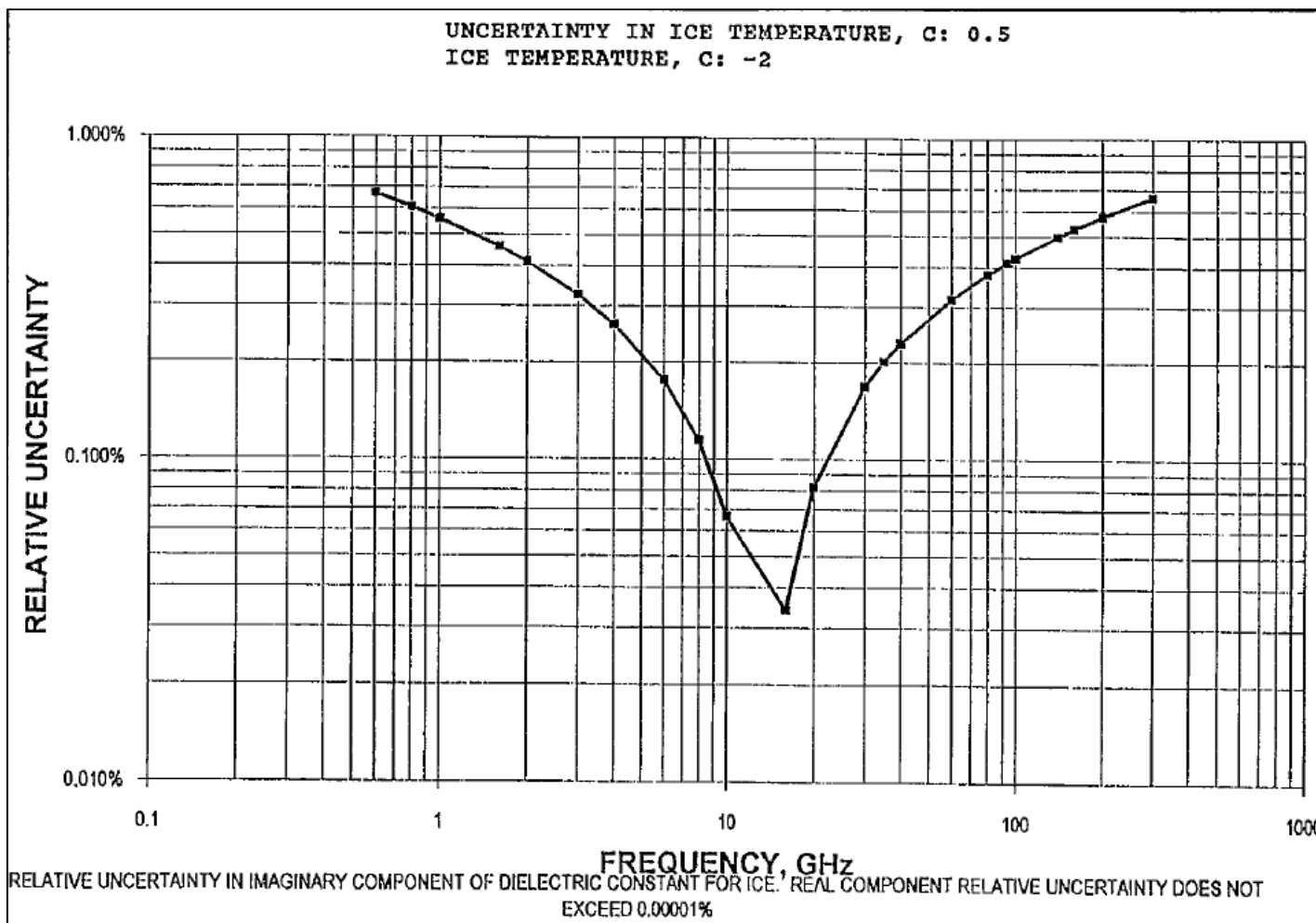


Figure G-6. Relative Uncertainty in the Imaginary Component of the Dielectric Constant of Ice as a Function of Frequency, -2°C Ice Temperature, and a 0.5°C Uncertainty. The Relative Uncertainty in the Real Component of the Dielectric Constant for These Variables Does Not Exceed 0.00001% .

This page intentionally left blank.

APPENDIX H

Citations

- Analytics, Inc. "Camouflage Effectiveness Evaluation System." Technical Memorandum 1900-03. Prepared for the U.S. Army Engineer Waterways Experiment Station, Vicksburg, MS, 1985.
- Alvin Schnitzler. "Image-detector model and parameters of the human visual system*." In *Journal of the Optical Society of America*, v63 n11, pp. 1357-1368. November 1973.
- Biltoft, Christopher A. and Rick D. Wald. *Dugway Optical Climatology Study*. DPG # DPG-FR-89-711. Available at <https://apps.dtic.mil/sti/citations/ADA220136>.
- Businger, J. A., J. C. Wyngaard, Y. Izumi, and E. F. Bradley. "Flux-Profile Relationships in the Atmospheric Surface Layer." In *Journal of the Atmospheric Sciences*, V28, I2, pp. 181-189. 1 March 1971.
- Churnside, J. H., Richard J. Lataitis, and Robert S. Lawrence. "Localized Measurements of Refractive Turbulence Using Spatial Filtering of Scintillations." In *Applied Optics*, V. 27, Issue 11, 1 June 1988. pp. 2199-2213.
- Clough, S.A., F.X. Kneizys, L.S. Rothman, and W.O. Gallery. "Atmospheric Spectral Transmittance and Radiance: FASCOD1B." In *Proceedings Volume 0277, Atmospheric Transmission*, 28 July 1981.
- Cook, J. and Stephen Burk. "Potential Refractivity as a Similarity Variable." *Boundary Layer Meteorology*, 58, pp 151-159, 1992.
- Edgar Andreas. "Atmospheric Stability from Scintillation Measurements." In *Applied Optics*, V. 27, Issue 11, pp. 2241-2246. June 1988.
- . "Estimating C_n^2 over Snow and Sea Ice from Meteorological Data." In *Journal of the Optical Society of America A*. V5, I4, pp. 481-195. 1 April 1988.
- . "Using Scintillation at Two Wavelengths to Measure Path-Averaged Heat Fluxes in Free Convection." *Boundary Layer Meteorology*, 54, pp 167-182, 1991.
- F. Roddier. "The Effects of Atmospheric Turbulence in Optical Astronomy." In *Progress in Optics*, V19, pp. 281-376. 1981.
- Farmer, W. M. and Roger Davis. "Computation of Broad Spectral Band Electro-Optical System Transmittance Response Characteristics to Military Smokes/Obscurants Using Field Test Data from Transmissiometer System Measurements." Technical Report AMCPM-SMK-CT-011-89. In *Proceedings of the Smoke/Obscurants Symposium XIII*, pp. 259-273, Aberdeen Proving Ground, MD 21005, 1989.

- Farmer, W. M., L. Rust, M. DeAntonio, and R. Davis. "Integrated Transmissometer Modeling System (ITEMS)." In *Proceedings of the Smoke/Obscurants Symposium XII*. pp. 385-397. Aberdeen Proving Ground, 1988.
- Farrell, T., D. Dixon, L. Heflinger, S. Klyza, and K. Triebes. "Low-Cost Experiment to Measure Optical Turbulence Between Two Buildings." In *Journal of Directed Energy*, V. 2, no. 4, pp. 297-311. Fall 2007.
- Fred Nicodemus. *Self-Study Manual on Optical Radiation Measurements*. NBS Technical Note 910-8. Washington: National Bureau of Standards, 1985.
- Frederickson, P. A., K. L. Davidson, C. R. Zeisse, and C. S. Bendall. "Estimating the Refractive Index Structure Parameter (C_n^2) over the Ocean Using Bulk Methods." In *Journal of Applied Meteorology*, Vol. 39, pp. 1770-1783. October 2000.
- G. J. Burton. "Transformation of Visual Target Acquisition Data Between Different Meteorological and Optical Sight Parameters: A Simple Method." In *Applied Optics*, V22 Issue 11, pp. 1679-1683. 1983.
- H. A. Panovsky. "The Structure Constant for the Index of Refraction in Relation to the Gradient of Index of Refraction in the Surface Layer." In *Journal of Geophysical Research*, V73, I18, pp. 6047-6049. 15 September 1968.
- James Lancombe. "A Technique for Measuring the Mass Concentration of Falling Snow." In *Optical Engineering for Cold Environments*, V. 0414, pp. 17-28.
- J. C. Wyngaard. "On Surface-Layer Turbulence." In *Workshop on Micrometeorology*, American Meteorological Society, Boston, 1973, pp. 101-149.
- J. J. Wesolowski et al. *Evaluation of the proposed ambient air monitoring equivalent and reference methods*. Springfield: National Technical Information Service, 1974.
- J. P. Welsh. *Smart Weapons Operability Enhancement (SWOE) Program Joint Test and Evaluation Program Test Design*. SWOE Report 92-5. June 1992. Retrieved 10 June 2022. Available at <https://apps.dtic.mil/sti/pdfs/ADA289660.pdf>.
- Kader, B. A., A. M. Yaglom, and S. L. Zubkovskii. "Spatial Correlation Functions of Surface-Layer Atmospheric Turbulence in Neutral Stratification." Chapter in *Boundary Layer Studies and Applications*, pp. 233-249. Dordrecht: Kluwer Academic, 1989.
- Kaskaoutis, D.G. and H.D. Kambezidis. "Investigation into the wavelength dependence of the aerosol optical depth in the Athens area." October 2006. In *Quarterly Journal of the Royal Meteorological Society*, V. 132 Issue 620: pp. 2217-2234.
- Kennedy, B. W., B. A. Locke, W. M. Farmer, W. G. Klimek, and F. E. Perron, "Joint U.S.-Canadian obscuration analysis for smokes in snow (Smoke Week XI), Final Report: Part I," Report No. SMK-001-90, Project Manager, Smoke/Obscurants, Aberdeen Proving Ground, MD (April 1990). This document is classified unclassified/limited.

- L. S. Gandin. *Objective Analysis of Meteorological Fields*. Jerusalem: Israel Program for Scientific Translation, 1965.
- Lyons, T. J. and W. D. Scott. *Principles of air pollution meteorology*. London: Belhaven, 1990.
- Marshall, J. S. and W. M. Palmer. "The distribution of raindrops with size." In *Journal of Meteorology*, ed. 5, pp. 165-166. August 1948.
- Matthew N. O. Sadiku. "Refractive Index of Snow at Microwave Frequencies." In *Applied Optics* V. 24, Issue 4, 15 February 1985. pp. 572-575.
- Miriam Sidran. "Broadband Reflectance and Emissivity of Specular and Rough Water Surfaces." In *Applied Optics*, V. 20, Issue 18, 15 September 1981. pp. 3176-3183.
- Noll, K. and T. Miller. *Air Monitoring Survey Design*. Ann Arbor: Ann Arbor Science Publishers, January 1977.
- Ochs, G. R. and Ting-I Wang. "Finite Aperture Optical Scintillometer for Profiling Wind and C_n^2 ." In *Applied Optics*, V. 17, Issue 23, 1 December 1978. pp. 3774-3778.
- Otto Schade. "Optical and Photoelectric Analog of the Eye." In *Journal of the Optical Society of America*, pp. 721-739. September 1956.
- Pruppacher, H.R. and J.D. Klett. *Microphysics of Clouds and Precipitation*. Dordrecht: Springer Science + Business Media, 2010.
- R. E. Munn. "Urban Meteorology: Some Selected Topics." In *Bulletin of the American Meteorological Society*, V. 54, I. 2, pp. 90-93. February 1973.
- Rachele, H. and Arnold Tunick. *Estimating C_n^2 , C_t^2 , C_q^2 , and C_q^2 During Unstable Atmospheric Conditions*. U.S. Army Laboratory Command, Atmospheric Sciences Laboratory. TR-0299, White Sands Missile Range, NM 88002-5501, August 1991.
- Radio Corporation of America. *Electro-optics handbook: a compendium of useful information and technical data*. Harrison, N.J., 1968, p. 5-3.
- Range Commanders Council. *A Guide for Quality Control of Surface Meteorological Data*. RCC 382-21. January 2021. May be superseded by update. Retrieved 10 June 2022. Available at <https://www.trmc.osd.mil/wiki/x/DIy8Bg>.
- Ridgway, W.L., R.A. Moose, and A.C. Cogley. *Atmospheric Transmittance/Radiance Computer Code FASCOD2*. AFGL-TR-82-0395. October 1982. Retrieved 10 June 2022. Available at <https://apps.dtic.mil/sti/pdfs/ADA130241.pdf>.
- R. J. Hill. "Implications of Monin-Obukhov Similarity Theory for Scalar Quantities." In *Journal of the Atmospheric Sciences*. V46, I14, pp. 2236-2244. 15 July 1989.

- R. T. Birge. "The Propagation of Errors." In *The American Physics Teacher*, V. 7, No.6, pp. 351-357. December 1939.
- "Rytov number", Wikipedia, last modified 17 March 2016,
https://en.wikipedia.org/wiki/Rytov_number.
- Sabatini, R. and M. Richardson. "New techniques for laser beam atmospheric extinction measurements from manned and unmanned aerospace vehicles." In *Central European Journal of Engineering*, 3, pp. 11-35. 2013.
- Schaefer, V. J. and J. A. Day. *A Field Guide to the Atmosphere*. Boston: Houghton Mifflin, 1998.
- Science and Technology Corporation. *Indirect Fire Battlefield Obscurants Test (Smoke Week VII) July 15-26, 1985, Fort Sill, OK*. STC-TR-2094. 1 February 1986. Retrieved 10 June 2022. Available to personnel from U.S. Government agencies only at <https://search.dtic.mil>.
- Smith, F. and A. C. Nelson. *Guidelines for development of a quality assurance program, reference method for continuous measurement of carbon monoxide in the atmosphere*. Springfield, VA: National Technical Information Service, 1973.
- Sutherland, R. A., F. Hansen, and W. Bach. "A Quantitative Method for Estimating Pasquill Stability Class from Windspeed and Sensible Heat Flux Density." In *Boundary Layer Meteorology*, V. 37, N. 4, pp. 357-369. 1996.
- T. Oguchi. "Electromagnetic wave propagation and scattering in rain and other hydrometeors." In *Proceedings of the IEEE*, V. 71, Issue 9, September 1983.
- U.S. Army Atmospheric Sciences Laboratory. *Interim SWOE Site Characterization Handbook*. SWOE Report 91-14. May 1991. Available to DoD personnel and contractors at <https://search.dtic.mil/>.
- V. I. Tatarski. *Wave propagation in a turbulent medium*. Mineola: Dover Publications, 2017.
- W. C. Eaton. *Use of the Flame Photometric Detector Method for Measurement of Sulfur Dioxide in Ambient Air: a Technical Assistance Document*. Research Triangle Park: Environmental Protection Agency, 1978.
- William Wolf. "Differences in Radiance: Relative Effects of Temperature Changes and Emissivity Changes." In *Applied Optics* V. 14, Issue 8, 1 August 1975. pp. 1937-1939.
- W. Michael Farmer. "Analysis of Emissivity Effects on Target Detection Through Smokes/Obscurants." In *Optical Engineering* V. 30, November 1991. pp. 1701-1708.

*** * * END OF DOCUMENT * * ***